

INFORMATION TO USERS

This material was produced from a microfilm copy of the original document. While the most advanced technological means to photograph and reproduce this document have been used, the quality is heavily dependent upon the quality of the original submitted.

The following explanation of techniques is provided to help you understand markings or patterns which may appear on this reproduction.

1. The sign or "target" for pages apparently lacking from the document photographed is "Missing Page(s)". If it was possible to obtain the missing page(s) or section, they are spliced into the film along with adjacent pages. This may have necessitated cutting thru an image and duplicating adjacent pages to insure you complete continuity.
2. When an image on the film is obliterated with a large round black mark, it is an indication that the photographer suspected that the copy may have moved during exposure and thus cause a blurred image. You will find a good image of the page in the adjacent frame.
3. When a map, drawing or chart, etc., was part of the material being photographed the photographer followed a definite method in "sectioning" the material. It is customary to begin photoing at the upper left hand corner of a large sheet and to continue photoing from left to right in equal sections with a small overlap. If necessary, sectioning is continued again – beginning below the first row and continuing on until complete.
4. The majority of users indicate that the textual content is of greatest value, however, a somewhat higher quality reproduction could be made from "photographs" if essential to the understanding of the dissertation. Silver prints of "photographs" may be ordered at additional charge by writing the Order Department, giving the catalog number, title, author and specific pages you wish reproduced.
5. PLEASE NOTE: Some pages may have indistinct print. Filmed as received.

Xerox University Microfilms

300 North Zeeb Road
Ann Arbor, Michigan 48106

76-10,644

ROSE, Rose Kfar, 1927-
THE SYNTHESIS AND CHARACTERIZATION OF
POTENTIALLY MESOMORPHIC ORGANO-PALLADIUM
COMPOUNDS.

The City University of New York, Ph.D., 1976
Chemistry, inorganic

Xerox University Microfilms, Ann Arbor, Michigan 48106

© COPYRIGHT BY
ROSE KFAR ROSE

1975

THE SYNTHESIS AND CHARACTERIZATION OF
POTENTIALLY MESOMORPHIC
ORGANO-PALLADIUM COMPOUNDS

by

ROSE KFAR ROSE

A dissertation submitted to the Graduate
Faculty in Chemistry in partial fulfillment of the
requirements for the degree of Doctor of Philosophy,
The City University of New York

1975

This manuscript has been read and accepted for the Graduate Faculty in Chemistry in satisfaction of the dissertation requirement for the degree of Doctor of Philosophy.

12/19/75
date

Bernard J. Bulkin
Prof. Bernard J. Bulkin
Chairman of Examining Committee

12/23/75
date

Leonard H. Schwartz
Prof. Leonard H. Schwartz
Executive Officer

Angelo Santoro
Prof. Angelo Santoro
Co-Mentor

W.F. Berkowitz
Prof. William F. Berkowitz
Supervisory Committee

The City University of New York

DEDICATION

This thesis is dedicated to the memory of my parents, Benzion and Esther Kfar, from whom I learned essential human values and a respect for learning. It is also dedicated to the memory of my husband, Alfred Rose, who had encouraged me in every way possible to further and maintain my interests in science, along with my new responsibilities of wife and mother. Finally, this thesis is dedicated to my daughter, Esther H. Rose, whose love, affection, and enthusiasm about my research, reinforced my perseverance and helped sustain my efforts throughout these years.

ACKNOWLEDGEMENTS

My appreciation is hereby expressed to Professors Bernard J. Bulkin and Angelo Santoro for suggesting this problem to me and for the guidance offered during the investigation. I wish to acknowledge the interest and enthusiasm about this project that Professors Bulkin and Santoro have shown, and the friendly spirit that marked our association. Special thanks are due to Professor Bulkin who, despite a busy schedule and many other responsibilities, made time available for frequent discussions of progress and offered numerous valuable suggestions. I am also grateful to Professor William F. Berkowitz for his valuable suggestions and criticisms.

A special acknowledgement is due to Professor Richard H. Wiley for his help in obtaining mass spectra of the compounds investigated. I also wish to acknowledge gratefully the time and effort of Dr. Nehama Yellin, who enthusiastically instructed me about the workings of the Raman instrument.

Thanks are due to the members of the Chemistry Department of Hunter College for providing a stimulating environment in which to pursue these studies. There was

usually someone available and willing to discuss with me some of the problems that impeded progress, and to offer me the benefit of their point of view. The new friends I made at Hunter in the course of the last few years are too numerous to mention individually, but I am confident that each one of them knows my feelings about the experiences, distressing moments, and feelings of comradeship we shared. I shall long treasure the memories of friendly times with my fellow students at Hunter College.

I wish to acknowledge gratefully the Faculty Fellowship leave awarded me for the 1972-73 academic year by Kingsborough Community College of CUNY, which made it possible for me to complete a substantial portion of the research reported in this thesis.

Last, but by no means least, I wish to acknowledge the influence of all my chemistry Professors: those at Hunter College, at Purdue University and at the City University of New York. It is through my association with them that my enthusiasm for and appreciation of chemistry has grown. It is from them that I learned that chemistry is an ever-growing and ever-expanding science, and that to keep up with its growth one should return to formal studies every once in a while.

Abstract

THE SYNTHESIS AND CHARACTERIZATION OF
POTENTIALLY MESOMORPHIC
ORGANO-PALLADIUM COMPOUNDS

by

Rose Kfar Rose

Advisers: Professor Bernard J. Bulkin
Professor Angelo Santoro

Of the several thousands known organic mesomorphic compounds, only a small group contain metal atoms. Mesomorphic substances, or "liquid crystals" share certain features of geometric anisotropy. Their molecules are elongated rod-like or lath-like in shape; they contain groups of atoms associated with permanent dipole moments; and the molecules themselves must be polarizable. The intermolecular forces operating between the molecules must be strong enough to help maintain the parallel arrangement after the crystal lattice has melted.

Based on the model system of mesomorphic p-n-alkoxybenzoic acids, two organo-palladium systems were investigated for potential mesomorphism. It was intended that the square planar geometry around the palladium(II) provide the rigidity essential for mesomorphic behavior.

In the first part of this investigation two substituted palladium carboxylates were prepared. Palladium(II)-

(p-octyloxy)-benzoate and palladium(II)-(p-propoxy)-benzoate were prepared by reacting palladium(II) acetate with the appropriate p-alkoxy benzoic acid. These compounds were dark, proved difficult to purify, were probably polymeric in nature, and their differential thermal analysis (DTA) did not indicate mesomorphic behavior.

Compounds prepared in the second system were substituted palladium beta-diketonates. The (p-octyloxy)-1-phenyl-1,3-butanedione, or "ligand" used, was synthesized by reacting p-octyloxy-benzoyl chloride with the sodium salt of acetylacetone, followed by hydrolysis of the intermediate formed. The structure of the ligand was confirmed by elemental analysis, mass spectrum, NMR, infrared, ultraviolet and Raman spectra.

The ligand was coordinated to Pd(II), and two products were obtained, henceforth described as PdL₂ Species I and PdL₂ Species II. These two compounds represent the cis and trans isomers, respectively, of bis [(p-octyloxy)-1-phenyl-1,3-butanedionato]-palladium(II). These compounds were characterized on the basis of elemental analysis, molecular weights, mass spectra, NMR, infrared, Raman and ultraviolet spectra.

Selection rules were derived for the motions involving the -PdO₄- subunit of the Pd-beta-diketonates studied.

Far infrared spectra (from 50 to 500 cm^{-1}) and low frequency Raman spectra of several compounds were determined and compared. Infrared and Raman spectra of bis(acetylacetonato)-palladium(II), or $\text{Pd}(\text{acac})_2$ as well as those of bis(1-phenyl-1,3-butanedionato)-palladium(II) or $\text{Pd}(\text{bzac})_2$ were obtained, extending into the far infrared and low frequency Raman regions.

The bands due to the fundamental metal-oxygen modes observed in the Raman spectrum of $\text{Pd}(\text{acac})_2$ were assigned by comparison with those previously reported for the 3 modes observed in the far infrared spectrum. Only one of the bands attributed to the M-O mode was previously reported for $\text{Pd}(\text{bzac})_2$. The other infrared and Raman active modes are reported and assigned here, and they follow selection rules for D_{2h} symmetry to which the trans $\text{Pd}(\text{bzac})_2$ belongs.

By comparison of the M-O fundamental modes observed and assigned in the far IR and Raman spectra, PdL_2 Species II was shown to be of D_{2h} symmetry, as expected for the trans isomer. PdL_2 Species I was shown to be of C_{2v} symmetry, as expected for the cis isomer.

The DTA thermograms of PdL_2 Species II indicate that the thermal behavior associated with the decomposition pattern of the Pd-beta-diketonates and other Pd-oxygen coordination compounds, has been modified by the introduction of the long p-octyloxy chain. The DTA of Species II is similar to that

of a mesomorphic compound, showing several endotherms preceding the melting point, then followed by decomposition. However, the compound does not possess the optical activity associated with mesomorphic compounds.

It is suggested that PdL_2 Species II is a "pseudo" mesomorphic compound, and that its high melting point (230°C) makes it difficult to establish its potential mesomorphism. A delicate balance of intermolecular attractions exists in mesomorphic systems. It is quite likely that the selective weakening of some of the cohesive forces does not occur until high temperatures are reached. When the melting process begins, the thermal vibrations are too great to maintain the ordered arrangement essential for the existence of a mesophase.

TABLE OF CONTENTS

	page
COPYRIGHT	ii
APPROVAL PAGE	iii
DEDICATION	iv
ACKNOWLEDGEMENTS	v
ABSTRACT	vii
TABLE OF CONTENTS	xi
LIST OF TABLES	xiii
LIST OF FIGURES	xv
INTRODUCTION	1
EXPERIMENTS AND RESULTS	11
Instruments	11
Chemicals Used	18
Synonyms and Abbreviations Used	20
Synthetic Procedures	21
Preparation of Palladium(II) Acetate	21
Preparation of Palladium(II) Benzoate	22
Preparation of Palladium(II) p-Octyloxy Benzoate	24
Preparation of Palladium(II) p-Propoxy Benzoate	29

TABLE OF CONTENTS (continued)

	page
Preparation of p-Octyloxy Benzoyl Chloride . . .	33
Preparation of (p-Octyloxy)-1-Phenyl-1,3- Butanedione	38
Preparation of bis-(1-Phenyl-1-3-Butanedionato)- Palladium(II)	45
Preparation of bis-[(p-Octyloxy)-1-Phenyl-1-3- Butanedionato]-Palladium(II)	59
Product Identification of Species I	61
Product Identification of Species II	71
Preparation of Dibenzonitrile Palladous Chloride	81
Details of Purification Procedures for Pd-carboxylates	82
DISCUSSION	98
Discussion of Pd-carboxylato Compounds	98
General Discussion of Vibrational Spectra of β -Diketones and Their Metal Chelates	107
Experimental Evidence for Structure Assignments. .	144
Discussion of Ultraviolet Spectra	198
Discussion of NMR Spectra	218
Discussion of DTA Data and Potential Mesomorphism	241
APPENDIX I	273
APPENDIX II	275
BIBLIOGRAPHY	276

LIST OF TABLES

Table		Page
I	Summary of Mass Spectral Data and Interpretation ("Ligand")	48
II	Comparison of Infrared Bands in Ligand with Literature Assignments	112
III	Selected Infrared Bands in Cu and Ni Complexes	134
IV	Comparison of Selected Infrared Bands of Ligand, Species I and Species II . .	139
V	Comparison of Far Infrared Data for Pd(acac) ₂	152
VI	Correlation Table for Symmetry Groups D _{4h} , D _{2h} and C _{2v}	158
VII	Comparison of Far Infrared and Raman Bands of Pd(acac) ₂	160
VIII	Comparison of Raman Bands of Pd(acac) ₂ with Ga(acac) ₃ and In(acac) ₃	161
IX	Correlation Diagram and Selection Rules For Symmetry Groups D _{4h} , D _{2h} and C _{2v}	163
X	Comparison of Far Infrared Bands and Raman Bands of Pd(bzac) ₂	176
XI	Comparison of Far Infrared and Raman Bands of PdL ₂ Species I	178
XII	Comparison of Far Infrared and Raman Bands of PdL ₂ Species II	188

LIST OF TABLES (continued)

Table		Page
XIII	Comparison of Gubin's Ultraviolet Data with Singh's Data on $\text{Pd}(\text{acac})_2$	200
XIV	Comparison of Our Ultraviolet Data with Singh's Data on $\text{Pd}(\text{bzac})_2$	203
XV	Comparison of Chemical Shifts in the NMR Spectra	227

LIST OF FIGURES

Figure		Page
1	Changes in Structure on Mesomorphic Transitions	4
2	Structures of Some Mesomorphic and Non-mesomorphic Compounds	7
3	Ultraviolet Spectrum of Palladium Acetate	23
4	Infrared Spectrum, Showing Band of Palladium Benzoate	25
5	DTA of Pd-octyloxy-benzoate	27
6	DSC of Pd-octyloxy-benzoate	28
7	Infrared Spectrum of Pd-octyloxy-benzoate	30
8	Ultraviolet Spectrum of Pd-octyloxy-benzoate	31
9	Infrared Spectrum of Pd-propoxy-benzoate	34
10	Ultraviolet Spectrum of Pd-propoxy-benzoate	35
11	DTA of Pd-propoxy-benzoate	36
12	Infrared Spectrum of "Ligand"	42
13	NMR Spectrum of "Ligand".	44
14	Mass Spectrum of "Ligand"	47
15	Ultraviolet Spectrum of "Ligand"	50

LIST OF FIGURES (continued)

Figure		Page
16	Infrared Spectrum of Pd(bzac) ₂	54
17	Ultraviolet Spectrum of Pd(bzac) ₂	56
18	NMR Spectrum of Pd(bzac) ₂	58
19	Infrared Spectrum of PdL ₂ Species I	63
20	Ultraviolet Spectrum of PdL ₂ Species I	66
21	NMR Spectrum of PdL ₂ Species I	68
22	Mass Spectrum of PdL ₂ Species I	70
23	Infrared Spectrum of PdL ₂ Species II	73
24	Ultraviolet Spectrum of PdL ₂ Species II	75
25	NMR Spectrum of PdL ₂ Species II	77
26	Mass Spectrum of PdL ₂ Species II	79
27	Infrared Spectrum of Benzene Solution of Crude Reaction Mixture, Showing Presence of Three Materials	86
28	Infrared Spectrum of Benzene Solution, Showing Less p-Octyloxy-benzoic Acid Contamination	87
29	Ultraviolet Spectrum of p-Octyloxy- benzoic Acid in Dioxane	88
30	Ultraviolet Spectrum of First Ligroin Extract of reaction Mixture to Prepare Pd-(p-propoxy)-benzoate	91
31	Ultraviolet Spectrum of Sixth Ligroin Extract of Reaction Mixture.	92

LIST OF FIGURES (continued)

Figure		Page
32	Infrared Spectrum of Benzene Solution of Crude Reaction Mixture, Showing Presence of Three Materials	93
33	Infrared Spectrum of Benzene Solution of Pd-(p-propoxy)-benzoate, Showing Less Contamination	94
34	DTA Thermogram of Pure p-Propoxy-benzoic Acid	96
35	DTA Thermogram of Crude Pd-(p-propoxy)-benzoate, Showing Contamination with p-Propoxy-benzoic Acid	97
36	Structures of Acetylacetonone and Its Metal Chelate	108
37	Raman Spectrum of Ligand	119
38	Raman Spectrum of Pd(acac) ₂	121
39	Raman Spectrum of Pd(bzac) ₂	123
40	Raman Spectrum of PdL ₂ Species I	125
41-A	Raman Spectrum of PdL ₂ Species II from 300 to 1650 cm ⁻¹	127
41-B	Raman Spectrum of PdL ₂ Species II from 2750 to 3500 cm ⁻¹	129
42	Normal Modes of a Square-planar MX ₄ Molecule.	147
43	Schematics of Vibrational Modes for Pd(acac) ₂	150
44	Far Infrared Spectrum of Pd(acac) ₂	155
45	Low Frequency Raman Spectrum of Pd(acac) ₂	157

LIST OF FIGURES (continued)

Figure		Page
46	Far Infrared Spectrum of Pd(bzac) ₂ . . .	173
47	Low Frequency Raman Spectrum of Pd(bzac) ₂	175
48	Far Infrared Spectrum of PdL ₂ Species I	180
49	Low Frequency Raman Spectrum of PdL ₂ Species I	182
50	Far Infrared Spectra of PdL ₂ Species II	185
51	Low Frequency Raman Spectrum of PdL ₂ Species II	187
52	Comparison of M-O Fundamentals in Pd(bzac) ₂ and PdL ₂ Species II trans. .	190
53	Comparison of M-O Fundamentals in Pd(acac) ₂ and PdL ₂ Species I cis . . .	192
54	Predicted and Observed Frequencies for the Accordion Mode	196
55	Ultraviolet Spectrum of Pd(acac) ₂ . . .	201
56-A	Ultraviolet Spectrum of Bzac	205
56-B	Alternative Structures for PdL ₂ Species I	238
57	DTA Thermogram of Ligand	243
58	DTA Thermogram of p-Octyloxy- benzoic Acid	245
59	DTA Thermograms of Three Organo- palladium Compounds	248

LIST OF FIGURES (continued)

Figure		Page
60	DTA Thermogram of PdL ₂ Species I, Showing Two Heatings	251
61	DTA Thermogram of PdL ₂ Species II, Showing Two Heatings	254
62	DTA Thermogram of PdL ₂ Species II, Showing Three Heatings	256

INTRODUCTION

Attempts to correlate mesomorphic behavior and the chemical constitution of a compound were begun by Vorlaender¹ and Lehmann² soon after the discovery of the first mesomorphic compound in 1888. Subsequently, various investigators attempted to find out why some compounds are mesomorphic and some are not, as well as to establish the manner in which chemical constitution of a compound determines whether the mesophase exhibited will be smectic, nematic or cholesteric. These findings are summarized in several reviews by Gray^{3,4} and by Brown and Shaw⁵, and these provide some of the guidelines outlined below for selection of a potentially mesomorphic structure. Predictions are still difficult to make, and a great deal remains to be learned about the relationship between mesomorphism and chemical constitution.

Although the melting point of an organic compound is quite unpredictable, one can generalize that compounds of high molecular weight, or those that are highly dipolar, will be high melting. On the other hand, relatively minor changes in molecular structure or geometry, can produce a

series of compounds with marked fluctuations among their respective melting points.³ At the melting point of an ordinary, non-mesomorphic compound, the three-dimensional, ordered, geometric arrangement of the molecules in the solid phase collapses suddenly, and a disordered isotropic liquid results. The temperature of this transition depends on the intermolecular attractive forces (i.e. dipole-dipole, induced dipole, van der Waal's) between the sides, the molecular planes, and the ends of the molecules. At the melting point the lateral, planar, and terminal intermolecular attractions have been weakened. The strength of the various intermolecular forces will also depend on the packing arrangement of the molecules in the crystal lattice.

The mesomorphic compound passes through one or more ordered intermediate states -- or mesophases -- before the increasing thermal agitations produce the isotropic liquid. For a mesomorphic compound each of these intermediate transitions involves a lesser decrease in the state of order than that occurring at the melting point of an ordinary compound.

In the smectic mesophase the terminal cohesions between the molecules have been weakened, and the strata of molecules become free to slide one over another. Within each particular layer, however, the ends of the molecules

remain aligned (Fig. 1-b). At the smectic-nematic transition, the molecules move in the direction of their long axes, out of the layers of the smectic mesophase. In the nematic mesophase (Fig. 1-c) the molecules remain parallel to one another, but their ends have moved out of alignment and into a more disordered state. The smectic-nematic transition will occur after the attractions operating between the sides and planes of the elongated molecules have been overcome, and when the molecules become free to slide out of the layers.

Before the change from the nematic melt to the isotropic liquid can take place, the residual intermolecular attractions between the planes, sides, and ends of the molecules must further decrease. The molecules will then break away rapidly from the parallel arrangement, the molecular clusters will decrease in size, and the isotropic liquid will result (Fig. 1d). The attractions between the ends of the molecules arranged in head-to-tail fashion, are probably very important in determining the temperature at which the final breakdown in molecular order of the nematic mesophase occurs.

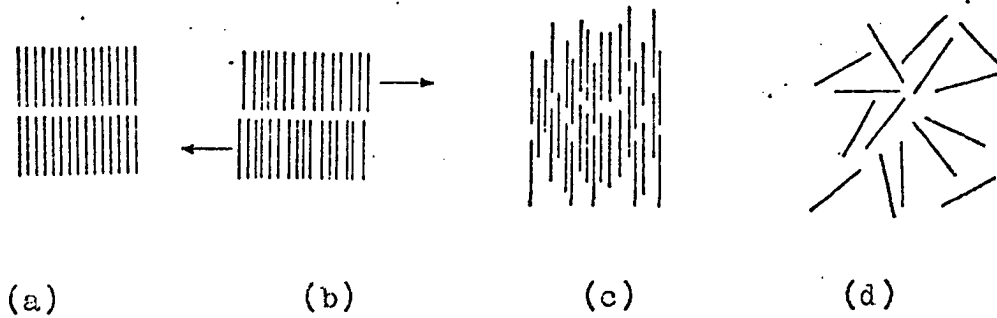


Figure 1 (a), (b), (c) and (d)

The changes in molecular arrangement involved in passing from (a) the crystal to (b) the smectic mesophase, to (c) the nematic mesophase and to (d) the isotropic liquid

The known mesomorphic compounds ("liquid crystals") can vary considerably in chemical composition, and they include many classes of compounds: alkali salts of fatty acids, alkoxy benzoic acids, alkoxy cinnamic acids, benzalamino-cinnamic acid esters, derivatives of benzidines and diphenyls, derivatives of stilbenes and similar unsaturated hydrocarbons, azo compounds, azoxy compounds, azine and hydrazones, esters of cholesterins and phytosterins.^{3,6,7} All of these different classes of compounds possess certain similar features of geometric anisotropy. Generally, the molecules of a mesomorphic substance are elongated and rod-like or lath-like in shape. It is also essential that the intermolecular forces operating between the molecules be strong enough to help maintain a parallel arrangement of the molecules after the crystal lattice has melted. To be a potentially mesomorphic system, the long and narrow molecules must contain groups of atoms associated with permanent dipole moments, and the molecule itself must be polarizable.³

The model system on which our investigations were based are the *p*-*n*-alkoxy benzoic acids. This homologous series is mesomorphic, beginning with the *n*-propoxy benzoic acid.^{8,9} The molecular geometry of these compounds satisfies

the requirements outlined above: they exist as elongated, linear dimers (Fig. 2), with two aromatic rings, dipolar ether groups, and the polarizable C=O bond. The importance of combining all of the above features in one molecule can be better appreciated by noting that benzoic acid itself, although it is also dimeric, is not mesomorphic, since it lacks the dipolar alkoxy group. Similarly, esters of the alkoxy benzoic acids are not mesomorphic, apparently because the monomeric ester molecule is much shorter than the corresponding hydrogen-bonded dimer of the alkoxy acid.

In aromatic compounds mesomorphic behavior is observed only in those with linear molecules that can maintain a fairly rigid molecular axis. The trans-p-n-alkoxycinnamic acids are mesomorphic,¹⁰ because they are linear dimers, with two aromatic rings, dipolar ether groups, and polarizable C=O and C=C bonds. On the other hand, the dimers formed by the cis-p-n-alkoxycinnamic acids are not linear, and these compounds are not mesomorphic. The requirement for a relatively rigid system can be understood by comparing the p-alkoxycinnamic acids with the p-alkoxy-3-phenyl-propionic acids which are not mesomorphic. In the dimerized cinnamic acids the aromatic rings, the olefinic linkages, and the dimerized carbonyl groups will tend to lie

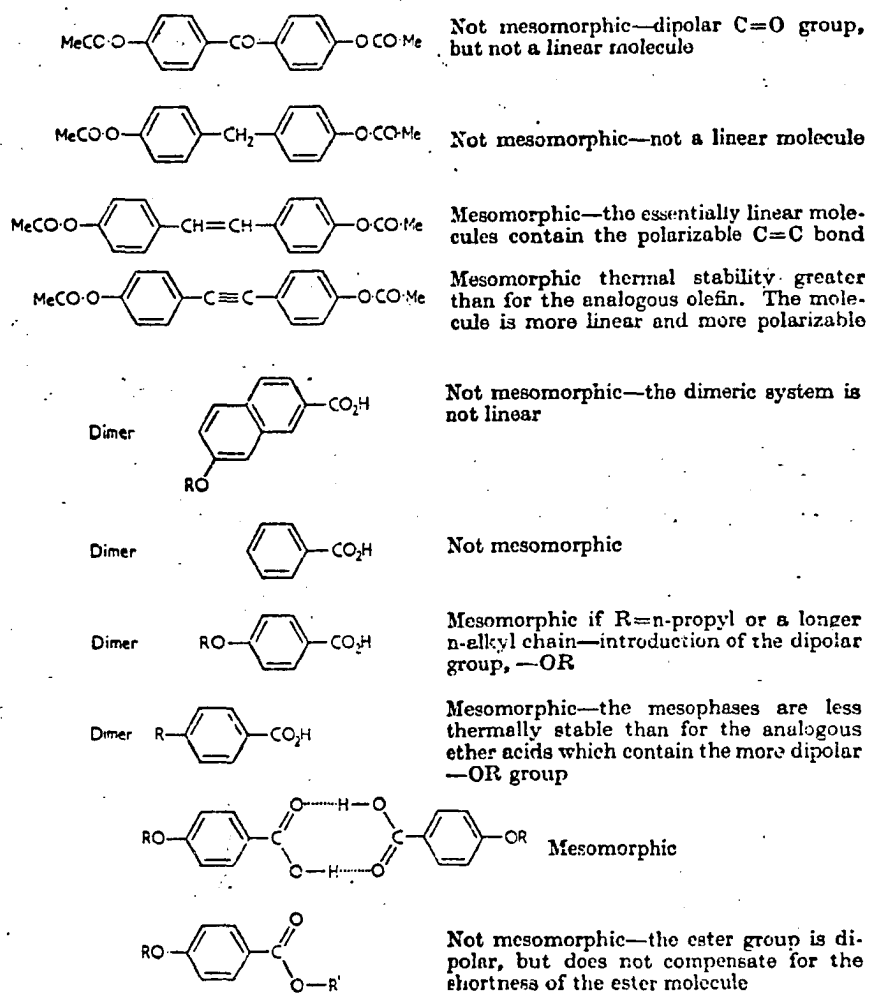


Figure 2. Structures of Some Mesomorphic and Non-mesomorphic Compounds

(Examples Selected from G.W. Gray, Reference 3)

in one plane, so that conjugation may occur as far as possible, to help maintain the energy of the system at a minimum. However, in the saturated molecule of the phenylpropionic acids the double methylene bridges, between the phenyl rings and the dimerized carbonyl groups, will be flexible like any other alkyl chain. Thermal vibrations will cause the dimeric molecule of the phenyl propionic acid to assume a non-linear and non-rigid arrangement.

After careful consideration of some of the above requirements of molecular geometric anisotropy, we proposed to design and prepare potentially mesomorphic organopalladium compounds, with Pd(II) coordinated to oxygen-bearing organic ligands. Such organopalladium compounds would represent a rather unique and interesting example of mesomorphism, since of the several thousands known organic compounds with mesomorphic behavior, only a small group contained metal atoms.⁶ Vorlaender in 1910¹¹ and Walter in 1926¹² showed that sodium, potassium, rubidium and thallium salts of aliphatic and aromatic carboxylic acids often have smectic phases. Several aromatic compounds of mercury related to Schiff bases, were reported by Urban in 1922¹³ and by Vorlaender in 1924¹⁴ to have a nematic phase. Eaborn and Hartshorne¹⁵ reported in 1955 a mesomorphic phase

associated with diisobutylsilanediol, but the phase was not classified. Young et al¹⁶ reported in 1971 several mesomorphic compounds of silicone, germanium and tin which were a series of Schiff bases with the groups containing Si, Ge, Sn terminally substituted.

The organopalladium compounds we proposed to investigate would have the metal centrally substituted. Since complexes of Pd(II) are known to assume a square planar geometry¹⁷, the Pd would provide the center around which the planarity and rigidity of the long molecule could be maintained.

One of the systems investigated involved the preparation of Pd(p-alkoxy)benzoates, in which the two molecules of p-alkoxybenzoic acid coordinate to the Pd II via the carboxylate. Based on the structure reported for palladium (II) acetate (monomer)¹⁸, and palladium (II) benzoate,¹⁹ it was assumed that the Pd-(p-alkoxy) benzoates would have the necessary features of being an elongated rod-like system, with polar alkoxy groups and polarizable C=O bonds.

The other potentially mesomorphic system of organopalladium compounds involved the coordination of the Pd(II) to a beta-diketo system designed to incorporate some of the essential features of the model system -- the p-alkoxy-

benzoic acids. In the latter system we coordinated Pd(II) to the ligand which we prepared: (p-octyloxy)1-phenyl-1,3-butanedione. Inasmuch as the X-ray structure of the trans-Pd(1-phenyl-1,3-butanedionato) compound had been determined by Hon et al²⁰, we reasoned that the trans isomer of the desired compound would have the Pd at the center, with the diketo-chelate rings coordinated to it, as well as the aromatic rings,-- all lying in one plane; and the long axis of the molecule would be extended through the oxygen of the alkoxy groups at the ends.

EXPERIMENTS AND RESULTS

Instruments

Infrared Spectrophotometer. Infrared spectra were obtained on a Perkin Elmer Model 521 dual grating spectrophotometer, with a range of 4000 cm^{-1} to 250 cm^{-1} . The instrument was run at a spectral slit width of about 1 cm^{-1} . The spectra were recorded on chart paper whose coordinate represents percent transmittance, and the abscissa is linear in wave number. The solid samples were either Nujol or hexachlorobutadiene mulls, placed as thin films between NaCl plates. Solution spectra were obtained in Beckman demountable liquid cells, with IRtran windows and Teflon spacers of appropriate thickness. Polyethylene film and water vapor²¹ were used as calibration standards.

For low wave number spectra (from 650 to 250 cm^{-1}) polyethylene cells were used. Dry nitrogen gas was used to purge the instrument free of water vapor for about 20 minutes prior to operation. A gentle stream of nitrogen was maintained while the spectra were recorded. The gain was increased from 4.5 to 6.0, the attenuator setting reduced

from 1100 to 900, and spectra were recorded at the slowest speed possible (scan time setting of 64).

Far Infrared Spectrophotometer. Far infrared spectra were obtained using a Block Engineering, Inc. Interferometer Spectrophotometer Model 296, in conjunction with Type 564 Storage Oscilloscope and Digilab NOVA FTS-14 high-speed Data System (serial No. 109116), and a recorder. The FTS-14 system is designed specifically for real-time laboratory Fourier spectroscopy. The three functions of the computer system are: a) data acquisition, signal averaging and experiment control; b) Fourier transformation and phase correction; c) ratio determination, display and data manipulation. The laser is a He-Ne unit with a line at 632.8nm. The white light source is a miniature incandescent bulb, and the associated detector is a germanium photodiode. A 3 micron mylar film was used as a beam splitter to obtain spectra from 50 to 450 or 500 cm^{-1} .

Raman Instrument. Raman spectra were taken with a Spex Industries Model 1401 spectrophotometer. The light source was a Spectra-Physics Krypton Model 165 or Argon Model 164 laser. The exciting lines used were either the 514.5 nm line of the Argon laser, or the 530.9 nm line of the Krypton laser. The power of the laser beam at the source ranged from 200 to 300 mw. Spectra were run at

spectral slit widths ranging from 1.0 to 4.0 cm^{-1} , with most of the spectra obtained at slit widths of 4.0 cm^{-1} . A Corrion Instruments Corp. Interference Filter was used with the Krypton laser, and an Ealing Corp. Interference Filter with the Argon laser.

Samples were generally contained in a capillary tube, about 8 cm. long and 0.5 to 1 mm in diameter. The ends of the capillary tube were sealed, using a microburner. Most spectra were obtained on solid samples, since the solubility of the organo-palladium compounds was too low, and the solutions of those compounds were very photosensitive. Neon lines were used to calibrate the spectra obtained.

Early attempts to obtain spectra of $\text{Pd}(\text{bzac})_2$ in CCl_4 and CHCl_3 solutions provided only limited data. In addition to the low solubility and low intensity of the spectral lines produced, the compounds in solution were subject to rapid thermal and photo-decomposition. These problems were even more acute with PdL_2 Species I and Species II. Therefore, most of the useful data were obtained on solid samples. As a result, bands due to crystal lattice vibrations also appear in both the Raman and the far infrared spectra of these compounds; nor was it possible to obtain Raman polarization data.

The bands in the region below 500 cm^{-1} , which were

of particular importance in establishing the symmetry of the $\text{-PdO}_4\text{-}$ subunit of some of the organo-palladium molecules, are generally much weaker than those above 500 cm^{-1} . Observations of these weak Raman bands were even further handicapped by thermal and photo-decomposition of samples. Each time the sample decomposed, a black spot formed on the walls of the capillary sample tube. To obtain better spectra, the weak Raman bands were enhanced by the combined use of zero suppression and scale expansion techniques (i.e. Raman spectra had to be taken at different ordinate scale expansion in different regions). Some spectra were obtained by running several "spots" of the sample tube in different spectral regions, so that a complete spectrum might be obtained by overlapping those regions. Visual examination of the Raman spectra was generally a good indication as to whether or not decomposition had taken place. Attempts to obtain Raman spectra by the "computer assisted method" were unsuccessful, since the computer continued to collect data even if the sample in the beam had decomposed and darkened.

Ultraviolet Spectrophotometer. A Cary Recording Spectrophotometer Model 14-R (Serial No. 1241), with a hydrogen lamp as a light source, was used to record ultra-

violet spectra. This instrument employs a double monochromator, consisting of a 30° fused silica prism in a series with a 600 line/mm echelette grating, each with its own collimating mirrors and slit systems. The resolving power of the monochromator is about 0.1 nm in the ultraviolet and near visible ranges. In the ultraviolet range the remote scattered radiation (more than 5.0 nm different from the monochromatic radiation) is generally less than 10 parts per million. The near scattered radiation (more than 0.5 nm different from the monochromatic) is less than 200 parts per million.

The absorbance scale on this instrument is effectively 20 inches for a density range of 0 to 2. A three-position Range Selector switch is provided, which permits operation in the 0-1, 1-2, or even over the entire 0-2 density range. In the latter case the appropriate range is automatically selected by limit switches and relays, which also control the 10:1 attenuators in the slidewire circuits. The recorder pointer accuracy limits are ± 0.002 absorbance unit from 0-1, and ± 0.005 unit near 2. Recorded accuracy may be slightly lower than these figures, by about 0.006 unit, because of chart paper shrinkage and slippage.

With proper sample handling technique, an analytical

accuracy of 0.1% may usually be obtained on measurements in the optimum absorbancy region (around 1). With the light source properly focused, at 350 nm the slits should balance at approximately .15 mm. In this investigation the slit widths were .35 mm. Samples were carefully weighed out, with an accuracy of ± 0.000002 g, and stock solutions with concentrations 0.005 to 0.01M prepared in volumetric flasks. These were diluted to proper concentrations using 1.0 and 2.0 ml. standard pipettes, as well as 5.00, 10.00 and 25.00 ml. volumetric flasks. Quartz sample cells were usually 1.0cm path-length, and well matched cells were used for reference (solvent) and sample, with the baseline of the solvent subtracted from the sample spectrum.

Differential Thermal Analysis. The studies reported here were made with the differential scanning calorimeter cell of the Dupont 900 Differential Thermal Analyzer. This DSC cell had been characterized by Baxter.²² Checks were made periodically to monitor the rate of temperature rise and to assure calibration of the instrument for transition temperatures. Most of the thermograms in this study were recorded at a heating rate of 10 degrees per minute, and at a maximum sensitivity of 0.1 to 0.2 degrees per inch. Samples were placed in small aluminum cups supplied by Dupont (part No. 900757), and those were covered and some-

times sealed hermetically with a special die press. A similar aluminum cup, filled with glass beads, served as reference. The heating rate was programmed, but the cooling rate was due to slow equilibration with ambient temperatures. Samples could also be rapidly cooled below ambient temperatures by use of a cooling jacket which was filled with liquid nitrogen.

The temperature programmer-controller operates on the basis of a feedback from a Chromel-Alumel control thermocouple. Cold junction compensation is provided for sample and control thermocouples by immersing another junction in a solid ice-water mixture. The 900 DTA can analyze samples as small as 0.1 mg or as large as 100 mg. Our samples generally weighed 1.000 mg to 4.000 mg. The 900 DTA contains a baseline compensator, so that it can accommodate differences in size, heat capacity and thermal conductivity between sample and reference.

The DTA contains an X-Y plotter, which is capable of simultaneous recording of sample temperature and temperature differential between sample and reference. A five-position switch permits selection of any of five X-axis scale settings: 10°C, 20°C, 50°C, 100°C and 200°C per inch. Most of the thermograms were obtained using the 20° per inch

setting. This setting corresponded to temperature changes recorded between 0° and 200°C with no shift of scale; or from 100° to 300°C with a shift of scale by minus 5 inches.

Other Instruments. The nuclear magnetic resonance spectra were obtained at 60Hz, using a Varian Associates Model A-60 Analytic NMR Spectrophotometer, and peak positions are expressed in parts per million (ppm) as downfield shifts from internal tetramethylsilane. Mass spectral data were taken with a Varian M-66 cycloidal double focussing mass spectrometer. Melting points were determined either in capillaries, using a Hoover-Thomas melting point apparatus; or on glass slides on a Mettler FP-2, and are uncorrected.

Microanalyses were performed by Schwartzkopf Micro-analytical Laboratory, Woodside, New York, 11377. Molecular weights were determined osmotically by Schwartzkopf at 37.5°C on a Mechrolab vapor pressure osmometer.

Chemicals Used. Palladium sponge was purchased from K & K Laboratories, Inc. Palladous chloride and palladium acetylacetonate were obtained from Alfa Inorganics Ventron Corp. Thionyl chloride was from MCB; sodium hydroxide flakes were from Fisher Scientific Co., and potassium hydroxide was obtained from J. T. Baker Chemical Co. The EDTA was from Fisher Scientific Co.

All of the alkoxy-benzoic acids used in synthetic work and for comparison with the compounds made, were purchased from Frinton Laboratories. The acetylacetone was obtained from Fisher Scientific Co. and distilled before using. Benzoylacetone was purchased from Aldrich Chemical Co. and recrystallized from ethanol. The solvents used for spectral investigations were from Mallinckrodt; chloroform was the nanograde and CH_2Cl_2 was the SpectrAR spectrophotometric grade. Absolute ethanol was obtained from Commercial Solvents Corporation.

All other solvents used in tlc and other purification procedures were from Fisher Scientific Co., of the ACS certified grade. All other ordinary chemicals were purchased as reagent grade.

Synonyms and Abbreviations Used

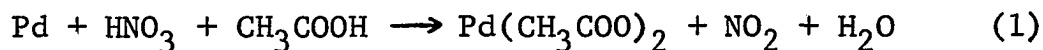
In description of procedure the following abbreviations were used: NMR, nuclear magnetic resonance; m, multiplet; q, quarter; t, triplet; d, doublet; s, singlet; tlc, thin layer chromatography; IR, infrared; sh, shoulder; s, sharp; m, medium; w, weak; vw, very weak; vs, very strong; b, broad; sym., symmetric; asym., asymmetric; UV, ultraviolet; mp, melting point; bp, boiling point; d, decomposes; DTA, differential thermal analysis; DSC, differential scanning calorimetry; HCBd, hexachlorobutadiene; TMS, tetramethylsilane.

In referring to chemicals used and compounds prepared the following abbreviations and synonyms were used: bzac, benzoylacetone, or 1-phenyl-1,3-butanedione; acac, acetylacetone, or 2,4-pentanedione; ligand, (p-octyloxy)-1-phenyl-1,3-butanedione, or p-OC₈H₁₇-bzac; Pd(ac)₂, palladium (II) acetate; PdL₂, Pd(ligand)₂, or bis- [(p-octyloxy)-1-phenyl-1,3-butandionato]- palladium; ether, diethyl ether; alkoxy b.a., alkoxy benzoic acid; ligroin, fraction boiling 60 to 90°C; EDTA, tetrasodium salt of ethylene diamine tetraacetate; Ph, phenyl; arom., aromatic; Ø, phenyl; Ar, aryl.

Synthetic Procedures

Preparation of Palladium(II) Acetate

This was prepared by following the general procedure of Stephenson et al¹⁹, with slight modifications.



To increase its reactivity, Pd sponge was pretreated with EDTA. The Pd sponge was left overnight in an aqueous solution of the sodium salt of EDTA. After filtration, the metal was washed three times with water, followed by three washes with absolute ethanol, and finally by three washes with anhydrous ether, then air dried. Best yields were obtained in those experiments where the EDTA pretreatment was used. In a typical experiment 3.23 g (0.03036 moles) palladium sponge, 75.0 ml (78.68 g or 1.31 moles) glacial acetic acid, 3.5 ml. of conc. HNO_3 were refluxed for 20 hours, until no more brown fumes were visible. The reaction mixture was filtered hot, and 1.98 g. of unreacted palladium was recovered. The hot filtrate was cooled, and from it obtained 2.32 g of crude palladium acetate. The yield based on the 1.2 g (0.01128 moles) of palladium used, and on the weight of the crude product, was 91.57%. The mp of the purified compound was 202-204^o(d), literature¹⁹ mp 205^o(d).

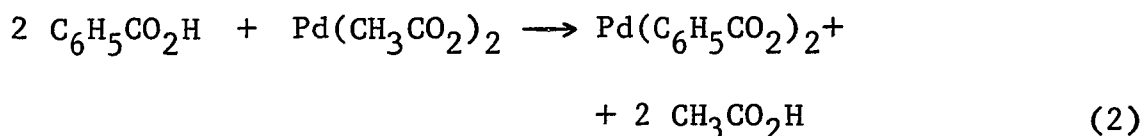
Product identification was based on the following

data: IR 1610 s(asym. C=O str.), 1430 s(asym. CH₃ bend and sym. CO str.); literature¹⁹ IR 1600, 1427 cm⁻¹.

UV spectrum (Fig. 3) in dioxane or benzene λ_{\max} 320, and 400 nm, with characteristic minimum at 355 nm, literature¹⁹ UV 394 nm. and 398 nm reported by Brandon and Claridge.^{22b}

Elemental analysis: Calcd. for PdC₄H₆O₄ C, 21.4; H, 2.7; Pd, 47.4%. Found: C, 22.02; H, 3.34; Pd, 46.65%.

Preparation of Palladium (II) Benzoate. For comparison purposes we prepared this compound on a small scale, following the directions of Stephenson.¹⁹ The palladium benzoate is prepared by an exchange reaction between Pd-acetate and benzoic acid.



Stephenson's directions state "a benzene solution of palladium diacetate and benzoic acid (mole ratio 1:3) was evaporated on a steam-bath and the residue washed with acetone or diethyl ether to remove benzoic acid. The product was recrystallized from benzene to yield the complex as a yellowish brown solid, mp 220^o(d)".

In this laboratory Stephenson's procedure resulted in the formation of a black decomposition product, and only

ABSORBANCE

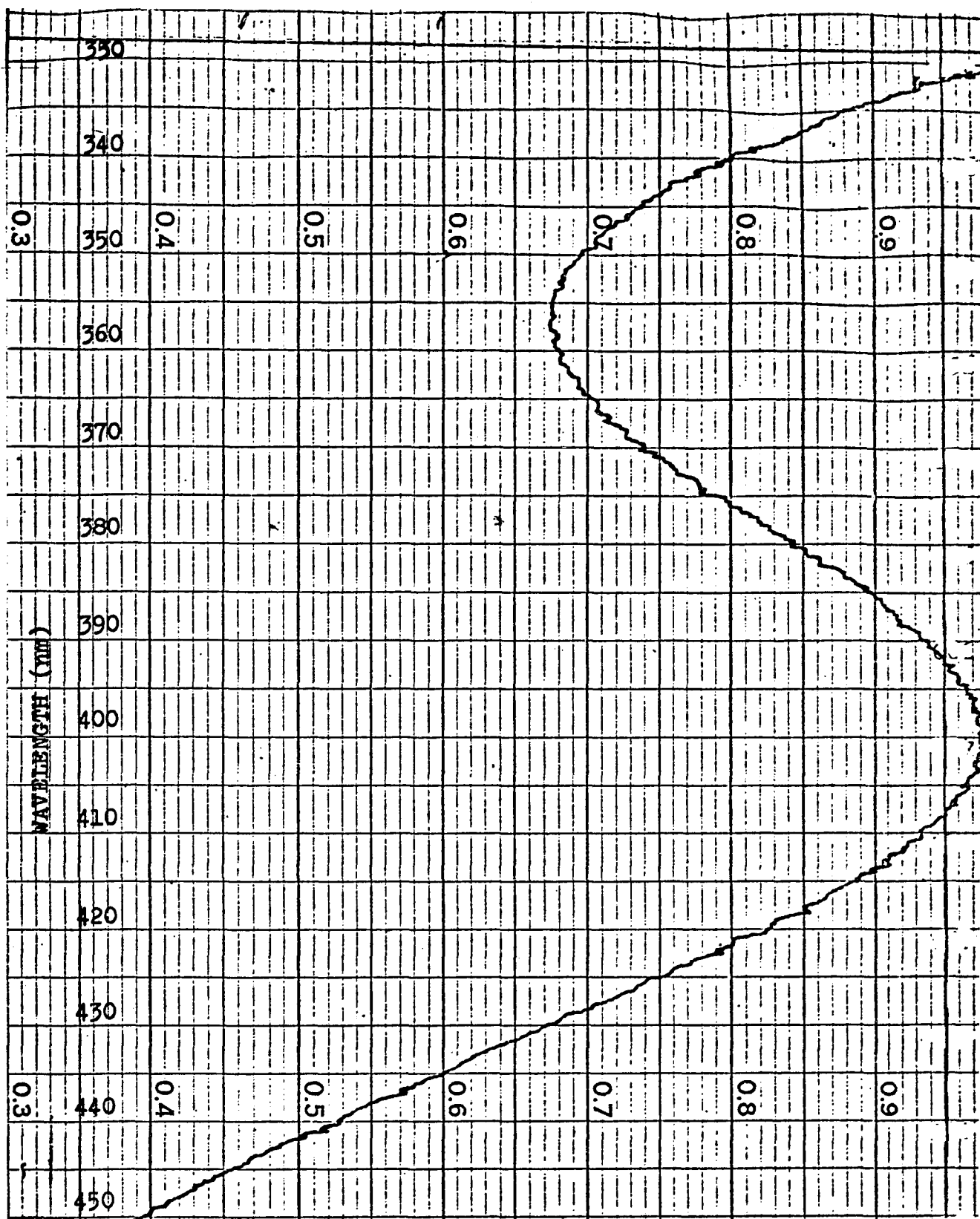
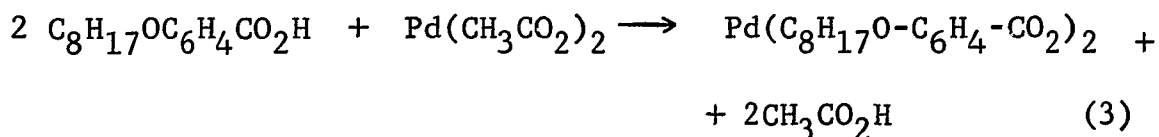


Figure 3. Ultraviolet spectrum of Pd-acetate in dioxane

a small amount of the desired yellowish product. The procedure was modified subsequently, with the reaction mixture heated in an oil bath maintained at 90-95°C, and the benzene-acetic acid mixture distilled off by using an adjustable reflux ratio take-off head. In a typical experiment 0.1291 g (5.753×10^{-4} moles) of $\text{Pd}(\text{ac})_2$, 0.1859 g (1.5238×10^{-3} moles) benzoic acid in 10 ml. of benzene were used. The weight of the crude product was estimated as 50 mg. or ca. 25% yield. The crude product melted over a broad range 210-220°(d), literature¹⁹ mp220°(d). The IR spectrum (Fig. 4) indicated that the correct product was formed in this reaction. IR bands in Nujol at 1570 (asym. C=O str.), 1410 (sym. C=O str.), 710 (C-H out-of-plane of aromatic, monosubstituted); literature IR¹⁹ 1567, 1404 cm^{-1} .

Preparation of Palladium (II) p-Octyloxy Benzoate.

The compound was prepared, using the modification described



above in the preparation of Pd-benzoate, maintaining the oil bath temperature at 94-97°C. In a typical experiment 0.5773g(2.573×10^{-3} moles) palladium acetate, 2.0268 g

TRANSMITTANCE (PERCENT)

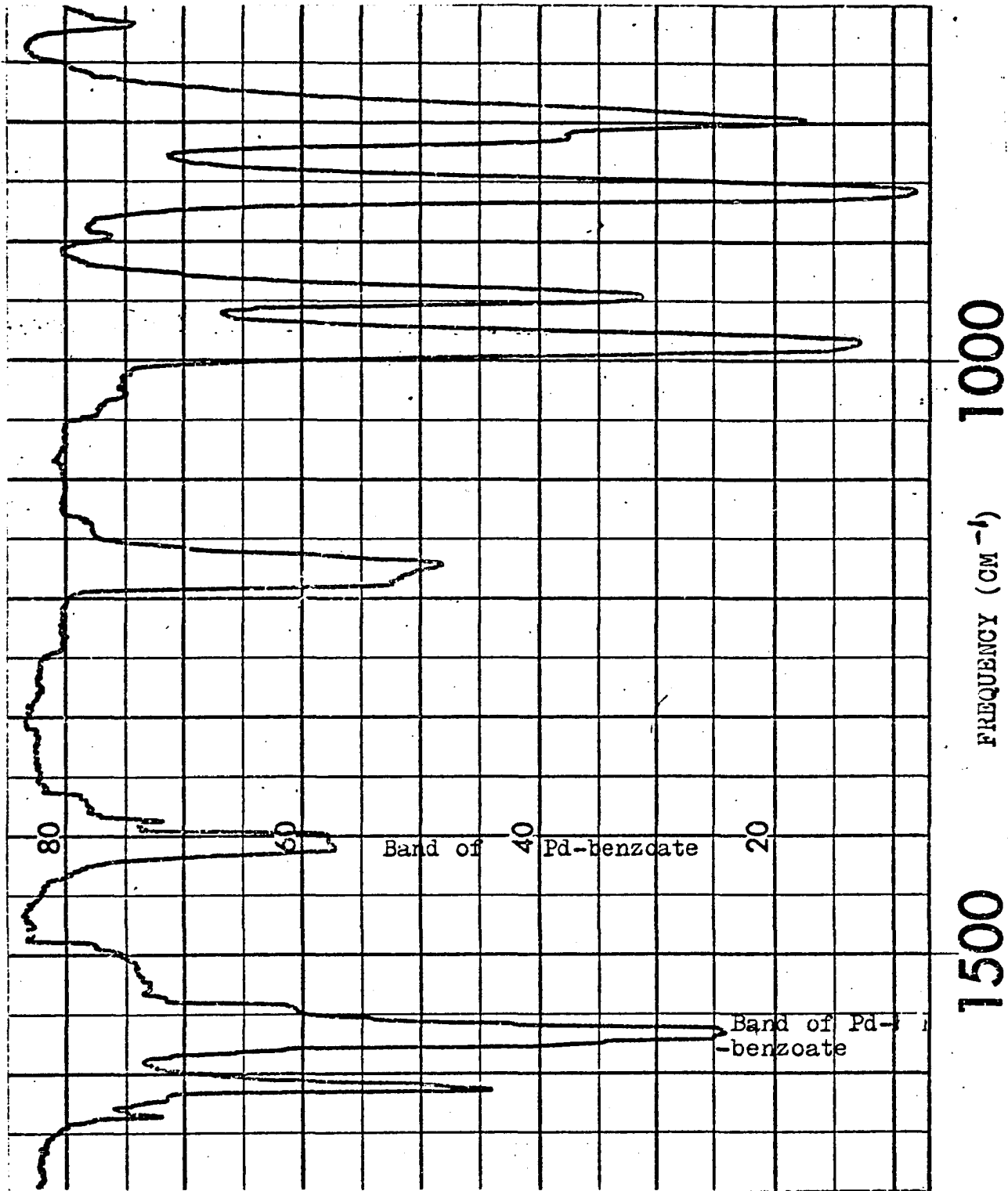


Figure 4. Infrared Spectrum of Pd-benzoate (HCBd mull)

(8.107×10^{-3} moles) of p-octyloxy benzoic acid, and 20 ml. of benzene were used. The reflux ratio was maintained between 3:1 and 5:1; the mixture was refluxed for 3 hours; then the benzene-acetic acid mixture was allowed to distill off very slowly, over a period of 2 hours. The residue was triturated with cold ligroin. A mixture of black and grayish-white residue remained, assumed to be unreacted octyloxy b.a. contaminated with palladium black. The grayish residue was separated from the Pd black, and it weighed 1.0772 g. Attempts to purify the product of this reaction by tlc were unsuccessful. Trials to sublime the excess unreacted octyloxy b.a., as well as trials to crystallize the Pd-(octyloxy)-benzoate by freezing a CHCl_3 solution, were also unsuccessful.

From elemental analysis results, it is possible to estimate that the product contains 86.5% Pd-(octyloxy)-benzoate, 12.3% Pd-acetate, and 1.2% Pd. The crude product was obtained by evaporation of the ligroin solution and weighed 1.1971g. Correcting this weight for 86.5% of product, estimates the yield at 1.035 g (90%, based on the 0.9496g or 3.798×10^{-3} moles of octyloxy b.a. that reacted.) The product is a blackish-brown, glassy, non-crystalline material. DTA and DSC show an endotherm at minus 34° . (Fig. 5, Fig. 6). Product identification based on IR

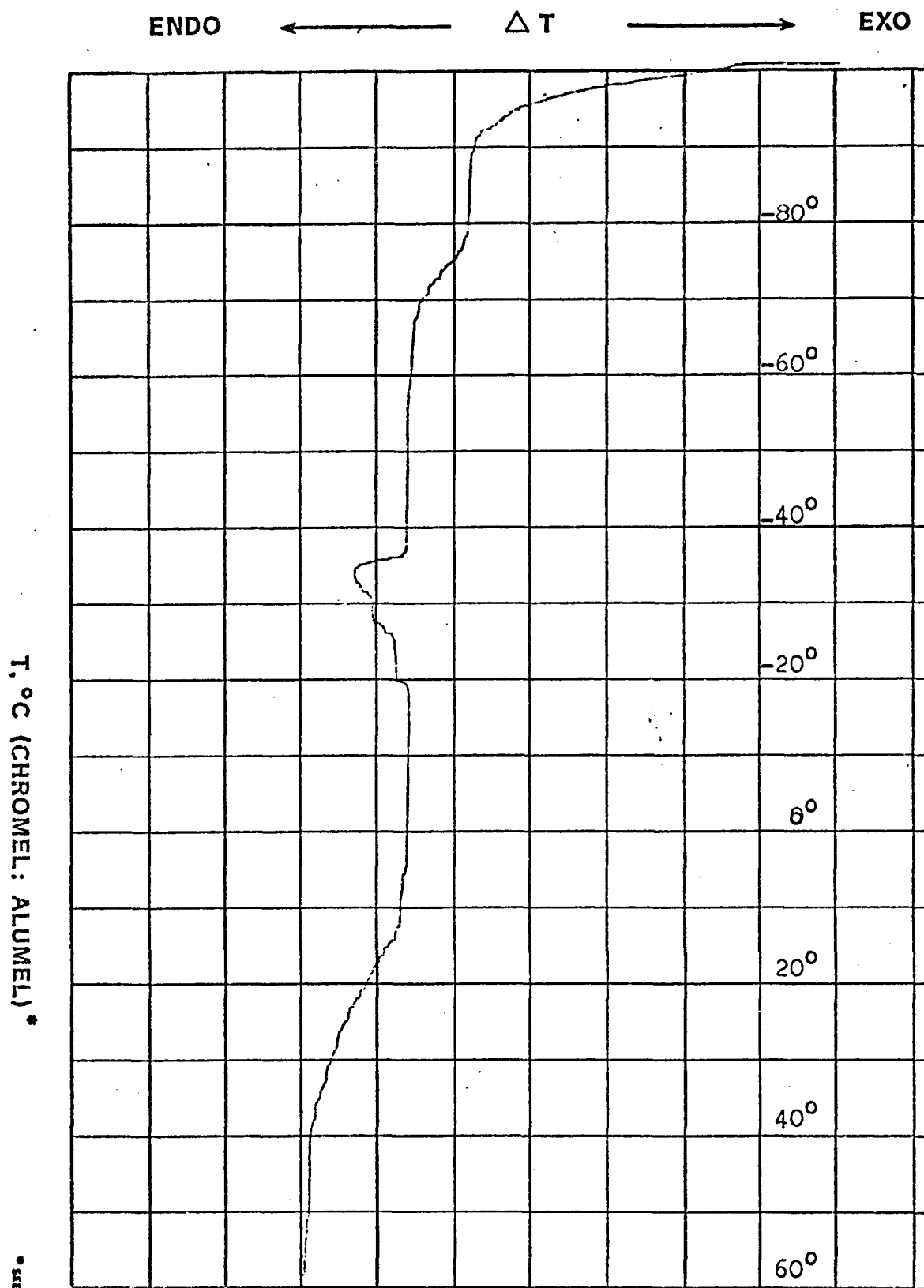


Figure 5. DTA thermogram of Pd-(p-octyloxy)-benzoate, showing endotherm at -34°C

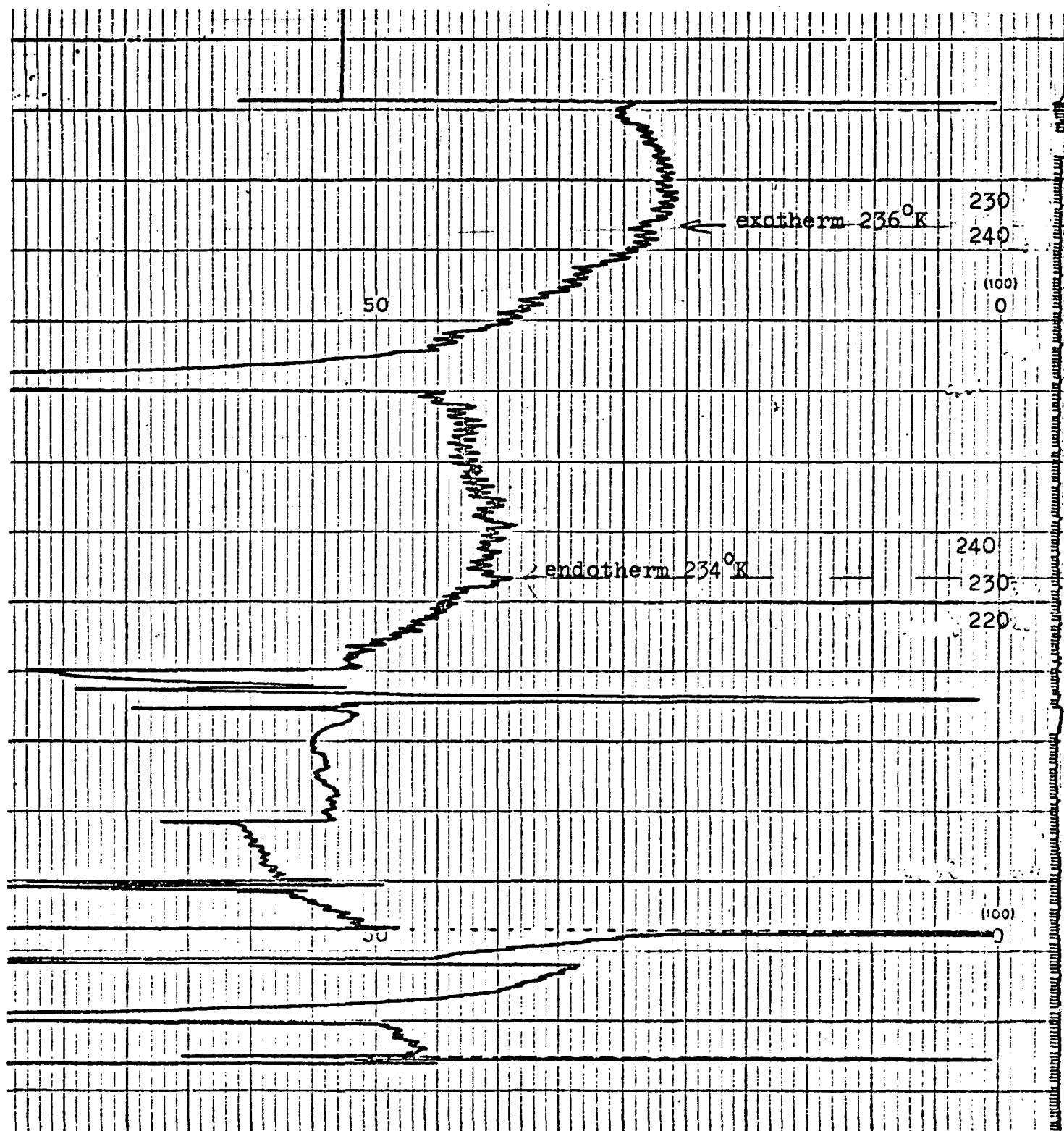


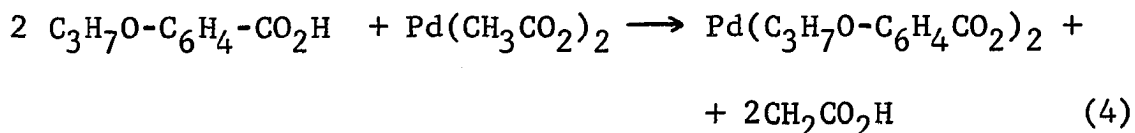
Figure 6. DSC thermogram of Pd-(p-octyloxy)-benzoate, showing an exotherm at 236°K (-37°C) on top and an endotherm at 234°K (-39°C) on bottom

(Fig. 7) (Nujol or C_4Cl_6): 1400s (C=O sym. str.)

UV (dioxane or benzene); λ_{max} (broad) 330-380 nm, ϵ_{max} (weak) 225 nm, characteristic minimum 240 nm; (Fig. 8).

Elemental Analysis: Calcd. for $PdC_{30}H_{42}O_6$: C, 59.5; H, 7.0; Pd, 17.6%; Found: C, 54.6; H, 6.38; Pd, 22.68%

Preparation of Palladium(II)-p-Propoxy Benzoate.



The procedure used was as outlined before, except that the reaction mixture was maintained under a stream of dry nitrogen gas and at room temperature, to minimize the rate of decomposition of the product. In the preparation 0.3908 g (1.77×10^{-3} moles) palladium acetate, 1.633g (9.04×10^{-3} moles) of propoxy b.a. in 30 ml. of benzene, previously dried over molecular sieves and degassed under nitrogen, were used. The reaction mixture was stirred magnetically for 20 hours under a gentle stream of nitrogen, in the absence of air. Most of the solvent had evaporated by that time, and the reaction mixture was brown, with a minimum of black decomposition product.

The residue was triturated with small portions of dried ligroin, in order to dissolve any unreacted Pd-acetate. Aliquots were taken and analyzed by UV. After 6 triturations,

TRANSMITTANCE (PERCENT)

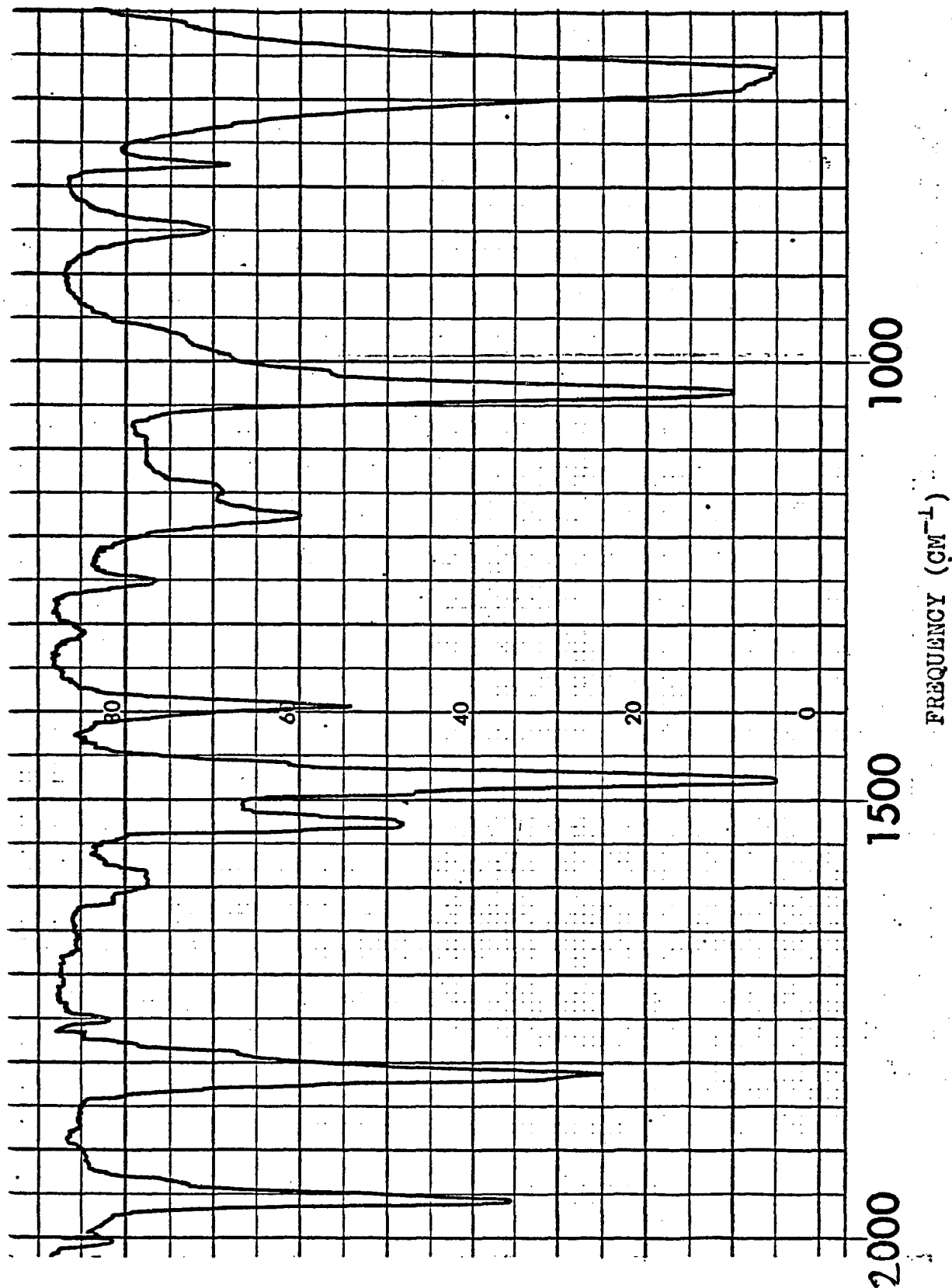


Figure 7. IR spectrum of Pd(p-octyloxy)-benzoate (C₆H₆ soln.)

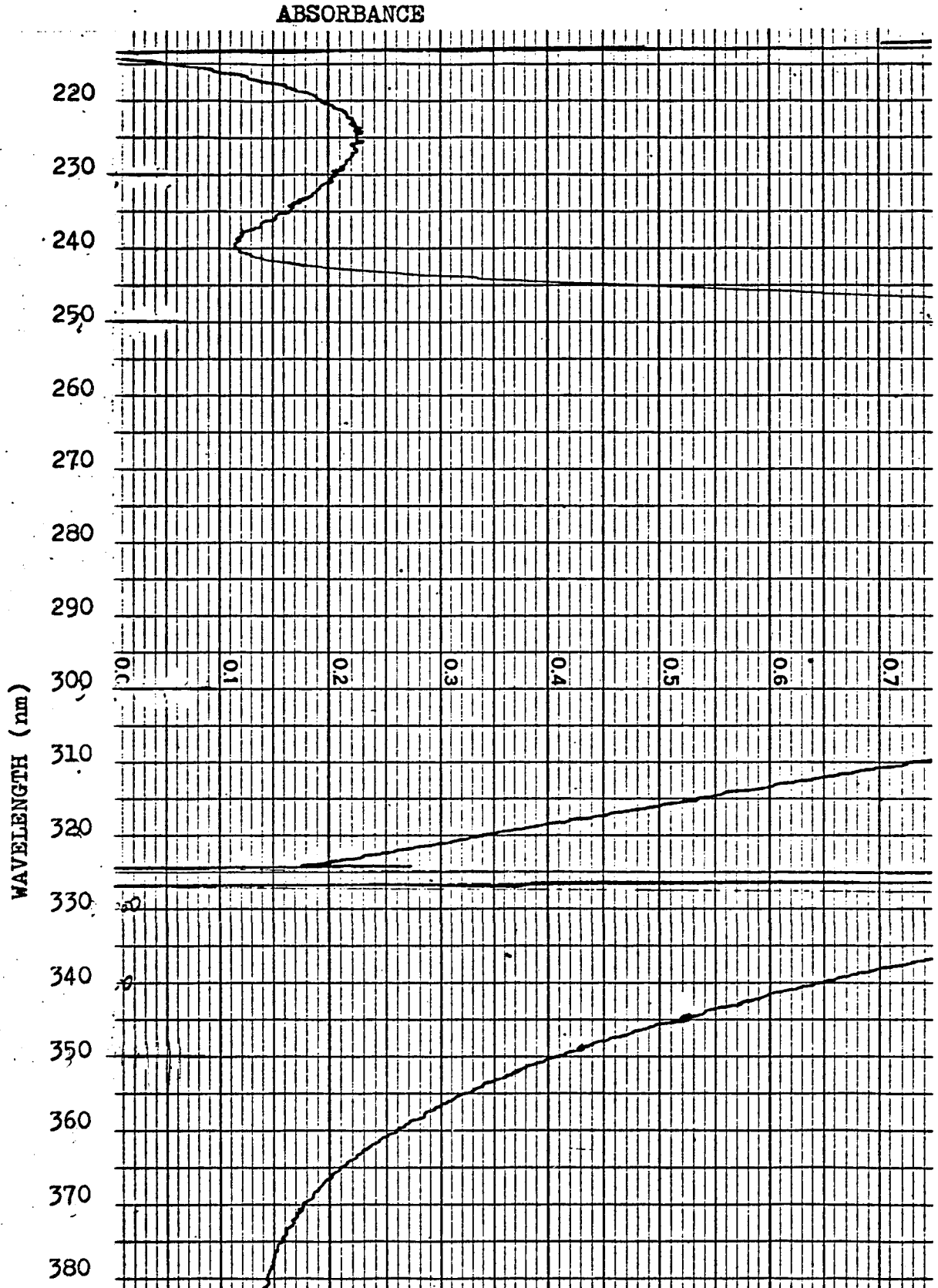


Figure 8. Ultraviolet spectrum of Pd(p-octyloxy)-benzoate in dioxane

the last ligroin solution was no longer colored, and its UV spectrum indicated absence of Pd-acetate. The solid residue was now triturated with dried benzene, yielding a dark brown solution and a grayish residue. The residue was washed, dried, and identified as 0.9096 g of unreacted propoxy benzoic acid.

Further purification of the Pd-(propoxy)benzoate involved a series of successive precipitations of the residual unreacted propoxy b.a. from a mixture of ca. 2:1 (by volume) of benzene and ligroin, which caused the propoxy b.a. to precipitate. If no precipitate appeared on cooling in ice, then the volume of the solution was reduced to one-half by evaporation under a gentle stream of nitrogen gas. The brownish-black supernatant was separated from the grayish precipitate after centrifuging, and the treatment of the solution was repeated by addition of further small portions of ligroin.

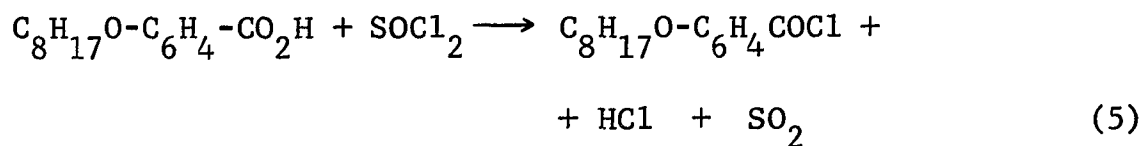
At various intermediate stages the solid material, obtained by total evaporation of solvents, was analyzed by DTA for the presence of traces of propoxy b.a. Generally, 4 to 6 successive "precipitations" by ligroin were sufficient to purify the product within the criteria used for purity checks. IR spectra were obtained on C_4Cl_6 (hexachlorobutadiene)

mulls as a further test for purity or absence of propoxy b.a. (absence of absorption at 1675 cm^{-1}). UV spectra were used to distinguish the Pd-(propoxy)-benzoate from Pd-acetate, and to determine when the product was free of Pd-acetate.

The yield of pooled solid fractions of Pd-(propoxy)-benzoate was estimated as 400 mg (ca. 50% yield). DTA (Fig. 11) showed an endotherm near 50°C , presumed to be the melting point of the solid dark brown compound which appeared non-crystalline (glassy). From elemental analysis it is possible to estimate that the product contains 89% of Pd-(propoxy)-benzoate, 6.7% of Pd-acetate, and 4.3% Pd.

The IR spectrum (Fig. 9) shows the characteristic bands at 1390 (asym. C=O str.) and 1250 cm^{-1} (C-O str.). Fig. 10 shows the UV spectrum with a broad λ_{max} at 270 nm . Elemental analysis: Calcd. for $\text{PdC}_{20}\text{H}_{22}\text{O}_6$: C, 51.7; H, 4.77; Pd, 22.85%. Found: C, 47.84; H, 4.61; Pd, 27.77%

Preparation of p-Octyloxy Benzoyl Chloride.



In a typical experiment 30.0 g (0.13 moles) of p-octyloxy b.a. were mixed with 24.0 ml. (39.8g or 0.335 moles) of thionyl chloride, and the mixture refluxed gently on a steam bath for $4\frac{1}{2}$ hours. The excess unreacted SOCl_2 was

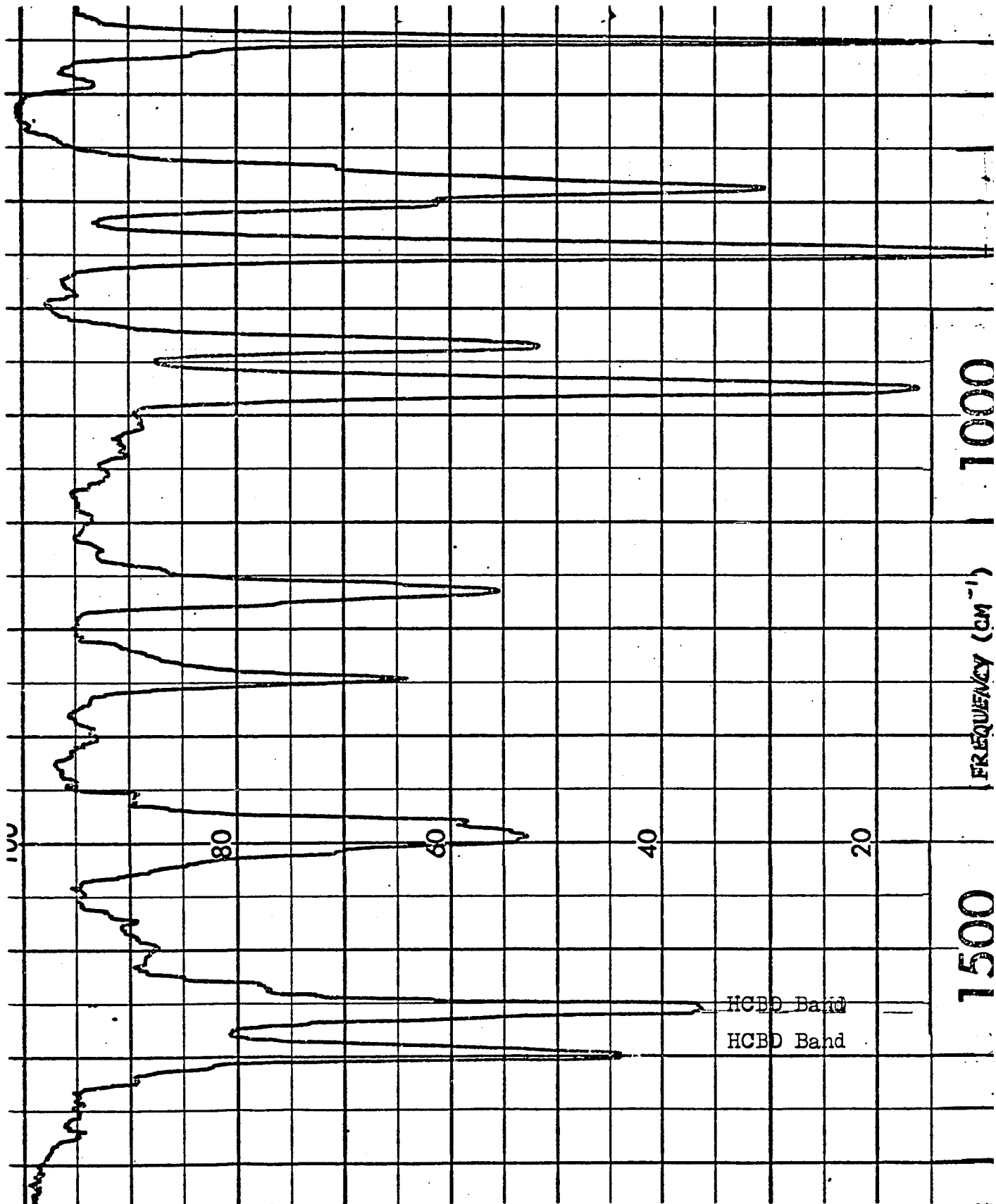


Figure 9. Infrared Spectrum of Pd-(p-propoxy)-benzoate (HCBD mull)

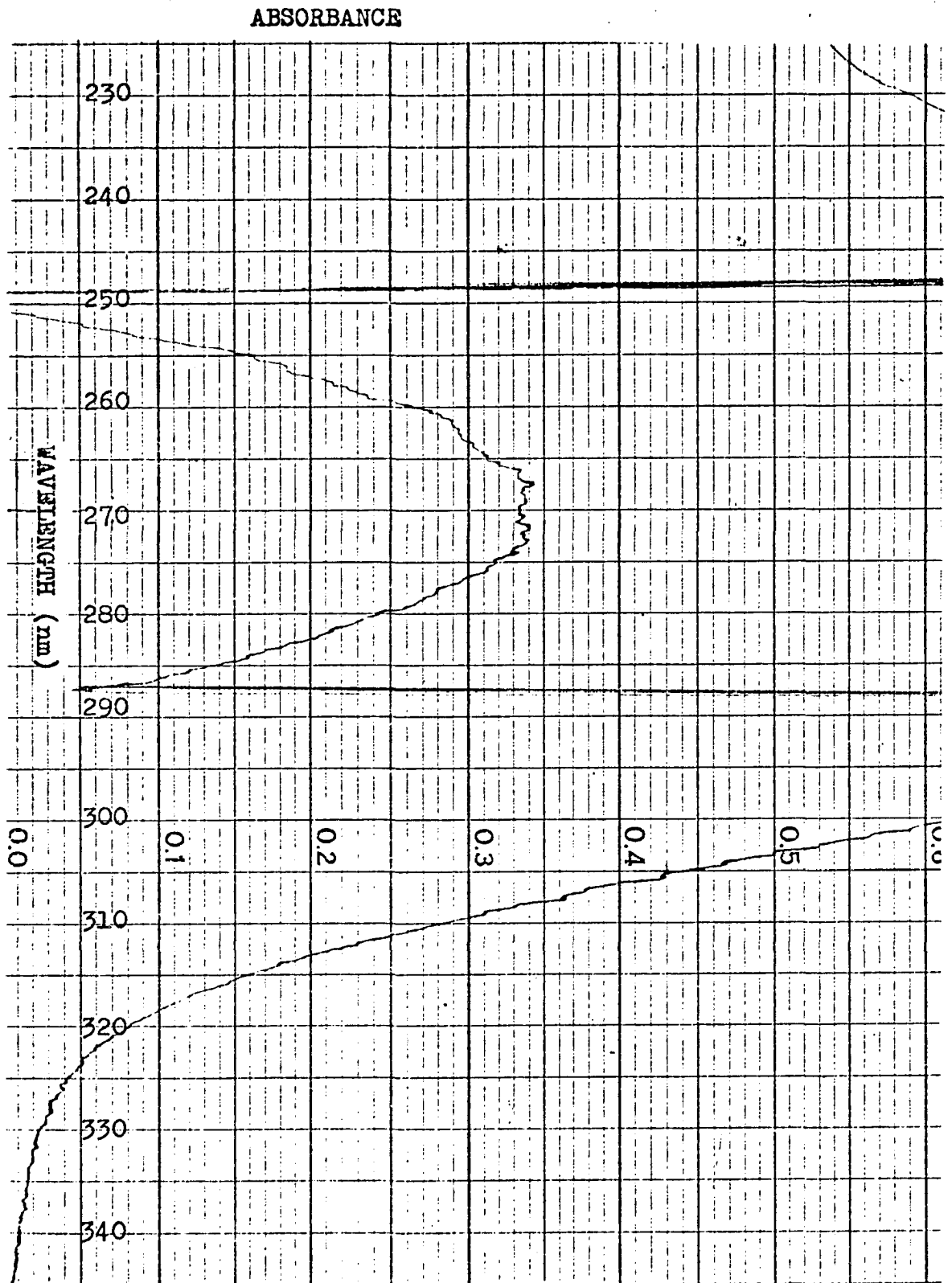


Figure 10. Ultraviolet spectrum of Pd(p-propoxy)-benzoate in dioxane

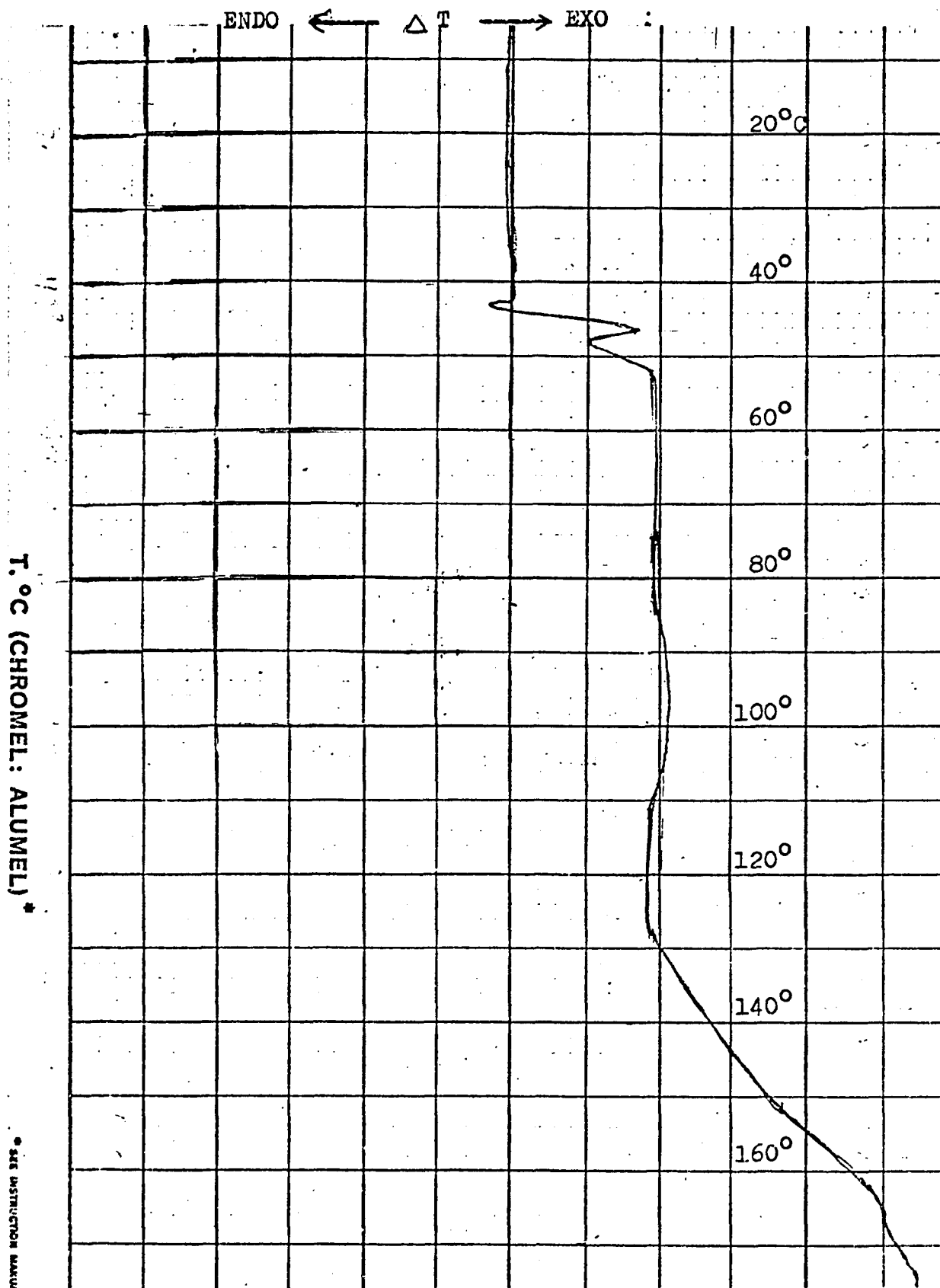


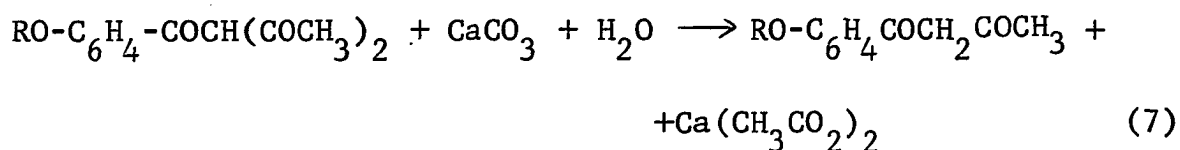
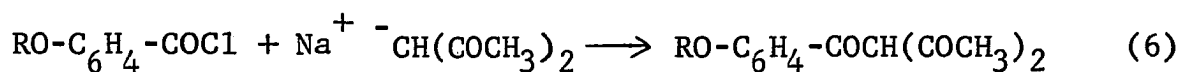
Figure 11. DTA Thermogram of Pd-(p-propoxy)-benzoate

removed by co-distilling it with several portions of added benzene, under a water aspirator vacuum, with the system protected from moisture by a CaCl_2 -packed drying tube. Three successive portions of 12-15 ml. of dried benzene were used in this initial purification. The remaining liquid was freed of any other low boiling materials by vigorous pumping for at least one hour after all visible bubbling had ceased. The crude product weighed 32.2 g (84.5% yield).

The aroyl chloride was purified by vacuum distillation, with the use of a tip-up McLeod gauge to determine its vapor pressure curve. It boiled at 146-148° at a pressure of 0.60 torr, and at 169-171° at 1.95 to 2.00 torr. These vapor pressure values were consistent with those reported for a series of other p-alkoxy-benzoyl chlorides prepared by McElvain, et al,²³ and by Pierce et al²⁴. Using the data in the literature, and applying the Hass-Newton equation, it can be calculated that this aroyl chloride should boil at 335° under 760 torr (see Appendix I). The yield of the purified acid chloride was 27.0 g (69.5% based on purified fraction), and it was a colorless liquid. No elemental analysis was obtained on this product, since its preparation involved a fairly straightforward and well-known reaction. The purified aroyl chloride was used in subsequent synthesis.

Preparation of (p-Octyloxy)-1-Phenyl-1,3-Butanedione.

This compound, which is also referred to as p-octyloxy-bzac or "ligand" was prepared by following the general procedure used by Sabnis et al²⁵ for the preparation of p-methoxy-bzac.



Whereas in Sabnis' case the R-group was CH₃, in this preparation the R- group was C₈H₁₇⁻. In a typical experiment 14.0 g of acetylacetone(acac) (0.14 moles) were converted to the sodium salt by stirring for 16 hours at room temperature with 3.9 g (8.4 x 10⁻² moles) of sodium hydroxide flakes in 75 ml. of dried benzene, under a reflux condenser equipped with a drying tube. To this mixture was slowly added a solution of 22.5 g (8.4 x 10⁻² moles) of the p-octyloxy-benzoyl chloride in 25 ml. of dried benzene, and gentle stirring was continued for another 18 hours.

The mixture was freed of solid inorganic materials by filtration, and the filtrate concentrated under reduced pressure. A pasty mass resulted, which was then warmed for 30 minutes with an aqueous suspension of calcium carbonate

(5.0 g or 0.05 moles in 25 ml. of water). The mixture was cooled, and subsequently extracted with several (5 or 6) 25 ml. portions of ether. The pooled ether extracts were yellow. They were dried overnight over anhydrous magnesium sulfate. The ether was then evaporated on a rotary evaporator under reduced pressure. The residue was an oily material, weighing 16.4g, with a yield of 67% based on the aroyl chloride used. In a similar preparation of p-methoxy-bzac, Sabnis²⁵ had reported a yield of 74%; Andrievskii et al²⁶ used an alternate method to prepare the p-methoxy-bzac and reported a yield of only 30%.

Initial attempts to purify our "ligand" by vacuum distillation, indicated that it is very high boiling (188^o at .70 torr). Attempts to vacuum distill produced a great deal of tarry brown materials and only a small amount of waxy yellow material that solidified inside the condenser. When impure, the "ligand" tends to form oils that resist crystallization. The best procedure for purification turned out to be alternate crystallizations from ethanol and carbon tetrachloride. The most persistent contaminant is the p-octyloxy b.a., apparently formed from some hydrolysis of the aroyl chloride. Since the acid is only sparingly soluble in CCl₄, the latter promotes the

separation of the product from the acid. When the ethanol solution is relatively free of the acid, chances for the "ligand" to crystallize are much improved. The pure ligand melts at 54-56°C, and is a yellowish white solid.

On a trial basis the "ligand" was prepared from the crude residue of p-octyloxy benzoyl chloride. Using 4.5g (0.0168 moles) of the aroyl chloride which had been filtered through glass wool, and 2.5 ml (2.62 g or 0.0262 moles) of acac, 0.68 g (0.0168 moles) of NaOH flakes and 15 ml. of benzene, a fairly good yield of 54% of the product was obtained. This suggests that one might omit the distillation of the aroyl chloride prior to its use in the condensation step in Reaction 6.

The following were used in the identification of "ligand". The infrared spectrum (Fig. 12) shows the characteristic 1630 cm^{-1} absorption due to C=O stretch, 1570m (aromatic ring), 1530m (C=C ring str, arom.), 1200m (C-CH₃ str. + C=C str), 1210m (C-H bend + C=O str.), 1065 w(arom. C-H in plane bend), 835m (arom. C-H out-of-plane bend, 2 adjacent H on ring), 790s (C-CH₃ str.) 475s (\emptyset ring in plane def); Fig. 13, the NMR (in CCl₄ or CDCl₃): δ 7.95, 7.75; 7.0, 6.95 (two d, 4H, aromatic), 6.10(s, 1H, CH=COH), 4.03 (t, 2H, CH₂O), 2.26, 2.15

Figure 12

Infrared spectrum of ligand.
Nujol bands are indicated by N

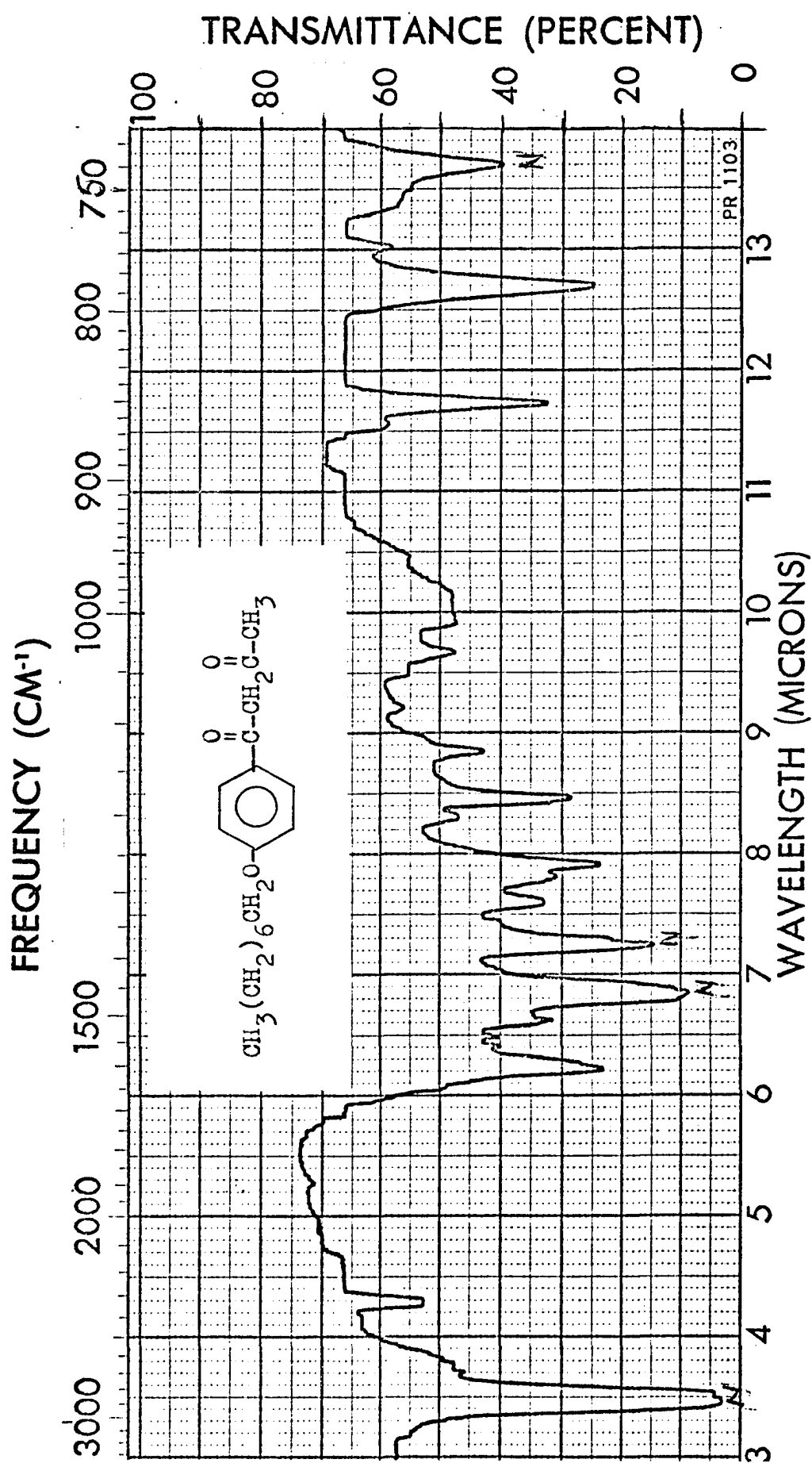


Figure 12

Figure 13

¹H-NMR spectrum of ligand in CDCl₃

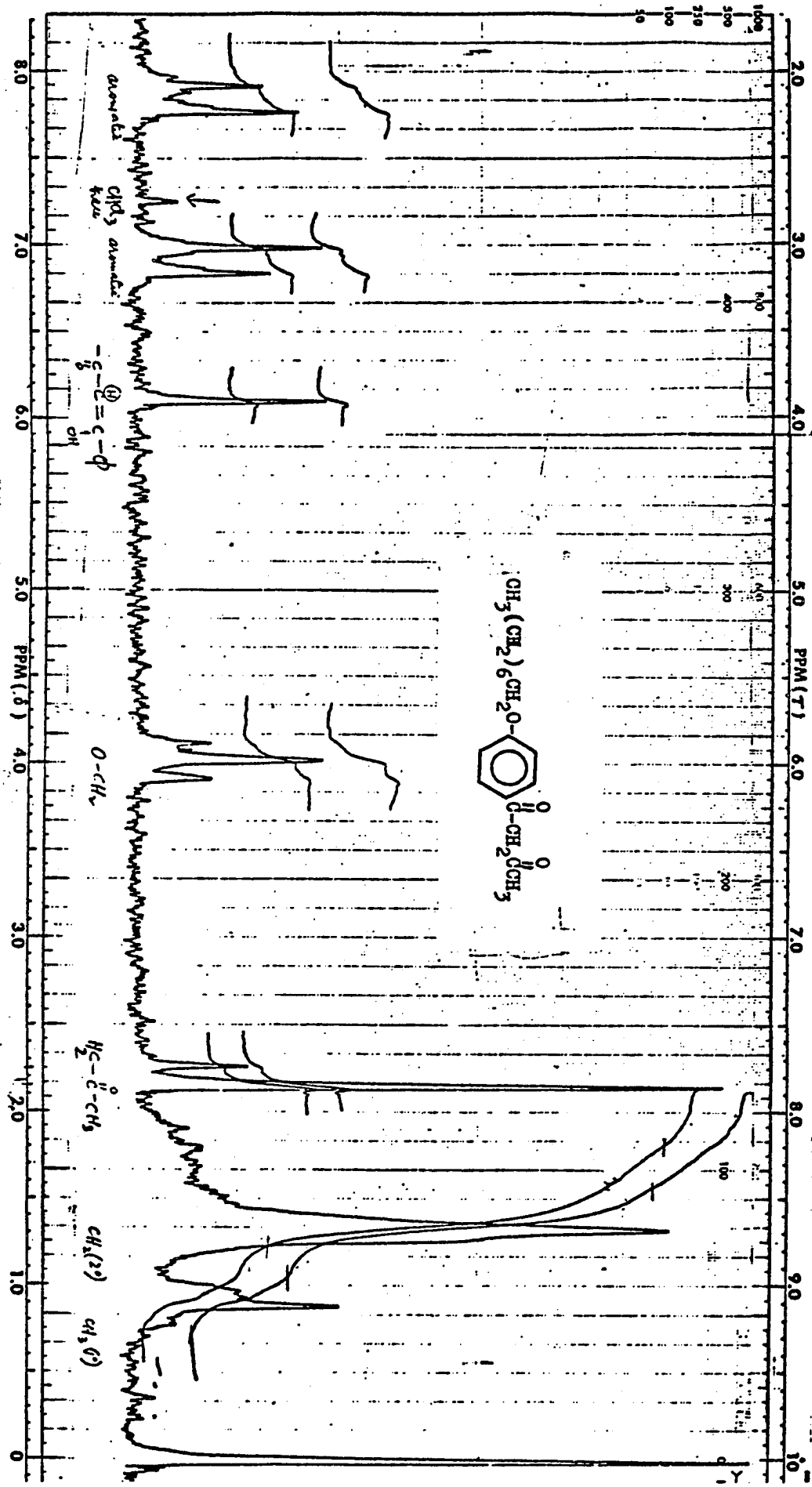
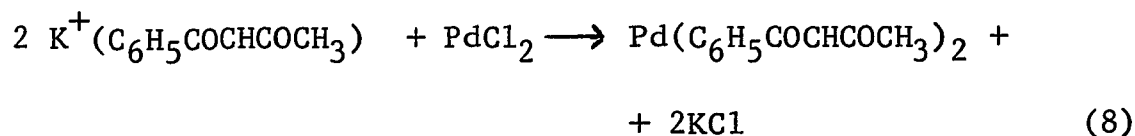


Figure 13

(d, 4H, $\text{CH}_3\text{C}=\text{OCH}$), 1.33 m, 12H, $\text{CH}_3(\text{CH}_2)_6\text{CH}_2\text{O}$, 0.90
 (t, broad, 3H, CH_3CH_2 --). The mass spectrum (Fig. 14)
 yields a molecular weight 290; calculated for
 $\text{C}_{18}\text{H}_{26}\text{O}_3$: 290. The mass spectrum is consistent with
 the structure assigned, as detailed in Table I. Fig. 15
 shows the UV spectrum in CH_2Cl_2 : λ_{max} 320 nm, molar
 absorptivity $\epsilon=35,000$; Elemental analysis: Calcd. for
 $\text{C}_{18}\text{H}_{26}\text{O}_3$: C, 74.45; H, 9.0%
 Found: C, 74.26, 74.49; H, 9.23, 9.23%

Preparation of bis-[(1-Phenyl-1,3-Butanedionato)]

Palladium (II). This compound, also referred to as $\text{Pd}(\text{bzac})_2$,
 was prepared by two slightly different procedures, one of
 them outlined by Hon et al,²⁰ and by Carmichael.²⁷



In one experiment a solution of 5 ml. of ethanol, containing
 0.5140 g (3.16×10^{-3} moles) of 1-phenyl-1,3-butanedione
 (or bzac), previously recrystallized from ethanol, was made
 slightly alkaline by the addition of several drops of an
 ethanolic solution of potassium hydroxide.

Figure 14
Mass spectrum of ligand

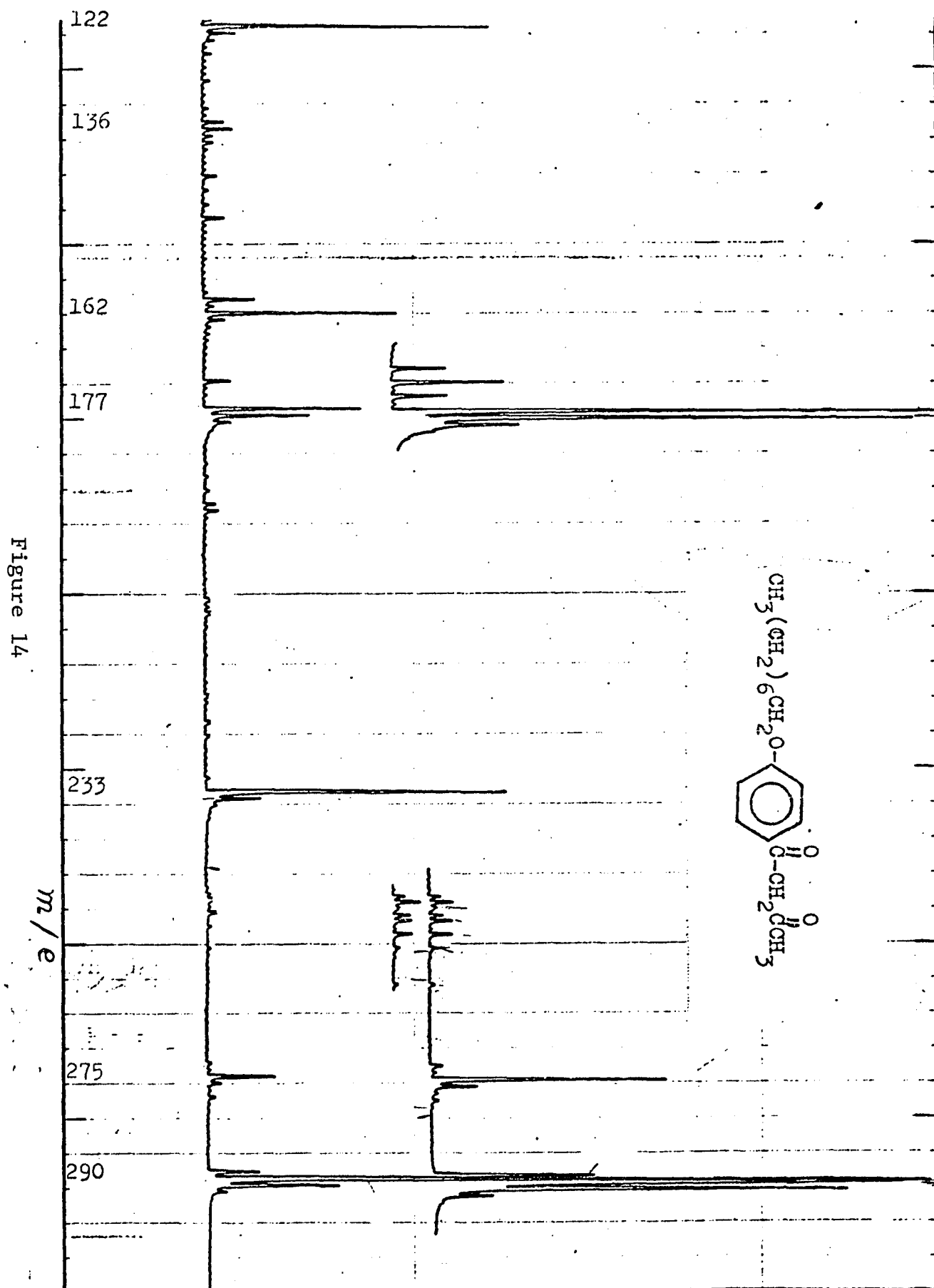


TABLE I
SUMMARY OF MASS SPECTRA INTERPRETATION (LIGAND)

Condensed Structural Formula of Possible Ion Fragment	Empirical Formula	Theoretical Mass Value	Mass Value Observed in Spectrum
$C_8H_{17}OC_6H_4COCH_2CO$	$C_{17}H_{23}O_3$	275	275
$C_8H_{17}OC_6H_4CO$	$C_{15}H_{21}O_2$	233	233
$C_4H_9OC_6H_4COCH_2COCH_3$	$C_{14}H_{18}O_3$	233	233
$OC_6H_4COCH_2COCH_3$	$C_{10}H_9O_3$	177	177
$C_6H_4COCH_2COCH_3$	$C_{10}H_9O_2$	161	161
$OC_6H_4COCH_2O$	$C_8H_6O_3$	162	162
$OC_6H_4COCH_2$	$C_8H_6O_2$	136	136
OC_6H_4CO	$C_7H_4O_2$	122	122

Figure 15

Ultraviolet spectrum of
ligand in CH_2Cl_2 ,
concentration $1.543 \times 10^{-5} \text{M}$

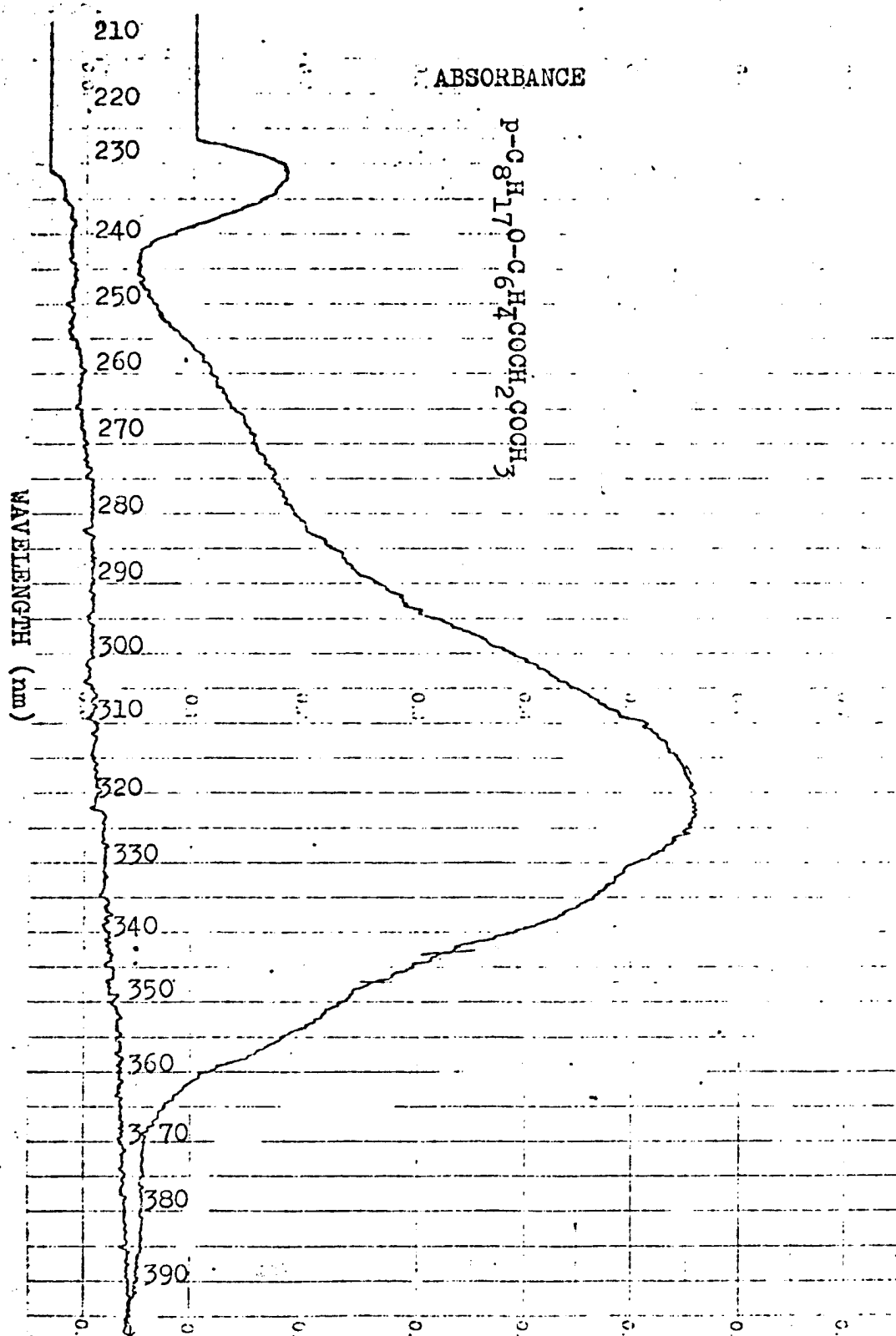


Figure 15

To this was added a suspension of 0.1450 g (8.2×10^{-4} moles) of palladous chloride in 1 ml. of water. The mixture was stirred at room temperature for $2\frac{1}{2}$ hours. The grayish-green product was filtered, washed twice with small portions of cold ethanol, and three times with cold water. Attempts to recrystallize this material from either CH_2Cl_2 , as suggested by Carmichael²⁷ or from CHCl_3 used by Hon²⁰, were not very successful. Recrystallizations yielded material that still had brownish or greenish contaminants, due probably to the decomposition of this material when it was warmed in the recrystallization solvent. The best purification procedure that was developed, involved dissolving the material in a minimum amount of CHCl_3 at room temperature, filtering away any insoluble Pd solids and PdCl_2 , then adding cold ethanol to the CHCl_3 solution to cause the precipitation of the organo-palladium complex. The yield, based on 0.1860 g of crude product, was 54%.

In the variation of that procedure the bzac was dissolved in an ethanolic solution containing a weight of KOH stoichiometrically equivalent to the weight of PdCl_2 used, with the bzac present in large excess. This time the reaction mixture was stirred at slightly elevated temperatures (40 to 50°C), but it was kept well below 60°C where

Grinberg and Simonova²⁸ noted decomposition of the Pd- β -diketonate they prepared, i.e. Pd(acac)₂. In this latter experiment 0.7100g (4.011×10^{-3} moles) of PdCl₂, an ethanolic solution containing 0.455 g KOH (8.110×10^{-3} moles), and 2.4820 g (15.2426×10^{-3} moles) of bzac in 55 ml of absolute ethanol were used. The flask was covered with aluminum foil, because the complex is light sensitive when in solution. The crude solid, obtained after 2 hours, was filtered, washed with ethanol and water, then air dried. It weighed 1.4320 g, representing a yield of 83.3%, based on the PdCl₂ used. Unreacted bzac was recovered in several fractions from the mother liquor by partial evaporation. A total of 0.74 g or 60% of the excess bzac used was recovered.

The product identification was based on IR spectrum (Fig. 16), which showed absorbances at 1590 (C=O str.), 1560sh(Ph ring stretch), 1540, 1520 (C=C coupled to Ph ring), 1480 (Ph ring str.), 790 cm^{-1} (C-CH₃ stretch), 710 cm^{-1} (C-H out-of-plane, monosubstituted arom.). The ultra-violet spectrum of Pd(bzac)₂ is shown in Fig. 17, and the λ_{max} values are listed here, with molar absorptivity ϵ_{max} given in parenthesis: 260 nm (35,950), 285 nm (29,520), 352 nm (19,670). The UV spectrum is in general agreement

Figure 16

Infrared spectrum of $\text{Pd}(\text{bzac})_2$.
Nujol bands are indicated by N

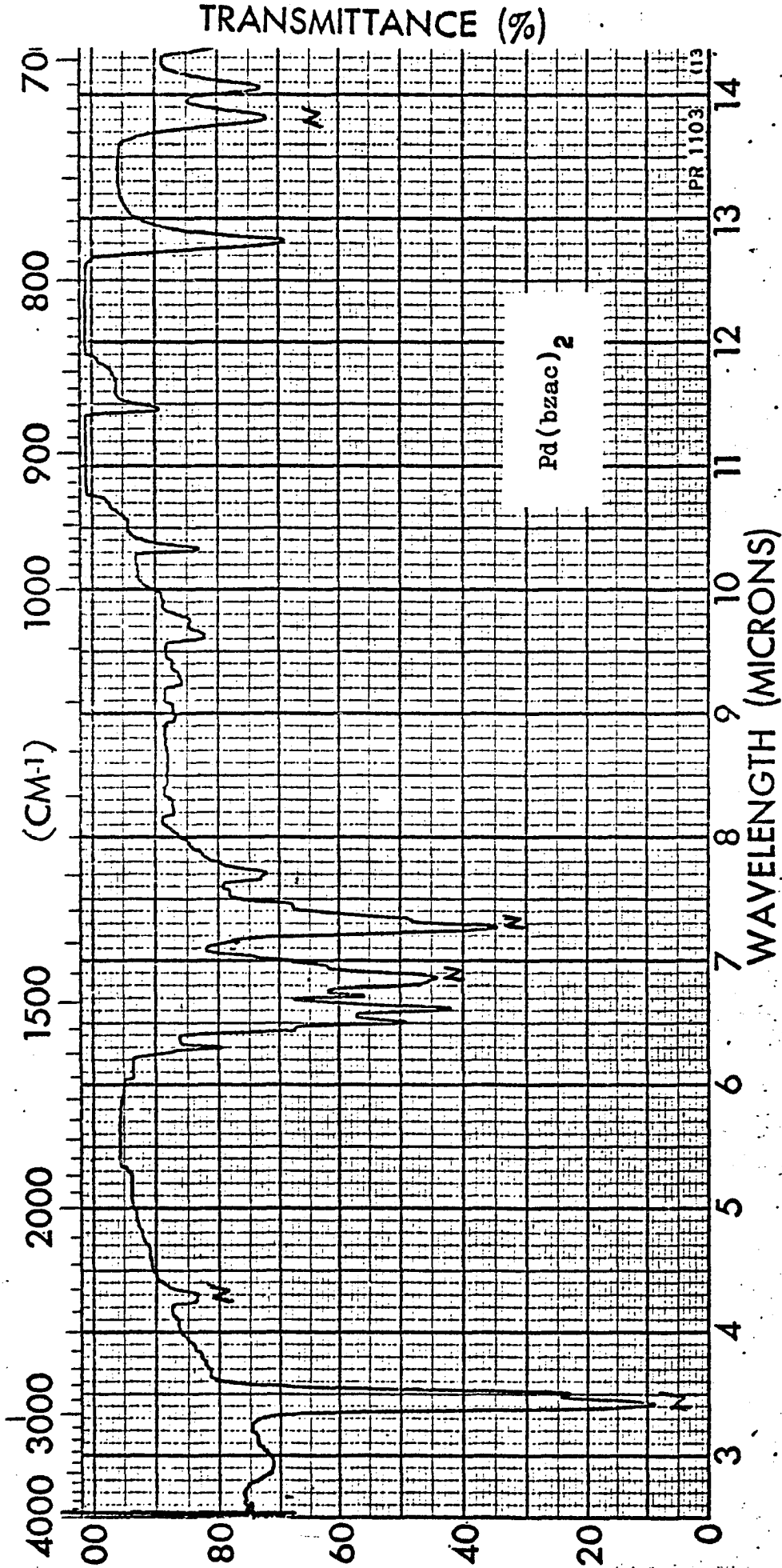


Figure 16

Figure 17

Ultraviolet spectrum of Pd(bzac)₂ in CHCl₃,
concentration $2.10 \times 10^{-5} \text{M}$

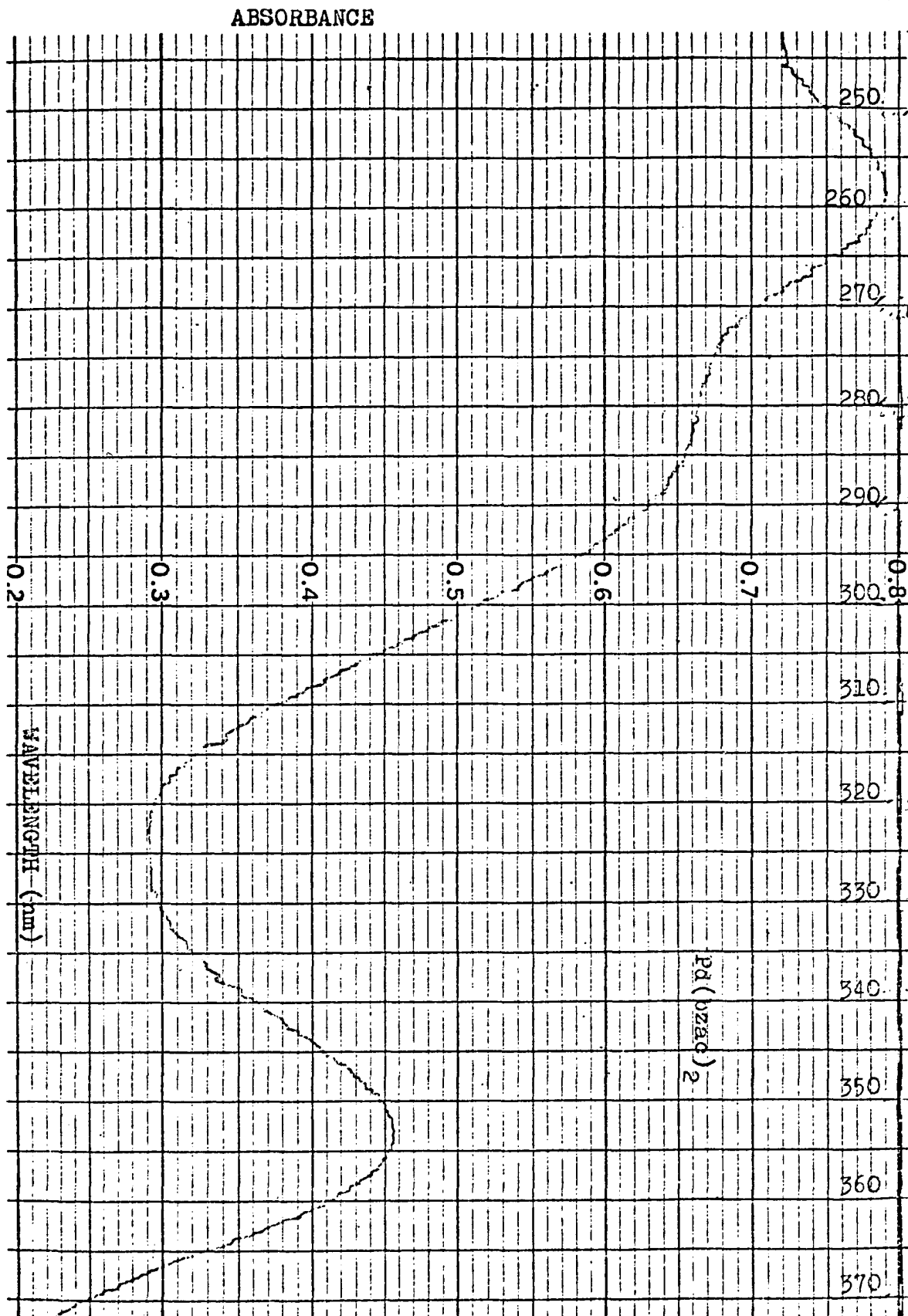


Figure 17

Figure 18

$^1\text{H-NMR}$ spectrum of $\text{Pd}(\text{bzac})_2$ in CDCl_3

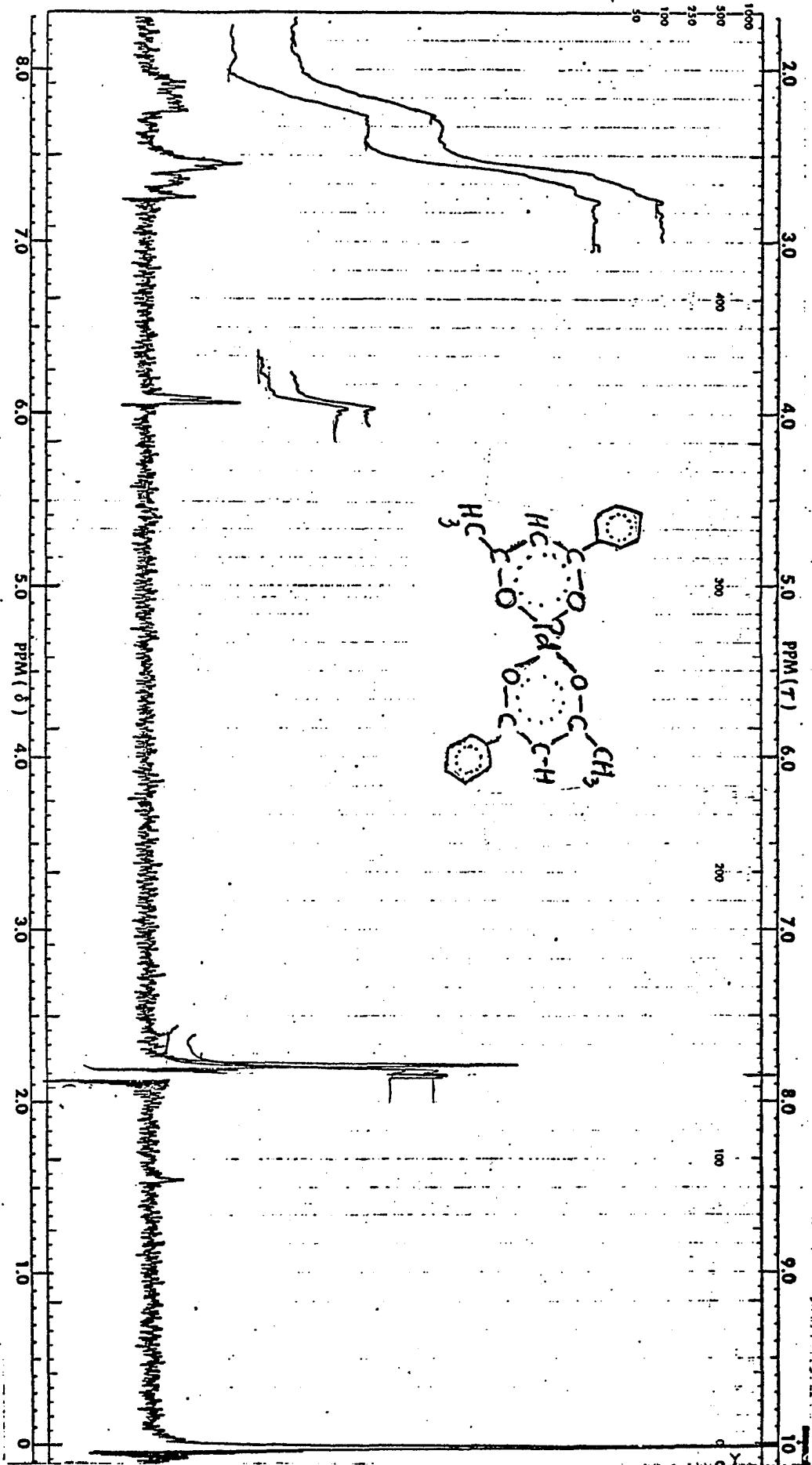
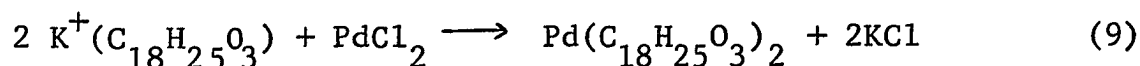


Figure 18

with that reported for Pd(bzac)₂ by Singh and Sahai.²⁹

The NMR spectrum of Pd(bzac)₂ is shown in Fig. 18. The δ values of each signal are listed here: 7.95, 7.75, (broad d, 2H, aromatic), 7.45 to 7.25 (m, 3H, aromatic), 6.05 (s, 1H, $\underline{\text{C}}\underline{\text{H}}=\text{CO}$), 2.11 (s, 4H, $\underline{\text{C}}\underline{\text{H}}_3\text{-CO-}\underline{\text{C}}\underline{\text{H}}$).
 Elemental analysis: Calcd. for PdC₂₀H₁₈O₄: C, 55.99; H, 4.23; Pd, 24.81%. Found: C, 55.64; H, 4.10; Pd, 24.32%
 Molecular weight calculated for PdC₂₀H₁₈O₄ 428.76; found osmometrically (in 1.143% wt/wt or ca. 0.027 molal solution in benzene) 417.

Preparation of bis-[(p-Octyloxy)-1-Phenyl-1,3-Butanedionato]-Palladium(II). This compound, also referred to as PdL₂ or Pd(ligand)₂, was prepared by the general procedure outlined for the preparation of Pd(bzac)₂, using only several drops of the ethanolic KOH solution, and keeping the reaction mixture at room temperature, protected from light by a cover of aluminum foil. From this reaction two products were isolated, which were designated Species I and Species II. It will be shown later that these two Species represent cis and trans isomers of PdL₂, respectively.



In a typical experiment 1.1680 g (4.0×10^{-3} moles) of the ligand were dissolved in 10 ml. of ethanol. To this were added several drops of ethanolic KOH, and an aqueous suspension of 0.2435 g of PdCl_2 (1.37×10^{-3} moles). Species I was isolated from the reaction after $2\frac{1}{2}$ to 3 hours. Species II was obtained from the mother liquor after standing in the absence of light for 24 to 72 hours. The yield of the crude organo-palladium compounds were: 0.3130 g of Species I, and 0.3150 g of Species II, or approximately a 66% overall yield. In addition, approximately 0.150 g of unreacted ligand was recovered from the mother liquor. Species I was found more soluble in organic solvents (CHCl_3 and C_6H_6) than Species II.

Species I is much more difficult to purify than Species II. It is frequently contaminated with unreacted PdCl_2 or "Pd black" that forms from the decomposition in the course of the reaction. Attempts to purify Species I by recrystallization from CHCl_3 or C_6H_6 were unsatisfactory, since they usually lead to additional decomposition with the production of more "Pd black". The best procedure developed for purification, involved dissolving the solid in a minimum volume of benzene at room temperature, filtering away any insoluble Pd and PdCl_2 solids, then adding cold ethanol to

the benzene solution, to cause precipitation of the organo-palladium compound. The solid was then quickly separated from the supernatant, washed with cold ethanol, dried under nitrogen, and then vacuum dried. The success depended on how rapidly the material was removed from contact with solution, since it was fairly stable when it was dry. Additional crops of lower purity could be obtained from the supernatant by adding more ethanol, partially evaporating the solution, and separating and washing the solid, as described.

Species II is usually obtained in much purer form, it is less soluble in organic solvents, and is more resistant to decomposition in solution. It is frequently contaminated with excess unreacted "ligand", and it can be freed of the ligand by repeated washings with ethanol. Species I is a yellow solid, melting at 138.3-139.6°C (d ca. 160 - 170°). Species II is a golden-yellow solid, mp 235-236° (d). The thermal behavior of these two compounds is discussed in another section.

Product identification of Species I was based on the data that follows. The infrared spectrum (Fig. 19) shows bands at 1630 (mainly C=O str.), 1580 (Ph-ring str.), 1550 (mainly C=C stretch); 1240 (C-O str.); 835 (2 adjacent

Figure 19

Infrared spectrum of PdL₂ Species I.
Nujol bands are indicated by N

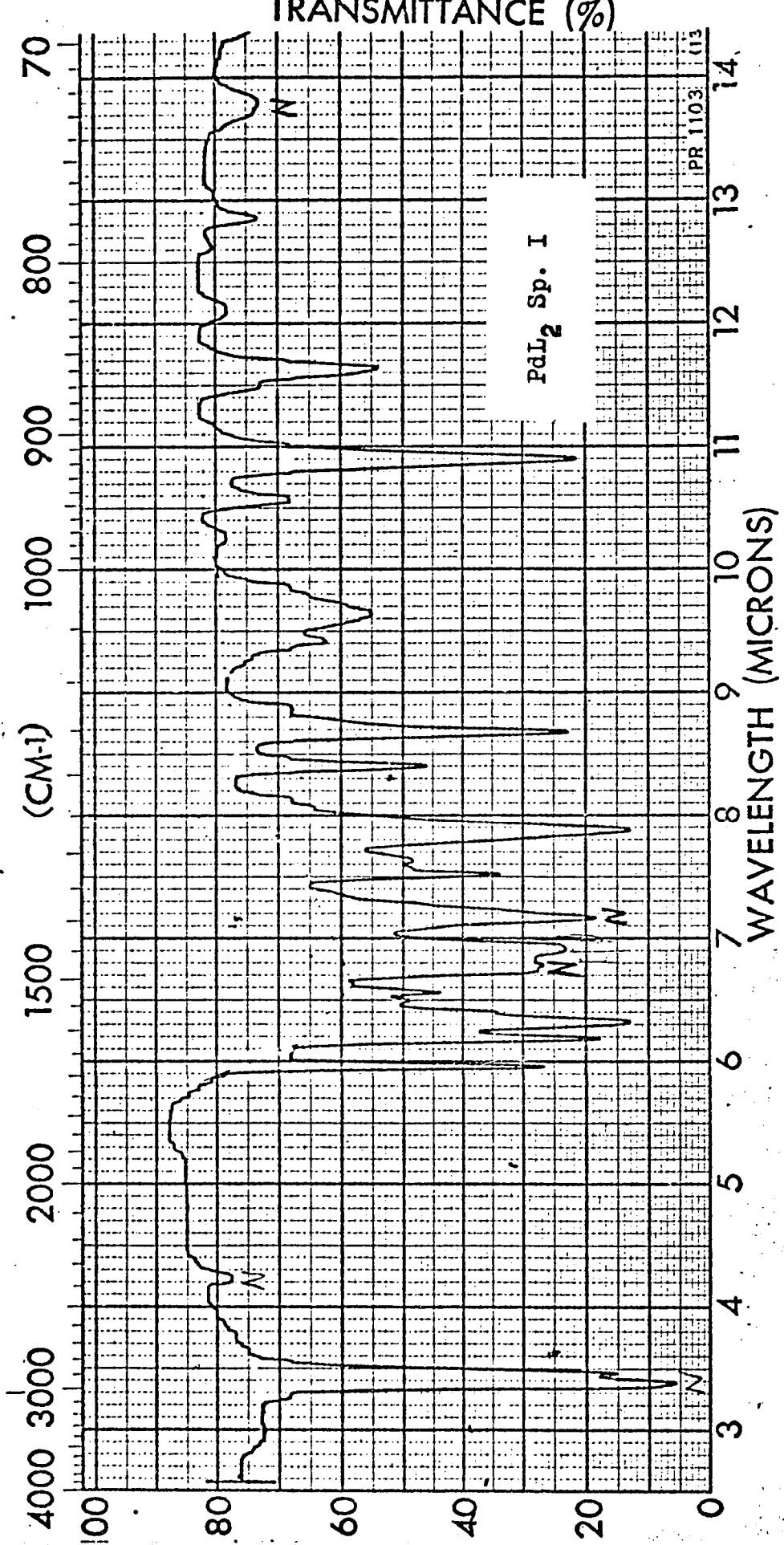


Figure 19

aromatic H). The UV spectrum (Fig. 20) shows absorbances at $\lambda_{\text{max}} = 330 \text{ nm}$ ($\epsilon_{\text{max}} = 10,540$) and at 290 nm (52,110). The NMR spectrum is shown in Fig. 21, with the following shifts downfield from TMS: δ 8.00, 7.86, 7.03, 6.88 (two d, 4H, aromatic), 4.05 (t, 2H, CH_2O), 2.00 (s, area larger than 4H, CHCOCH_3), 1.35 to 1.55 m, 12H, $\text{CH}_3(\text{CH}_2)_6\text{CH}_2\text{O}$, 0.9 (t, broad, 3H, CH_3CH_2 --).

The mass spectrum of PdL_2 Species I is shown in Fig. 22. In order to obtain that, it was necessary to heat the sample to very high temperatures (analyzer 150° and 300°C), and no peaks are observed corresponding to the parent ion. A peak due to the ligand molecular ion is seen at 290, and fragments of the ligand at 233. There were no peaks above mass value of 330, nor above mass 550 up to 800 that could be attributed to Pd-containing fragments. Due to the natural abundance distribution of Pd isotopes, a characteristic pattern of "triplet" lines of almost equal intensity can be seen for Pd, corresponding to mass values of 105, 106 and 108, with shorter lines for ^{104}Pd and ^{110}Pd . This characteristic Pd pattern was seen only at 318 and 205, using the highest line as corresponding to ^{108}Pd . The fragment at 318 could be due to $\text{COC}_2\text{-Pd-CH}_2\text{COC-COC}_6\text{H}_4$ or $\text{C}_{13}\text{H}_6\text{O}_3\text{Pd}$, which in theory gives

Figure 20

Ultraviolet spectrum of PdL₂ Species I
in CH₂Cl₂, concentration 1.708 x 10⁻⁵M

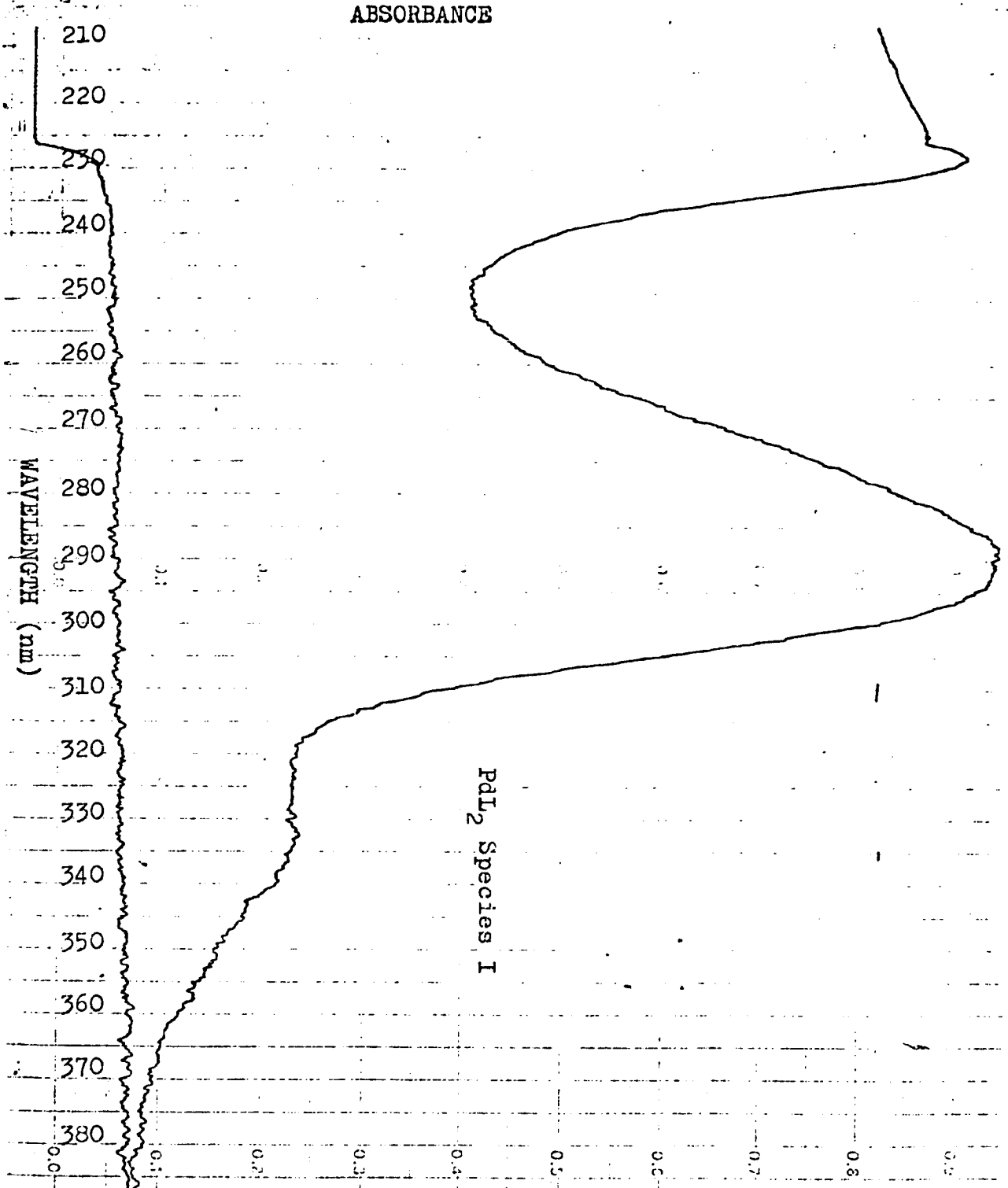


Figure 20

Figure 21

$^1\text{H-NMR}$ spectrum of PdL_2 Species I in CDCl_3

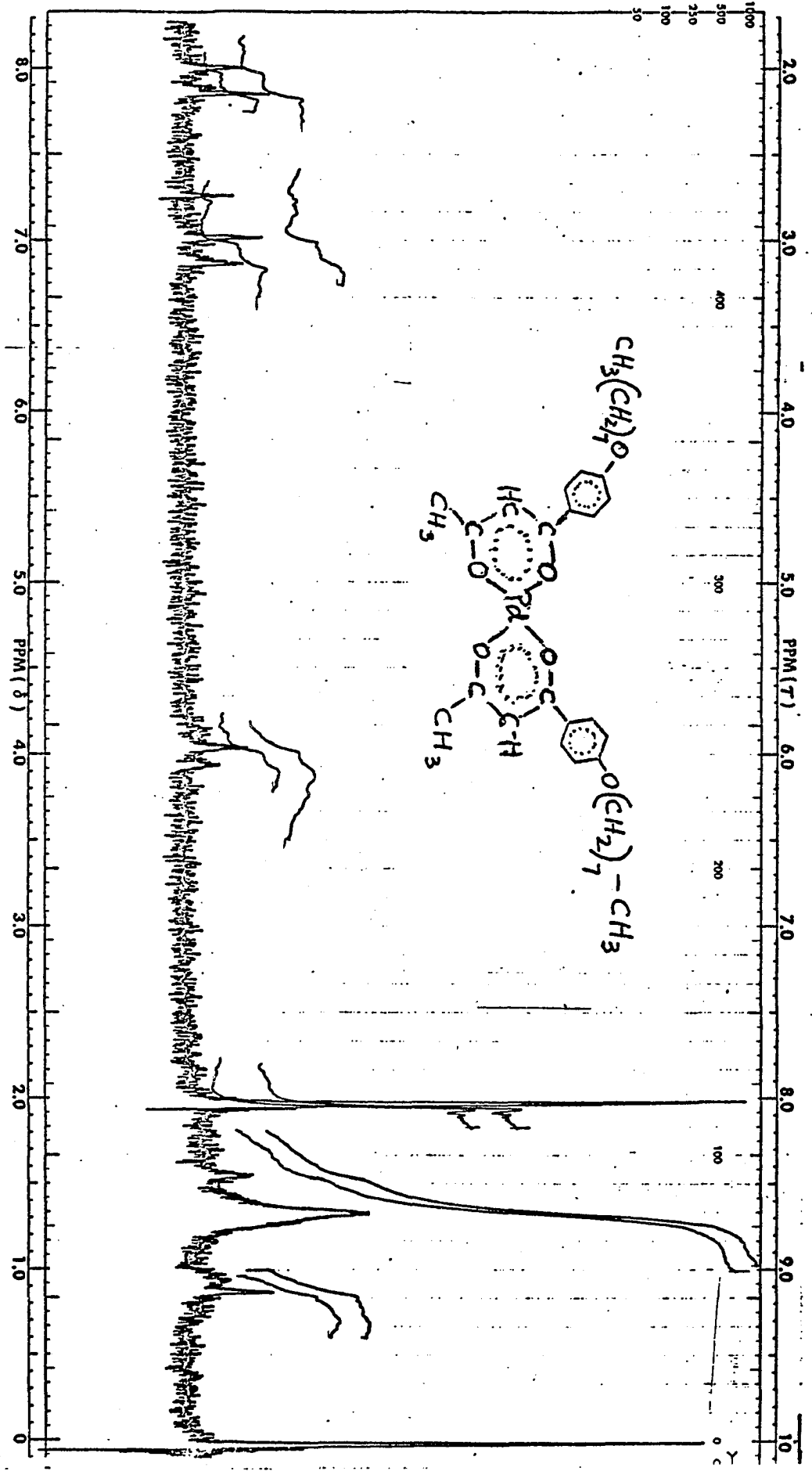


Figure 21

Figure 22

Mass spectrum of PdL₂ Species I.
The upper curve starts from 330 m/e

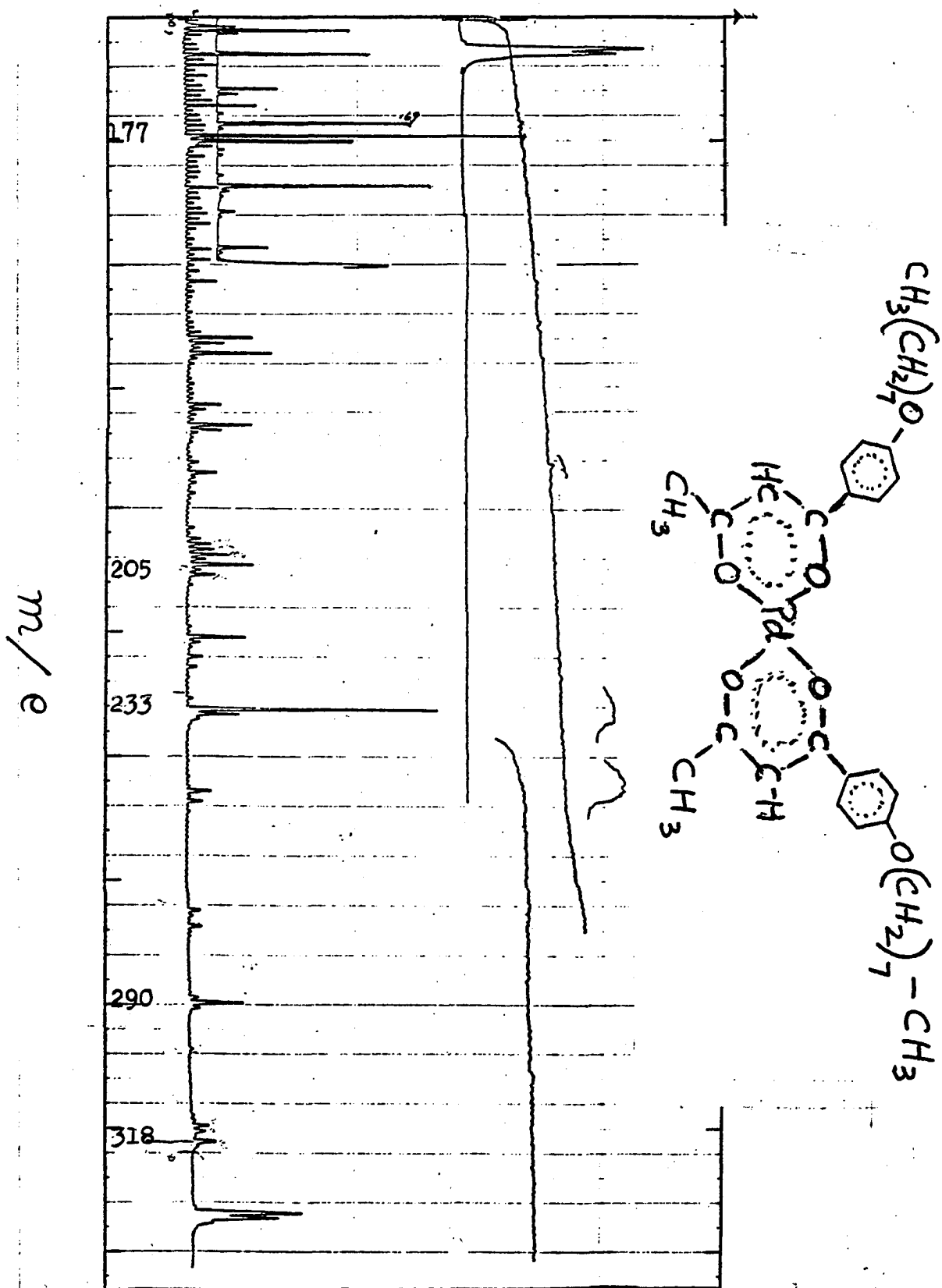


Figure 22

318. The fragment at 205 could be $\text{CH}_2\text{CO-Pd-COCHCH}_2$ or $\text{C}_5\text{H}_5\text{O}_2\text{Pd}$, with theoretical mass of 205.

Molecular weight of PdL_2 Species I was determined osmometrically in benzene (1.406% wt/wt solution or 0.0205 molal) to be 705 (% error 2.92); and 673 in CHCl_3 (0.492% wt/wt solution, or 0.0072 molal) with a relative error of 1.75% from the value of 685 calculated for $\text{PdC}_{36}\text{H}_{50}\text{O}_6$.

Elemental analysis: Calcd. C, 63.10; H, 7.36; Pd, 15.52%. Found: C, 62.81; H, 7.15; Pd, 13.3 by ash residue and 13.56% by atomic absorption.

Product identification of Species II was based on the data that follows. The infrared spectrum (Fig. 23) shows bands at 1620 (mainly C=O stretch), 1590 (Ph ring stretch), 1550sh and 1530 (mainly C=C str), 1250 and 1220 (C-O str.), 840 (2 adjacent aromatic H), 780 (C- CH_3 str.) The ultraviolet spectrum (Fig. 24) shows absorbances at $\lambda_{\text{max}} = 310 \text{ nm}$ ($\epsilon_{\text{max}} = 43,780$) and at 355 nm (34,750). The NMR spectrum is shown in Fig. 25, with the following shifts downfield from TMS: δ 7.95, 7.75, 7.45, 7.25 (two d, 4H, aromatic), 6.03 (s, 1H, $\text{CH}=\text{CO}$), 4.0 (t, 2H, CH_2O), 2.20 (d, 4H, CH_3COCH), 1.33 m, 12H, $\text{CH}_3(\text{CH}_2)_6\text{CH}_2\text{O}$, 0.90 (t, broad, 3H, CH_3CH_2 -).

The mass spectrum of PdL_2 Species II is shown in

Figure 23

Infrared spectrum of PdL₂ Species II.
Nujol bands are indicated by N

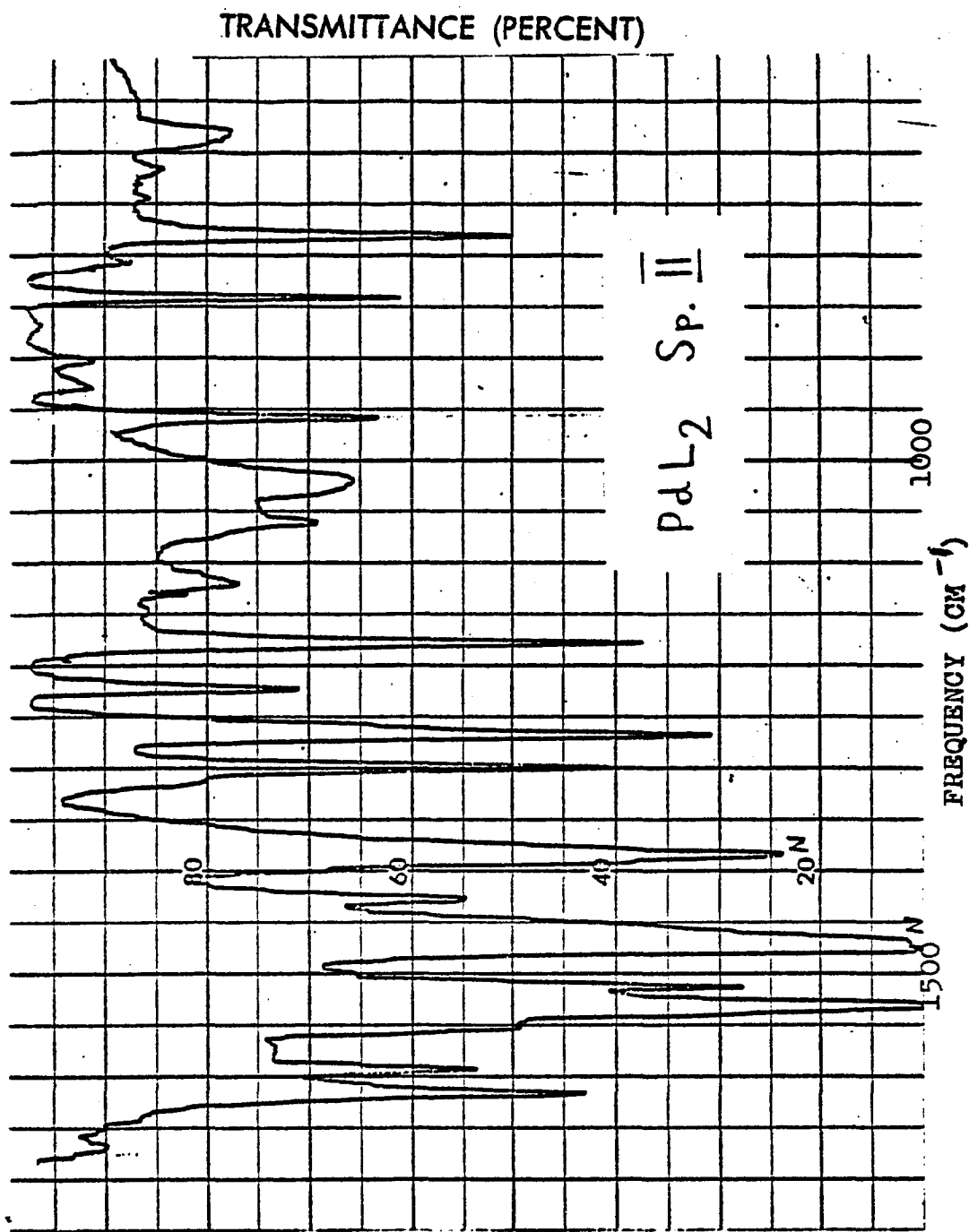


Figure 23

Figure 24

Ultraviolet spectrum of PdL₂ Species II
in CH₂Cl₂, concentration 1.439 x 10⁻⁵M

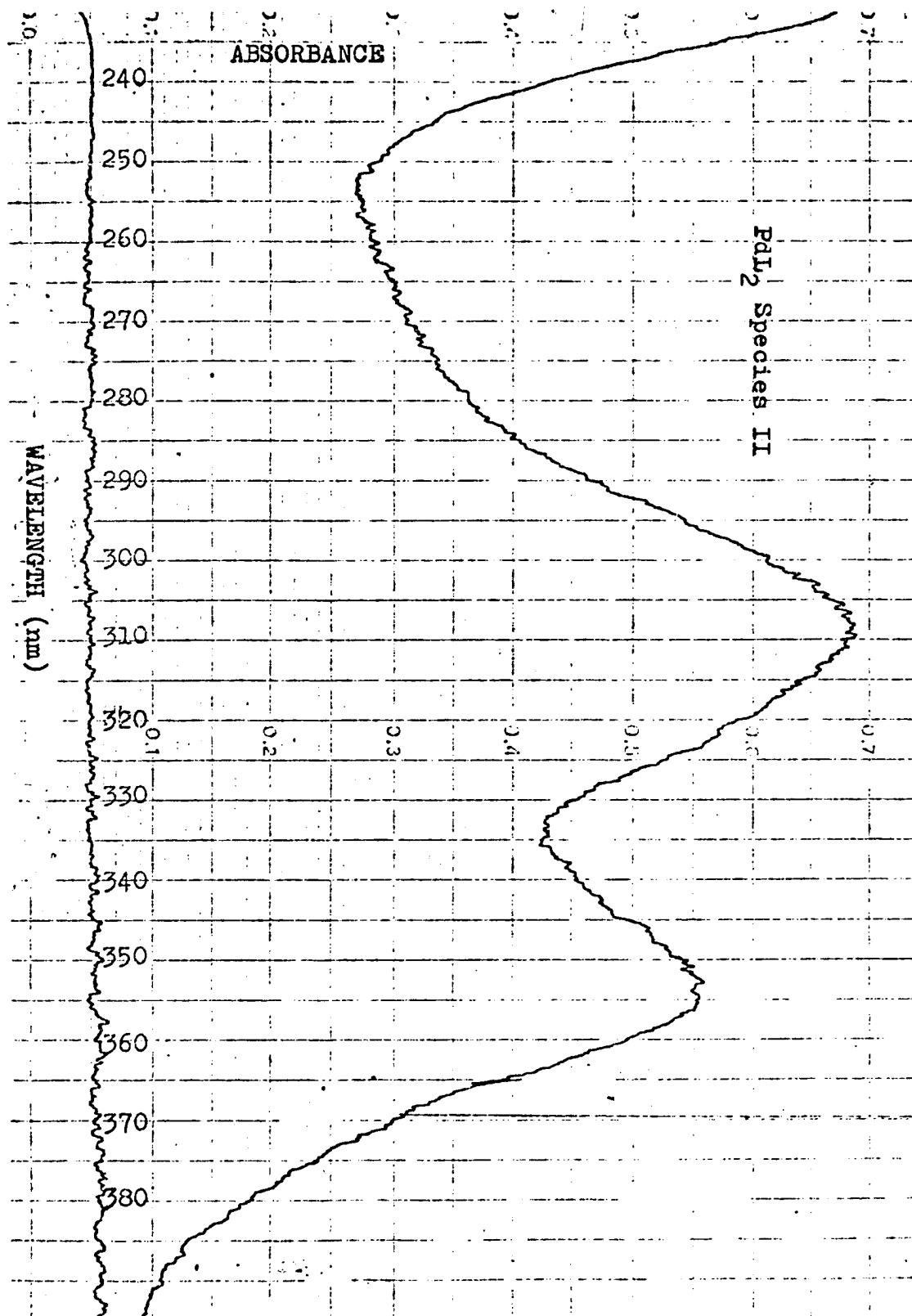


Figure 24

Figure 25

^1H -NMR spectrum of PdL_2 Species II in CDCl_3

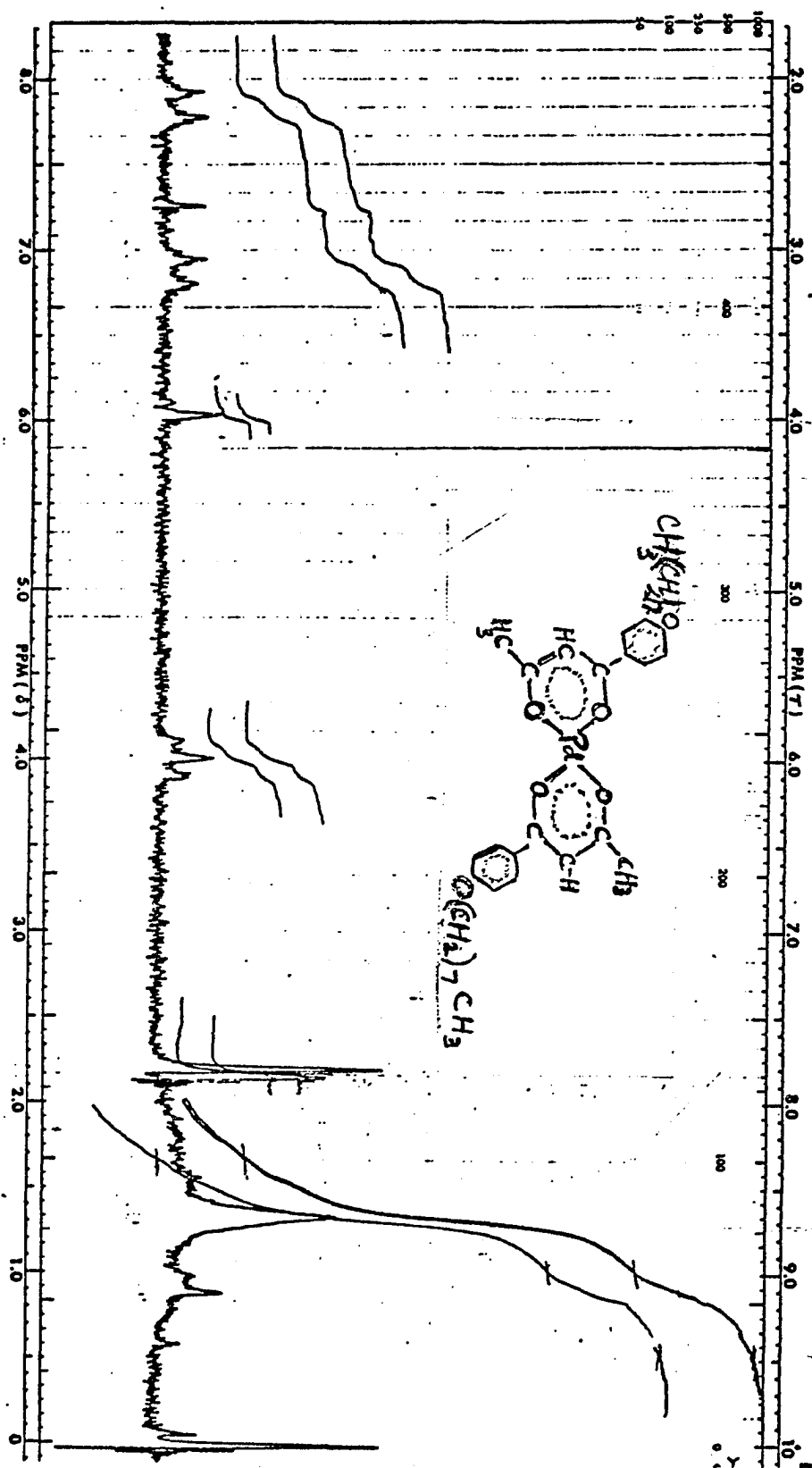


Figure 25

Figure 26

Mass spectrum of PdL₂ Species II.
The lower curve ranges from 100 m/e,
the middle curve from 250, the
upper curve from 450 m/e

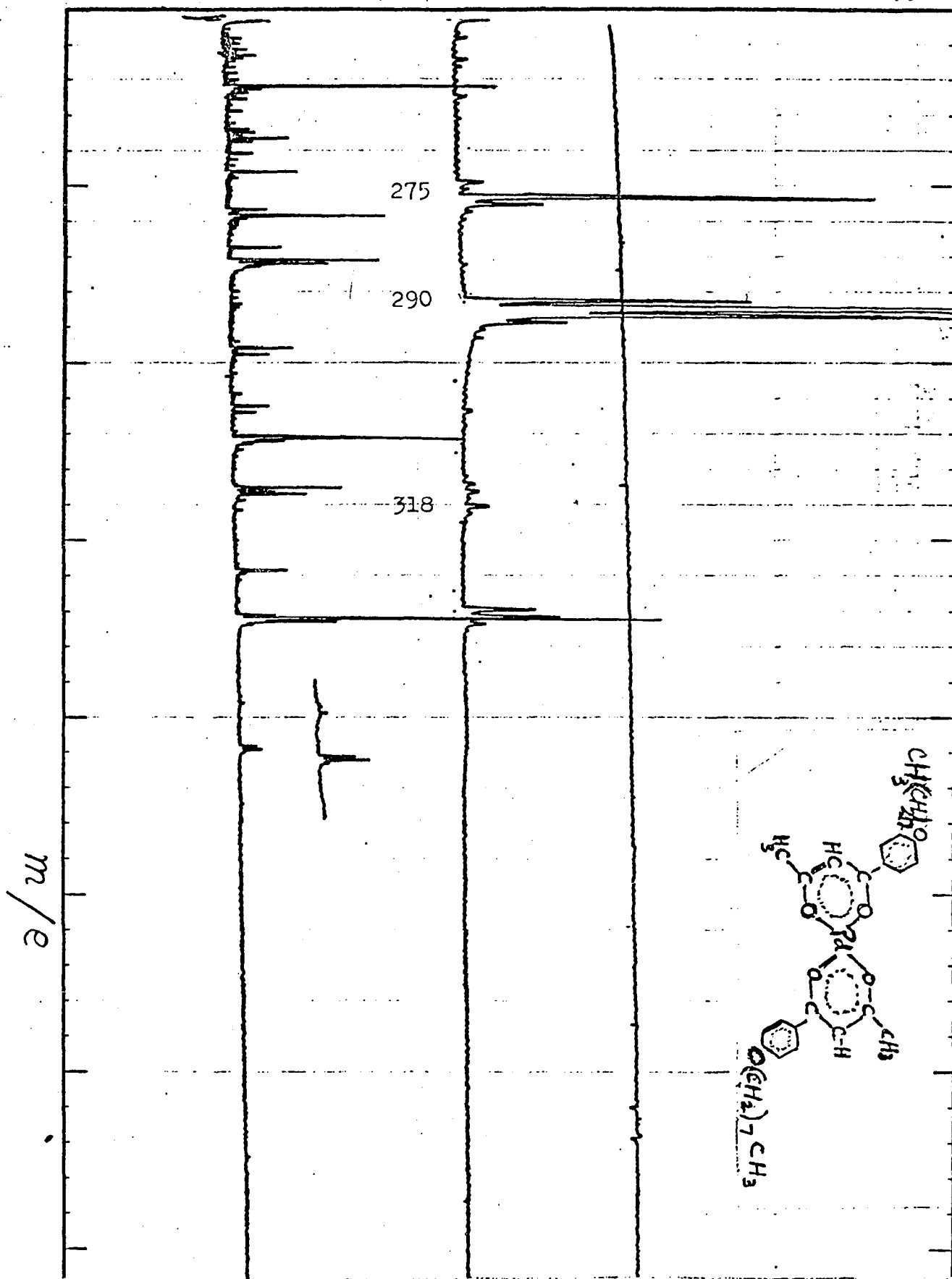


Figure 26

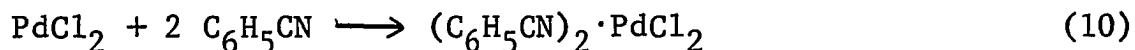
Fig. 26. As in the case of PdL_2 Species I, high temperatures were needed: the probe was heated to 190° , with the analyzer at 150° and 250°C . The highest mass value peak seen is at 634, but this one does not show any characteristic Pd isotope "splitting pattern". There is a peak at 290 due to the ligand, and a peak at mass value of 318 that does show the Pd pattern. This is the same peak observed in the mass spectrum of PdL_2 Species I, and is probably also due to a $\text{C}_{13}\text{H}_6\text{O}_3\text{Pd}$ fragment (theory 318).

The molecular weight of PdL_2 Species II was more difficult to determine than that of Species I, because of the lower solubility of this compound. A value of 717 was found (error of ca. 5% from calculated value of 685) by osmometric method in CHCl_3 (0.453% wt/wt solution or 0.0066 molal). The compound was insufficiently soluble in benzene to obtain reproducible results in that solvent.

Elemental analysis: Calculated for $\text{PdC}_{36}\text{H}_{50}\text{O}_6$
C, 63.10; H, 7.36; Pd, 15.52%. Found: C, 63.04%, H, 7.47;
Pd, 15.24% by ash residue; Pd, 14.74% by specific colorimetric reagent.

Preparation of Dibenzonitrile Palladous Chloride.

This compound was prepared, following the procedure described by Kharash et al³⁰ in 1938.



0.7740g of PdCl_2 (4.36×10^{-3} moles), dissolved in a minimum volume of benzonitrile (used 10ml., in excess of stoichiometric amount needed) at 80-100°C. The reaction mixture, with a reflux condenser attached, was heated for one hour at 80°C, and it was filtered hot to remove a blackish-brown residue. The filtrate was cooled in an ice-water bath, and an orange-yellow precipitate formed, which was collected by vacuum filtration. More precipitate was also obtained from the first mother liquor by diluting it with low-boiling petroleum ether. The solid material was washed three times with 5 ml. portions of cold pet ether, then it was air dried, and finally dried for 2 days in a vacuum dessicator over drierite, after some preliminary pumping to remove excess solvent. The yield of the solid product was 1.0340 g, or 65% (literature reports yields up to 90%). In appearance the solid was like the material described by Kharash, i.e. orange-yellow and stable in air.

No elemental analysis was obtained on this compound, but it was used in a subsequent attempted preparation of $\text{Pd}(3\text{-phenyl-acac})_2$.

Details of Purification Procedures for Pd-carboxylates

The purification of these compounds proved difficult and tedious. It was anticipated that the palladium-oxygen bond in this series of compounds would be quite labile. Stephenson et al had reported that the carboxylate group in $\text{Pd}(\text{ac})_2$ and Pd(II)-propionate could be easily replaced by various mono-, bi-, and tetradentate ligands. They found that those palladium carboxylates reacted, even in the cold, with acetylacetone, with salicylaldehyde, and with various nitrogen donor ligands, as well as with tri-phenylphosphine and triphenylarsine. Their investigations of relative stability of the organo-palladium compounds indicated that the most stable ones were those with palladium-nitrogen bonds. They also reported that the palladium carboxylates were stable in air (presumably in the solid and dry state). However, the compounds decomposed when warmed with alcohols and other solvents to give palladium metal.¹⁹

In our laboratory attempts to recrystallize the crude product indicated that the compounds decomposed when

heated to produce more "Pd-black". Solvents that were potential proton donors were unsatisfactory, and the compounds decomposed even in dioxane and chloroform. Attempts to purify the Pd-(p-octyloxy)-benzoate by thin layer chromatography (tlc) on sheets coated with activated alumina or silica gel were unsuccessful. More extensive studies were conducted in an effort to develop proper conditions for tlc purification on sheets coated with silica gel, with polyvinyl alcohol as a binder and fluorescent indicator (Eastman Chromagram #6060). The following solvent system were tried to effect the separation of the reaction product from the unreacted Pd-acetate and the p-octyloxy-benzoic acid by tlc on #6060 sheets: ligroin (b.p. range 60-90^oC), chloroform, benzene, ethyl acetate, ether, methyl ethyl ketone, and various mixtures of these solvents. In most cases, the solvent caused the migration of the alkoxy-benzoic acid, and some slow migration of the Pd-acetate; but the desired product did not migrate, and it remained adsorbed to the plate coating. Subsequently, larger scale separation was attempted on glass plates coated with 0.25 mm adsorbent (plates #5765), and again only the p-octyloxy benzoic acid had separated from the colored residue.

The residue was scraped off the glass tlc plates, and separation of the colored materials was attempted by the use of more polar solvents. The solvents used in these trials included chloroform, acetone, CH_2Cl_2 and dioxane; the solvents were tried at room temperature, as well as warmed to ca. 50°C . Dioxane and CH_2Cl_2 seemed to offer some chance of dissolving or extracting the organo-palladium compounds from the adsorbent. (Fig. 10 and 29). Attempts to use a continuous extraction Soxhlet apparatus, with dioxane or chloroform as the solvents, were even less successful, inasmuch as the heated solvents and their vapors seemed to speed up the decomposition of the organo-palladium compounds, with the production of more "Pd-black". Because of these results, there were no further attempts to separate the products by chromatography.

Along with the tlc purification attempts, ultra-violet spectra of the various fractions of materials were determined. The UV spectra, together with infrared spectra of the reaction mixture and of various fractions obtained during the stages of purification, were useful in following the course of the procedures. In the IR the presence of the p-alkoxy-benzoic acids can be readily detected by the band at 1685 cm^{-1} for the p-octyloxy-, and at 1675 cm^{-1} in

the p-propoxy-benzoic acid. The $\text{Pd}(\text{ac})_2$ absorbs at 1600 cm^{-1} (asymmetric stretch) and at 1427 cm^{-1} (symmetric stretch), as reported by Stephenson et al.¹⁹ The Pd-benzoate had been reported by them to absorb at 1567 and 1404 cm^{-1} .

The organo-palladium compounds prepared in our laboratory had characteristic absorptions at 1400 cm^{-1} (Pd-p-octyloxy-benzoate) and at 1390 (Pd-p-propoxy-benzoate). The latter bands were sufficiently well separated from the symmetric stretch of Pd-acetate (at ca. 1430), to be useful in determining the purity of the mixture of the two organo-palladium compounds by following the changes in the IR spectrum (Figs. 9, 27 and 28 to be compared).

The alkoxy-benzoic acids are white crystalline substances that do not absorb in the visible; and in the UV they absorb below 310 nm . The Pd-acetate is orange-brown, while the two Pd-(p-alkoxy)-benzoates prepared here are brownish black. In the ultraviolet spectrum these three compounds can be distinguished even better than in the IR. The Pd-acetate has a characteristic "minimum" where the other two compounds absorb. Ultraviolet spectra could be obtained in dioxane, benzene, ligroin and CH_2Cl_2 .

In the UV region Pd-acetate (Fig. 3) absorbs at 400 nm , with its characteristic minimum at 355 nm , and

TRANSMITTANCE (PERCENT)

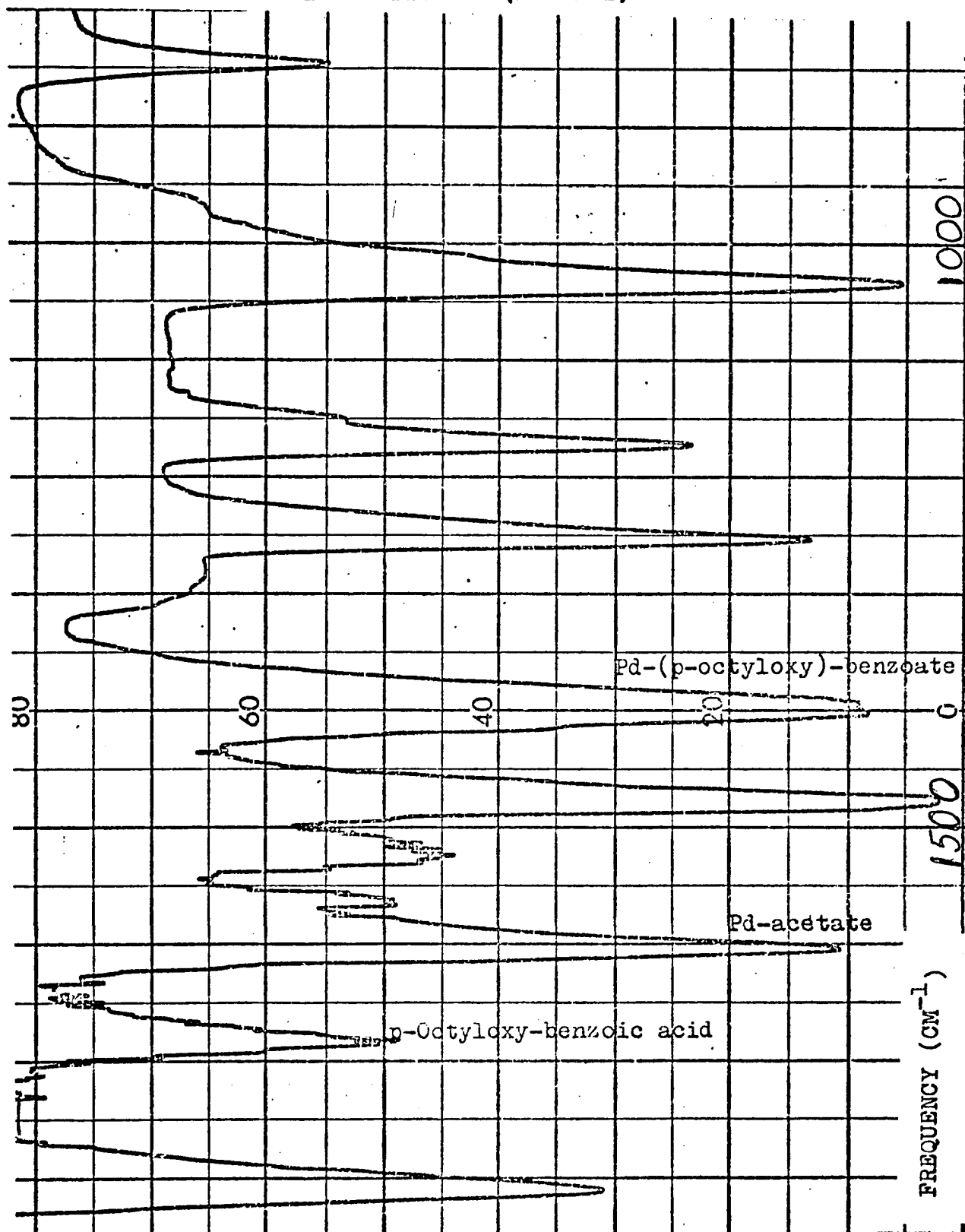


Figure 27. IR spectrum of benzene solution of crude reactn. mixture, showing presence of three materials

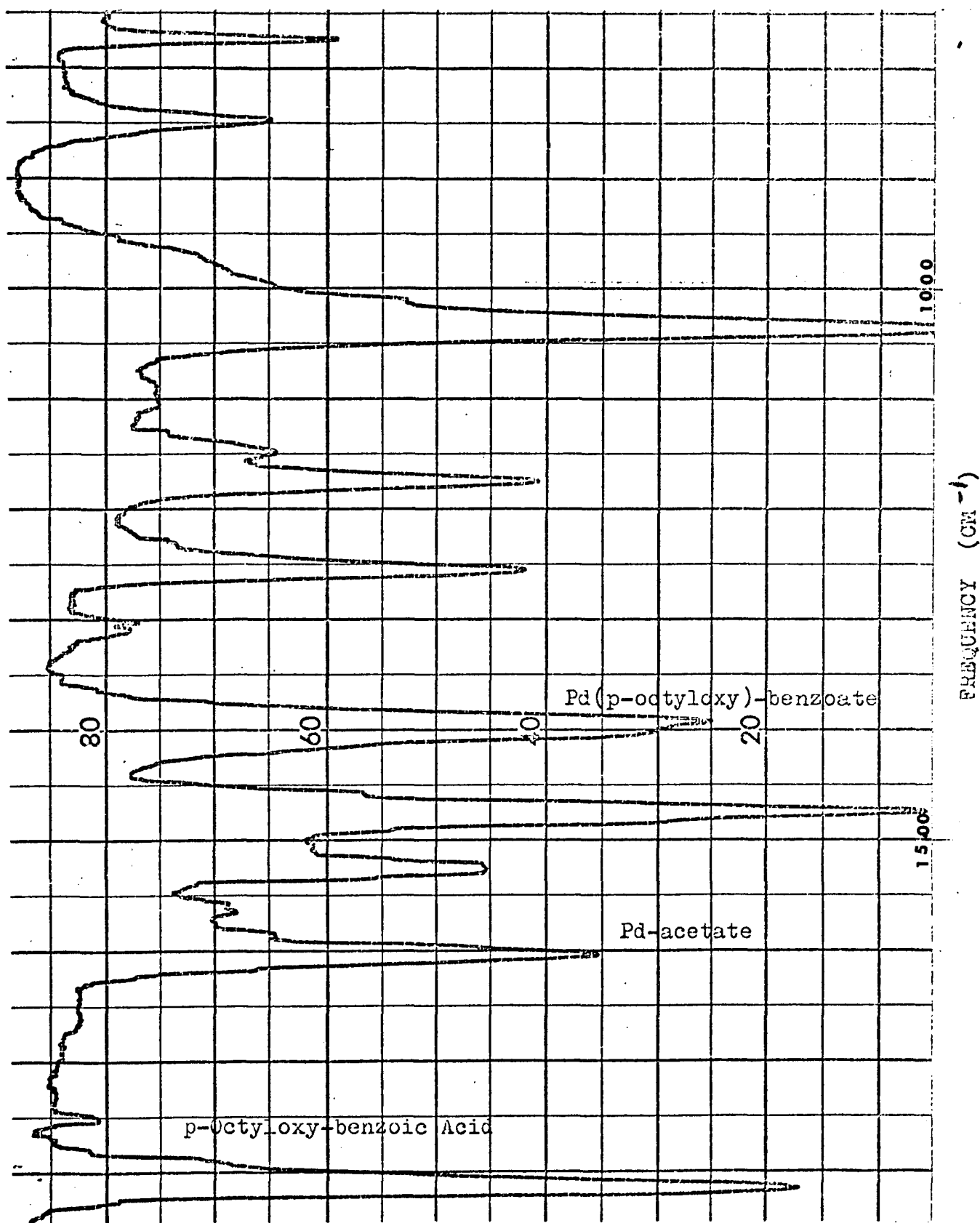


Figure 28. IR spectrum of benzene solution of Pd(octyloxy)-benzoate, showing less contamination

ABSORBANCE

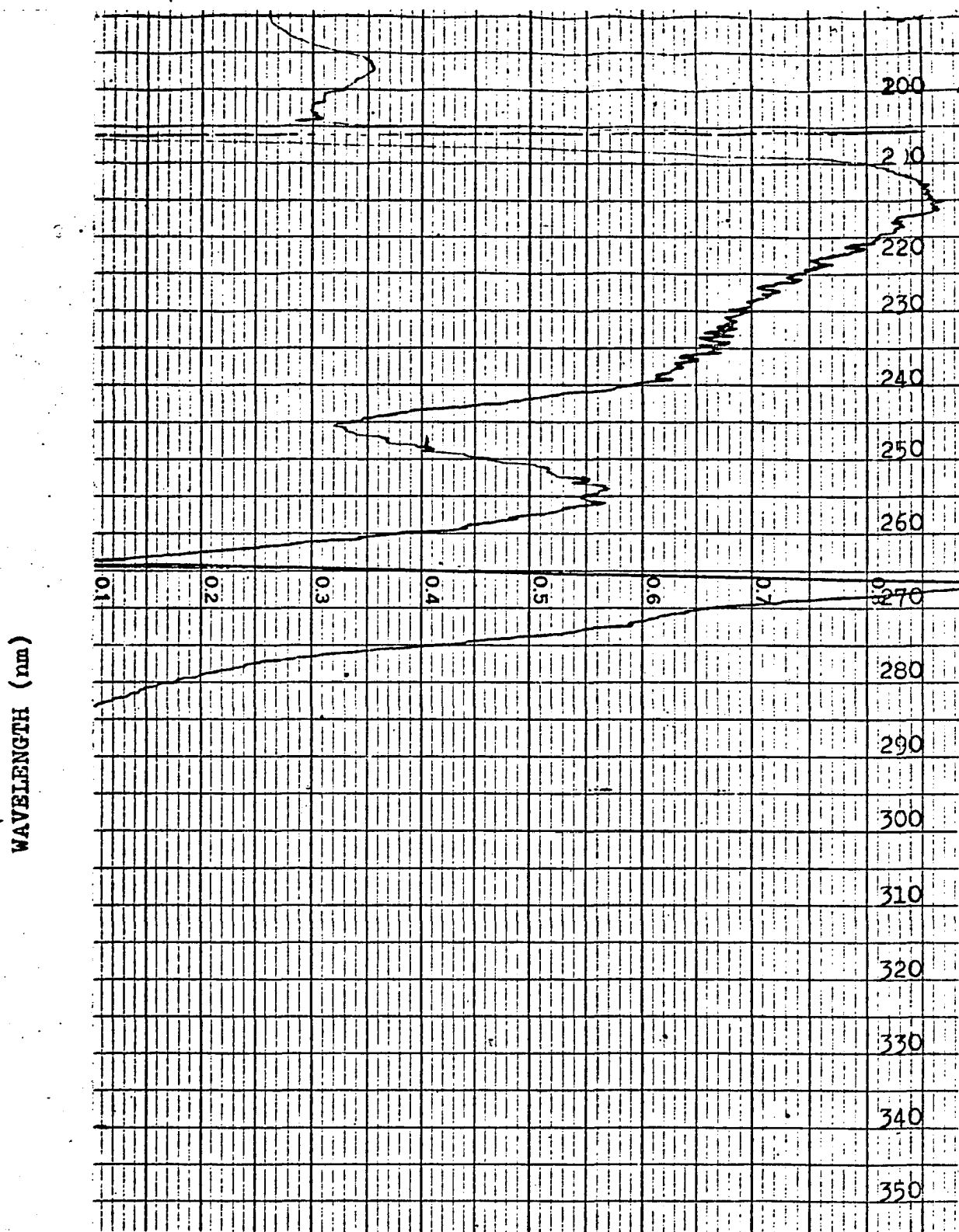


Figure 29. Ultraviolet spectrum of p-octyloxybenzoic acid in dioxane

another absorption at 320 nm. The Pd-(p-octyloxy)-benzoate has a band between 330 and 380 nm, with a minimum at 240 nm, and another weaker absorbance band at 225 nm (Fig. 8). The Pd-(p-propoxy)-benzoate has a UV spectrum similar to that of the p-octyloxy-analogue, with an absorbance below 380 nm. On the basis of differences in UV spectra, it was possible to determine whether the crude reaction mixture contained the desired product, and whether or not the purification procedures were effecting any separation of the materials.

In the purification procedure for the Pd-(propoxy)-benzoate, it was possible to take advantage of the differences in solubility of the three components of the reaction mixture, i.e. p-propoxy-benzoic acid, Pd-acetate and Pd-(p-propoxy)-benzoate. The alkoxy-benzoic acid was essentially insoluble in cold ligroin, while the Pd-acetate was more soluble in it than the Pd-(p-propoxy)-benzoate. The reaction mixture was triturated with cold ligroin, and the various ligroin extracts were examined in the ultra-violet. If the UV spectrum showed a "minimum" at 350 nm, it was judged to be a fraction containing mostly Pd-acetate; if there was an absorption at 350 nm, the solution was deemed to contain also the desired reaction product. After

six successive ligroin triturations, the concentration of Pd-acetate in the extract was reduced considerably (Figures 30, 31, 32, 33); the remaining mixture was judged essentially free of Pd-acetate.

The crude product, which had been previously separated by filtration from any excess unreacted alkoxybenzoic acid, still contained a mixture of the desired product and the acid, as judged from the appearance of the IR spectrum (Fig. 32, 33). A minimum volume of benzene, previously dried over molecular sieves, was added to dissolve the material. Since both components were known to be soluble in benzene, some ligroin was added to the benzene solution, so that the solvent mixture was approximately 66% benzene-33% ligroin, by volume. If no propoxy benzoic acid precipitated on cooling (white or grayish solid), the volume of the solution was reduced to one-half under a gentle stream of nitrogen gas. In the course of the evaporation, more acid precipitated, and it was separated from the supernatant solution. The separation step and further precipitation by addition of more ligroin were repeated several more times, until no more propoxy-benzoic acid separated from the mixture upon refrigeration.

Infrared spectra were used to follow the progress of the purification procedure. At various intermediate

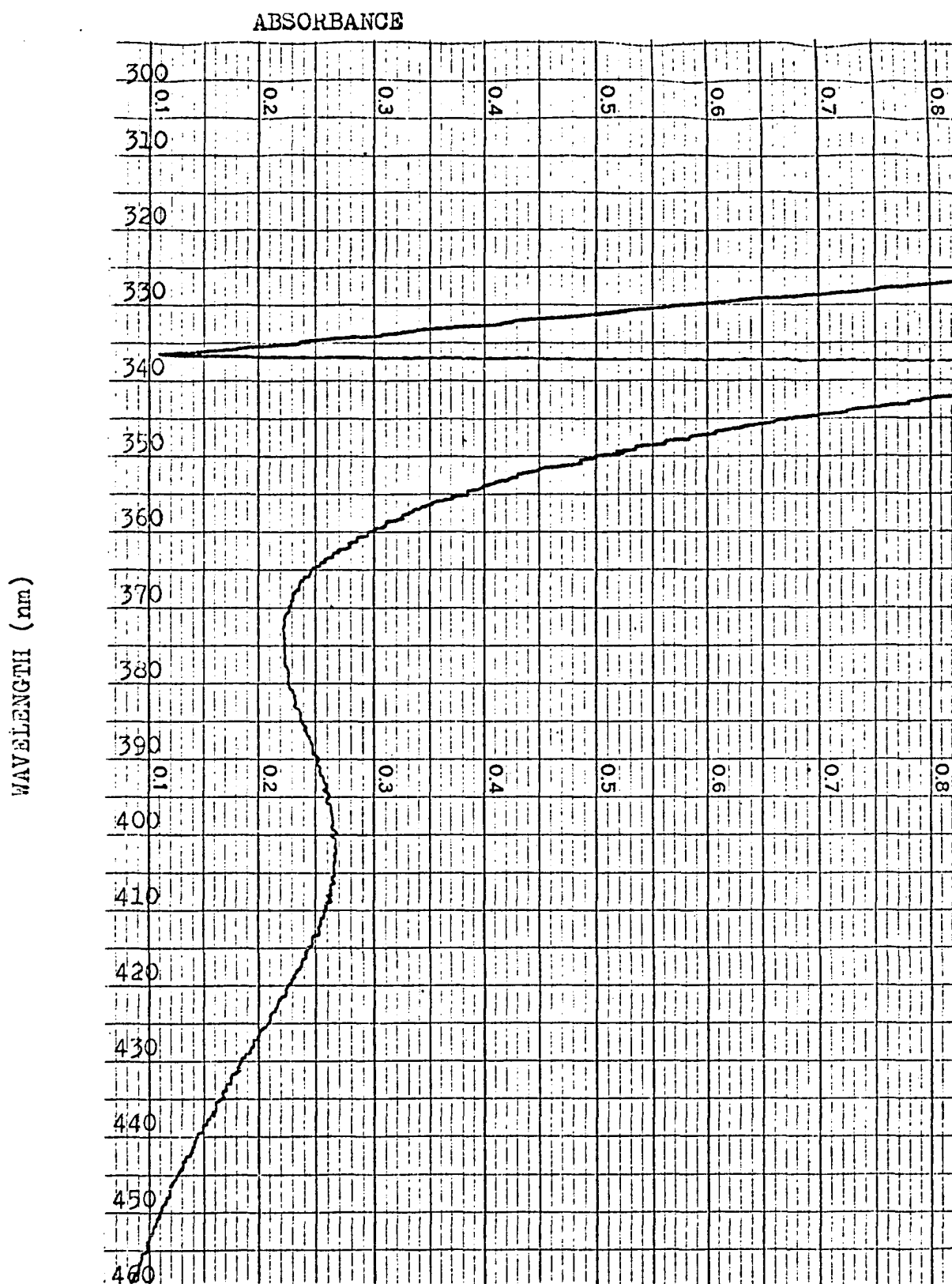


Figure 30. UV spectrum of first ligroin extract, showing absorbance at 400 nm due to Pd-acetate and absorbance below 360 nm of Pd-(p-propoxy)-benzoate

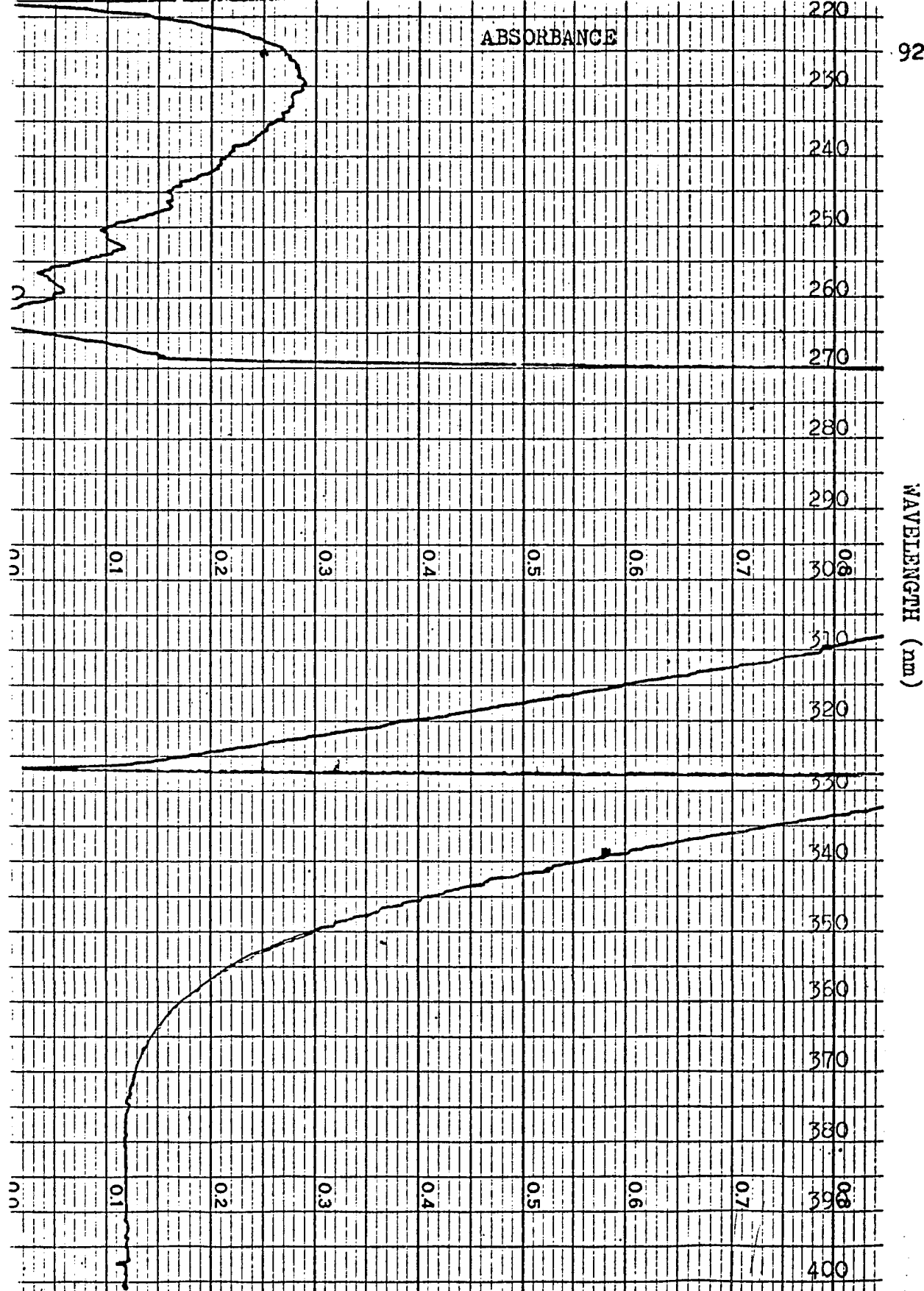


Figure 31. UV spectrum of sixth ligroin extract, showing absence of Pd-acetate (at 400 nm) and presence of Pd(p-propoxy)-benzoate (below 340, 230 nm)

TRANSMITTANCE (PERCENT)

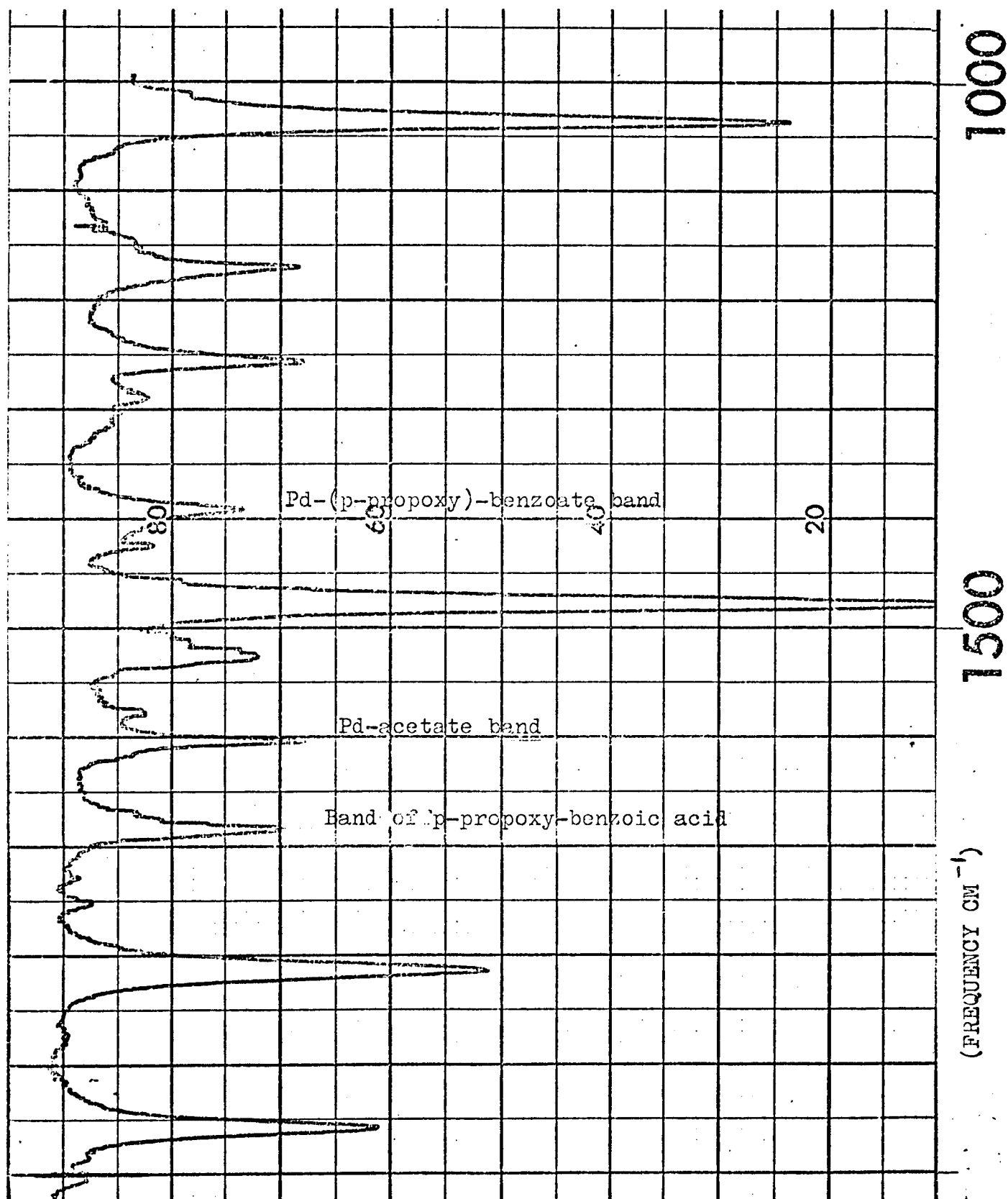


Figure 32. IR spectrum of benzene solution of crude reaction mixture, showing presence of three materials

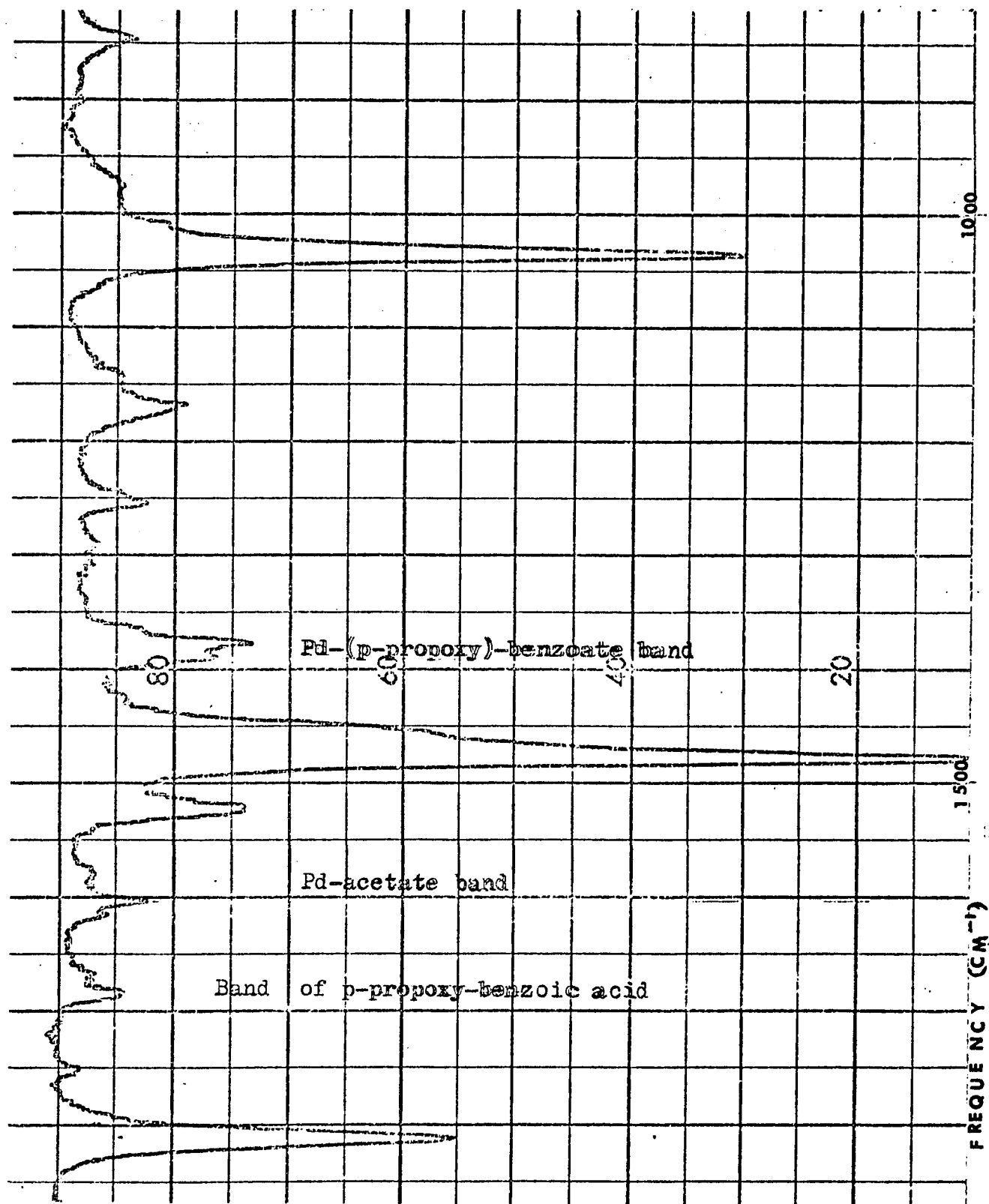


Figure 33. IR spectrum of benzene solution of Pd(propoxy)-benzoate, showing less contamination

stages, small aliquots were taken, the solvents evaporated to dryness, and the solid residue analyzed by DTA to detect any traces of the propoxy-benzoic acid. Generally, 4 successive precipitations by addition of ligroin to the benzene-ligroin mixture, yielded a product deemed sufficiently pure on the basis of the combined IR, UV and DTA criteria mentioned. If the material still contained some propoxy-benzoic acid, the DTA thermograms showed one or more endotherms in the 120 to 150°C region (Figs. 34, 35), with decomposition above 140 due to the decomposition of the organo-palladium compound. The Pd-(p-propoxy)-benzoate, when sufficiently pure, is a dark non-crystalline solid. If the sample is first cooled below -40°C and then heated, its DTA thermogram shows one or two closely spaced endotherms ca. 43 and 50°C, with decomposition above 140°C. Otherwise, the DTA does not indicate mesomorphic behavior. (Fig. 11).

Two samples of Pd-(p-propoxy)-benzoate were analyzed, judged to be the best samples on the basis of the combined UV, IR and DTA criteria. From the results of the elemental analysis it was possible to estimate that the purer of the two samples contained 89.0% of Pd-(propoxy)-benzoate, 6.7% Pd-acetate and 4.3% Pd. It can be calculated that such a mixture would yield 47.44% C, 4.43% H and 27.82% Pd.

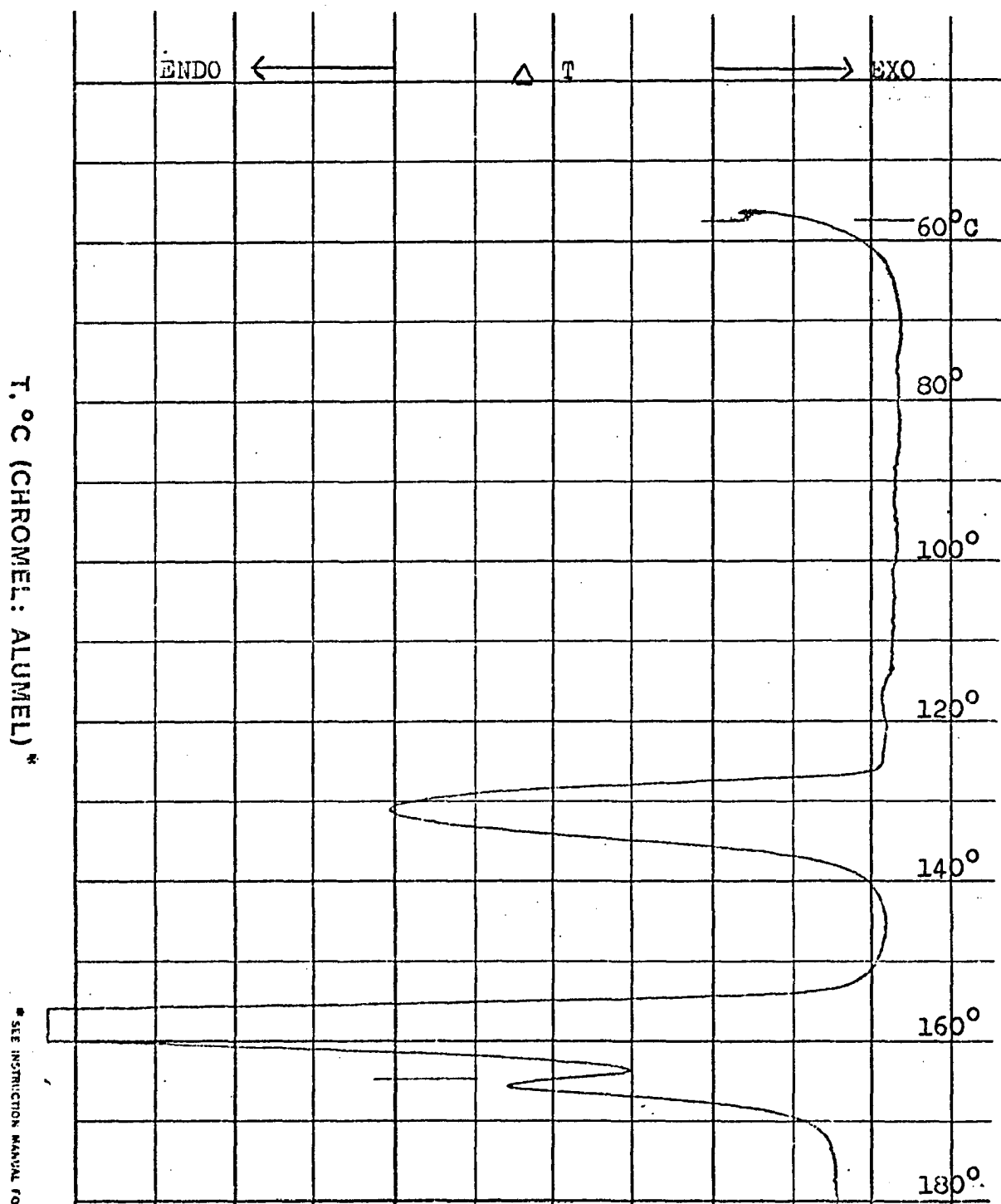


Figure 34. DTA thermogram of pure p-propoxy-benzoic acid

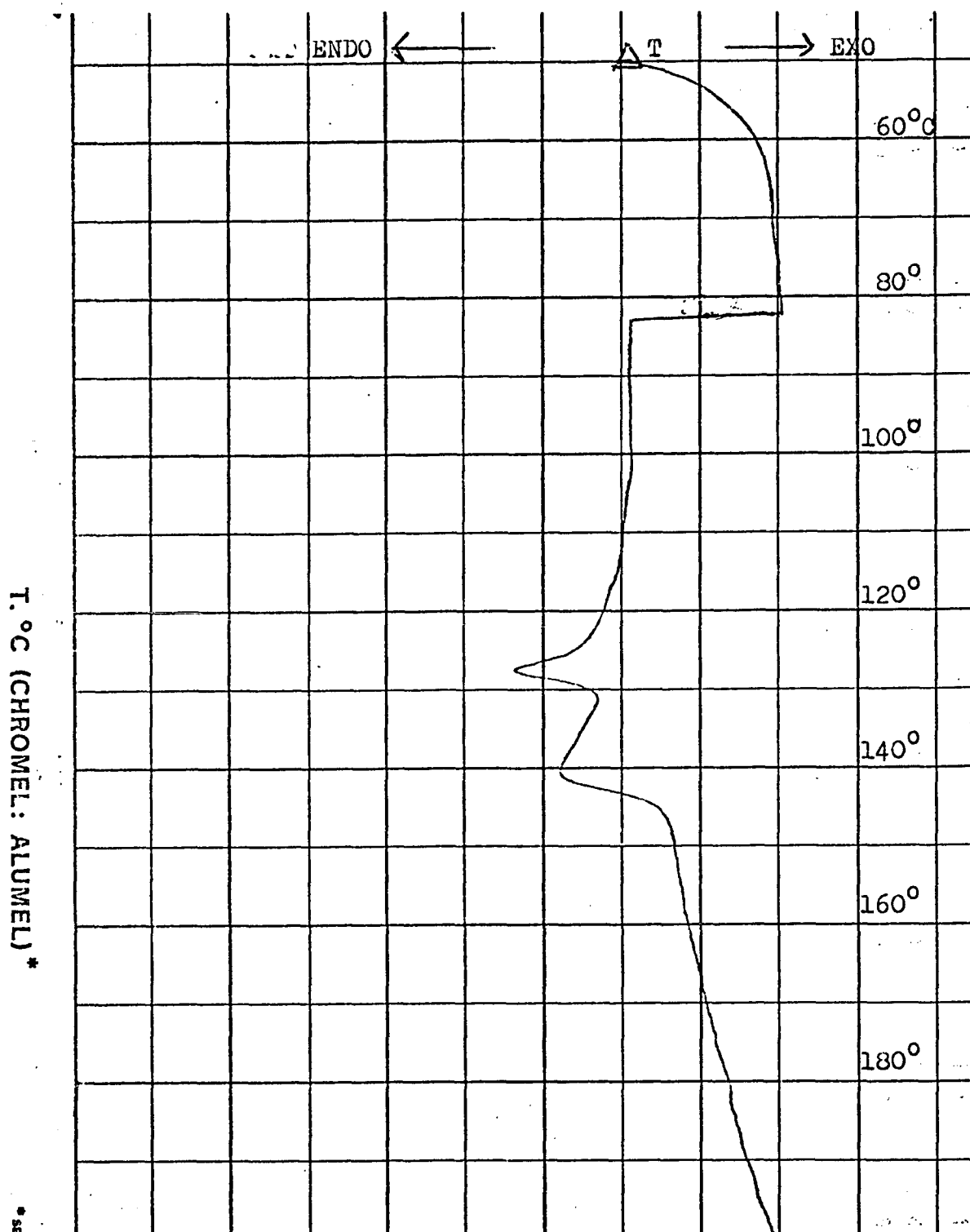


Fig. 35 DTA thermogram of crude Pd-(p-propoxy)-benzoate, showing contamination with p-propoxy-benzoic acid

DISCUSSION

Discussion of Pd-carboxylato Complexes

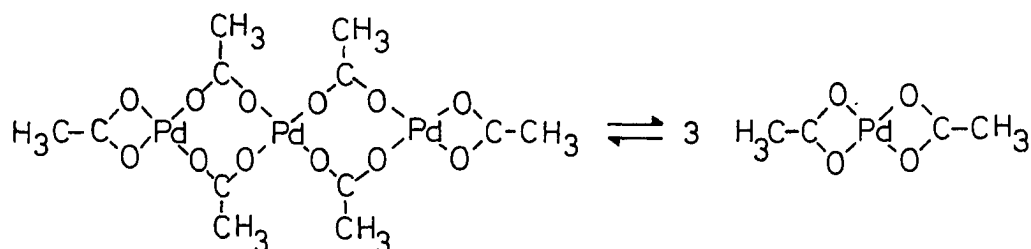
The first system of potentially mesomorphic organo-palladium compounds investigated in this study was the palladium(II)-carboxylato series. The more tedious procedure developed for the purification of Pd-(p-propoxy)-benzoate yielded material of generally higher purity and less Pd(ac)₂ contamination than the results in the preparation of the Pd-(p-octyloxy) analogue. Analysis of the two samples of the propoxy analogue indicated that the purer sample contained 89.0% of the desired product, 6.77% Pd(ac)₂ and 4.3% Pd as contaminants. The less pure sample contained 84% of Pd-(p-propoxy)-benzoate, 8.0% Pd(ac)₂ and 8.0% Pd. In case of the octyloxy analogue, it was estimated to be 86.5% pure, with 12.3% Pd(ac)₂ and 1.2% Pd as contaminants.

DTA data did not indicate that either of the two compounds prepared was potentially mesomorphic. Since these compounds were also very dark, they could not be properly examined under a polarizing microscope, so that any potential mesomorphism would have been very difficult to establish.

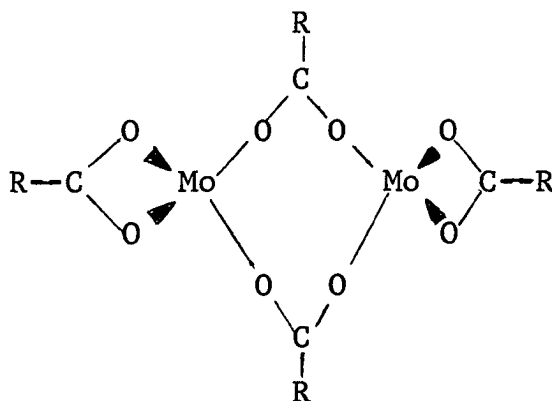
The difficulties in synthesizing and purifying encountered in this earlier endeavor, suggested a need to re-examine the problem and the approach. In line with

the requirements for mesomorphic behavior, as outlined in the Introduction, the geometry of the compounds prepared in our laboratory had to be derived from the structures reported for Pd-acetate and Pd-propionate by Stephenson et al.¹⁹ and by Morehouse et al.¹⁸ Those structures had been assigned on the basis of molecular weight determinations. Ebullioscopically in benzene and acetone, Pd-acetate and Pd-propionate were reported to be monomeric,^{18,19} yet osmometric measurements in benzene at 37°C indicated that both of those compounds were trimeric (found 714 in benzene for the acetate, calculated for trimer 675; found 767 in benzene for propionate, calculated for trimer 759). Although monomeric structures were assumed, those were apparently based on ebullioscopic values intermediate between monomer and trimer: for the Pd-acetate Stephenson et al.¹⁹ found 253 and 357 (calculated for monomer 225); for the Pd-propionate they found 249 and 386 (calculated 253). Stephenson et al.¹⁹ had suggested that the compounds existed in a monomer-trimer equilibrium, but also noted that they were unsuccessful in attempts to study that equilibrium "by infrared, absorption, and high-resolution NMR spectral measurements over a temperature range, since the spectra of the two species appear to show no features that are characteristic (single peak only)".

Morehouse et al¹⁸ had assumed that in the Pd-acetate, as well as in the propionate, the metal atom retained its normal square planar coordination; and that the trimer-monomer system is one that involved both bridging and chelate groups in the trimer, but only chelate groups in the monomer, as shown below.



A similar structure, involving both bridging and chelating carboxyl groups, had been reported by Stephenson et al³¹ for $\text{Mo}(\text{O}-\text{COR})_2$, as shown below. That structure had



been assigned on the basis of osmometric and ebullioscopic molecular weight determinations, as well as some preliminary X-ray diffraction results reported to the authors by Lawton

and Mason.

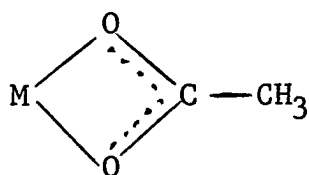
In addition to postulating a trimer-monomer equilibrium for the $\text{Pd}(\text{ac})_2$ and $\text{Pd}(\text{II})$ -propionate, Morehouse et al¹⁸ reported that the trimers were readily cleaved by nitrogen, phosphorus, oxygen and sulfur donor ligands, to produce crystalline monomeric species, such as $\text{Pd}(\text{OCOCH}_3)_2(\text{C}_5\text{H}_5\text{N})_2$, or $\text{Pd}(\text{ac})_2\text{L}_2$. Such adduct compounds with the new ligands, i.e. the $\text{Pd}(\text{ac})_2\text{L}_2$, had low dipole moments, indicating that they had a trans configuration. The adduct compounds also showed an IR band at ca. 1700 cm^{-1} , arising from a singly bound carboxylate group, while the bridged or chelated carboxylate groups had absorbed at ca. 1600 and 1425 cm^{-1} .

Stephenson and Wilkinson³² had reported IR data on some other adducts of palladium(II) carboxylates, of the general type $\text{Pd}(\text{OCOCH}_3)_2\text{L}_2$ with L being Ph_3P or Ph_3As . In those dimeric adducts they reported carboxylate groups as both bridging and unidentate ligands. They saw the IR bands of the bridging acetate at 1580 and 1410 cm^{-1} ; those of the unidentate acetate at 1630 and 1314 cm^{-1} .

In case of the compounds prepared and investigated in this work, it was essential that the Pd -(p-alkoxy)-benzoates be similar in structure to the monomeric,

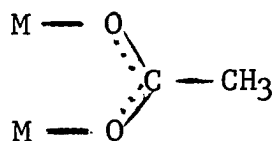
chelated compound, if they were to exhibit potentially mesomorphic behavior. In view of the facile decomposition of the compounds prepared here, and from the report of Stephenson et al¹⁹ about the decomposition of the organo-palladium compounds on warming in various solvents, it seemed probable to us that the ebullioscopic data on molecular weights were incorrect. Seen from that point of view, it seems likely that the "intermediate values" of molecular weights from ebullioscopic measurements in benzene and acetone were, in fact, average values of the decomposition products. As might be expected, the lower molecular weights in benzene than in acetone, could be due to more decomposition at the boiling point of benzene (80°C) than at the boiling point of acetone (56°C). On the other hand, the osmometric measurements taken at 37°C probably represented the true molecular weights of those compounds, and those yielded data suggesting that Pd(ac)₂ and Pd(II)-propionate were trimers.

We were also aware of the fact that the carboxylate ligand could coordinate to a divalent metal in more than one way, and that some X-ray structures had been reported for other divalent metals. For example, Talbot³³ had reported that a structure, schematically represented below,



was found in $\text{Zn}(\text{ac})_2 \cdot 2\text{H}_2\text{O}$, in which the carboxylate was a bidentate ligand, and each ligand was coordinated to only one metal. Many anhydrous salts, such as $\text{Cr}(\text{ac})_3$ and $\text{Mn}(\text{ac})_3$ are usually considered to have that structure also,³⁴ since in it the metal attains its maximum coordination number.

A bridging structure for the acetate ion, as drawn below had been reported for $\text{Cr}_2(\text{ac})_4 \cdot 2\text{H}_2\text{O}$ by van Niekerk and Scheoning,³⁵ as well as for $\text{Cu}_2(\text{ac})_4 \cdot 2\text{H}_2\text{O}$ by



van Niekerk and Schoening in 1953.³⁶ Similarly, the structure of $\text{Be}_4\text{O}(\text{ac})_6$ with bridging acetate ligands had been reported by Bragg and Morgan in 1923;³⁷ that of $\text{Zn}_4\text{O}(\text{ac})_6$ by Koyama and Saito in 1954.³⁸

The organo-palladium compounds prepared in this

laboratory showed no IR band in the region of 1700 cm^{-1} , where Morehouse et al¹⁸ had reported the absorbance of a unidentate carboxylate. Nor were there absorbances at 1630 and 1314 cm^{-1} , where Stephenson and Wilkinson³² had seen the bands of a unidentate acetate. The bands at 1600 and 1400 cm^{-1} in our compounds suggest that there are no unidentate carboxylates; the ligands are probably bridging or chelating, or both. It is also conceivable that these compounds are polymeric, which would be in keeping with their low solubility. The carboxylate ligands could serve as bridging units between the palladiums in such a polymeric species. However, those polymeric structures would probably not have the geometry needed to be mesomorphic.

It should be mentioned further that in 1970, after our investigation of the Pd-carboxylato series had been in progress, the X-ray structure of palladium acetate had been reported by Skapski and Smart.³⁹ They found that the molecular formula of the compound was $2\text{ Pd}_3(\text{ac})_6 \cdot \text{H}_2\text{O}$. The molecule is trimeric, with only bridging acetate groups used to bond to the palladium. The crystal structure shows that the molecule consists of a nearly equilateral triangle of Pd atoms that are about 3.15 Å apart. These are joined together by double acetate bridges, so that the coordination

at the metal atoms is approximately square-planar. The reported Pd-O-C angles are 127.8 to 133.2^o; the O-C-O angles are 124.8 to 128.7^o; and the O-Pd-trans-O angles are 163.5 to 168.9^o. Skapski and Smart point out that a certain amount of strain is involved in such a structure, and this seems to them a likely explanation for the relatively low stability that had been reported for the trimeric molecule by Stephenson et al.¹⁹ Skapski also reported that "to relieve some of the strain the metal atoms are pushed out of the plane of the oxygens, ca. 0.25 Å towards the center of the triangle." However, they found no evidence for metal-metal bonding, and reported a Pd-Pd distance ranging between 3.105 and 3.203 Å. They concluded that the position of the metal atoms was a compromise between square-planar coordination and reasonable angles at the coordinating oxygens.

Skapski and Smart report that, although the water molecule lies between two independent trimers, in a potentially hydrogen bonding position, its nearest approach to an acetate oxygen is 3.08 Å. They conclude by stating that "the role of the water molecule is not clear".²⁵

In view of the difficulties encountered in the synthesis and purification of the Pd(p-alkoxy)-benzoates,

and in order to avoid further trials and difficulties in synthesizing compounds whose geometry did not meet the requirements for potential mesomorphic behavior, it was decided to reexamine the literature and search out data available on the X-ray structures of other potential organo-palladium systems. In the course of that search it was decided to use substituted acetylacetonate ligands, and to use the known structure of $\text{Pd}(\text{bzac})_2$ trans described by Hon et al²⁰ as our second model system. The p-octyloxy chain had to be introduced into the benzoylacetone ligand prior to coordination with the palladium, and the results of that attempt constitute the major portion of this investigation, as discussed in subsequent sections.

General Discussion of Vibrational Spectra of β -Diketones
and Their Metal Chelates

Any discussion of the vibrational spectra of metal β -diketones should start with a consideration of the spectra and structure of the ligand, the simplest of them being acetylacetonone (acac). There is extensive literature on the subject of infrared spectra, including several excellent reviews. The literature reports through 1958 are reviewed by Cotton in the chapter on Infrared Spectra of Transitional Metal Complexes, which is part of Modern Coordination Chemistry by Jack Lewis and R. G. Wilkins.⁴⁰ Nakamoto's book, Infrared Spectra of Inorganic and Coordination Compounds⁴¹ reviews the literature up till 1968. A more recent book by John R. Ferraro, published in 1971, on Low Frequency Vibrations of Inorganic and Coordination Compounds, includes references to papers published up to 1969.⁴² In 1971 a review article by B. Bock et al appeared,⁴³ which discusses the bond character of β -diketo-metal chelates. More recent literature references were selected for this discussion by the writer.

Acetylacetonone exists in tautomeric equilibrium at ordinary temperatures, with at least three molecular forms present, as evidenced by its spectrum (Fig. 36, Structures

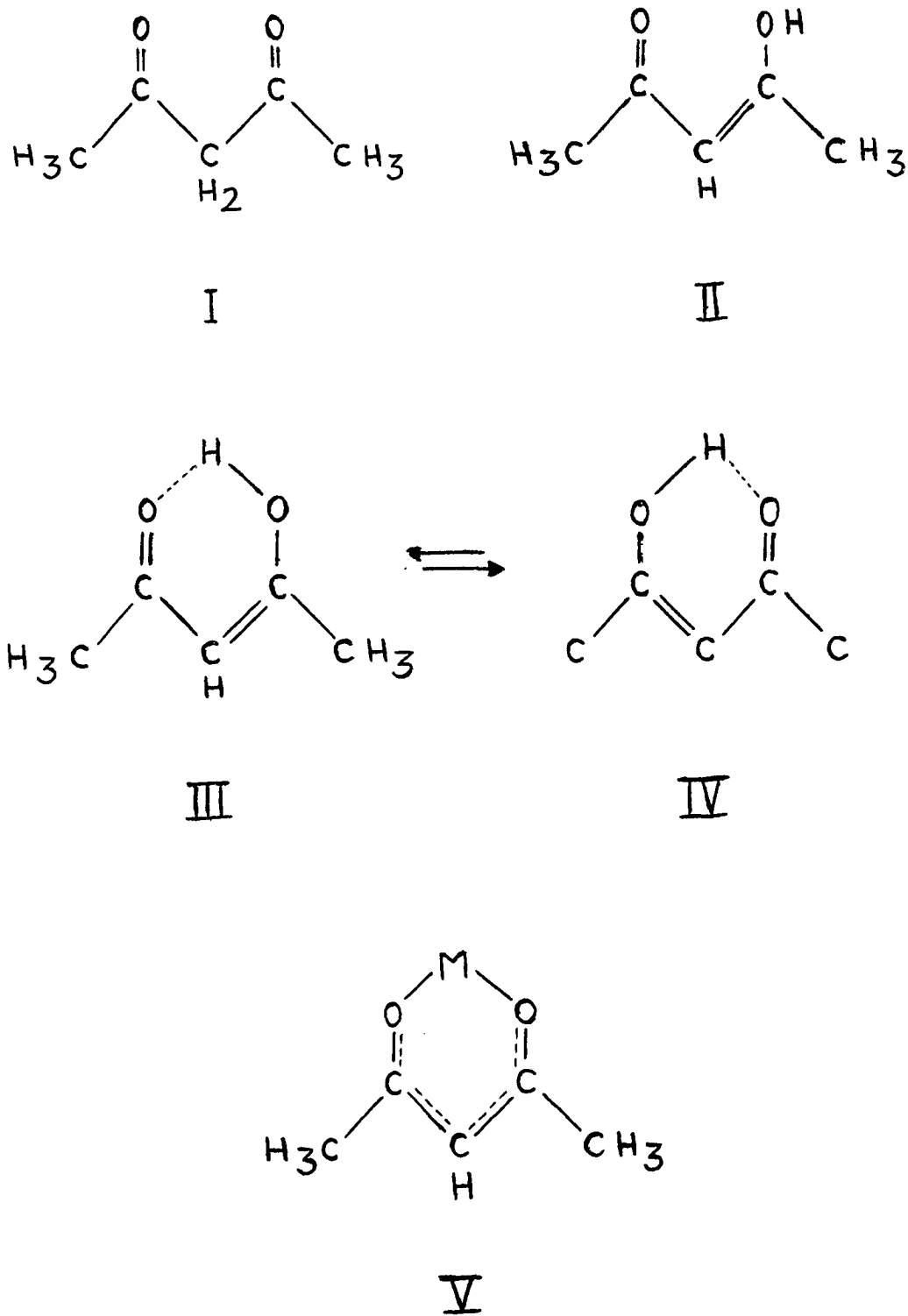


Figure 36. Structures of acetylacetone and its metal chelate

I, II and III). In acac one should consider the following important features of the spectrum: there is an O-H absorption near 2700 cm^{-1} ; there is no C=O absorption at about 1670 cm^{-1} which would be typical of a conjugated ketone; there is an unusually intense broad band in the range of 1640 to 1530 cm^{-1} . All of the above mentioned features of the IR spectrum are consistent with a conjugated chelate structure, that resonates between forms III and IV in Fig. 36, as has been suggested by Rasmussen et al in 1949.⁴⁴

Due to the equilibrium between structures III and IV, in Fig. 36, the double bond character in acac is reduced below that of an ordinary aliphatic ketone, with a corresponding shift of the C=O band to lower frequency. Cotton⁴⁰ also points out that the absence of any overtone band of a hydrogen bonded O-H around 7000 cm^{-1} , as well as the low fundamental O-H absorption, indicate that a hydrogen bridge exists in form III which is of much greater strength than is the ordinary O-H...O bonding. A small absorption band at 1720 cm^{-1} confirms the presence of a small amount of Structure I which possesses normal carbonyl groups. The absence of a band near 1675 , that is characteristic of conjugated aliphatic ketones, is evidence that form II is not very probable. These interpretations of the infrared

spectrum of acac are in agreement with the NMR spectrum of the pure liquid, as reported by Jarrett et al in 1953.⁴⁵

In addition to the spectra of β -diketones reported by Nakamoto et al,^{63b} Lowe and Ferguson⁴⁸ reported the IR spectra of benzoylacetone (bzac) and p-methoxy-benzoylacetone (p-OCH₃-bzac). Liang et al⁴⁹ reported the IR and Raman spectra of Eu(bzac)₄·piperidinium. The IR bands and interpretation by Lowe and Ferguson⁴⁸ for bzac are: 3574 w; 3461 (associated OH); 2520-2460w (intramolecular OH...O=C); 1714w (CH₃-C=O); and 1610-1598s (C=O...H-O). Liang et al listed more bands and included more assignments attributed to the bzac ligand: 1600vs (C=O stretch); 1570s (Ph ring stretch); 1520vs (C=C stretch); 1355m(CH₃ symmetric bend); 1280vs (C-CH₃ stretch and C=C stretch); 1200 m (C-H bend and C=O stretch); 1070w (Ph C-H in-plane bend); 1025m (Ph C-H in-plane bend). For the p-OCH₃-bzac Lowe and Ferguson⁴⁸ reported IR bands at 3636w (free OH); 3484w(assoc. OH); 2793-2591 w (intramolecular OH...O=C); 1712w (CH₃C=O); and 1635-1577s (broad C=O...H-O and C=C).

Bellamy and Beecher⁵⁰ assigned only the carbonyl frequencies in benzoylacetone in 1954. They had assigned the 1724 cm⁻¹ band to the keto and the 1600 cm⁻¹ band to the enol form.

Table II, lists the bands observed in the IR spectrum of our "ligand"-- the p-octyloxy-benzoylacetone (Fig. 12). The relative intensities and the assignments of the more intense bands are in general agreement with those reported for bzac and related compounds by Bellamy⁵⁰, Lowe⁴⁸, by Liang⁴⁹, and Holtzclaw.^{51,52} Ligand bands in the IR region below 1700 cm^{-1} are listed here with their assignments: 1660sh (C=O and C=C stretch); 1630s (mainly C=O stretch); 1570m (Phenyl ring stretch); 1530m (mainly C=C stretch); 1360m (CH_3 symmetric bend); 1280s (C- CH_3 stretch and C=C stretch); 1210m (C-H bend and C=O stretch); 1065w (Phenyl C-H in-plane bend); 1030m (Phenyl C-H in-plane bend); 835s (2 adjacent protons of p-substituted aromatic ring); 790s (C- CH_3 stretch).

The absence of appreciable absorption bands in the ligand at or near 1720 and 1675 cm^{-1} , is taken as evidence that the ligand does not exist in forms analogous to structure I (the diketo form) or structure II (transoid enol) shown in Fig. 36. Most likely the ligand forms an intramolecular hydrogen bonded structure, represented by a hybrid of structures analogous to III and IV. The position of the C=O stretch at 1630 cm^{-1} would be in accord with the estimation by Blout et al⁵³ that conjugation of a carbonyl

TABLE II

COMPARISON OF BAND ASSIGNMENTS IN "LIGAND" WITH
 REPORTED BANDS AND ASSIGNMENTS IN Bzac^(a)
 AND Eu(bzac)₄·PIPERIDINIUM^(b)

Ligand (in Nujol)	Bzac (neat, l.)	Eu(bzac) ₄ piperid	Assignments ^(c)
1660 sh			C=O stretch
1630 s	1604s,b	1600 vs	mainly C=O stretch
1570 m		1570 s	Ph-ring stretch
1530 m		1520 vs	mainly C=C stretch
(Nujol region)		1480 s	Ph-ring stretch
		1460 vs	C-H bend + C=O str.
1360 m		1355 m	CH ₃ symmetric bend
1320 m	1298m,b	1300 m	- - - - -
1280 s		1280 vs	C-CH ₃ str. + C=C str.
1210 m	1198 b	1200 m	C-H bend + C=O str.
1185 s	1178 b	1175 w	- - - - -
1140 m		1155 vw	- - - - -
1120 w	1082 m	1105 m	- - - - -
1065 w	1065 m	1070 w	Ph C-H in-plane bend
1030 m	1025 m	1025 m	Ph C-H in-plane bend
(Nujol region)		995 m	- - - - -
	960 m,b	945 w	complex mode involving C=O stretch
		925 vw	- - - - -
870 m		865 vw	- - - - -
835 s	836 m	840 m	2 adj. arom. H (p-substit.)
790 s			C-CH ₃ stretch

- (a) These absorbance bands reported by Holtzclaw and Collman in reference 51 for benzoylacetone liquid, neat.
 (b) Infrared bands reported by Liang et al in reference 49.
 (c) Most of the assignments were made by comparison with those of Liang et al, which were based on the approximate coordinate analysis for a single chelate ring in Eu(bzac)₄·piperidinium and related compounds.

group by an $\alpha - \beta$ double bond usually lowers the frequency of that carbonyl absorption by about 20 to 30 cm^{-1} . Further evidence for this frequency shift, especially in the aromatic series of carbonyl compounds, comes from a report by Hunsberger et al⁵⁴, who had established the existence of a linear relationship between the carbonyl frequency shift and the double bond character of the ring bond that plays a part in the chelation.

In attempting to interpret the infrared spectra of metal chelates of acac, i.e. either the bis or the tris metal acetylacetonates, most investigators found it necessary to make the simplifying assumption that the two or three chelate rings are independent to some extent. Cotton⁴⁰ points out that such a simplification is probably quite satisfactory for the interpretation of most C-C, C-O and C-H stretches. On the other hand, the metal-oxygen bonds probably have to be considered in terms of the symmetry of the entire molecule, since M-O stretches in one ring will be rather strongly coupled to those in the other rings, through the common metal atom.⁴⁰

In contrast to the numerous literature reports on the IR spectra of acetylacetonates and other metal- β - diketonates, only a handful of pertinent Raman spectra have

been reported. The Raman spectra of benzoyl-acetone, dibenzoylmethane, $\text{Be}(\text{acac})_2$ and $\text{Zn}(\text{acac})_2$ were reported by Kahovec and Kohlrausch⁵⁵ in 1940. D. N Shigorin^{56,57} had reported the existence of two weak bands in the Raman spectra of Mg, Ni, Zn and Al acetylacetonates in 1953. The Raman spectra of the tris acac chelates of Al, Ga and In were reported by Hester and Plane in 1964.⁵⁸ The Raman spectra of $\text{Eu}(\text{acac})_3 \cdot 2\text{H}_2\text{O}$ and of $\text{Eu}(\text{bzac})_4$ piperidinium salt were reported by Liang et al⁴⁹ in 1970. Assignments of Raman bands are included only in the reports by Hester and Plane,⁵⁸ and by Liang⁴⁹ in the region below 1650 cm^{-1} .

Most of our discussion of the pertinent Raman data will be deferred to the discussion of the region below 500 cm^{-1} . It will be shown that the selection rules based on group theoretical considerations, and a comparison of infrared and Raman bands due to the M-O vibrations, were extremely helpful in the assignment of molecules to a particular symmetry group, and thus provided a basis for the assignment of geometry in $\text{Pd}(\text{bzac})_2$, PdL_2 Species I, and PdL_2 Species II. The discussion of the infrared spectra of metal-acac complexes can be conveniently divided into several important regions: (a) 4000 to 1650 cm^{-1} , (b) 1650 to 1200 cm^{-1} , (c) 1200 to 400 cm^{-1} . In addition, (d) infrared

evidence for the presence of a metal-carbon bond will be discussed; i.e. bonding between the metal and the "gamma" carbon of the chelate ring.

(a) Considering first the 4000 to 1650 cm^{-1} region of the IR spectrum, it has been reported that the OH...O absorption of the acac disappears upon chelation with the metal (Structure V in Fig. 36). The symmetric and anti-symmetric methyl stretching frequencies appear around 2870 and 2970, respectively.⁴⁰ Cotton and Holm⁵⁹ reported that the C-H stretch of the "middle" or "gamma" carbon of the unchelated acac ring moves to slightly higher frequencies upon chelation. It seems quite reasonable that resonance in the ring changes the environment of that proton from an olefinic to a pseudo-aromatic proton. Calvin and Wilson⁶⁰ have suggested that the conjugation is extended through the metal atom. They have used that conjugation as an explanation of the high stability of metal-acac complexes. Cotton and Holm⁵⁹ found that the "gamma" C-H stretching absorption in complexes of Fe(III), Co(III), Mn(III) and Cr(III) occurred at about 3090 cm^{-1} (in spectra of CHCl_3 solutions of the compounds). It should be noted that in compounds of the type $\text{R}'\text{R}''\text{C}=\text{H}_2$ the C-H infrared frequency is at 3075 - 3085 cm^{-1} , while in benzene a similar stretch is at 3099 cm^{-1} .

Thus, in the metal-chelated β -diketonates the C-H infrared frequency lies closer to the aromatic frequency.

Inasmuch as the organo-palladium compounds investigated in our laboratory have a very limited solubility in CCl_4 , CS_2 , CHCl_3 and other IR solvents tried, most of the IR spectra were obtained on Nujol mulls. It is difficult, therefore, to discuss any changes in either the CH_3 or C-H stretching frequencies upon chelation, since those regions of the spectrum (2800 to 3100 cm^{-1}) show strong Nujol bands. It was attempted to compare those regions in the Raman spectra of the ligands (bzac, acac, and p-octyloxy-bzac) with those of the appropriate palladium chelates.

In the Raman spectra of the acetylacetonato complexes Hester and Plane⁵⁸ observed a doublet, which they attributed to $\nu(\text{C-H})$ Fermi resonance; the stronger line was observed around 2930 and the weaker line around 2950 cm^{-1} . In $\text{Al}(\text{acac})_3$ the doublet was seen at 2927 and 2952 cm^{-1} ; in $\text{Ga}(\text{acac})_3$ at 2930 and 2950 cm^{-1} ; and in $\text{In}(\text{acac})_3$ at 2928 and 2950 cm^{-1} . Kahovec and Kohlrausch⁵⁵ reported a strong Raman band in benzoylacetone at 2919 cm^{-1} , with no assignment given. It seems likely that in the Raman spectra of those compounds the C-H stretching frequency is seen in the region of 2920 to 2930 cm^{-1} .

In the Raman spectra investigated here a band was seen at 2920 cm^{-1} in acac, in bzac, and in the ligand (Fig. 37). In the Pd-chelates this band was observed at 2930 in $\text{Pd}(\text{acac})_2$ (Fig. 38), in $\text{Pd}(\text{bzac})_2$ (Fig. 39), and in PdL_2 Species II (Fig. 41-b). In PdL_2 Species I (Fig. 40) the band was observed at 2920 cm^{-1} . If the shift of the C-H band to higher frequencies upon chelation is taken as a measure of greater "aromaticity", as suggested by Cotton and Holm⁵⁹, one would conclude that PdL_2 Species II is more "aromatic" than PdL_2 Species I.

(b) The next region to be considered in the IR spectrum is from 1650 to 1200 cm^{-1} . This is the region potentially most informative about the electronic distribution in the chelate ring. Because of resonance all the carbon-carbon and carbon-oxygen bond orders should average out to about 1.5. In addition, as pointed out by Holtzclaw and Collman⁵¹, if there is more conjugation between the metal ion and oxygen in one acetylacetonate than in another, there should be also variation in the C-O bond order and in the C-O stretching frequency. Several attempts have been made to correlate stability constants with variations in the frequency bands assigned as carbonyl stretching frequencies.

Figure 37

Raman spectrum of solid sample of ligand.
Regions omitted showed no Raman scattering bands.

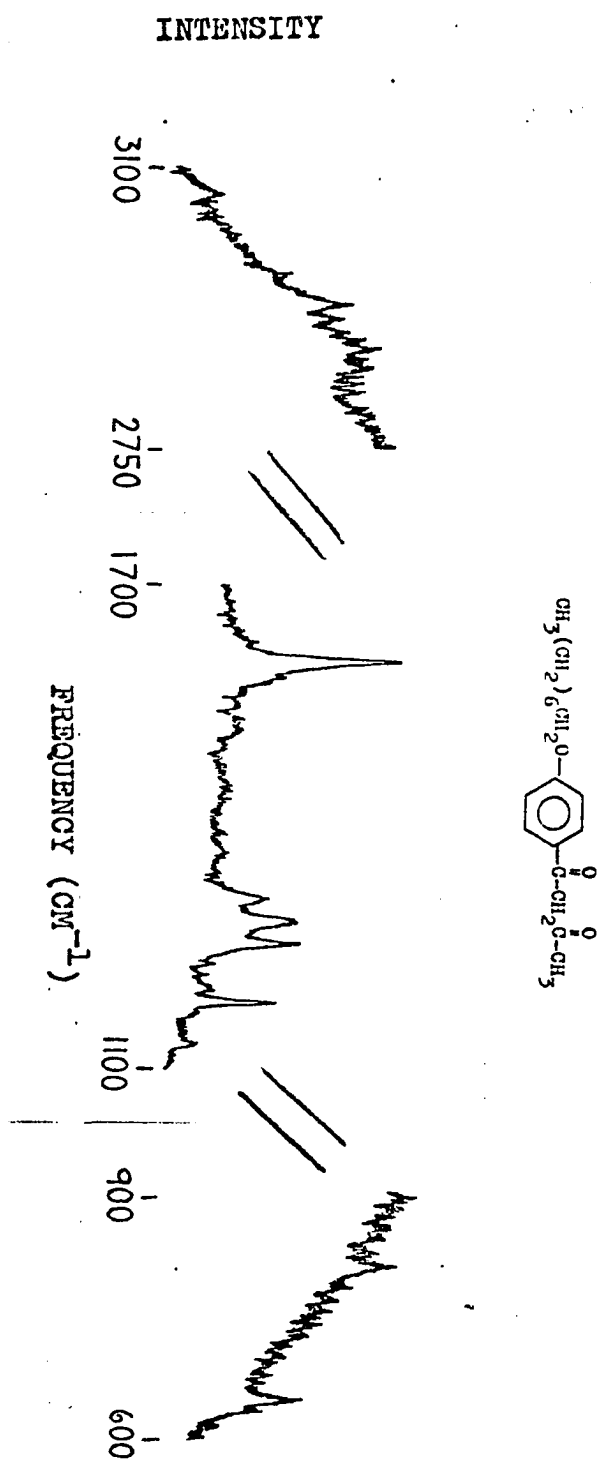


Figure 37

Figure 38

Raman spectrum of solid sample of $\text{Pd}(\text{acac})_2$.
Regions omitted showed
no Raman scattering bands.

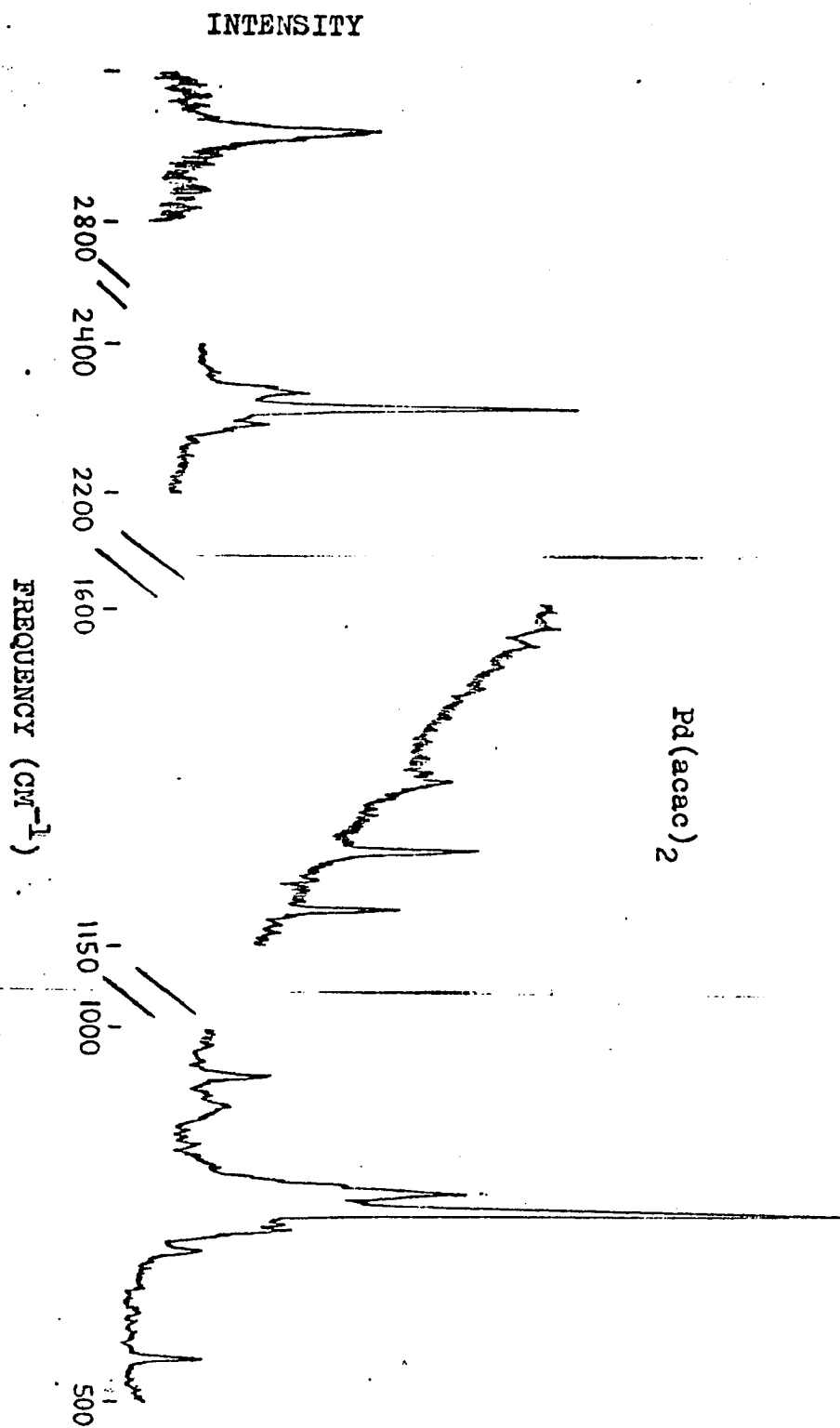


Figure 38

Figure 39

Raman spectrum of solid sample of $\text{Pd}(\text{bzac})_2$.

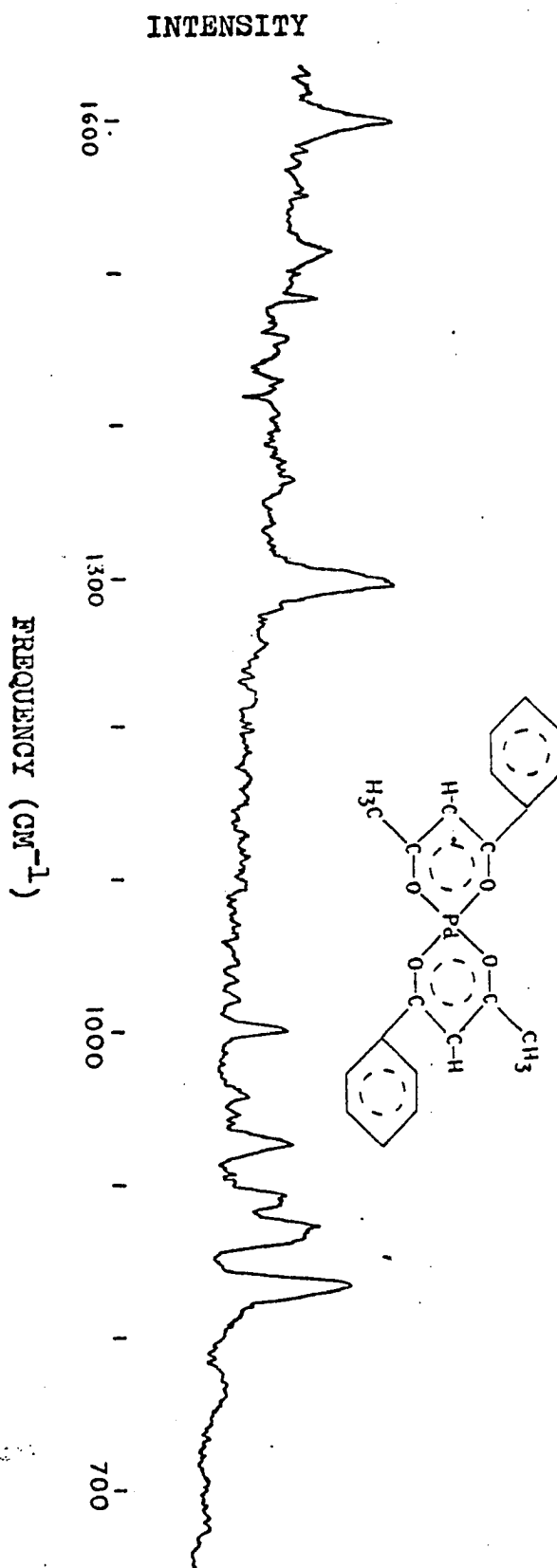


Figure 39

Figure 40

Raman spectrum of PdL₂ Species I.
Regions omitted showed no Raman scattering bands.

PdL₂ Species I

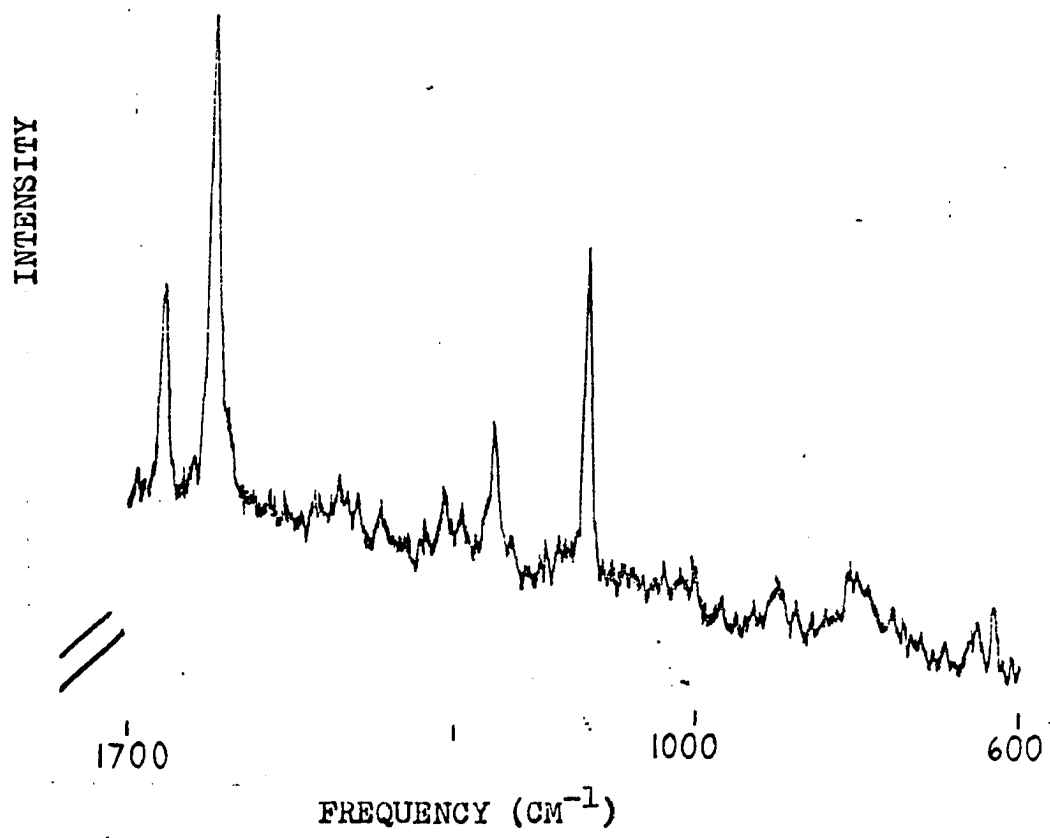
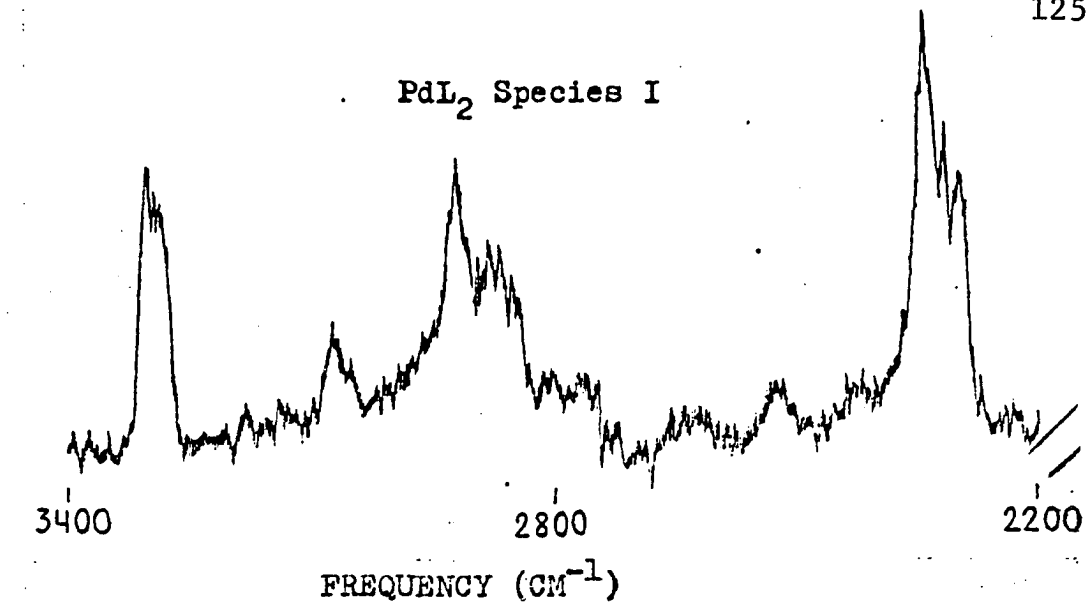


Figure 40

Figure 41-A

Raman spectrum of PdL₂ Species II,
showing region from 300 to 1650 cm⁻¹

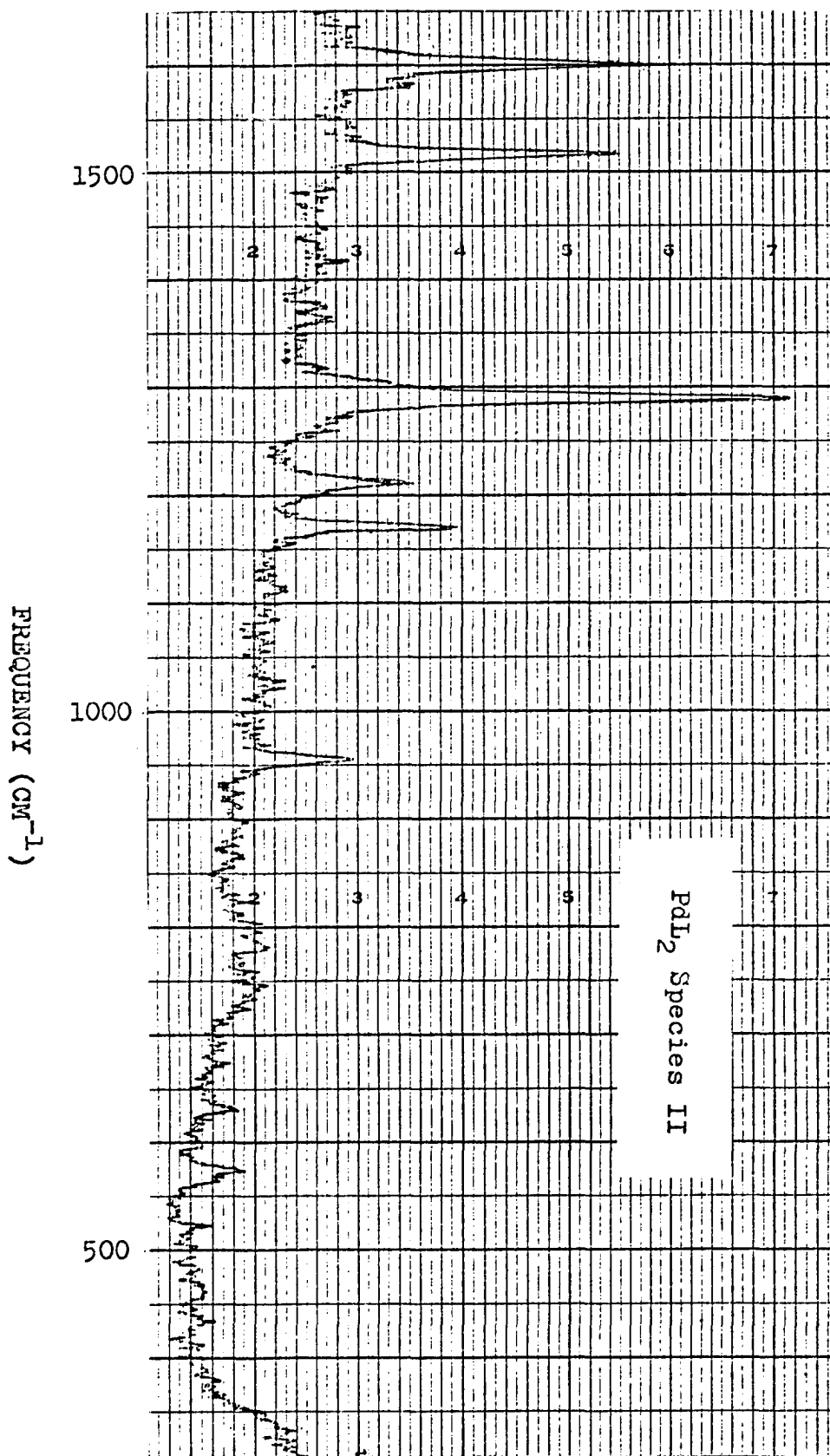


Figure 41-A

Figure 41-B

Raman spectrum of PdL₂ Species II,
showing region from 2750 to 3500 cm⁻¹

INTENSITY

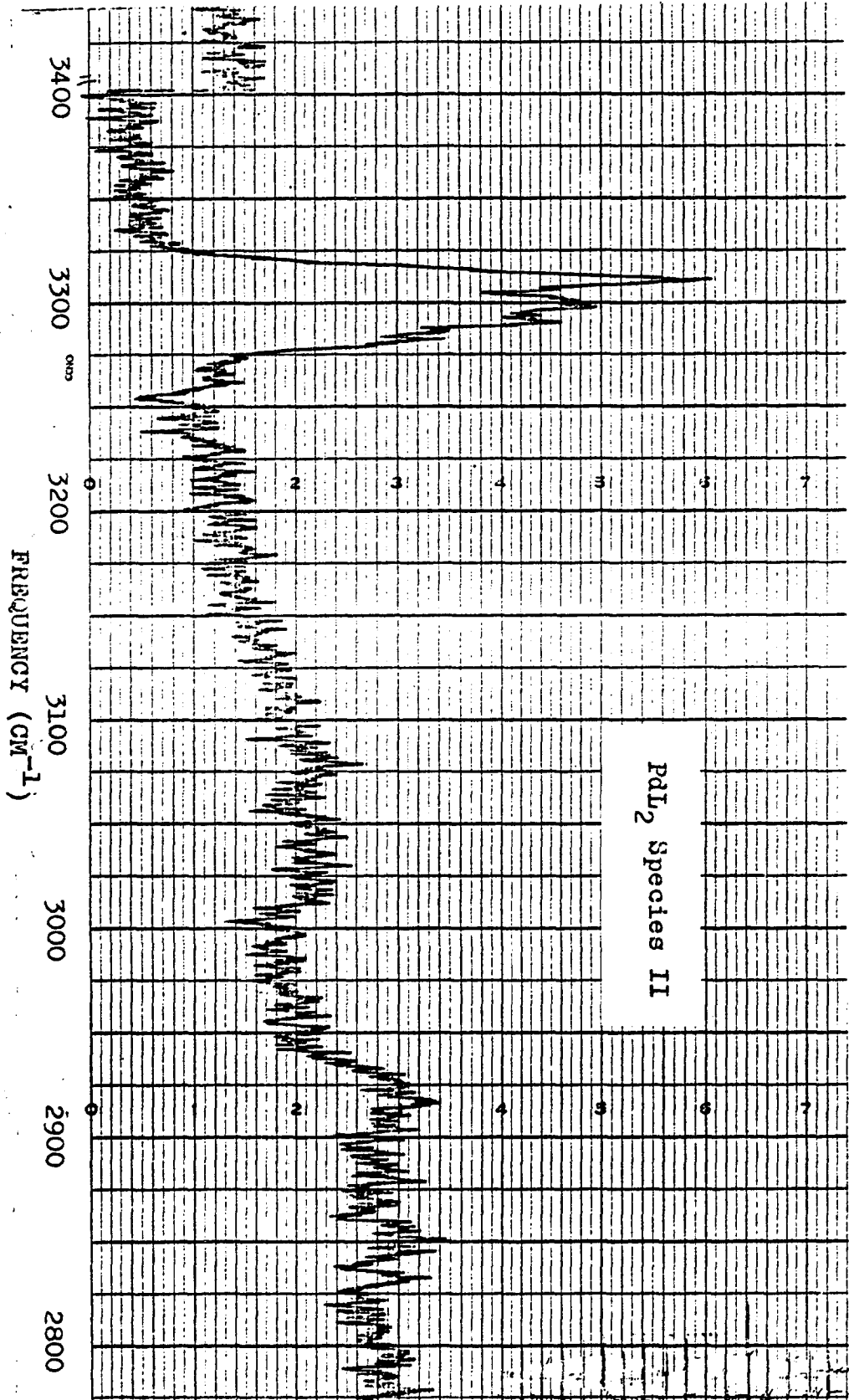


Figure 41-B

The nature of the 1577 and 1529 cm^{-1} band in $\text{Cu}(\text{acac})_2$ and other related metal acetylacetonates has been the subject of much controversy. Originally, Nakamoto and Martell in a series of papers^{61,62} assigned the former band to a $\text{C}=\text{C}$ stretching and the latter to a $\text{C}=\text{O}$ stretching mode, indicating that the first band had 75% $\text{C}=\text{C}$ and only 25% $\text{C}=\text{O}$ character, while the second band arose from the same bonds with the proportions reversed. This assignment has been accepted in some of the reports that followed, and criticized by others. It might be pointed out that among the papers that contributed to this controversy are reports by Pinchas et al^{63a}, Bock et al⁴³, Musso and Junge⁶⁴, Mikami et al⁶⁵, Bellamy and Branch⁶⁶, Holtzclaw and Collman⁵¹, West and Riley⁶⁷, Benke and Nakamoto^{68,69}, and Nakamoto et al.^{46,47,70} While some of the reports agree with the original assignment, others believed that the two assignments should be reversed. The results of recent isotope substitution studies, involving ^{13}C and ^{18}O , by Pinchas et al^{63a} as well as Musso and Junge⁶⁴, suggest that the band in the 1580 cm^{-1} region is the $\text{C}=\text{O}$ stretching and the one in the 1530 cm^{-1} region is the $\text{C}=\text{C}$ stretching frequency. Further confirmation of bands assigned in metal acac complexes, especially those due to the metal-

ligand vibrations, came from metal isotope substitution studies by Nakamoto et al⁷⁰ in pentanedionato complexes of Fe(III), Cr(III), Pd(II), Cu(II) and Ni(II), which were highly enriched in the heavier metal isotopes.

Holtzclaw and Collman⁵¹, who had used the higher frequency band as the carbonyl, and the second one as the C=C stretching vibration, attempted to correlate stability constants of the chelate with variations in the frequency of the carbonyl band. They pointed out that a relationship should exist between the strength of the metal-oxygen bond and the frequency of the C-O bond, since the bond strength of the C-O bond should decrease as the M-O bond strengthens. Using their assignments of the carbonyl frequency, Holtzclaw and Collman obtained good "qualitative correlation" between band position and the known order of stability constants for the acac complexes of Na(I), Ni(II), Mg(II), Cd(II), Mn(II), Co(II), Cu(II) and Pd(II). With the exception of nickel complexes which were out of "sequence", the frequencies of the carbonyl band decreased in the order given, while the stability constants of the complexes are known to increase in the same order. The stability constants of the metal acac complexes had been estimated from pH values by Van Uitert.⁷¹

Inasmuch as the compounds investigated here are

structurally closer to $\text{Pd}(\text{bzac})_2$ than to $\text{Pd}(\text{acac})_2$, one should examine previous investigations of the effect of substituting a phenyl group (or some other group) for one or both of the methyl group in the acac chelate. Bellamy and Branch⁶⁶ reported and compared the spectra of dilute CHCl_3 solutions of $\text{Cu}(\text{acac})_2$, $\text{Cu}(\text{bzac})_2$ and $\text{Cu}(\text{dibenzoylmethane})_2$. The latter compounds will henceforth be referred to as $\text{Cu}(\text{dbm})_2$. Holtzclaw and Collman^{51,52} reported the IR spectra of acac, $\text{Pd}(\text{acac})_2$, bzac; the spectrum of $\text{Cu}(\text{bzac})_2$, was reported by Holtzclaw et al.⁷² Although in 1959 Nakamoto et al⁴⁷ investigated the infrared spectra of several substituted metal β -diketonates of Cu(II), Ni(II), Cu(II), Pd(II) and Al(III), including $\text{Cu}(\text{acac})_2$, $\text{Cu}(\text{bzac})_2$, $\text{Pd}(\text{acac})_2$ and $\text{Pd}(\text{bzac})_2$, they had reported only the metal-oxygen stretching frequencies in those, and not the carbonyl frequencies. In a 1962 report Nakamoto et al⁷³ reported the spectra of Cu(II) and Ni(II) substituted metal acac complexes, with the CF_3 and C_6H_5 - substituents replacing one, or both, of the CH_3 groups of the acac ring.

Nakamoto et al⁷³ believe that the inductive electron-withdrawing effect of the phenyl substituent can be neglected. The most important electronic effects of the phenyl "lie in its mesomeric interaction with the semi-aromatic metal chelate ring". As a result of the latter resonance effect,

the pi-electrons are shifted from the phenyl to the chelate ring, which leads to a general strengthening of the M-O bonds through an increase of the negative charge on the oxygen atoms, as in contributing resonance structures B and C shown below.

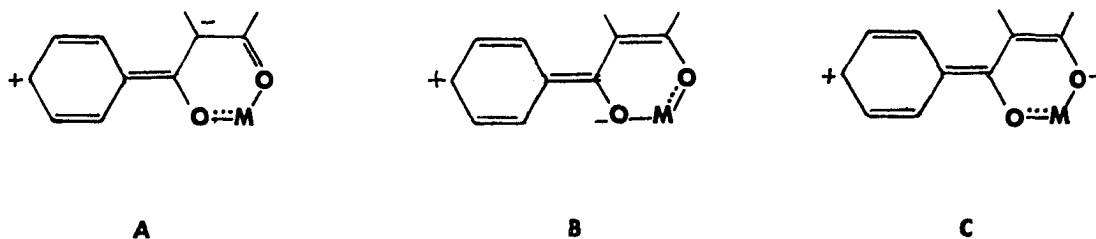


Table III shows the frequencies listed by Nakamoto et al.⁷³ for the C=C stretch, the C=O stretch, as well as the M-O stretch for the acac, bzac and dbm complexes of Cu(II) and Ni(II). Attention should be called, however, to the assignment of the upper frequency band to the carbonyl stretch, and the lower to the C=O stretch. In view of the more recent reports on the controversy of these two assignments discussed before, these two bands should probably be reversed. It should also be pointed out that in Nakamoto's report there was satisfactory agreement between the calculated and observed bands for the symmetrical ligands, but there were no calculations for the "unsymmetrical" benzoylacetone complexes.

TABLE III
 SELECTED INFRARED BANDS IN Cu AND Ni COMPLEXES

$\text{Cu}(\text{acac})_2$	$\text{Cu}(\text{bzac})_2$	$\text{Cu}(\text{dbm})_2$	$\text{Ni}(\text{acac})_2$	$\text{Ni}(\text{bzac})_2$	$\text{Ni}(\text{dbm})_2$	Stretching Mode
1580	1590	1593	1598	1591	1595	C=C
1548, 1524	1554	1544	1508	1591	1595	C=O
455	458	462	452	455	458	M-O

One should be able to compare the shifts of the carbonyl and the M-O bands due to phenyl substitution. These bands were compared by Nakamoto with the stability constants of the complexes, as calculated by Van Uitert⁷¹ in a 75% dioxane-water mixture. The $\log K_1K_2$ calculated in the Cu(II) series had been reported as 23.66 for the acac complex, 23.01 for the benzac and 24.94 for the dbm complex. In the Ni(II) series, the respective values of $\log K_1K_2$ were 17.08, 18.00 and 20.72.

Whether one considers the upper bands or the lower bands reported by Nakamoto to represent the C=O stretch, there is no regular correlation between the frequency shift and the stability constants of the complexes. Nor is there a pronounced regular trend in the changes in the stability constants, although it does appear that in the Ni(II) series the introduction of the phenyl ring makes the complex more stable. On the other hand, the trend in the M-O frequency shift seems more regular; i.e. the introduction of one phenyl substituent shifts the M-O frequency to higher values - from 455 to 458 in Cu(II), and from 452 to 455 cm^{-1} in Ni(II) - indicating a strengthening of the M-O bond. This trend is also observed in the introduction of a second phenyl substituent, since the frequencies shift from 458 cm^{-1} to 462 cm^{-1}

in Cu(II) and from 455 to 458 cm^{-1} in Ni(II), on going from $\text{M}-(\text{bzac})_2$ to $\text{M}-(\text{dbm})_2$.

It is not the intent of this discussion to suggest that the comparisons of the effects of phenyl substitution on M-O stretching frequencies in the compounds investigated by Nakamoto constitutes a definite trend to be expected in all cases. In fact, one should keep in mind the suggestions by Holtzclaw and Collman⁵¹ on this subject. Holtzman pointed out that one should expect a qualitative correlation between stability of complexes and the carbonyl frequency shift, but only when comparing a series of complexes of different metals with the same ligand. The position of the carbonyl band depends largely on three factors: (1) the masses of the groups attached to the carbonyl; (2) the interaction of the carbonyl with any neighboring π - or d-orbitals; and (3) the relative electron density of the sigma-bonds, which is largely controlled by the electronegativity of the groups attached to the carbon of the carbonyl group.

In practice it may be difficult to evaluate each of the above three factors separately. In comparing a series of metal acac complexes, according to Holtzclaw, any effect which strengthens the metal oxygen bond also weakens the

carbon-oxygen bond. On the other hand, when comparing a series of various β -diketonates of the same metal, one or more of the three effects -- i.e. difference in mass, in resonance, and in inductive effects -- must be attributed essentially to the ligand, since the metal remains the same. The relative magnitudes of these three effects as one changes from ligand to ligand need not be the same, nor are they necessarily expected to change in the same direction. Hence, the overall relative effects on the metal-oxygen bond and on the carbonyl bond need not be the same.

Considering next the position of the carbonyl band and other important bands in the 1650 to 1200 cm^{-1} region observed in the organo-palladium compounds in this investigation, it should first be pointed out that the complete IR spectrum of $\text{Pd}(\text{bzac})_2$ has not been previously reported, since only the M-O stretching frequency was listed by Nakamoto et al.⁴⁷ In 1967 and 1968 Singh and Sahai^{74,75} investigated the nitro-substituted analogues of $\text{Pd}(\text{acac})_2$ and $\text{Pd}(\text{bzac})_2$, with the $-\text{NO}_2$ group substituted in each case for the "gamma" proton of the chelate ring. In the nitro-analogue of $\text{Pd}(\text{acac})_2$ Singh⁷⁴ reported the carbonyl band at 1560 cm^{-1} , or about 10 cm^{-1} lower than the band in $\text{Pd}(\text{acac})_2$ reported by Nakamoto et al.⁶¹ and by Mikami et al.⁶⁵ The carbonyl

band in the nitro-analogue of $\text{Pd}(\text{bzac})_2$ was reported by Singh and Sahai at 1550 cm^{-1} .

The infrared spectrum of $\text{Pd}(\text{bzac})_2$ is shown in Fig. 16. The uppermost band in that region is seen at 1590 cm^{-1} , probably due mainly to the carbonyl stretch. The shoulder at 1560 is due to one of the phenyl ring stretches, the doublet at 1540 and 1520 is due mainly to the C=C, probably coupled to the phenyl ring stretch; the band at 1480 cm^{-1} is due to another phenyl ring stretch.

Table IV lists the absorbances in this region of the "ligand", and both chelates; i.e. PdL_2 Species I and PdL_2 Species II. It can be seen that the carbonyl band appears in the ligand at 1630, with a shoulder at 1660, appears in Species I of PdL_2 at 1630 cm^{-1} , and in Species II of PdL_2 at 1620 cm^{-1} . The phenyl ring stretch, seen in the ligand at 1570 cm^{-1} , is assigned to 1580 cm^{-1} in Species I and 1590 cm^{-1} in Species II. The band attributed mainly to the C=C stretch appears in the ligand at 1530 cm^{-1} ; at 1550 cm^{-1} in Species I; and at 1530 cm^{-1} , with a shoulder at 1550 cm^{-1} , in Species II. No generalization will be attempted as to the relative strength of the C-O bonds in these compounds, as judged from the frequency shift of the carbonyl band. (Figs. 12, 19, 23)

TABLE IV

COMPARISON OF INFRARED STRETCHING FREQUENCIES
OF LIGAND, SPECIES I AND SPECIES II
IN CARBONYL REGION

<u>Ligand</u>	<u>PdL₂, Species I</u>	<u>PdL₂, Species II</u>	<u>Assignment</u>
1660sh 1630	1630	1620	mainly C=O stretch
1570	1580	1590	Ph-ring stretch
1530	1550	1550 sh and 1530	mainly C=C stretch

(c) The region from 1200 to 400 cm^{-1} will be considered next. As pointed out by Cotton⁴⁰, the assignment of absorption bands in this region is extremely difficult and "has not often been attempted in any systematic way". This is the region in which C-H deformations, ring deformations and metal-oxygen bonding and stretching modes may be expected, probably with considerable coupling between those modes.

The most important assignments in this region are for the M-O stretching frequencies, and these should be extended into the far IR. In 1959 Nakamoto et al⁴⁷ measured the spectra of 32 compounds in the 1700 to 300 cm^{-1} region, using optical components of sodium chloride, potassium bromide and cesium bromide. In their report of the M-O band frequencies in the 420 to 480 cm^{-1} region, they point out that the bands shift to higher frequencies and increase in intensity as the metal is changed. The order of the shifts corresponds to the order of stability for the following metals investigated:



In the acetylacetonato complexes the M-O bands shift, respectively, from 420 cm^{-1} in $\text{Co}(\text{acac})_2$ to 453, 455, and to 465 in $\text{Pd}(\text{acac})_2$. In case of the bzac complexes, the bands are as follows: 423 in $\text{Co}(\text{bzac})_2$, 455 in $\text{Ni}(\text{bzac})_2$, 458 in $\text{Cu}(\text{bzac})_2$ and 478 in $\text{Pd}(\text{bzac})_2$.

In the compounds investigated in this laboratory, the metal-oxygen bands have been assigned, in the far IR region and in the Raman, as discussed in the next section. The metal-oxygen modes were assigned in $\text{Pd}(\text{bzac})_2$, PdL_2 Species I and PdL_2 Species II by comparison with those previously assigned by Nakamoto^{47,61} and Mikami⁶⁵ and by comparison with the appropriate Raman bands, as predicted by selection rules. Here only one of the strongest bands in the far IR region around 450 cm^{-1} , in all four Pd-diketonates, will be considered, with its symmetry representation given.

The band which is seen in $\text{Pd}(\text{acac})_2$ at 464 cm^{-1} (B_{1u}), appears at 480 cm^{-1} (B_{1u}) in $\text{Pd}(\text{bzac})_2$; at 469 cm^{-1} (B_2) in PdL_2 Species I, and at 448 cm^{-1} (B_{1u}) in PdL_2 Species II. From the trend in the frequency of that single metal-oxygen band, which is due to a fundamental angle deformation mode ν_2 , one might conclude that the Pd-O bond in both PdL_2 compounds prepared is weaker than the corresponding bond in $\text{Pd}(\text{bzac})_2$. However, this lowering of the frequency of the M-O bond may be simply due to the greater mass of the ligand employed, and need not represent a change in bond strength. Comparing only the two PdL_2 compounds, Species I and II, in which the mass of the ligand is identical, it appears that

the Pd-O bond is weaker in Species II (448 cm^{-1}) than in Species I (470 cm^{-1}).

(d) Collman et al⁷⁷ discuss some infrared criteria for the presence of the so-called "gamma" proton of the chelate ring. These complexes that do have a proton on the central carbon of the chelate, show two infrared bands: a doublet in the 1500 to 1600 cm^{-1} region. However, substituted metal acac complexes, show only a single band at about 1550 cm^{-1} . This feature of the spectrum was also reported by Dryden and Winston in 1958,⁷⁸ and they attributed the upper frequency band to the doublet of the chelated carbonyl group; the lower band had been assigned to the partial double bond of the chelate ring. This lower frequency band was thought to disappear upon substitution of another group in the "gamma" position, due to a mass effect.

In 1974 Baba et al⁷⁹ reacted bis(acetylacetonato)-palladium(II) with triphenylphosphine and nitrogen bases such as pyridine, diethylamine, and N-methylbenzylamine. They found that one of the chelating acac ligands was transformed into a carbon-bonded ligand, with the base L occupying the fourth coordination site of the palladium. The product complexes of the type $\text{Pd}(\text{acac})_2\text{L}$ were characterized by their IR and NMR spectra. In case of the oxygen-bonded acac ligand

Baba reported bands, assigned to the $\nu(\text{C}=\text{O})$ and $\nu(\text{C}=\text{C})$ in the 1500 to 1600 cm^{-1} region. In the carbon-bonded ligand the $\nu(\text{C}=\text{O})$ vibration was seen in the 1600 to 1700 cm^{-1} . In addition, strong bands were observed in the 500 to 550 cm^{-1} region, attributed to the $\nu(\text{Pd}-\text{C})$ vibration. The Pd-C vibration was observed at 518, 519, 524 and 540 cm^{-1} , the position of that band differing slightly with the differing bases used as the L group.

The compounds in this investigation have no bands in the Pd-C region, so one can eliminate from consideration structures involving palladium-carbon bonded isomers.

Experimental Evidence for Structure Assignments

The most important evidence for the assignment of structures and distinguishing between Species I and Species II of the PdL_2 compounds prepared, comes from the comparison of the Raman and infrared spectra of the two compounds. In this connection, the most relevant motions to be examined and analyzed are those directly involving the $-\text{PdO}_4$ -subunit of the molecule, since those modes will be most directly affected by changes in the geometry of the molecule. In this investigation we derived the selection rules predicted by group theoretical considerations, as well as compared our band assignments with those reported in the literature for similar systems, where assignments had been made from force constant calculations⁶¹ and metal isotope effects on certain vibrations.^{46,70}

For a general N-atom molecule, or in our case a subunit of the molecule containing N atoms, the number of normal vibrations is only $3N - 6$, since six coordinates are required to describe the translational and rotational motion of the molecule as a whole. Using group theory it is possible to find the number of normal vibrations belonging to each species. The principle of the method is that all representations are irreducible if normal coordinates are used as the basis for the representations.

Selection rules for infrared and Raman spectra are based on quantum mechanics. The selection rule for the infrared spectrum is determined by the integral:

$$[\mu]_{\nu, \nu'} = \int \Psi_{\nu'}(Q_a) \mu \Psi_{\nu}(Q_a) dQ_a \quad (11)$$

In equation 11 μ is the dipole moment in the electronic ground state, Ψ is the vibrational eigenfunction, and ν and ν' are the vibrational quantum numbers before and after the transition, respectively. The activity of the normal vibration with normal coordinate Q_a is being determined. By resolving the dipole moment into the three components in the x, y and z direction, the selection rule can be restated in terms of those coordinates. Thus, a fundamental mode will be infrared active, i.e. it will give rise to an absorption band, if the normal mode belongs to the same representation as any one of the Cartesian coordinates.⁸⁰

Similarly, the selection rule for the Raman spectrum is determined by the integral:

$$[\alpha]_{\nu, \nu'} = \int \Psi_{\nu'}(Q_a) \alpha \Psi_{\nu}(Q_a) dQ_a \quad (12)$$

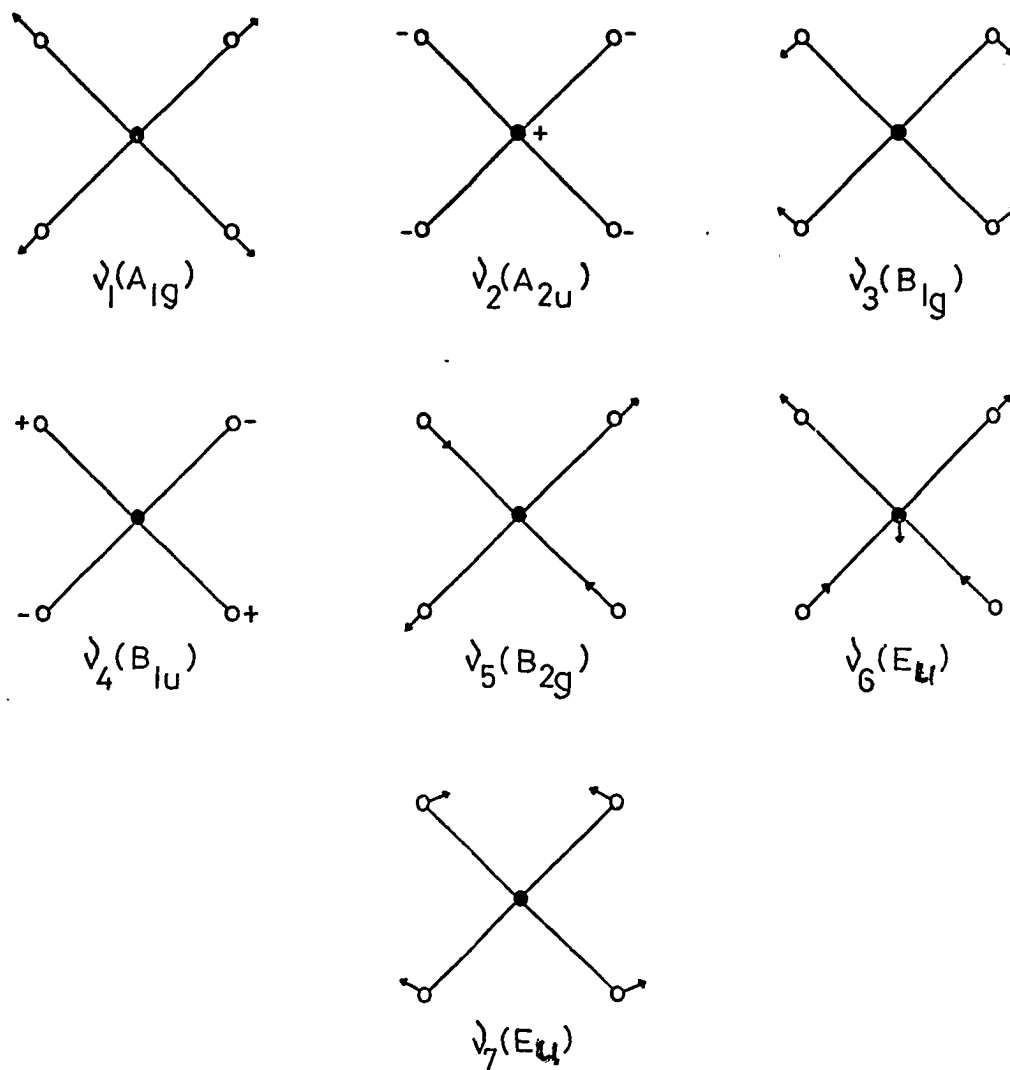
Equation 12 may be resolved into six components; α_{xx} , α_{yy} , α_{zz} , α_{xy} , α_{yz} , α_{xz} . If one of these integrals is not

zero, the normal vibration associated with Q_a is Raman active. If all the integrals are zero, the vibration is Raman inactive. In practice it is possible to decide whether or not the integrals are zero or nonzero from a consideration of symmetry. Therefore, a fundamental transition will be Raman active if the normal mode involved belongs to the same representation as one or more of the components of the polarizability tensor of the molecule.⁸⁰

A truly square-planar molecule of the type MX_4 , in which all the M—X bonds are of equal length, would be of D_{4h} symmetry. The fundamental modes of such a system are shown in Fig. 42.

For a group of five atoms the number of fundamental vibrations would be $3N - 6$ or nine. In actuality, as seen in Fig. 42, there are two doubly degenerate stretching modes (ν_6 and ν_7). The seven fundamental modes divide themselves in the following manner: $\nu_1 (A_{1g})$ is the symmetrical stretch; $\nu_2 (A_{2u})$ is a deformation mode; $\nu_3 (B_{1g})$ is a deformation mode; $\nu_4 (B_{1u})$ is inactive by both Raman and IR selection rules; $\nu_5 (B_{2g})$ is the asymmetric stretch; ν_6 and ν_7 are the above mentioned doubly degenerate modes of E_u symmetry.

Character tables for the D_{4h} group (Appendix II) can



Normal modes of a square planar MX_4 molecule (D_{4h})
 (From Adams, reference 81, p. 30)

Figure 42

be used to determine the selection rules. Thus, the ν_1 , ν_3 , and ν_5 modes should be Raman active, while the ν_2 , ν_6 and ν_7 should be IR active, with ν_4 being inactive in Raman and IR, as mentioned before. In D_{4h} symmetry one would expect no coincidences between Raman and IR active bands, and only 6 bands should be observed.

In the $--PdO_4--$ subunit of any of the molecular systems that will be considered here the four Pd-O bonds are not identical; the symmetry of the system is reduced. We used correlation tables to work out selections rules for the lower symmetry molecules.⁸¹ For example, the simplest of the Pd-beta-diketonates, the $Pd(acac)_2$ molecule, has been investigated and described by Nakamoto et al in 1961⁶¹ and by Mikami et al in 1967.⁶⁵ Both of those reports contain careful assignments of the infrared bands, based on calculations. $Pd(acac)_2$ had been analyzed by Mikami and assigned to the D_{2h} symmetry group. Nakamoto⁶¹ and Mikami⁶⁵ had reported the IR and far IR spectra of $Pd(acac)_2$, but no Raman spectra were reported by either of those investigators.

Of the modes that involve the M--O stretching or deformations, or modes that are coupled with either of the above, Nakamoto calculated that the M--O stretch (ν_5) should

appear at 472 cm^{-1} (observed at 464), and the ring deformation M--O stretch (ν_4) was calculated at 648 cm^{-1} and observed at 676 cm^{-1} . Mikami's report included observations of bands in the lower cm^{-1} and into the far IR region. The actual modes that are of interest for purposes of comparison in the present research are shown on Fig. 43. For the entire molecule the Mikami modes are shown in his article, and here only the three modes of interest: ν_{11} (B_{1u}) which is like the ν_2 mode previously described in a D_{4h} hypothetical MX_4 or $-\text{PdO}_4-$ subunit; the ν_{25} (B_{2u}) mode that is similar to the ν_7 mode in D_{4h} symmetry; and the ν_{32} (B_{3u}) mode which is similar to the ν_6 mode in D_{4h} . Mikami⁶⁵ had calculated that the ν_{11} should appear at 456 cm^{-1} , and observed it at 463 cm^{-1} ; (within the experimental error limits in good agreement with Nakamoto). The ν_{25} mode Mikami calculated to be at 302 cm^{-1} and observed at 294 cm^{-1} ; and the ν_{32} mode was calculated for 263 cm^{-1} and observed at 259 cm^{-1} . In addition, Mikami⁶⁵ also observed several bands in the far IR at 220, 174, 105 and 94 cm^{-1} ; these he calculated to correspond to ν_{13} (B_{1u}) at 221, the ν_{33} (B_{3u}) at 181, ν_{34} (B_{3u}) at 103 cm^{-1} , respectively. These three calculated absorptions appear in fairly good agreement with the weak bands observed. Mikami also

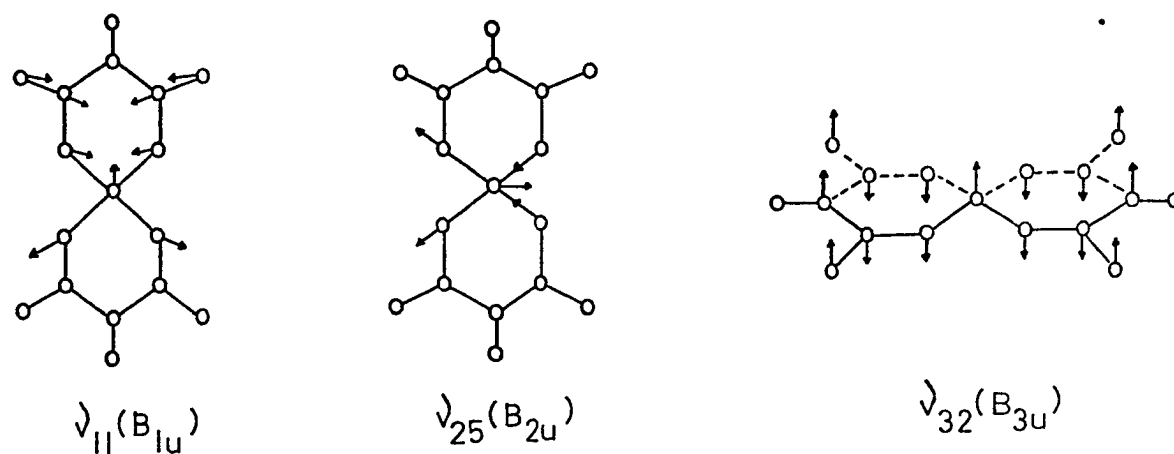


Figure 43

Schematics of vibrational modes for $\text{Pd}(\text{acac})_2$

(Selected from modes shown in reference 65 by Mikami et al)

calculated a ν_{26} (B_{2u}) at 68 cm^{-1} , and a ν_{35} (B_{3u}) at 53 cm^{-1} , with no clear assignment of any of the latter band.

Table V summarizes the data on the far infrared spectrum of $\text{Pd}(\text{acac})_2$, comparing the bands observed in this laboratory and their assignments, with the data from Mikami⁶⁵ and Nakamoto⁶¹. For easy comparison the bands (Fig. 44) assigned to the M-O modes have been underlined, and they are seen at 265 cm^{-1} (B_{3u}), at 295 cm^{-1} (B_{2u}), and at 464 cm^{-1} (B_{1u}). It should also be pointed out that these are generally consistent with the assignments of the M-O bands in $\text{Eu}(\text{acac})_2$ by Liang et al⁴⁹ at 200 , 225 and 410 cm^{-1} .

In this investigation the Raman spectrum of $\text{Pd}(\text{acac})_2$ is being reported (Fig. 45). The bands observed in the Raman spectrum have been assigned in accord with group theoretical selection rules for D_{2h} symmetry. Correlation Table VI shows how the symmetry species of D_{4h} transform in the case of D_{2h} symmetry. In addition, since one of the compounds to be discussed later (PdL_2 Species I) will be shown to be of C_{2v} symmetry, this is also included in the table.

As can be seen from the correlation Table VI, in D_{2h} symmetry to which $\text{Pd}(\text{acac})_2$ had been previously assigned by Mikami,⁶⁵ the Raman active modes belong to A_g , A_g .

TABLE V
COMPARISON OF FAR INFRARED DATA FOR Pd(acac)₂

Observ. (cm ⁻¹)	Relative Intensity (1-10)	Assigned	Mikami ⁶⁵ Data			Nakamoto ⁶¹ Data		
			Rept'd	Calc'd	Assigned	Rept'd	Calc'd	Assigned
60	4	ν_{35}	53	$\nu_{35}(\text{B}_{3u})$			
(70)	2	ν_{26}		68	$\nu_{26}(\text{B}_{2u})$			
95			94					
			(105)	103	$\nu_{34}(\text{B}_{3u})$			
120	1.5	lattice						
152	2	C-CH ₃ torsion						
170b	1.5	C-CH ₃ torsion	(174)	181	$\nu_{33}(\text{B}_{3u})$	186	ν_7 ring deform.
225	2	ring deform.*	(220)	221	$\nu_{13}(\text{B}_{1u})$			
<u>265</u>	8	M-O mode ν_{32}	<u>263</u>	259	$\nu_{32}(\text{B}_{3u})$	268	ν_6 C-CH ₃ bend
<u>295</u>	6	M-O mode ν_{25}	<u>294</u>	302	$\nu_{25}(\text{B}_{2u})$			
						317	ν_{14} M-O stretch

(Table continued on next page)

TABLE V (CONTINUED)

COMPARISON OF FAR INFRARED DATA FOR Pd(acac)₂

Observ. (cm ⁻¹)	Relative Intensity (1-10)	Assigned	Mikami ⁶⁵ Data			Nakamoto ⁶¹ Data		
			Rept'd	Calc'd	Assigned	Rept'd	Calc'd	Assigned
						373	ν_{13} ring deform.
440	4	ν_{24} (B _{2u})	441	432	ν_{24} (B _{2u})	442		out-of-plane
<u>464</u>	10	M-O str. ν_{11}	<u>463</u>	456	ν_{11} (B _{1u})	<u>464</u>	472	ν_5 M-O stretch

The bands assigned to the M-O modes have been underlined. The relative intensity of the observed bands has been expressed on a scale of 1 to 10.

* The ring deformation modes have been assigned by analogy with Pt(acac)₂, as assigned by Benke and Nakamoto in 1967 in references 68 and 69.

Figure 44

Far infrared spectrum of $\text{Pd}(\text{acac})_2$, Nujol mull

ABSORBANCE

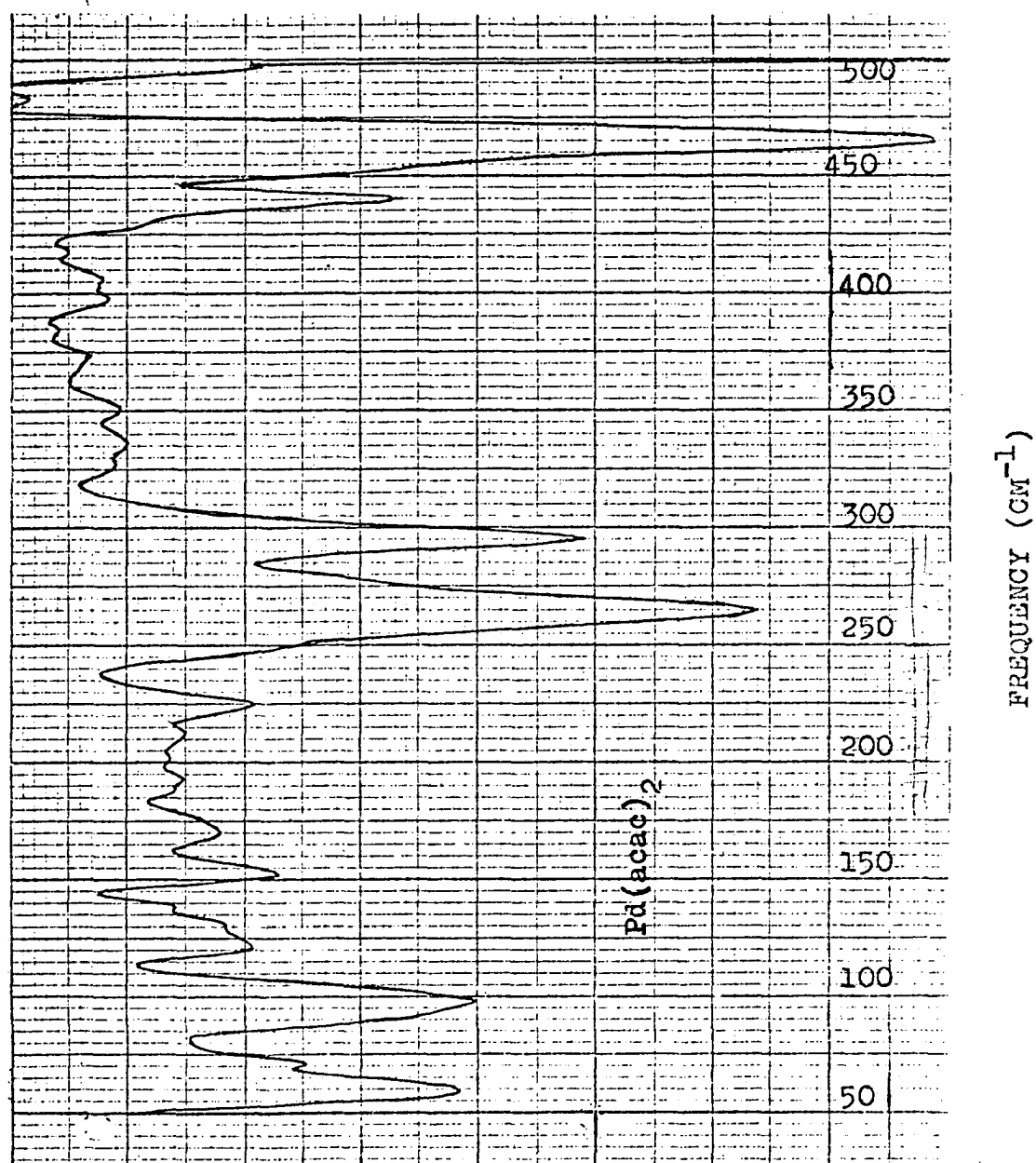


Figure 44

Figure 45

Low frequency Raman spectrum of $\text{Pd}(\text{acac})_2$.
Dashed lines indicate changes
in ordinate scale expansion.

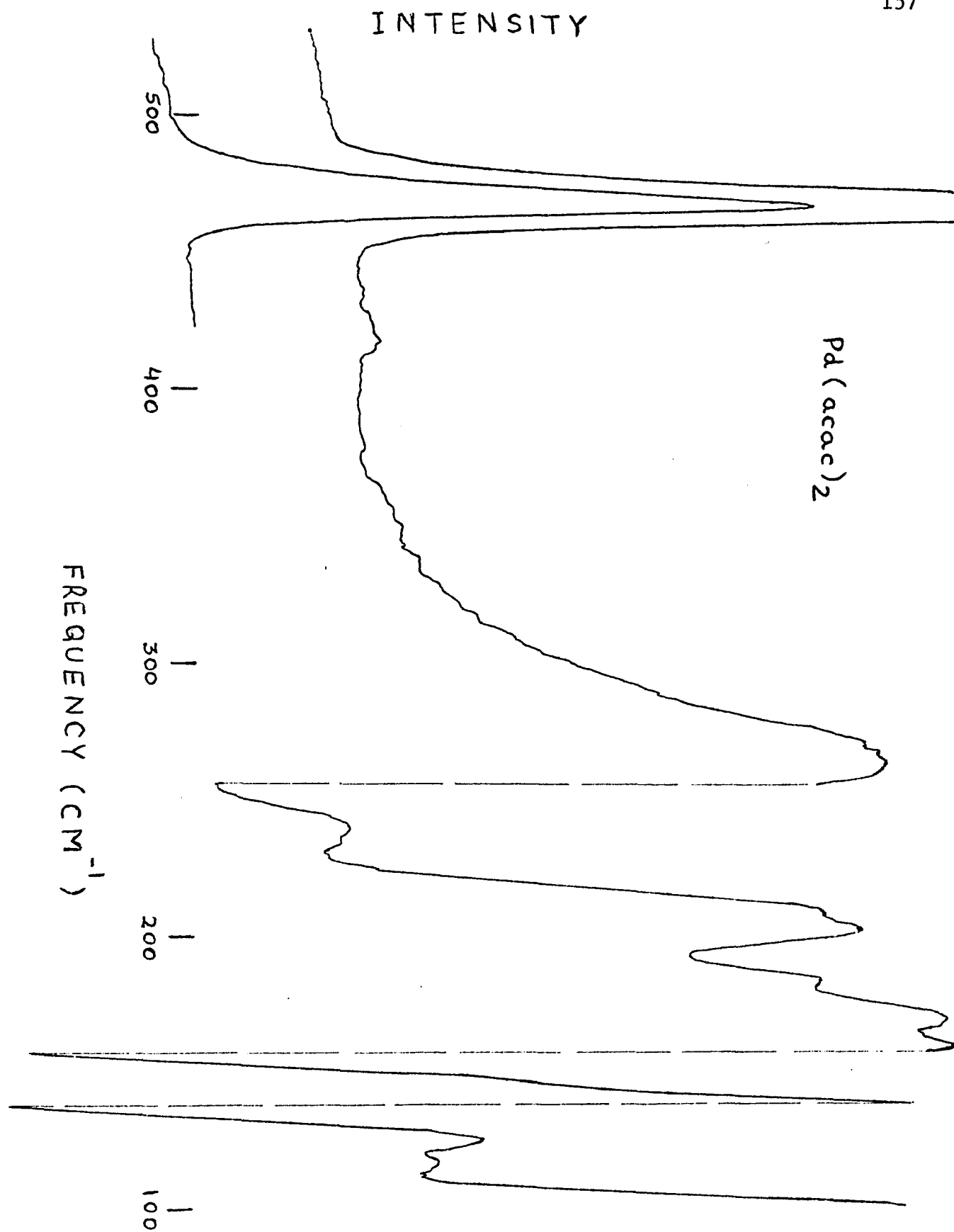


Figure 45

TABLE VI

CORRELATION TABLE FOR SYMMETRY GROUPS D_{4h} , D_{2h} and C_{2v}

Mode	Group D_{4h} Symmetry Species (Activity)	Group D_{2h} Symmetry Species (Activity)	Group C_{2v} Symmetry Species (Activity)
ν_1	A_{1g} (Raman)	A_g (Raman)	A_1 (IR + Raman)
ν_2	A_{2u} (IR)	B_{1u} (IR)	B_2 (IR + Raman)
ν_3	B_{1g} (Raman)	A_g (Raman)	A_1 (IR + Raman)
ν_4	B_{1u} (inactive)	A_u (inactive)	A_2 (Raman)
ν_5	B_{2g} (Raman)	B_{1g} (Raman)	B_1 (IR + Raman)
ν_6	E_u (IR)	B_{2u} (IR) B_{3u} (IR)	B_1 (IR + Raman) A_1 (IR + Raman)
ν_7	E_u (IR)	B_{2u} (IR) B_{3u} (IR)	B_1 (IR + Raman) A_1 (IR + Raman)

and B_{1g} , corresponding to the ν_1 (symmetric stretch), ν_3 (deformation mode) and ν_5 (assymmetric stretch) depicted in the hypothetical case of MX_4 . The discussion on how the correlation table is used to distinguish between possible cis and trans isomers will be deferred to the consideration of $Pd(bzac)_2$ and PdL_2 Species I and Species II. It can also be seen that in D_{2h} symmetry the selection rules predict three IR active bands, three Raman active bands, and no coincidences between those bands.

Table VII shows our data on the far IR spectra and Raman spectra of $Pd(acac)_2$, with relative intensities of the bands, and the assignments given to all the bands below 500 cm^{-1} . (Figs. 44 and 45). As in Table V, relative intensities are expressed on a scale of 1 to 10. As predicted by selection rules for D_{2h} symmetry, there are three bands observed in the far IR, seen at 265, 295 and 464 cm^{-1} ; and three Raman active bands at 203, 227 and 462 cm^{-1} . There are no coincidences between the observed Raman and infrared bands. In addition to the fundamental bands, the table shows which bands have been assigned as overtone or combination bands.

Table VIII compares our assignments of the Raman bands in $Pd(acac)_2$ with assignments previously reported for

TABLE VII

COMPARISON OF FAR IR AND RAMAN BANDS OF Pd(acac)₂

Far Infrared Bands			Raman Bands		
cm ⁻¹	Intens.	Assignment	cm ⁻¹	Intens.	Assignment
60	4	ν_{35} (B _{3u})*			
70(sh)	2	ν_{26} (B _{2u})*	112	10+	lattice mode
120	1.5	lattice mode	123	6	lattice mode
152	2	C-CH ₃ torsion	168	3	C-CH ₃ torsion.
170b	1.5	C-CH ₃ torsion.	182	3	C-CH ₃ torsion.
225	2	ring deform.	<u>203</u>	8	M-O fund. (A _g)
			<u>227</u>	4	M-O fund. (B _{1g})
			233(sh)	1	comb. 112+123
<u>265</u>	8	M-O fund. (B _{3u})	259	1	overtone (2x123)
<u>295</u>	6	M-O fund. (B _{2u})	288	2	comb. 168+123
440	4	ν_{24} (B _{2u})*			
<u>464</u>	10	M-O fund. (B _{1u})	<u>462</u>	10	M-O fund. (A _g)

* These assignments follow Mikami's previous assignments. ⁶⁵

The fundamental M-O bands have been underlined for easier comparison.

TABLE VIII

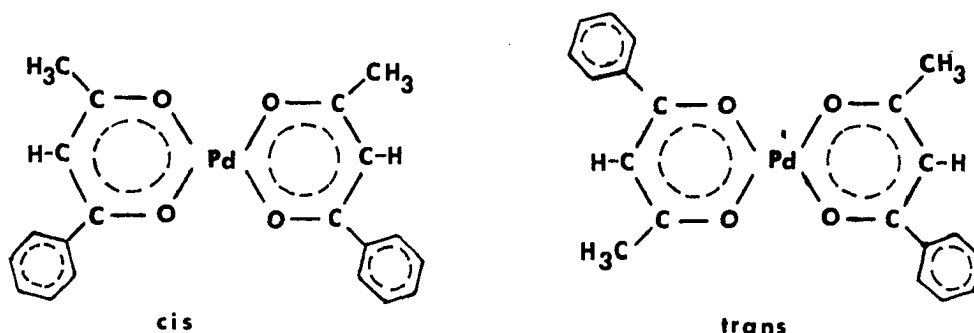
COMPARISON OF RAMAN DATA FOR Pd(acac)₂, Ga(acac)₃ and In(acac)₃

Data for Pd(acac) ₃ Observ. (cm ⁻¹)	Assigned	Data for Ga(acac) ₃ (cm ⁻¹)	Data for In(acac) ₃ (cm ⁻¹)	Assigned
112	lattice mode			
123	lattice mode			
168	C-CH ₃ torsion.			
182	C-CH ₃ torsion.			
<u>203</u>	M-O fund. (A _g)	208 vw, dp	230 w, dp	in-plane ring deform.
<u>227</u>	M-O fund. (B _{1g})			
233sh	comb. 112+123			
259	overtone (2x123)	283 vw, dp	C-CH ₃ deform.
288	comb. 168+123			
		420 vw, dp	410 vw, dp	in-plane ring deform.
<u>462</u>	M-O fund. (A _g)	460s, dp	444 m, p	M-O symmetric
		525 wv, dp	M-O asymmetric
		570 w, dp	570 w, dp	C-CH ₃ wag
		685 m, dp	675 mw, dp	M-O + ring deform.

Data and assignment for Ga(acac)₃ and In(acac)₃ are from Hester and Plane, in reference 58.

$\text{Ga}(\text{acac})_3$ and for $\text{In}(\text{acac})_3$ by Hester and Plane.⁵⁸ In addition, Liang et al⁴⁹ had reported the Raman spectrum of $\text{Eu}(\text{acac})_3 \cdot 2\text{H}_2\text{O}$, but the only band observed in that region and attributed to a possible M-O mode was at 410 cm^{-1} , assigned to a "complicated mode involving Eu-O stretch." One should not expect very close correlations in the M-O band frequencies of various metals, due to the differences in the mass effect of each metal (Pd = 106.4; Eu = 151.96; In = 114.82; Ga = 69.72). Furthermore, differences in electronegativity would definitely affect the strength of the M-O bond and its frequency. It is obvious, however, that in each case a band attributed to one of the M-O modes is seen in the Raman spectrum in the region from 400 to 480 cm^{-1} .

The next palladium β -diketonate to be considered is $\text{Pd}(\text{bzac})_2$. Because benzoylacetone (bzac) is not a symmetrical ligand, the chelate $\text{Pd}(\text{bzac})_2$ can exist in the form of two geometric isomers, cis and trans, as shown below.



An alternative presentation of the correlation diagram is shown in Table IX A and B. Here the fundamental

TABLE IX

CORRELATION DIAGRAM AND SELECTION RULES FOR D_{4h} , D_{2h} and C_{2v}

A. Stretching Modes, Their Assignments and Activity

	MX_4 (D_{4h})	MX_2Y_2 trans (D_{2h})	MX_2Y_2 cis (C_{2v} , with σ_d)
ν_1	sym. str. (A_{1g}) (Raman active)	$\longrightarrow A_g$ (Raman)	$\longrightarrow A$ (IR and Raman)
ν_5	asym. str. (B_{2g}) (Raman active)	$\longrightarrow B_{1g}$ (Raman)	$\longrightarrow B_1$ (IR and Raman)
ν_6	asym. str. (E_u) (IR active)	B_{2u} (IR)	$\longrightarrow B_1$ (IR and Raman)
ν_7		B_{3u} (IR)	$\longrightarrow A_1$ (IR and Raman)
ν_7	asym. str. (E_u) (IR active)	B_{2u} (IR)	$\longrightarrow B_1$ (IR and Raman)
		B_{3u} (IR)	$\longrightarrow A$ (IR and Raman)

B. Deformation Modes, Their Assignments and Activity

	MX_4 (D_{4h})	MX_2Y_2 trans (D_{2h})	MX_2Y_2 cis (C_{2v})
ν_2	angle def. (A_{2u}) (IR active)	$\longrightarrow B_{1u}$ (IR)	$\longrightarrow B_2$ (IR and Raman)
ν_3	deformation (B_{1g}) (Raman active)	$\longrightarrow A_g$ (Raman)	$\longrightarrow A_1$ (IR and Raman)
ν_4	deformation (B_{1u}) (inactive)	$\longrightarrow A_u$ (innactive)	$\longrightarrow A_2$ (Raman)

M-O modes have been separated into two groups: the stretching modes and the angle deformation modes. A comparison of Table IX with character tables (Appendix II) shows which symmetry representations are spanned by Cartesian coordinates (and which should be IR active), as well as those modes that belong to the same representation as the polarizability tensor (and should be Raman active).

In D_{4h} symmetry of the hypothetical MX_4 molecule the Cartesian coordinates span A_{2u} and E_u representations, and the polarizability tensor spans A_{1g} ; B_{1g} ; B_{2g} ; E_g . In D_{2h} symmetry, to which a hypothetical MX_2Y_2 trans isomer would belong, the Cartesian coordinates span B_{1u} B_{2u} B_{3u} . The polarizability tensor in D_{2h} symmetry spans A_g B_{1g} B_{2g} B_{3g} . Finally, in C_{2v} symmetry, to which the hypothetical MX_2Y_2 cis isomer belongs, the Cartesian coordinates span A_1 B_1 B_2 : the polarizability tensor spans A_1 A_2 B_1 B_2 . Thus, the selection rules predict that in the trans isomer the stretching modes will appear in the IR (B_{3u} and B_{2u}), and in the Raman (A_g and B_{1g}), with no coincidental lines. The bending or deformation modes in the trans isomer will be B_{1u} (IR active), A_g (Raman active) and A_u (inactive). As indicated before, in D_{2h} symmetry -- to which $Pd(acac)_2$ $Pd(bzac)_2$ trans and PdL_2 trans belong -- a total of six bands

corresponding to the Pd-O fundamental modes should be observed: three in the IR and three in the Raman, with no coincidences.

Regarding the Pd(bzac)₂ system, or the more general M(bzac)_n system, only limited far infrared and Raman data can be found in the literature. The Cu(bzac)₂ and Ni(bzac)₂ were investigated by Nakamoto et al,⁷³ and in the far IR region only one M-O stretching mode was reported and assigned: at 458 cm⁻¹ in Cu(bzac)₂ and at 455 cm⁻¹ in Ni(bzac)₂. As was pointed out before, the calculations by Nakamoto involved only the symmetrical β-diketo ligands, so no other far IR bands were calculated or recorded for the benzoylacetone complexes of Cu(II) and Ni(II). For the dibenzoylmethane complexes of these two divalent metals Nakamoto⁷³ also calculated and reported a ring deformation mode in the far infrared region: it was observed at 337 cm⁻¹ for Cu(dbm)₂ (calculated 373), and at 337 cm⁻¹ in Ni(dmb)₂ (calculated 373). For Pd(bzac)₂ Nakamoto et al⁴⁷ reported only one metal oxygen stretching frequency at 478 cm⁻¹. They also reported⁴⁷ the M-O stretching frequency for Co(bzac)₂ at 423 cm⁻¹, and for Al(bzac)₃ at 470 cm⁻¹. Holtzclaw and Collman reported the spectra of benzoylacetone and Cu(bzac)₂^{51,52}, but the lowest frequency band reported by them was in the 680 cm⁻¹ region, and no assignments were made for any bands below 1420 cm⁻¹.

The only Raman data for a $M(\text{bzac})_n$ type compound was included in the report by Liang et al⁴⁹ for $\text{Eu}(\text{bzac})_4 \cdot \text{piperidinium}$, along with the infrared data.

In the far IR region Liang reports four bands: 440m, 400m, 300 vw, and 270 vw, with only two assignments; the band at 400 cm^{-1} assigned to a complicated mode involving the Eu-O stretch, and at 270 cm^{-1} , to the C-CH₃ bending mode.

Only one medium intensity band is reported in the Raman low frequency region: at 460 cm^{-1} , with no assignment given. Presumably, this Raman band may be due to one of the metal-oxygen modes. It should be pointed out, however, that in the $\text{Eu}(\text{bzac})_4 \cdot \text{piperidinium}$ one is dealing with a positive ion of $\text{Eu}(\text{bzac})_4^+$ of Eu(III), and not with a neutral $M(\text{bzac})_n$ system, as was with the complexes of Cu, Ni, Pd, Co and Al investigated by Nakamoto.^{47,76}

Before presenting the far infrared and Raman data for $\text{Pd}(\text{bzac})_2$, one should consider the literature reports on the existence of two isomers of that species: trans and cis. In 1967 Hon et al²⁰ reported the crystal structure of the trans form. They deduced that the palladium, and the four oxygens which form a parallelogram centered on the Pd, are completely planar, giving rise to a center of symmetry

at the Pd atom. The pattern of bond lengths around the chelate ring follows an alternating single and double bond arrangement. These investigators point out, however, that the differences between the two metal-oxygen bond lengths in $\text{Pd}(\text{bzac})_2$ are smaller than in the copper chelate they had previously investigated,⁸² and even less pronounced than the differences they had observed in the vanadyl chelate of benzoylacetone.⁸³

Hon et al report that the phenyl group in the trans $\text{Pd}(\text{bzac})_2$ is joined to the chelate ring by a somewhat shorter bond than the usual carbon-carbon single bond, and that the phenyl group is rotated about this linkage by an angle which is not large enough to destroy effective conjugation between phenyl and chelate rings (angle of 23°). They reported that the Pd--O distances are 1.965 Å and 1.976 Å, with the shorter distance being to the oxygen closest to the phenyl substituent, and the shorter Pd--O distance to the oxygen closest to the methyl substituent of the chelate ring.

It should also be mentioned that the packing in the crystal form of $\text{Pd}(\text{bzac})_2$ was reported by Hon et al to be different from the packing in the $\text{Cu}(\text{bzac})_2$.⁸² They found that in the trans $\text{Pd}(\text{bzac})_2$ there are two

molecules per unit cell, and "the metal of one molecule in the unit cell is in contact (3.75 Å) with a methyl group of the other molecule". The molecules so connected "form a crinkled sheet in the (100) plane. The sheets are joined by van der Waals contacts between the projecting phenyl side groups." In spite of the differences in packing between the $\text{Cu}(\text{bzac})_2$ and $\text{Pd}(\text{bzac})_2$, Hon et al "emphasize that the geometries of the two chelate rings are, within experimental error, identical".

The Hon et al report makes no mention of any cis isomer of the $\text{Pd}(\text{bzac})_2$. However, Shugam et al reported in 1966, in the Russian *Zhurnal Strukturnoi Khimii*,⁸⁴ crystallographic data on several "inner complexes" of beta-diketones. Included in that report are data for a cis $\text{Pd}(\text{bzac})_2$ compound. The Russian investigators do not describe any details of their method of preparation, nor do they give any other spectrographic data or physical measurements. They found that the $\text{Pd}(\text{bzac})_2$ was not centrosymmetric, with the molecule located in the crystal on two-fold rotation axes. They also point out that only in the case of symmetrical ligands (f.e. acetylacetonone and dibenzoylmethane), are the copper and palladium

chelates isomorphous. However, in the case of the unsymmetrical benzoylacetone ligand, the copper chelate has a trans structure, while the palladium chelate is cis.

The cell parameters reported are another direct difference between the results of Hon et al²⁰ and those of Shugam et al.⁸⁴ Hon et al described a diamond-shaped crystal, rotating along one of the diagonal axes, with monoclinic parameters, as follows: $a = 9.367 \text{ \AA}$, $b = 10.518 \text{ \AA}$, $c = 9.454 \text{ \AA}$, $\beta = 108.0^\circ$. The Russian investigators, on the other hand, report their cell parameters as $a = 10.44 \text{ \AA} \pm 0.04 \text{ \AA}$; $b = 11.10 \pm 0.03 \text{ \AA}$; $c = 15.07 \pm 0.04 \text{ \AA}$; and $N = 4$. The densities of the compounds are identical. As described by Hon et al, and determined by flotation in potassium iodide solution, the density was 1.609 g/ml . Shugam et al report $d = 1.61$, and give no details on the method of determination.

Neither of the investigators who determined the crystal structures, reported any infrared or ultraviolet spectra, nor did they report any NMR data. The electronic spectroscopic data pertinent to the $\text{Pd}(\text{bzac})_2$ compound or compounds are in a series of papers by Singh and Sahai.^{74,75,86}

Those reports include UV data on Pd(acac)₂, Pd(bzac)₂ and Pd-dibenzoylmethane, as well as a comparison of these "parent" compounds with several in which the "gamma" hydrogen of the chelate ring has been substituted by Cl, Br, NO₂ or SCN. As discussed in a previous section, the IR data in those reports are only for the gamma-substituted compounds, with no IR data for Pd(bzac)₂ itself.

The results show that the compound we have prepared, as well as the one investigated by Singh and Sahai,⁸⁶ is the trans isomer of Pd(bzac)₂. The comparison of our UV spectra with those of Singh will be discussed in another section. At this point in the discussion it can be stated that our UV spectra are in general agreement with those of Singh as far as the position of the absorption maxima, but differ only in the calculated values of the extinction coefficients. (Incidentally, those can be attributed to differences in slit widths between our instrument and that used by the Indian authors.)

In our research the assignment of structure in the case of the Pd(bzac)₂, -- which was prepared in accordance with the procedure briefly outlined by Hon et al²⁰ -- is based on the comparison of Raman and far IR spectra and the application of the appropriate selection rules. As discussed before, if the Pd(bzac)₂ is trans, it belongs to the D_{2h}

symmetry, and selection rules predict two stretching modes and one bending mode in the infrared, and two stretching modes and one bending mode in the Raman, with no coincidental lines. Fig. 46 shows the far IR spectrum of $\text{Pd}(\text{bzac})_2$, and the low frequency Raman region is shown in Fig. 47. Our assignments of the bands involving the M-O modes of the $-\text{PdO}_4-$ subunit are detailed in Table X. It can be seen that the appropriate M-O bands follow the selection rules for a trans molecule of D_{2h} symmetry.

In the far IR we found fundamental modes at 265 cm^{-1} (assigned to B_{3u}), at 280 cm^{-1} (B_{2u}) and at 480 cm^{-1} (B_{1u}). The latter band is in agreement with the one reported at 478 cm^{-1} by Nakamoto in 1969,⁴⁷ within the experimental error. The Raman active bands due to the appropriate fundamental modes are at 210 cm^{-1} (assigned to A_g), at 273 cm^{-1} (B_{1g}), and at 430 cm^{-1} (A_g). There are no coincidental lines, as predicted by selection rules.

The data pertinent to the assignment of structure for Species I and Species II of the PdL_2 compounds prepared here (with L = p-octyloxy-1-phenyl-1,3-butanedione), are summarized in Tables XI and XII, respectively. The fundamental modes were generally assigned to the most intense

Figure 46

Far infrared spectrum of $\text{Pd}(\text{bzac})_2$, Nujol mull

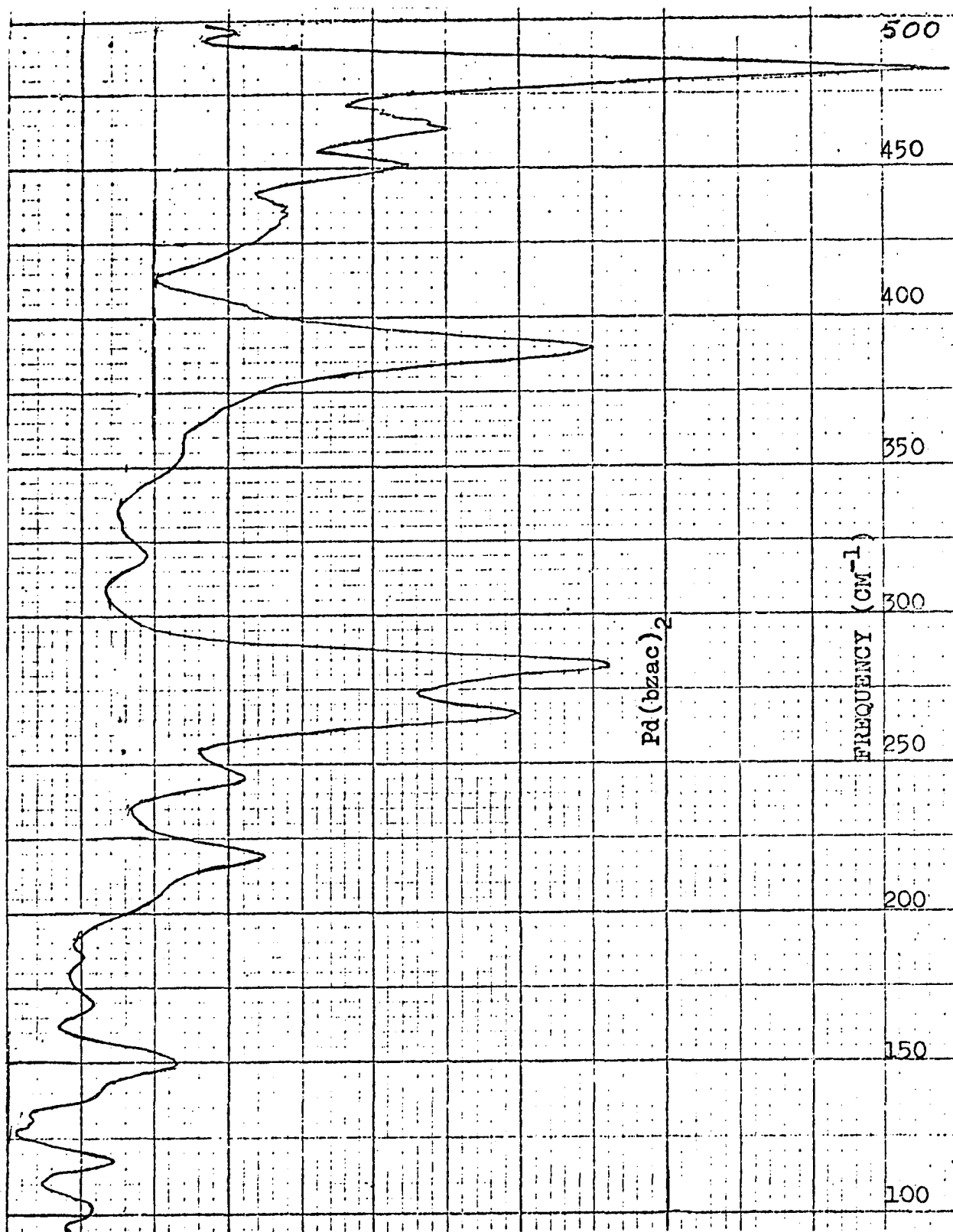


Figure 46

Figure 47

Low frequency Raman spectrum of $\text{Pd}(\text{bzac})_2$.
Dashed lines indicate changes
in ordinate scale expansion.

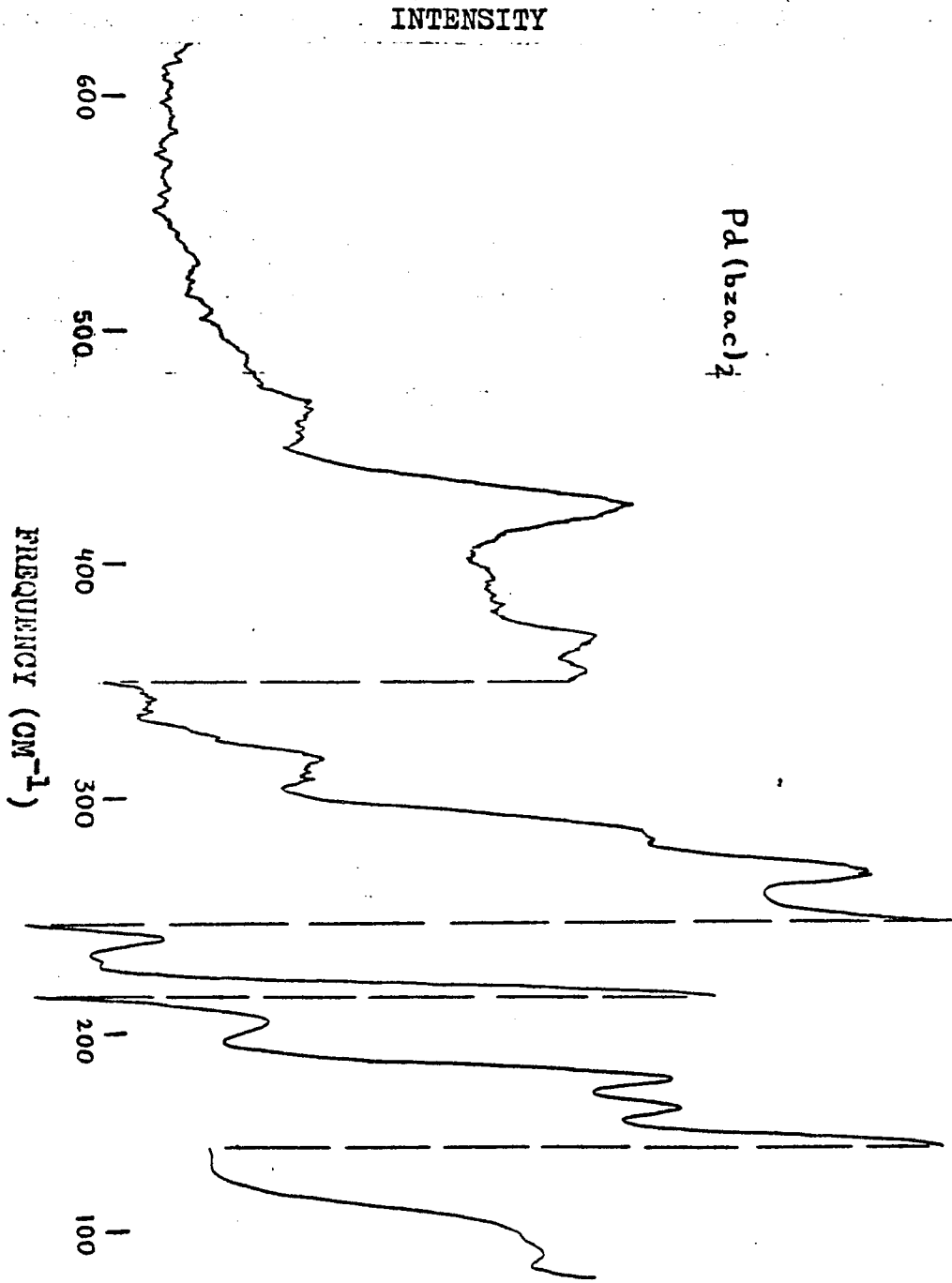


Figure 47

TABLE X

COMPARISON OF FAR IR AND RAMAN BANDS OF Pd(bzac)₂

Far Infrared Bands			Raman Bands		
cm ⁻¹	Intens.	Assignment	cm ⁻¹	Intens.	Assignment
70	2	C-Ph torsion.*			
105	1	lattice mode	110	10+	lattice mode
120	1	lattice mode			
150	1.5	C-CH ₃ torsion.	172	8.5	combination (lattice + C-Ph torsion)
			185	10+	C-CH ₃ tort.
220	2	comb. 150+70	<u>210</u>	10	M-O fund. (A _g)
240	1.5	Overtone(2x120)	245	5	comb. 172+70 ^g
<u>265</u>	5	M-O fund. (B _{3u})	<u>273</u>	2.5	M-O fund. (B _{1g})
<u>280</u>	6.5	M-O fund. (B _{2u})	(287)sh	1	comb. 110+172 ^g
			322	1	comb. 210+110
			346	1	comb. 245+110
			360	1	comb. 245+110
			374	1	overtone(2x185)
390	6	(280+105 or comb. (265+120)	<u>430</u>	3	M-O fund. (A _g)
450	3	combination (280+105+70=455)			
465	3.5	unassigned			
<u>480**</u>	10	M-O fund. (B _{1u})			

The fundamental M-O bands have been underlined for easier comparison.

*Details of estimation of the C-phenyl torsional mode are given in subsequent discussion.

**This is in agreement with band reported by Nakamoto et al⁴⁷

bands, and by comparison with the region assigned to the fundamental modes that were observed and calculated by Mikami⁶⁵ and Nakamoto⁶¹ for Pd(acac)₂, as well as the band reported by Nakamoto et al⁴⁷ and those assigned by us for Pd(bzac)₂. All of the bands observed in the far IR and Raman spectra below 500 cm⁻¹ have been assigned, including crystal lattice vibrations, overtones and combination modes. In addition, the position of the C-phenyl torsional mode and the "accordion mode" of the p-octyloxy chain have been estimated and assigned, as detailed later.

In Table XI it can be seen that Species I, assigned as the cis isomer of C_{2v} symmetry, has far IR and Raman spectra in accordance with the selection rules. The fundamental modes and their assignments in the far IR are at 225 cm⁻¹(A₁); at 305 cm⁻¹(A₁); at 395 cm⁻¹(B₁); at 422 cm⁻¹(B₁); at 433 cm⁻¹(B₁) and at 470 cm⁻¹(B₂). There are six absorptions in the Raman spectrum, coincidental with the far IR bands and of the same symmetry: at 223 cm⁻¹, at 308 cm⁻¹, 397 cm⁻¹, 424 cm⁻¹, 435 cm⁻¹ and 469 cm⁻¹. The small differences are within the experimental error of ± 1 cm⁻¹ involved in calibration of the lines. In addition, in accordance with the selection rules, a seventh mode, predicted to be only Raman active, is seen at 355 cm⁻¹ (assigned to A₂; bending mode). (See Figs. 48 and 49.)

TABLE XI

COMPARISON OF FAR IR AND RAMAN BANDS OF PdL₂ Sp. I, cis

Far Infrared Bands			Raman Bands		
cm ⁻¹	Intens.	Assignment	cm ⁻¹	Intens.	Assignment
75	2.5	C-Ph torsion	115	10+	lattice mode
105b	2.5	lattice mode	125	10+	lattice mode
153	2.5	C-CH ₃ torsion.	155	10+	C-CH ₃ torsion.
175	1.5	C-CH ₃ torsion	190	10+	comb. 125+C-Ph torsion.
<u>225</u>	2	M-O fund. (A ₁)	<u>223</u>	10	M-O fund. (A ₁)
268	1.5	comb. 153+105	240	3	accordion mode*
280	2	comb. 175+105	273sh	1	comb. 155+115
<u>305</u>	2	M-O fund. (A ₁)	<u>308</u>	1	M-O fund. (A ₁)
325	1	comb. 225+105	<u>355</u>	1	M-O fund. (A ₂) Raman only)
<u>395</u>	3	M-O fund. (B ₁)	<u>397</u>	1	M-O fund. (B ₁)
<u>422</u>	2	M-O fund. (B ₁)	<u>424</u>	1	M-O fund. (B ₁)
<u>433</u>	1	M-O fund. (B ₁)	<u>435</u>	1	M-O fund. (B ₁)
<u>470</u>	10	M-O fund. (B ₂)	<u>469</u>	5	M-O fund. (B ₂)

The fundamental M-O bands have been underlined for easier comparison.

*Details of estimation of the Raman active accordion mode are given in subsequent discussion.

Figure 48

Far infrared spectrum of PdL_2
Species I, Nujol mull

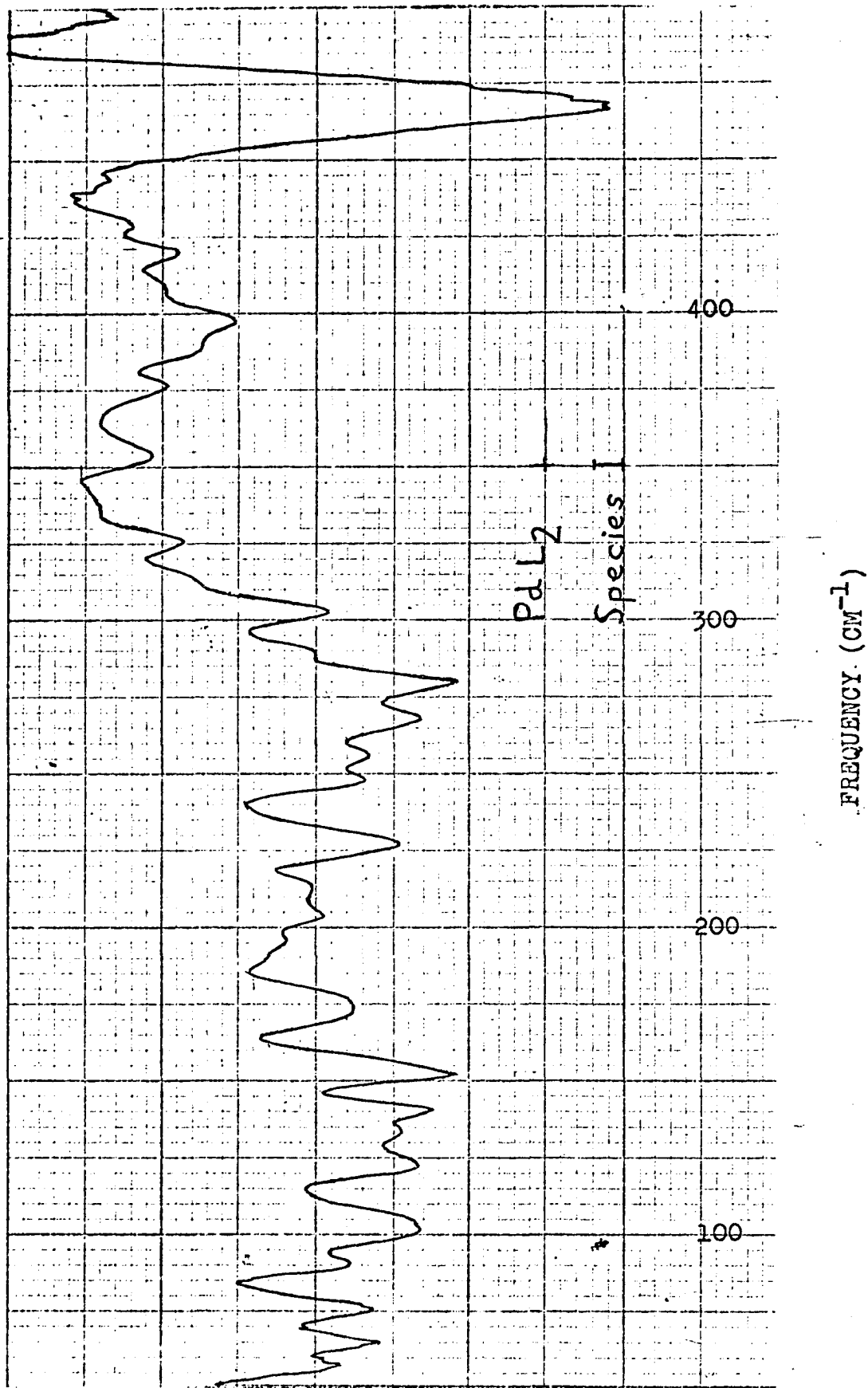


Figure 48

Figure 49

Low frequency Raman spectrum of PdL₂ Species I.
Dashed lines indicate changes
in ordinate scale expansion.

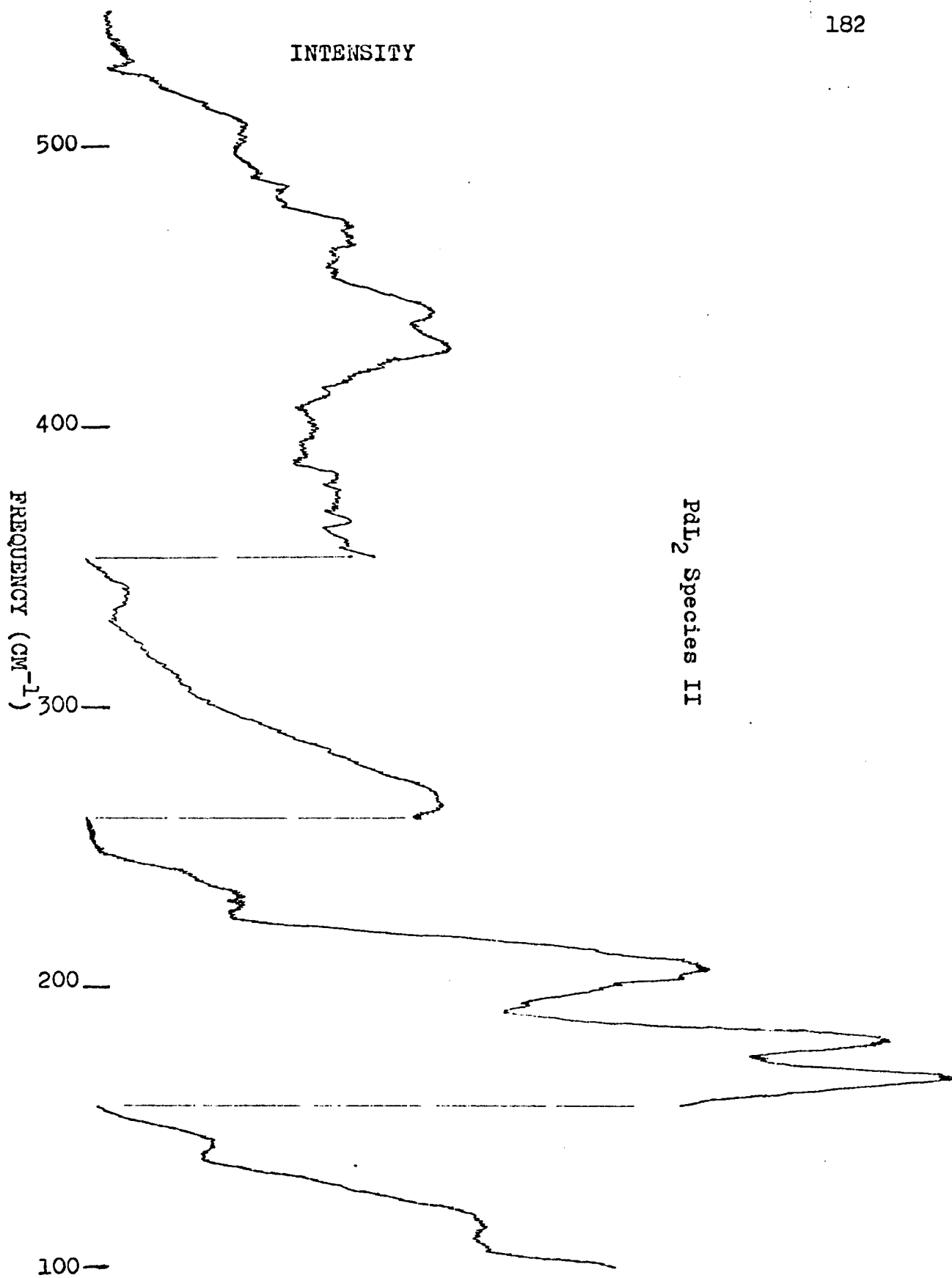


Figure 49

Table XII summarizes the data and band assignments for Species II of PdL_2 , shown to be the trans isomer. The fundamental modes in the far IR are at 255 cm^{-1} (assigned to B_{3u}); at 288 cm^{-1} (B_{2u}) and at 448 cm^{-1} (B_{1u}). In the Raman spectrum the fundamental modes can be seen at 211 cm^{-1} (assigned to A_g), 266 cm^{-1} (B_{1g}) and at 441 cm^{-1} (A_g). In agreement with selection rules for a trans isomer of D_{2h} symmetry, there are no coincidental lines in the far infrared and Raman spectra. (See Figures 50 and 51)

Figures 52 and 53 summarize the fundamental modes assigned here to the motions of the $-\text{PdO}_4-$ subunits in each of the four compounds examined: 53 for $\text{Pd}(\text{acac})_2$, 52 for $\text{Pd}(\text{bzac})_2$ trans, 52 for PdL_2 Species II trans, and 53 for PdL_2 Species I cis. As would be expected from similarities in structures, Fig. 52 shows that the assignments of the fundamental modes are fairly similar in $\text{Pd}(\text{bzac})_2$ trans and PdL_2 Species II trans.

Details of estimation of the C-phenyl torsional mode (henceforth abbreviated as C-Ph) follow. The C- CH_3 torsional mode generally appears at about 150 cm^{-1} . According to the vibrational equation for a harmonic oscillator (Equn. 13) substitution by a heavier group

$$\nu = \frac{1}{2\pi} \sqrt{\frac{k}{\mu}} \quad (13)$$

Figure 50

Far infrared spectra of PdL₂ Species II. The region from 50 to 350 cm⁻¹, shown in A, was determined on the far infrared spectrophotometer. The region from 275 to 700 cm⁻¹ was determined on the Perkin Elmer Model 521 spectrophotometer, and is shown in B. Bands due to Nujol and/or polyethylene are indicated by N.

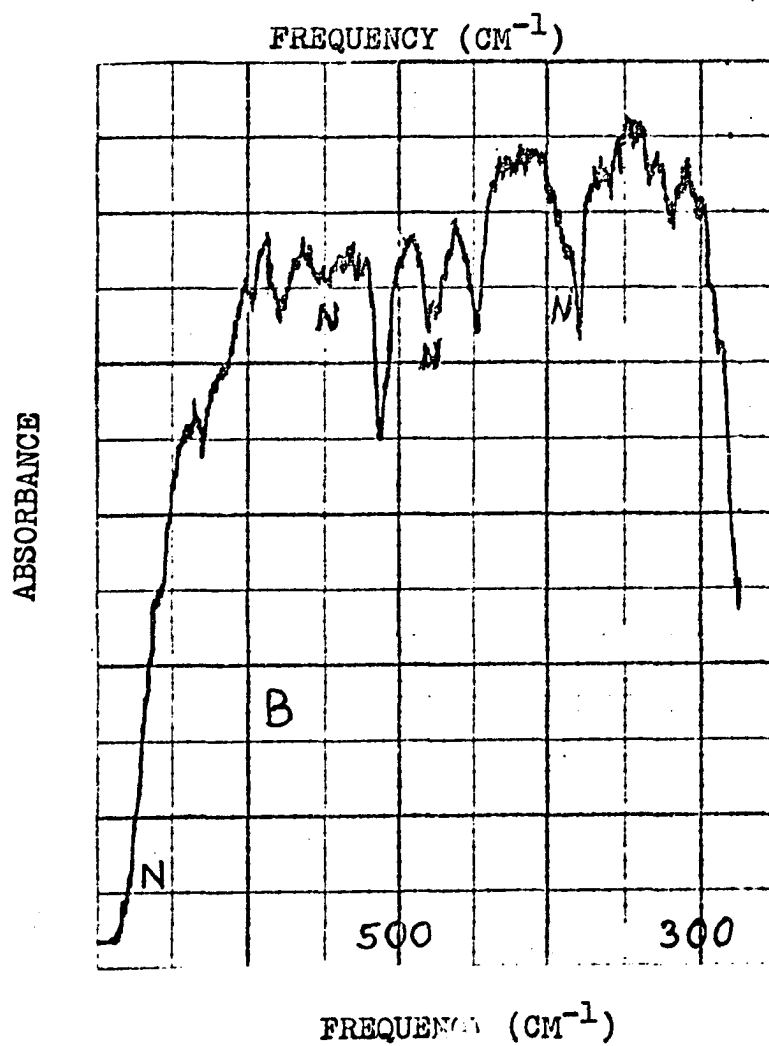
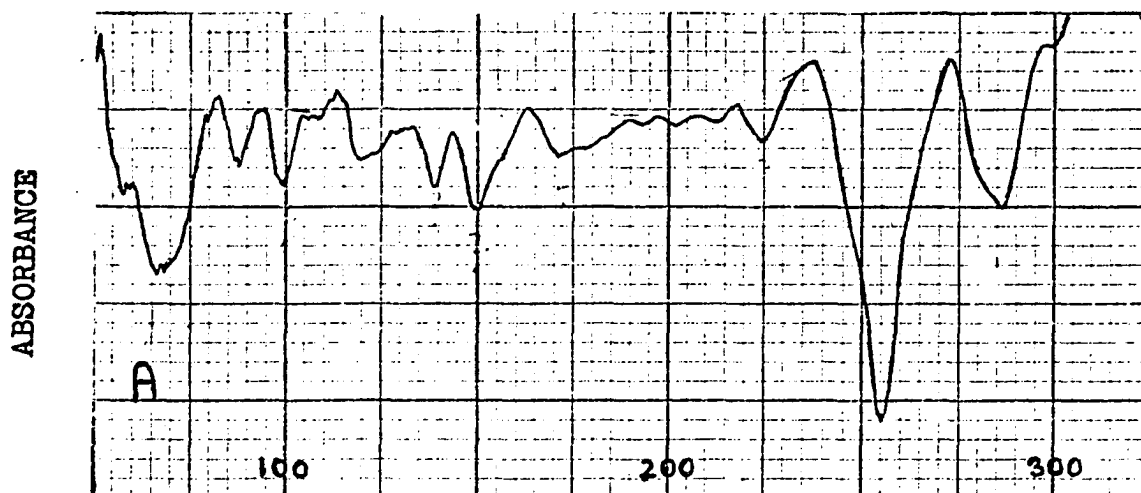
PdL₂ Sp. II

Figure 50

Figure 51

Low frequency Raman spectrum of PdL₂ Species II.
Dashed lines indicate changes
in ordinate scale expansion.

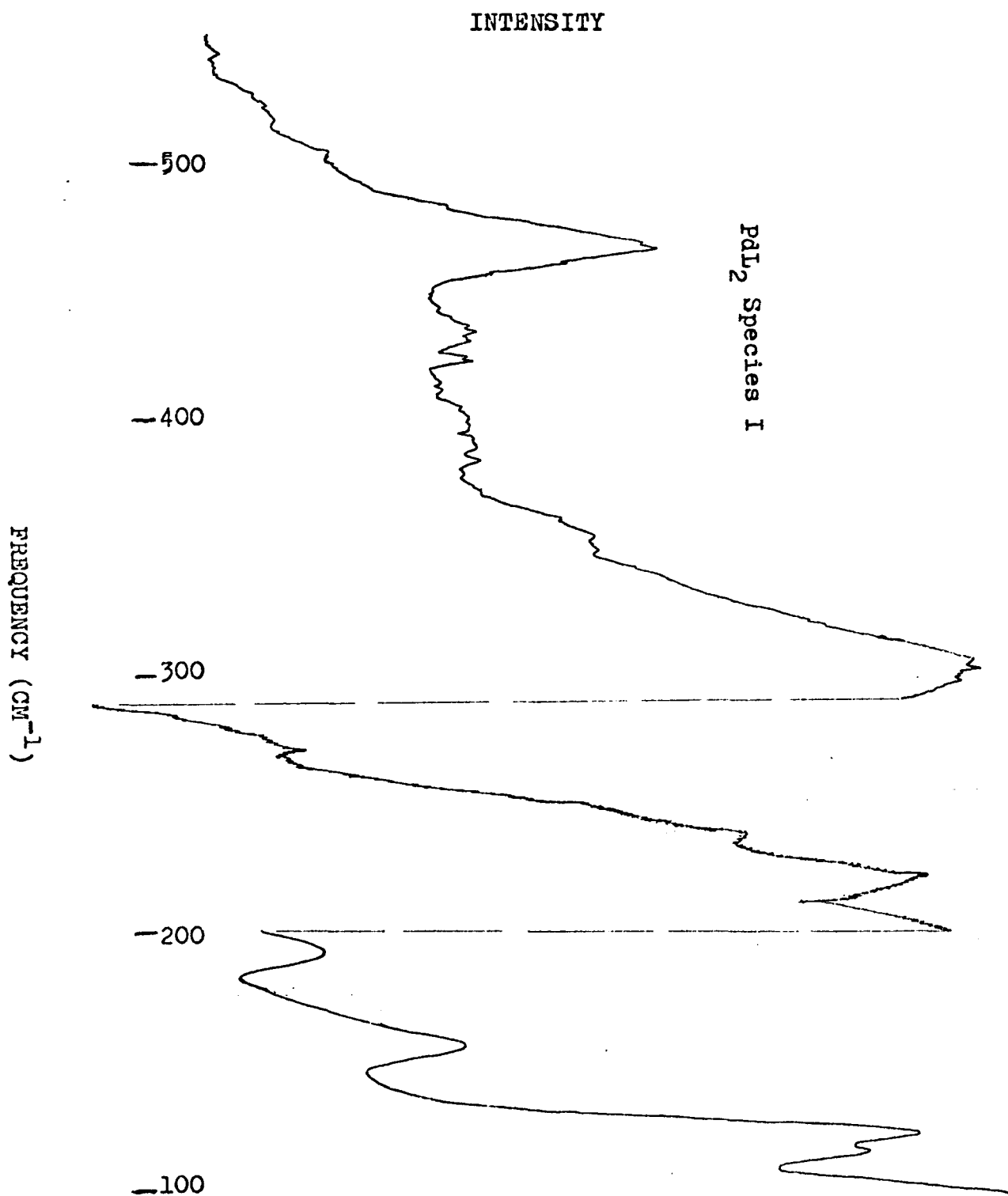


Figure 51

TABLE XII

COMPARISON OF FAR IR AND RAMAN BANDS OF PdL₂ Sp. II trans

Far Infrared Bands			Raman Bands		
cm ⁻¹	Intens.	Assignment	cm ⁻¹	Intens.	Assignment
65	6	C-Ph torsion	120	10+	lattice mode
150	4.5	C-CH ₃ torsion	147	8	lattice mode
170	3	C-CH ₃ torsion	172	10+	C-CH ₃ torsion
			187	10	C-CH ₃ torsion
			<u>211</u>	10	M-O fund. (A _g)
225	2.5	comb. 170+65	235	1.5	overtone (2x120)
<u>255</u>	10	M-O fund. (B _{3u})	243	3	accordion mode*
<u>288</u>	5	M-O fund. (B _{2u})	<u>266</u>	2	M-O fund. (B _{1g})
320	2.5	comb. 170+150			
340	1.5	overtone (2x170)	342	1	overtone (2x172)
			422	1	overtone (2x211)
<u>448</u>	6	M-O fund. (B _{1u})	<u>441</u>	1	M-O fund. (A _g)
			467	1	overtone (2x235)

The fundamental M-O bands have been underlined for easier comparison.

*Details of estimation of the Raman active accordion mode are given in subsequent discussion.

Figure 52

Comparison of fundamental M-O frequencies and their assignments in Pd(bzac)₂ trans (upper chart) and PdL₂ Species II trans (lower chart).

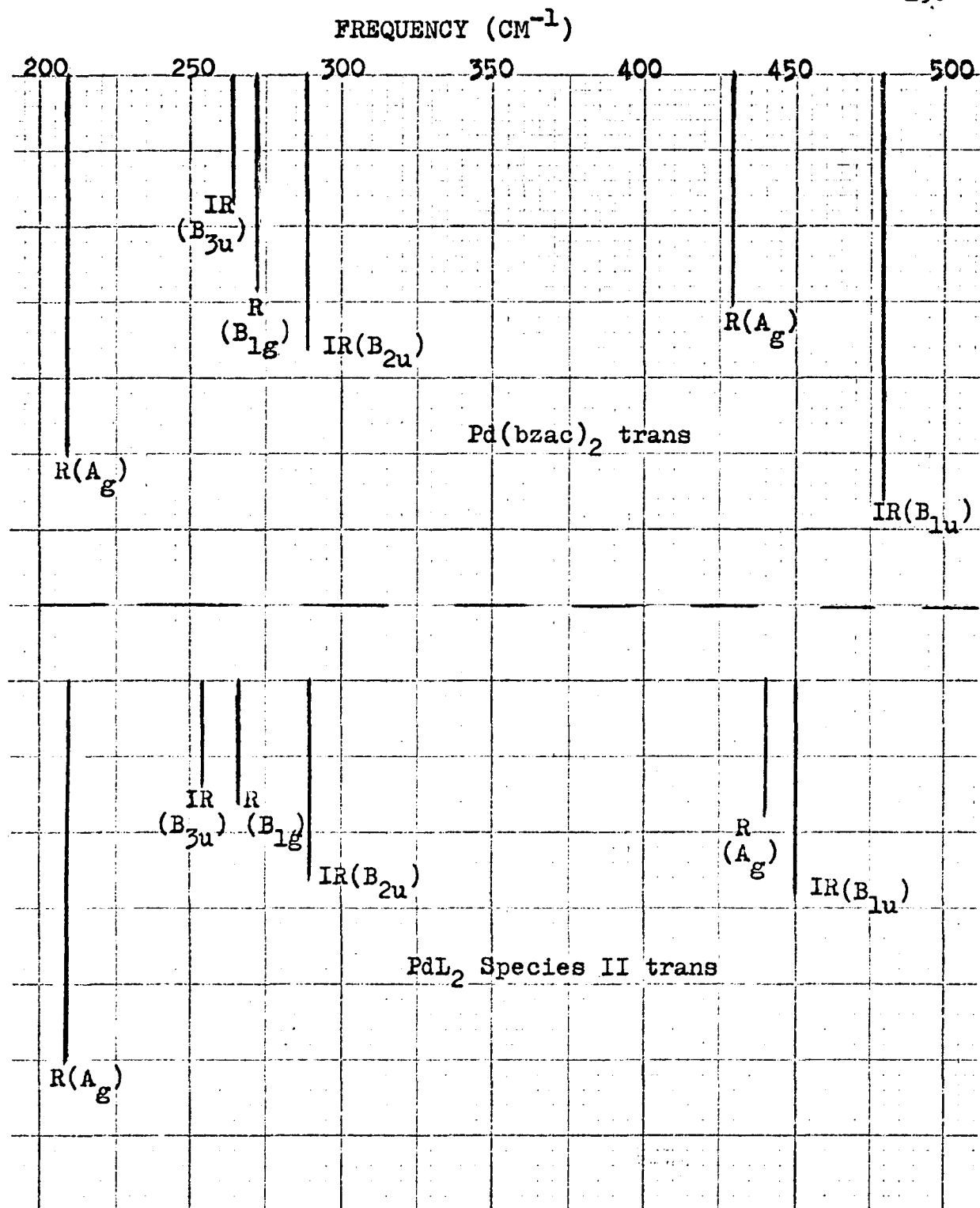


Figure 52

Figure 53

Comparison of fundamental M-O frequencies and their assignments in $\text{Pd}(\text{acac})_2$ (upper chart) and PdL_2 Species I cis (lower chart)

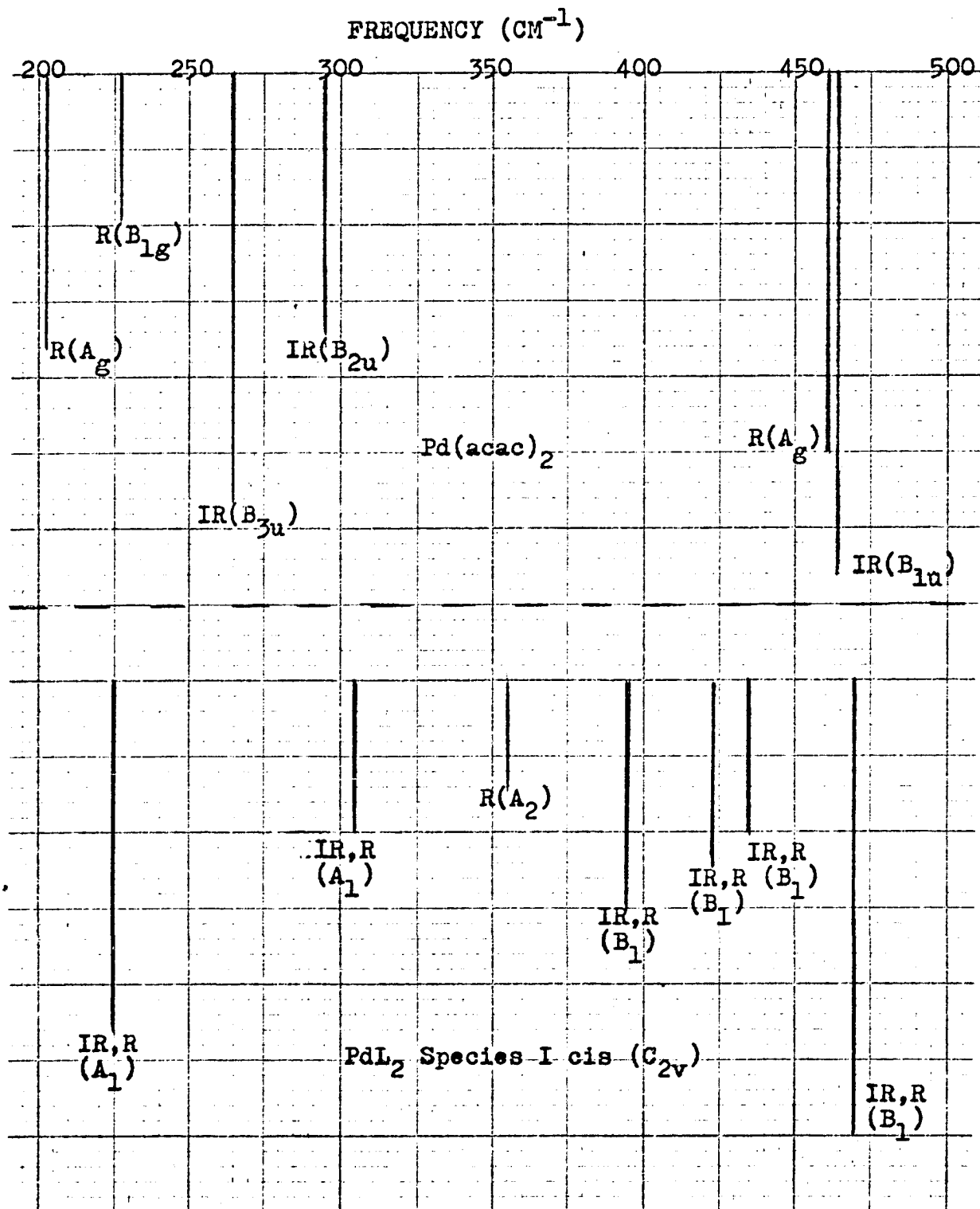
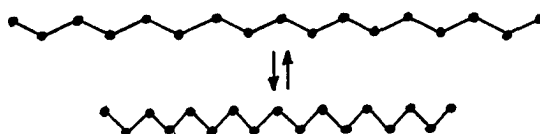


Figure 53

leads to a displacement of the absorption band to longer wavelength and lower frequency, since the reduced mass of the vibrating group of atoms appears in the denominator in the square root. If a CH_3 group, with a mass of 15 amu is replaced by C_6H_5 or Ph with a mass of 77 amu, the band will move to lower frequency. Since $77/15 = 5.13$, and the square root of $5.13 = 2.265$, it is easily calculated that if the CH_3 torsional appears at 150 cm^{-1} , the corresponding C-Ph torsional mode absorbance should be seen at about $150/2.265 = 66 \text{ cm}^{-1}$, or slightly higher, probably around 70 to 75 cm^{-1} .

The C-Ph torsional bands were generally observed in the far IR, but they were difficult to observe in the Raman spectra, due to main line interference. However, some combination bands were attributed in the Raman to coupling with the C-Ph torsional mode.

The so-called "accordion mode" had been first investigated in finite polymethylene chains by Mizushima and Shimanouchi in 1949⁸⁷, and by Schaufele and Shimanouchi in 1967.⁸⁸ This mode, also called the longitudinal acoustical (LA) accordion mode, reproduced below, as it was shown by Schaufele and Shimanouchi.⁸⁸



LA accordion mode of hydrocarbon chain

In 1973 J. M. Schnur⁸⁹ investigated the Raman spectra of homologous alkoxy-azobenzenes (AAB), and the changes in those spectra as a function of the alkoxy chain length, as well as a function of temperature. He analyzed the data known about the group frequencies of n-alkanes, with particular discussion of the normal vibration known as the "accordion mode". It had been established by Schaufele and Shimanouchi⁸⁸ that this mode is characteristic of the motion of the chain backbone, and its frequency is inversely proportional to the length of the polymethylene chain. In alkanes this band is only Raman active. Schnur⁸⁹ found that the motion of each alkoxy chain can be approximated by an alkane "accordion" with one free and one fixed end. Using this model, Schnur found good agreement between the predicted and observed bands in the dialkoxyazobenzenes (dialkoxy AB) investigated.

In the AAB series Schnur treated the oxygen of the alkoxy chain as if it were a carbon that participated in the accordion mode. He found that the frequency of the

accordion mode bands in the AAB compounds exhibited the inverse frequency shift with carbon number, similar to that previously described and analyzed by Schaufele and Shimanouchi.⁸⁸ Fig. 54 is reproduced from Schnur's article. As can be seen, the original includes data from $n=5$ (i.e. corresponding to the dibutoxy AB) to $n = 8$ (for diheptyloxy AB).

Schnur's plot of frequency shift versus chain length includes three curves. The lowest one is the calculated curve, based on a model of an alkane with one free and one fixed end. The top curve shows the observed accordion mode in alkanes. Schnur's middle curve, which does follow the inverse frequency shift with carbon number, is of interest in the assignments of accordion mode to the *p*-octyloxy chain. However, this curve would have to be extrapolated to $n = 9$, so that it could be applied to estimate the position of the accordion mode in both species of PdL_2 .

For $n = 6$ Schnur observed the accordion mode at about 310 cm^{-1} ; for $n = 7$ at 285 cm^{-1} ; and for $n = 8$ at about 265 cm^{-1} . Extrapolating those values for the alkoxy chain, one would estimate that the accordion mode for the *n*-octyloxy chain, where $n = 9$, should be seen around $245 \text{ cm}^{-1} \pm 5 \text{ cm}^{-1}$. In the Raman spectra of PdL_2 Species I the accordion mode

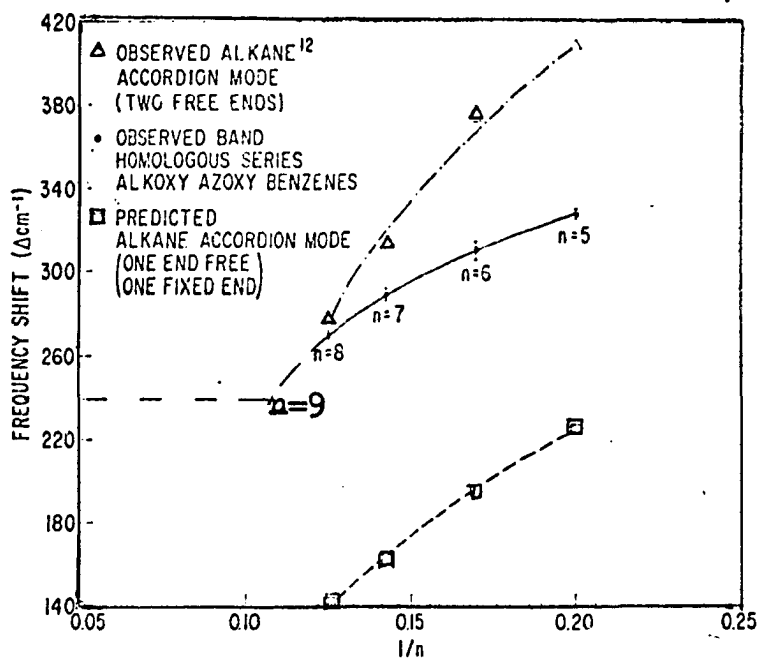


Figure 54. Predicted and observed frequencies for the accordion mode.

The curve for the observed band in the homologous series of alkoxy azoxy benzenes reported in Schnur's article (reference 39) was extrapolated to $n=9$, as shown by the dashed line. In this curve n is the number of carbons in the alkoxy tail plus one (for the oxygen)

has been tentatively assigned to 240 cm^{-1} . In the Raman spectrum of PdL_2 Species II this mode has been assigned to 243 cm^{-1} .

Discussion of Ultraviolet Spectra

The ultraviolet spectrum of the (p-octyloxy)-1-phenyl-1,3-butanedione("ligand") is shown in Fig. 15. It shows an absorbance at 320 nm, with a ϵ value of 35,000. The UV spectrum of PdL₂ Species I, cis, is shown in Fig. 20. Two absorbances can be seen: one at 330 nm, with a ϵ value of 10,540 and another at 290 nm, with an ϵ value of 52,110. The UV spectrum of PdL₂ Species II, trans, is shown in Fig. 24; this shows two absorbances: at 310 nm, with an ϵ value of 43,780, and another at 355 nm, with an ϵ value of 34,750.

The discussion of these spectra will involve an examination of the effect of substitution of a phenyl ring for a methyl group in the metal acetylacetonato complexes of several known compounds. Since one of the important reference compounds to be considered is Pd(bzac)₂, it seems important to discuss first the differences between the values of extinction coefficients calculated for that compound from our results, and those reported by Singh and Sahai²⁹, as mentioned in a preceding section of the discussion of spectroscopic band assignments.

Singh and Sahai²⁹ reported the UV spectra of Pd(acac)₂, Pd(bzac)₂, as well as a series of compounds in which the

"gamma" proton of the chelate ring was replaced by groups such as Cl, Br, NO₂ and SCN. Similarly, they reported spectra for analogous compounds of Cu and Al. Their extinction coefficients are reported in the form of log ϵ , and in order to compare their results with our data, it was necessary to convert Singh's reported values to the antilogs. The data reported by Singh are compared with those reported by another investigator, Gubin et al.⁹⁰ As can be seen in Table XIII, the ϵ_{\max} values reported for Pd(acac)₂ by Gubin are considerably lower (by about 50%) than those reported by Singh. It can be seen that Gubin⁹⁰ reported four absorbances; at 208.5, 225, 250 and 328 nm. Singh reports band I at 250; a shoulder at 260 - 270, attributed to band II, band III at 330, and a shoulder at 400 nm assigned to band IV. Table XIII lists only those bands for which ϵ_{\max} values were reported by either Gubin or Singh.

In view of this discrepancy between ϵ values reported by Gubin and by Singh, we determined the UV spectrum in CHCl₃ of Pd(acac)₂ purchased from Alpha Inorganics (Fig. 55). We find absorption bands at 328 nm, with ϵ_{\max} of 12,080, and at 250 nm with $\epsilon_{\max} = 15,160$. Our values, when compared with those in Table XIII, seem to be closer to those reported by

TABLE XIII

COMPARISON OF GUBIN'S DATA AND SINGH'S DATA ON Pd(acac)₂

λ_{\max} (in nm)	Gubin's ϵ	Singh's $\log \epsilon$	Our Recalculation of Singh's ϵ	Ratio $\frac{G's \epsilon}{S's \epsilon}$
208.5	42,800	not reported		
225	35,400	not reported		
250	16,300	$\log = 4.53$	33,900	$\frac{1.63}{3.39} = .481$
328±2	12,700	$\log = 4.38$	24,000	$\frac{1.27}{2.40} = .529$
400	not reported	$\log = 2.47$		

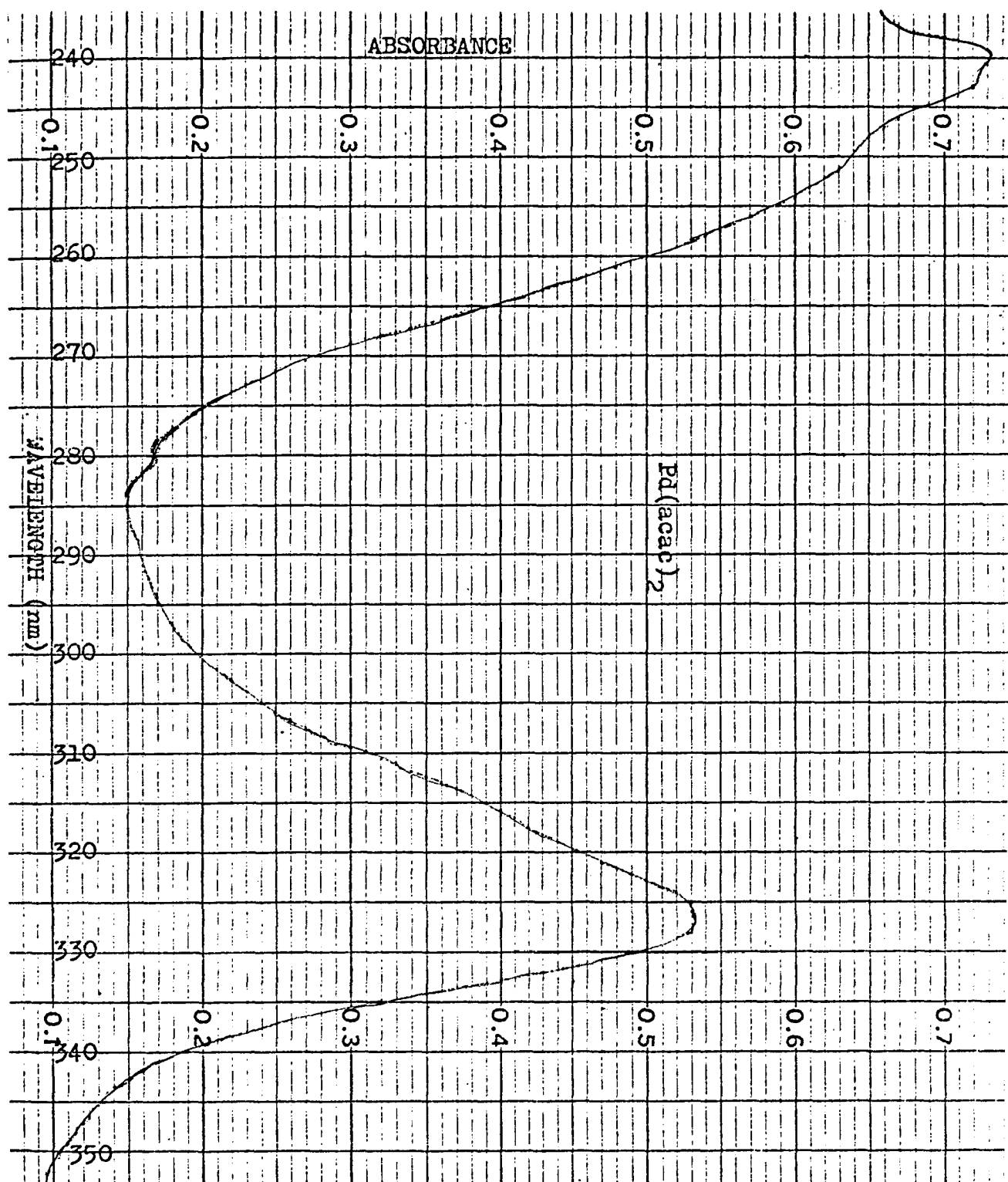


Figure 55. Ultraviolet spectrum of $\text{Pd}(\text{acac})_2$ in CHCl_3 , concentration $3.892 \times 10^{-5} \text{M}$

Gubin. We conclude from this comparison that the slit width used in our instrument is probably much closer to that used by Gubin, and quite different from the slit width apparently used by Singh and Sahai. Probably Singh used a narrower slit width to obtain the higher absorbance. This conclusion is further supported by a comparison of UV data for two more compounds: a $\text{Pd}(\text{acac})_2$ analog with -Cl substituted for the "gamma" proton, and one with -Br substituted in that position. Both compounds were studied by Gubin⁹⁰ and by Singh.⁸⁵ For the chloro-substituted compound, the ratio of Gubin's to Singh's ϵ_{max} values (after recalculation of antilog) is $6.70/12.3 = 0.545$; for the bromo-analog the ratio is $6.9/8.7 = 0.79$.

We similarly compared our ϵ_{max} values for $\text{Pd}(\text{bzac})_2$ with those reported by Singh and Sahai. The data are shown in Table XIV.

Inasmuch as data from chemical analysis and molecular weight determinations indicate that our $\text{Pd}(\text{bzac})_2$ is pure, we feel justified in attributing the discrepancy between our ϵ_{max} values and those reported by Singh⁸⁶ to differences in slit width. Neither Gubin nor Singh reported the slit width used, but Singh's values on the $\text{Pd}(\text{acac})_2$ seem much more out of line with ours than those of Gubin. Singh reported using

TABLE XIV
COMPARISON OF OUR DATA AND SINGH'S FOR Pd(bzac)₂

λ_{\max} (in nm)	Our ϵ_{\max}	Singh's log ϵ	Our calcul. of Singh's ϵ	Ratio $\frac{\text{Our } \epsilon}{\text{Singh's } \epsilon}$
260 (band I)	35,950	log = 4.70	50,120	$\frac{3.595}{5.012} = 0.717$
285 (band II)	29,520	log = 4.69	48,980	$\frac{2.952}{4.898} = 0.603$
352 (band III)	19,670	log = 4.49	30,900	$\frac{1.967}{3.090} = 0.637$

a Cary 14R spectrophotometer, and estimated that their ϵ values were generally reproducible within 5%.

For comparison we also determined the UV spectrum of bzac which had been recrystallized from ethanol. The spectrum for a 8.508×10^{-3} M solution of bzac in CHCl_3 is shown in Fig. 56A. The band at 310 nm corresponds to an ϵ_{max} value of 16,930; the one at 250 nm has an ϵ_{max} value of 54,070. The UV spectrum of bzac was reported by Lowe and Ferguson⁴⁸, with a band at 307 nm, $\epsilon_{\text{max}} = 38,000$ in heptane; or a band at 307 nm, with $\epsilon_{\text{max}} = 15,800$ in isopropyl alcohol. Our ϵ value is in good agreement with the one reported in isopropyl alcohol, and we would expect it to differ from the one in the non-polar heptane.

Lowe and Ferguson discuss the positions of λ_{max} in benzoylacetone p-methoxy-benzoylacetone and $\text{Cu}(\text{bzac})_2$, and compare them with those observed in aliphatic beta-diketones. They point out that all reported values of λ_{max} for enols and their methyl ethers, of the type $\text{R-CO-CH}=\text{C}(\text{OH})-\text{R}$ and $\text{R-CO-CH}=\text{C}(\text{OCH}_3)-\text{R}$, (where R is an alkyl group) are below 300 nm. This is true even for the methyl ethers of the two possible enols of benzoylacetone investigated by Eistert and Merkel.⁹¹ On the other hand, the aryl substituted chromophore has λ_{max} above 300 nm, whenever the steric requirements do

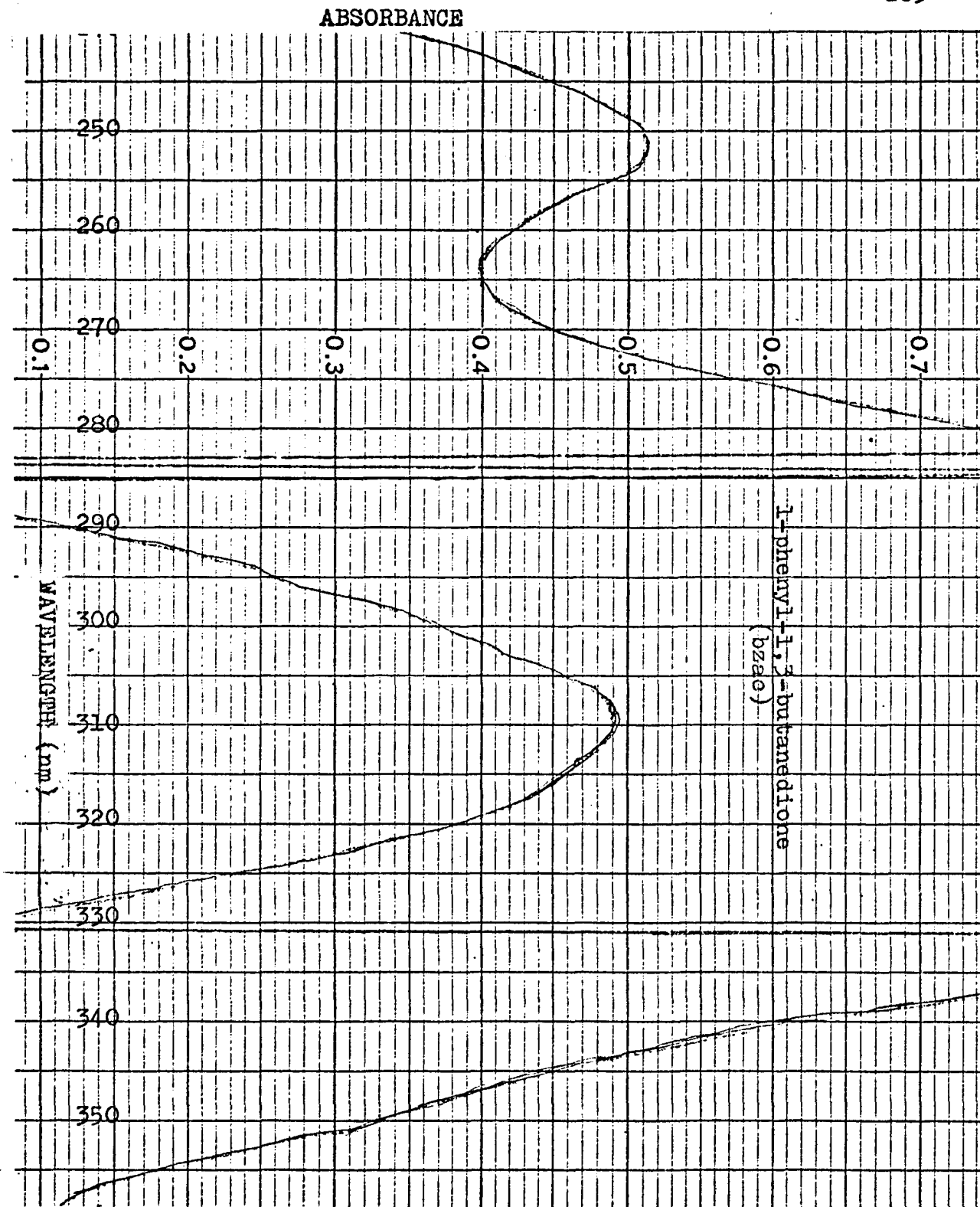
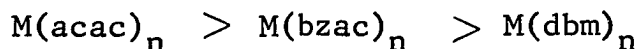


Figure 56A. Ultraviolet spectrum of bzac in CHCl₃,
concentration $8.508 \times 10^{-3} M$

In turning to the examination of the effect of phenyl substituents on the UV spectra of substituted metal acetylacetonates, it should be noted that two opposite effects must be considered. It has been well established that the phenyl ring can withdraw electrons by an inductive effect, but it can also donate electrons by a resonance effect, provided the phenyl ring is coplanar with the chelate ring attached to the metal. In examining this effect we will consider band III, for which data have been collected on a series of compounds. This band Gubin and Singh report as most sensitive to substitution. Singh and Sahai⁸⁶ reported that in the Cu, Pd and Al compounds studied, replacing a methyl group by a phenyl group in the metal (acac)_n results in a shift of all absorption bands in the UV and visible towards lower energy (longer wavelengths) in all transitions. They believe that this indicates the dominance of the resonance effect over the weak inductive effect of the phenyl ring. Shifts to lower energy for the Pd(II), Cu(II) and Al(III) beta-diketonates are of the order



with the M(acac)_n absorbing at the shortest wavelengths and the M(dbm)_n absorbing at the longest wavelengths. (dbm = dibenzoylmethane). Similar shifts were noted by Sasaki et al⁹²

when the methyl group in metal acetylacetonates was replaced by a furoyl ring.

It is the purpose of the discussion to show next that while the weak inductive effect remains constant, the resonance effect of the phenyl group is dominant but variable. The extent of the shift in the UV spectrum attributed to that resonance effect is also dependent on the angle τ , which is the out-of-plane twist of the phenyl ring with respect to the chelate ring plane. The resonance interaction between two p- π orbitals depends on the cos of the angle τ , or on the $\cos^2 \tau$.^{20,93} Therefore, the relative resonance interactions in two molecular systems can be compared in terms of the $\cos \tau$ or $\cos^2 \tau$. Comparisons could be made by us only for those compounds for which ultraviolet and/or visible spectra were known, and for which crystal structure data on the angle τ were also available.

Prior to discussing the organometallic compounds, it might be pointed out that a similar qualitative treatment of the effect of twisting a "single" bond in a conjugated system had been discussed by Ingraham in a review on Steric Effects on Certain Physical Properties.^{85a} In a conjugated system the single bond will have some double bond character, and the strength of that bond will be

maximal when all atoms attached to that bond lie in the same plane. Such a planar arrangement allows for maximum overlap of the p-orbitals across the bond.

The changes in the electronic spectra due to steric effects have been investigated in biphenyls and other poly-phenyl systems. The additional resonance of the biphenyls over two isolated benzene rings was plotted by Dewar^{85b} as a function of the \cos^2 of the angle of twist. The curve for that \cos^2 dependence shows that for twist angles as large as 45° , there is still 50% resonance energy; and that the resonance energy becomes negligible as the angle of twist approaches 90° . In some respect the experimental studies on spectra of the biphenyl systems could serve as a model for the organometallic compounds to be discussed, where the phenyl ring is attached to the "quasi-aromatic" acac chelate ring.

In 1951 Turner and Voitle^{85c} pointed out that twisting a single bond away from coplanarity in a conjugated system may produce three effects on the spectrum. (1) Relatively small twist angles will result in no change in the wavelength of maximum absorption, but will cause a decrease in the absorption intensity. (2) Larger twists shift the absorption maximum to shorter wavelengths, in

addition to decreased intensity. (3) When the twist is large enough almost to eliminate interaction between the two portions of the molecule, the spectrum is similar to the sum of the spectra of "component parts" on either side of the twisted bond.

Our comparisons focus on band III, which had been attributed by Singh and Sahai to a π_3 to π_4 transition, based on the Huckel LCAO-MO calculations carried out by Barnum⁹⁴ and by Fackler et al.^{95,96} This band has been selected, because most of the compounds include data on this band, while bands I, II, and IV are absent from several compounds.

In the Cu-beta-diketonate series, Singh and Sahai²⁹ had reported the UV spectra of $\text{Cu}(\text{acac})_2$ and $\text{Cu}(\text{bzac})_2$ in methanol. In the $\text{Cu}(\text{acac})_2$ band III appears at 294 nm, with $\epsilon = \text{antilog } 4.40 = 25,120$. In the $\text{Cu}(\text{bzac})_2$ band III appears at 320 nm, with $\epsilon = \text{antilog } 4.322 = 21,000$. The bathochromic shift (to longer wavelengths and lower energy) is 26 nm, and it can be attributed to the resonance effect of the phenyl group. Hon et al.⁸² reported that in $\text{Cu}(\text{bzac})_2$ the out-of-plane twist angle τ was 14.3° . Since $\cos \tau$ is 0.969 (\cos^2 is 0.939), it can be estimated that the resonance interaction is 97% (94%). Here one would certainly expect

the resonance effect of the phenyl group to dominate over the inductive effect.

Extending this approach consider next the $\text{Cu}(\text{dibenzomethane})_2$ or $\text{Cu}(\text{dbm})_2$, in which two phenyl rings were substituted for the two methyl groups of the acac. Its crystal structure has been reported by M. Blackstone et al⁹⁷ with τ angles of 9.3° and 4.6° . In this case the $\cos \tau$ values are .987 and .997 (\cos^2 are .904 and .994), respectively, and the resonance interaction is even higher than in $\text{Cu}(\text{bzac})_2$. Since there are two phenyl groups, each of them capable of contributing electron density, one would expect the band III in $\text{Cu}(\text{dbm})_2$ to appear at considerably lower energy (longer wavelength) than either $\text{Cu}(\text{acac})_2$ or $\text{Cu}(\text{bzac})_2$. In fact, Singh reports band III at 350 nm, or 56 nm higher than band III in $\text{Cu}(\text{acac})_2$, and with a higher ϵ_{max} value for the $\text{Cu}(\text{dbm})_2$, or a value equal to $\text{antilog } 4.58$ which is 38,020, as would be expected from this discussion.

In the palladium beta-diketonates, ultraviolet and crystal structural data are available only for $\text{Pd}(\text{bzac})_2$, with some limited data available on the $\text{Pd}(3\text{-}\phi\text{-acac})_2$ compound. First, one should compare the UV spectra of $\text{Pd}(\text{acac})_2$ and $\text{Pd}(\text{bzac})_2$. It should be noted that the angle τ reported²⁰

for $\text{Pd}(\text{bzac})_2$ is 23° , and that $\cos 23^\circ$ is 0.921 (\cos^2 is 0.847). One would anticipate resonance interaction of 92% (85%), which is slightly less than in the analogous copper compound. Considering the UV spectra of $\text{Pd}(\text{acac})_2$ and $\text{Pd}(\text{bzac})_2$, we observed a bathochromic shift of 24 nm in the $\text{Pd}(\text{bzac})_2$ -- from 328 nm for $\text{Pd}(\text{acac})_2$ up to 352 nm in $\text{Pd}(\text{bzac})_2$. The intensity of the band in the $\text{Pd}(\text{bzac})_2$ is greater, as measured by a higher ϵ_{max} of 19,670 in $\text{Pd}(\text{bzac})_2$, and only 12,080 in $\text{Pd}(\text{acac})_2$. These changes are consistent with the estimation of resonance interaction from $\cos \tau$ ($\cos^2 \tau$) dependence.⁹³ Furthermore, the bathochromic shift is slightly less in the Pd compounds (24 nm) than in the analogous Cu compounds (26 nm), also consistent with the lower percentage in resonance interaction (92% for Pd vs. 97% for Cu based on \cos values, or 85% vs. 94% based on \cos^2 values, respectively).

A further indication of the relationship between the magnitude of the τ angle and the shift in band III of the UV spectrum, can be found by comparing the "limited" data on the effect due to substituents on the "gamma" carbon of the chelate ring of $\text{Pd}(\text{acac})_2$. For example, $\text{Pd}(3\text{-}\phi\text{-acac})_2$ had been prepared by Nesmeyanov et al.⁹⁸ and by Carmichael.²⁷ Although its crystal structure has not been reported, that

of the $\text{Cu}(3\text{-}\phi\text{-acac})_2$ had been determined by Carmichael et al.⁹⁹

In the $\text{Cu}(3\text{-}\phi\text{-acac})_2$ molecule the phenyl ring is twisted 70° from the plane of the chelate ring, probably due to steric crowding. If we assume that the angle of twist in $\text{Pd}(3\text{-}\phi\text{-acac})_2$ is also large, and of the same order of magnitude as in the Cu analogue, and using the $\cos \tau$ ($\cos^2 \tau$) dependence to estimate the resonance interaction, we conclude that it is reduced to only 34% (or 11% using \cos^2). Therefore, in the $\text{Pd}(3\text{-}\phi\text{-acac})_2$ one would expect a negligible resonance effect, and one might expect that the inductive electron withdrawing effect of the phenyl could predominate.

Gubin et al⁹⁰ had reported the UV spectra of $\text{Pd}(3\text{-}\phi\text{-acac})_2$ as well as that of $\text{Pd}(3\text{-methyl-acac})_2$, and it is useful to compare those with the UV spectrum of $\text{Pd}(\text{acac})_2$ itself. In case of the methyl substituent, it can only donate electrons inductively, so its effect would be to lower the energy. In the methyl-substituted compound band III is observed at 344 nm, or a bathochromic shift of 16 nm from the absorbance at 328 of $\text{Pd}(\text{acac})_2$. Since the resonance interaction in the $\text{Pd}(3\text{-}\phi\text{-acac})_2$ was estimated as negligible, one would expect the phenyl ring's inductive electron withdrawing effect to be much more important than in the other compounds discussed. Therefore, if a bathochromic shift is to be

observed, its magnitude should be quite small. Indeed, the band seen in $\text{Pd}(\text{acac})_2$ at 328, is observed in $\text{Pd}(3\text{-}\phi\text{-acac})_2$ at 340, or at a bathochromic shift of only 12 nm. This comparison of the ultraviolet band positions of $\text{Pd}(\text{acac})_2$, $\text{Pd}(3\text{-me-acac})_2$ and $\text{Pd}(3\text{-}\phi\text{-acac})_2$ seems to lend further validity to the qualitative relationship we suggest between resonance contribution of the phenyl ring, the out-of-plane tilt angle \mathcal{T} , and the bathochromic shift.

Proceeding now to the discussion of the UV spectra of PdL_2 Species I and PdL_2 Species II, it must be noted that no data are available on the crystal structure and angle \mathcal{T} for these compounds. Some of the discussion is, therefore, speculative, but it is qualitatively related to the arguments outlined above. We shall focus on band III, and compare the UV spectra of $\text{Pd}(\text{bzac})_2$, PdL_2 Species I (cis) and PdL_2 Species II (trans). (Figs. 17, 20, 24)

It will be assumed that the crystal structure of the trans isomer, PdL_2 Species II, is similar to that of $\text{Pd}(\text{bzac})_2$ trans. It is expected that the effect of the p-octyloxy substituent is small. However, since the alkoxy group is an electron donor on a phenyl ring, we would expect band III to be shifted to lower energy (longer wavelength) than its counterpart in $\text{Pd}(\text{bzac})_2$. Consistent with this

expectation, the absorbance is at 355 nm, or 3 nm higher than in $\text{Pd}(\text{bzac})_2$, with an ϵ value of 34,750. It should be emphasized that this value is higher than the ϵ_{max} of 19,670 we found for $\text{Pd}(\text{bzac})_2$ or that of 30,900 reported by Singh and Sahai.²⁹ Therefore, this small bathochromic shift, and the general similarity in appearance of the UV spectra of $\text{Pd}(\text{bzac})_2$ trans and PdL_2 Species II are consistent with our assignment of trans structure to PdL_2 Species II. Comparing the relative intensities of band III and II in both compounds: in $\text{Pd}(\text{bzac})_2$ the intensity of band III is 66% of that of band II; in PdL_2 Species II the relative intensity of band III is 79% of band II.

On the other hand, the UV spectrum of PdL_2 Species I is considerably different from that of $\text{Pd}(\text{bzac})_2$. In terms of relative intensities of bands III and II, in PdL_2 Species I the intensity of band III is only 20% of the intensity of band II. It should be noted that in a cis configuration, both bulky phenyl rings with their p-alkoxy substituents, would be on the same side. We might speculate that steric crowding would tilt the p-substituted phenyl rings farther from the plane of the chelate rings, much beyond the 23° angle reported for the trans $\text{Pd}(\text{bzac})_2$.²⁰ Such an increased tilt would reduce effective conjugation between the phenyl

and chelate rings, and the inductive electron withdrawing effect of the phenyl group might become dominant. If those assumptions are correct, the cis isomer of PdL_2 would absorb at a higher energy (or shorter wavelength) than the trans isomer, with a corresponding lowering in the intensity. In fact, PdL_2 Species I absorbs at 330 nm, at considerably shorter wavelength (higher energy) than either the PdL_2 trans or the $\text{Pd}(\text{bzac})_2$ trans. Incidentally, this is the approximate position of the absorption of $\text{Pd}(\text{acac})_2$, perhaps suggesting that the resonance effect and the opposing inductive effects of the phenyl group are almost equalized in this compound. An alternative explanation might assume that as in the case of the biphenyls discussed by Turner and Voitle, the angle of twist is large enough to eliminate the interaction between the $\text{Pd}(\text{acac})_2$ subunit of the molecule and the attached p-alkoxy-phenyl substituent.

The fact that the relative intensity of band III in PdL_2 Species I cis is considerably lower (only 20% of the intensity of band II) than the appropriate relative intensity of band III in Species II, is another indication that the phenyl ring in Species I is probably considerably twisted out of the plane of the acac ring. As discussed in the case of the biphenyls, even relatively small twist angles lead to

considerable decreases in the absorption intensity.

Conceivably, one of the phenyl rings might be twisted to a greater extent than the other, as was found in the X-ray structure of the cis form of vanadyl-benzac, $\text{VO}(\text{C}_6\text{H}_5\text{COCHCOCH}_3)_2$, determined by Hon et al.⁸³ In the cis form of that compound one of the phenyl rings was twisted by 13° more than the other. Shugam et al.⁸⁴, who reported the X-ray structure assigned to the cis form of $\text{Pd}(\text{bzac})_2$ did not report the angle of twist between the phenyl ring and the acac plane.

While no data is available on the twist of the phenyl rings in compounds PdL_2 Species I and PdL_2 Species II, the analysis of their ultraviolet spectra, as outlined above, especially in terms of the shifts in the position of maximum absorbance and the changes in intensity in band III, is consistent with and lends further support to the assignments of cis and trans form to PdL_2 Species I and PdL_2 Species II, respectively.

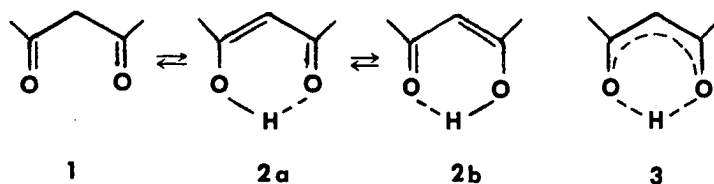
Discussion of NMR Spectra

The discussion of our NMR data will begin with a brief survey of the information and data in the literature on analogous compounds. An attempt will be made to show how other investigators used the NMR data to deduce the structure of beta-diketones and their metal chelates, as well as to point out some of the limitations of NMR, and some of the ways in which NMR complements or reinforces data obtained from vibrational spectroscopy. Literature data from investigations of the extent of anisotropy of the chelate ring will also be included.

Before discussing the data obtained in this work, it is necessary to review some of the NMR data and interpretations in the literature. Lowe et al⁵¹ reported the following NMR spectrum (in τ) for benzoylacetone: 7.87 (enol--CH₃); 7.84 (keto -CH₃); 6.09 (CH₂); 3.92 (vinyl); multiplet with center at 2.34 (aromatic), and minus 6.02 (OH). For the p-methoxy benzoylacetone Lowe's NMR data are (in τ values): 7.92 (enol -CH₃); 7.84 (keto -CH₃); 6.23 (CH₃O); 4.03 (vinyl); 2.71 aromatic quartet (J = 9cps); minus 6.16 (OH).

It is known that in pentanedione (acac) the equilibrium between the keto and enol forms (1 and 2 below) is established

so slowly at room temperature that the two forms can be easily detected in each other's presence by their NMR spectra. Reeves¹⁰⁰ reported that the two methyl groups of the enol form give only one sharp signal in the ¹H-NMR spectrum, even though their environments are different in the usual notation, and it is very unlikely that the signals coincide by accident. It has been suggested that either the interconversion of the two tautomers (2a and 2b) with equal energy is very fast even at low temperatures; or the molecule has a symmetrical structure (structure 3), in which the bonds between the acidic enolic proton and the two oxygen atoms are of exactly the same length.



2,4-Pentanedione or acac reacts with many metal ions to form complexes. Some of those chelates are so stable that the methine proton behaves almost like an aromatic proton, and it can be substituted by several reagents (i.e. Br, Cl, NO₂, etc.) In 1945 M. Calvin¹⁰¹ first tried to explain the stability of these chelates by a benzenoid resonance. It should be pointed out that while in the keto form of acac

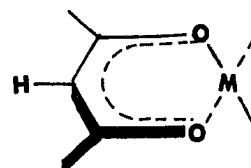
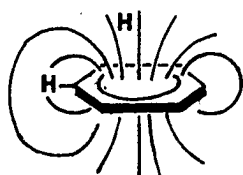
(Structure 1) the acetyl groups can rotate about the bond joining them to the central carbon atom, the enol form is fixed in a planar or nearly planar structure in the cis configuration, because of the hydrogen bond formed (structures 2a, 2b). X-ray structures have shown different lengths for the C--O and C--C bonds in some of the beta diketones investigated (1,3-phenyl-1,3-propanedione), as reported by Williams in 1966¹⁰² as well as in $\text{Cu}(\text{acac})_2$, as reported by Shugam in 1952.¹⁰³ However, in the majority of the chelates of acac with a wide variety of metals reviewed in Bock's article,⁴³ the X-ray structural analyses indicate a symmetrical electron distribution in the chelate ring. An average values of 1.27 Å for the C--O distance and 1.39 Å for the C--C distance was reported by Lingafelter and Brawn.¹⁰⁴

Bock points out, however, that results of X-ray analyses refer to the crystal, in which the structure may be different from that in solution on which NMR studies are carried out; that difference due possibly to interactions with neighboring groups in the crystal lattice. In addition, the X-ray analysis yields only distances, and provides no direct information as to whether the conjugation in the chelate ring passes cyclically through the metal ion, even

though the average C--C distance is 1.39 Å, as in benzene. Attempts have been made to use NMR spectroscopy to detect the two tautomers separately, but within the time scale of NMR spectroscopy this has not been detected. Bock emphasizes that vibrational spectroscopy is more promising, because structures with lifetimes as low as 10^{-12} seconds should still be recognizable in the region of C--C, C--O and O--H stretching vibrations.

Some NMR criteria for distinguishing between an open enolate, a chelate, and a C-bonded structure in the metal complexes of beta-diketones, are summarized in the review article by Bock et al.⁴³ The authors point out that these three possible structures can be adequately distinguished on the basis of the vibrational spectrum. In discussing the bond character of the metal chelates of the beta-diketones, the authors emphasize that the bonding in the chelate is not the same as it is in the aromatic benzene ring, even though the metal-oxygen bond should have some pi character.

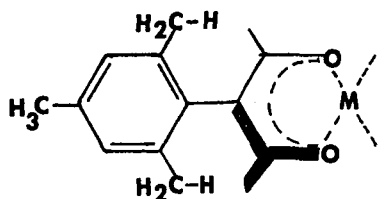
The magnetic anisotropy of the chelate ring is compared with that of the benzene, as shown below. Protons



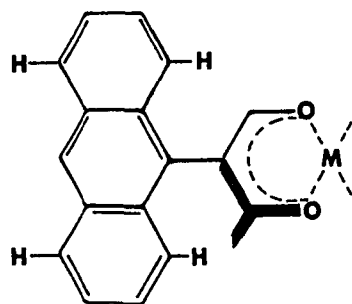
in the plane of the aromatic ring are shifted downfield, and protons above and below this plane are shifted to higher fields. Attempts to deduce the aromatic character of the metal chelates of acac, as related to the chemical shift, had been interpreted in different ways by various authors. While some argued in favor of aromaticity, others argued against it. It has been shown that the position of these protons is influenced by polar effects, and additional evidence for this idea came from calculations on the shift of the C-H signal and of the $^{13}\text{C}-\text{H}$ coupling with the aid of the electric field in the plane of the ring by Hammett et al.^{105a,105b}

As a further test for the "aromaticity" of the six electron system by cyclic conjugation via the metal atom, the extent of magnetic anisotropy was estimated and compared with benzenoid systems. For this purpose Kuhr and Musso prepared pentanedionates in which protons were situated above and below the plane of the chelate ring.¹⁰⁶ These pentanedionato compounds were compared with model aromatic compounds to determine the magnitude of the shifts for such protons in aromatic systems. Kuhr determined the difference in changes in δ in the shifts of the o- and p-methyl groups in the NMR spectra of phenylmesitylene, bimesityl, 9-mesityl-

anthracene and several other compounds of this type. (See structures below.)



Mesityl-derivative



Anthryl-derivative

Kuhr and Musso had shown that the difference was about 0.5 ppm if the system is truly aromatic. The range of differences was 0.30 to 1.06 ppm, and the variation was attributed partly to the different average twisting angles of the two aromatic systems in relation to each other, and partly to the fact that the 1,8-anthryl hydrogen atoms are more firmly fixed above the other ring than the protons of the rapidly rotating methyl groups. The observed shifts agreed with values calculated, taking into account the local contributions of the atoms to the total anisotropy.

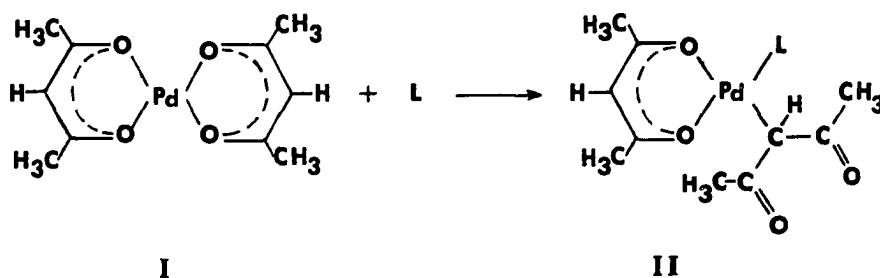
The NMR spectra of the corresponding mesityl- and anthryl-substituted acetylacetones and their metal chelates were determined by Kuhr and Musso.

The shift differences for the proton, shown above, in the substituted acac compounds were only 0.20 for the

mesityl-substituted ones and 0.05 for the anthryl-substituted compounds. In case of the Pd chelates in CDCl_3 , the change in δ was 0.22 ppm for the mesityl- and 0.08 for the anthryl-substituted chelate. It is pointed out that the shift differences are essentially the same for the metal chelates, for the free enolic acid forms, and for the alkali metal salts. With increasing stability of the metal chelates, as in going from Be, Al, Co to Pd compounds, there is no additional shift of the protons above the plane to higher magnetic fields. The values for the anthryl derivatives are smaller instead of greater than those for the mesityl compounds. Kuhr and Musso have concluded from these results at the angular C—C—C part of the chelate ring has no magnetic anisotropy comparable with that of the benzene.

NMR spectra of metal chelates of beta-diketones can also be analyzed to determine whether or not there is any metal-carbon bonding. This possibility was considered and investigated by Baba et al⁷⁹ with Pd as the metal, by Lewis and Oldham¹⁰⁷ for compounds of Pt. Baba and coworkers investigated the reaction of bis (acetylacetonato)palladium (II) with triphenylphosphine and other nitrogen bases (pyridine, diethylamine, N-methylbenzylamine). One of the chelating

acac ligands of the $\text{Pd}(\text{acac})_2$ was transformed in the course of the reaction into a Pd-carbon bonded unit, and the fourth coordination site of the palladium was taken up by the base. The palladium was bonded to the gamma carbon of the unchelated acetylacetone, and a methine proton was also present on that carbon. (Structures and reaction shown below.)



Baba et al⁷⁹ determined that in structure I the $\nu(\text{C}=\text{O})$ and $\nu(\text{C}=\text{C})$ bands of the chelating acac ligand appear in the 1500 to 1600 cm^{-1} region. In structure II new bands were observed in the 1600 to 1700 cm^{-1} region, which could be assigned to the $\nu(\text{C}=\text{O})$ of the carbon bonded acac ligand. In addition a strong band, observed for Structure II in the 500-550 cm^{-1} region, was attributed to the $\nu(\text{Pd}-\text{C})$ vibration.

The coexistence of one oxygen-chelating acac ligand and one carbon-bonded ligand was revealed also by proton NMR spectra. In compound II the methine proton on the carbon

bonded to the palladium appears at the following τ values relative to internal TMS (in CDCl_3 solution): at 6.46 when the L (ligand) is $\text{P}\phi_3$ (triphenyl phosphine), at 5.76 with pyridine as the L group and at 5.50 with $\text{NH}(\text{CH}_3)\text{CH}_2\text{C}_6\text{H}_5$ (N-methylbenzylamine). All of the above signals appear as singlets, except in the phosphine complex, where the signal appears as a doublet because of coupling with the phosphorus nucleus. As in the case of similar platinum complexes investigated by Lewis et al¹⁰⁷ the methine proton of the carbon bonded acac ligand absorbs at higher fields in comparison with that of the chelating acac.

NMR data on some Pd-beta diketones and compounds related to them are also included in the report by A. N. Nesmeyanov et al⁹⁸, who prepared $\text{Pd}(\text{acac})_2$, $\text{Pd}(3\text{-me-acac})_2$ and $\text{Pd}(3\text{-}\phi\text{-acac})_2$, as well as five other halo- and cyano-gamma-substituted palladium bisacetylacetonates. In $\text{Pd}(\text{acac})_2$ they reported the chemical shifts of the chelate protons at 2.00 ppm for the methyl groups and at 5.4 ppm for the gamma proton. In $\text{Pd}(3\text{-methyl-acac})_2$ the signals of the methyl groups of the chelate ring were seen at 2.10 ppm, while the protons of the gamma-substituted methyl groups signals appeared at 1.85 ppm.

Table XV summarizes the position of the NMR signals for the compounds that had been described before,^{45,48,98}

TABLE XV. CHEMICAL SHIFTS IN THE NMR SPECTRA OF PERTINENT COMPOUNDS

Compounds	acac ^a	bzac ^b	p-OCH ₃ - -bzac ^b	Ligand	Pd(acac) ₂ ^c	Pd(bzac) ₂	PdL ₂ Sp. II	PdL ₂ Sp. I
1°H, alkyl chain	----	----	----	0.90	-----	-----	0.9	0.9
2°H, alkyl chain	----	----	----	1.33	-----	-----	1.33	1.34-1.55
CO-CH ₃ , enol form	2.0	2.12	2.08	2.15	2.00	2.11	2.20	2.00 ^d
COCH ₃ , keto form	2.2	2.16	2.16	2.26	-----	-----	----	----
CO-CH ₂ , keto form	3.5	3.91	----	----	-----	-----	----	----
OCH ₂ or OCH ₃ (ether)	----	----	3.77	4.03	-----	-----	4.00	4.05
C=C-H, "vinylic" H	5.48	6.08	5.97	6.10	5.40	6.08	6.03	----- ^e
aromatic	----	7.66	7.29 (J=9)	6.95 7.00	-----	7.25 7.45	6.79 6.96	6.88 7.03
aromatic	----	----	----	7.75 7.95	-----	7.75 7.95	7.78 7.95	7.86 8.00

(a) NMR data are from Jarrett et al.⁴⁵

(b) NMR data are from Lowe and Ferguson⁴⁸

(c) NMR data are from Nesmeyanor et al.⁹⁸

(d) Very strong signal; area larger than expected for 4H

(e) No signal where "vinylic" methine seen in other compounds

and with which our data should be compared.

Several points need to be made concerning the data shown in Table XV. It can be seen from the summary and comparison of chemical shifts in the NMR spectra of our compounds and those reported in the literature, that the assignments are generally consistent. The "ligand" — p-octyloxy-benzoylacetone (Fig. 13)—should be compared with both PdL₂ compounds, Species I cis (Fig. 18) and Species II trans (Fig. 21).

The areas and multiplicities of each of the signals in the NMR spectrum of the ligand correspond to the assignments of each set of protons in the compound. The signals, with their δ value position, multiplicity and area, as well as assignments, are listed below: 0.90 (t, broad, 3H, CH_3CH_2 --); 1.33 (m, 12H, C- CH_2OH_2 -, for 6 CH_2 groups); 2.15, 2.26 (d, 4H, CH_3COCH); 4.03 (t, 2H, CH_2O); 6.10 (s, 1H, $\text{CH}=\text{COH}$); 6.95, 7.00; 7.75, 7.92 (two doublets, 4H, aromatic). The NMR spectrum of our ligand is generally similar to that reported⁴⁸ for the p-methoxy-benzyolacetone, except that the ligand also has the signals due to secondary methylene groups in the larger alkyl chain.

The absence of any signal from the CO-CH₃ or CO-CH₂ protons in the ligand prepared, is evidence that it exists

completely in the enol form. The signal due to the keto form in the case of acac (Ref. 45) indicates that only 15% is present in the keto form, as judged by the integrated intensities of the signals. Lowe and Ferguson⁴⁸ had reported that in benzoylacetone 94.5% was present in the enol form; in p-methyl-benzoyl-acetone the percentage of enol was 95.7; and in p-methoxy-benzoylacetone the enol was present in 94.7%. They also reported⁴⁸ that when the para position of benzoylacetone was substituted by a strongly electro-negative group, i.e. -Br or -NO₂, the enol form accounted for 100% of the compound. In Lowe's report⁴⁸ the ratios of enol were based on integrated intensities of vinyl and methylene signals in the NMR.

The NMR spectrum of Pd(bzac)₂ is similar to that of the unchelated benzoylacetone (Fig. 18). In the organo-palladium compound there is no signal due to the keto form, and the signal due to the "gamma" or "vinylic" methine appears as a doublet with a very small coupling constant of 0.05 ppm. In all likelihood this splitting is due to second order perturbations. One of the isotopes of palladium, ¹⁰⁵Pd, with a natural abundance of 22.6%, has a nuclear spin moment of 5/2.¹⁰⁸ Since the "gamma" methine protons of both trans chelate rings in Pd(bzac)₂ are closest to the central

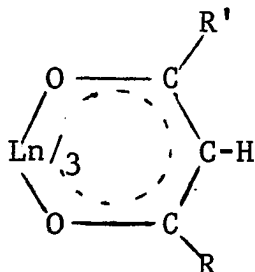
Pd atom, they would be subject to second order perturbations. It should be noted that Baba et al reported that in their Structure II, the methine proton of the Pd-carbon bonded acac ligand appeared as a doublet, when the base used was triphenyl phosphine; this doublet, with $J_{P-H} = 6.3$ Hz, was attributed to coupling with the phosphorus nucleus which has a nuclear spin of $\frac{1}{2}$.⁷⁹

The NMR spectrum of PdL₂ Species II (Fig. 25) is similar to that of the unchelated ligand. The areas and multiplicities are as expected. The methyl group (enol form) is shifted slightly downfield (2.20 vs 2.15 in the ligand), and the gamma or "vinyl" proton is shifted slightly upfield (6.03 vs. 6.10 in the ligand). There is also a downfield shift in one of the aromatic protons (6.79 in Species II vs. 6.95 in the ligand).

The spectrum of PdL₂ Species I (Fig. 21) shows more changes when compared with the NMR spectrum of the ligand. The methyl group of the chelate ring is shifted upfield (2.00 vs. 2.15 in the ligand), and the signal in this area is very strong, with an area that is larger than four protons. The aromatic protons are also shifted, and their coupling constants are greater (from 6.88 to 8.00, vs. 6.95 to 7.95 in the ligand for the four signals in the aromatic region).

Furthermore, the signal due to the "gamma" or "vinylic" proton is not seen in the usual 5.4 to 6.1 region. It appears from the spectrum that the gamma proton has shifted considerably upfield, and its signal coincides with that of the methyl group. It is tempting to speculate on the nature of this shift and to relate it to the structure of the compound.

This shift could be due to a pseudocontact mechanism similar to that caused by NMR shift reagents.¹⁰⁹ Those reagents are lanthanide chelates of beta-diketones, with the general structure shown below, with Ln the symbol for a lanthanide.



The NMR shift reagents can associate with a wide variety of substrates, by readily expanding their coordination number beyond six. Since shift reagents were first introduced in 1969 by Hinckley,¹¹⁰ they have been used to magnify chemical shift differences of nonequivalent protons. Most of those reagents are complexes of Eu, Pr and Ho, such as $\text{Eu}(\text{dpm})_3$ in which $\text{R} = \text{R}' = t\text{-butyl}$ in the structure shown

above; or $\text{Eu}(\text{fod})_3$ in which $\text{R} = \text{t-butyl}$ and $\text{R}' = \text{perfluoropropyl}$.

The europium shift reagents generally produce downfield shifts, but upfield shifts can be affected by the use of diamagnetic shift reagents, such as complexes of promethium (Pr).¹¹¹ T. J. Marks et al¹¹² reviewed the effect of shift reagents on various organometallic compounds, and they emphasized that the effectiveness of a given shift reagent system is a complex function of the magnetic anisotropy, electron spin relaxation time, solubility, and substrate affinity. They found that when the organometallic substrate was $(\text{C}_6\text{H}_5)\text{Fe}(\text{CO})_2\text{CN}$ and the lanthanide metal ions used in the shift reagents were Ho or Pr, the shifts were upfield (from C_6H_6 used as standard for comparison). When Ho chelates were used, the observed shifts were a function of lanthanide to substrate ratio. The shifts ranged in magnitude from 4.0 ppm with a low ratio of shift reagent to substrate, to 18.9 ppm for a 1:2 ratio, and finally to 34.1 ppm for a 1:1 ratio of shift reagent to substrate. In case of Pr shift reagents, the magnitude of shift ranged from 4.0 ppm for very low ratio, to about 8.5 ppm for a 1:1 ratio of reagent to substrate.

If one assumes that in solution there are interactions between adjacent molecules of PdL_2 cis, then one molecule

could act as a pseudo "shift reagent" on another molecule within the same molecular aggregate. In the case of the trans isomer of PdL_2 , however, the bulky phenyl groups with their large p-octyloxy chains, prevent close contact between two adjacent molecules. On the other hand, in the cis isomer both phenyl groups are on one side of the Pd-chelate plane, and the other side is free to interact with an adjacent molecule. It seems likely that any pseudo contact shifts would be noted in the cis isomer of PdL_2 , but not in the trans.

In addition to the shifts of the signals that have apparently taken place in PdL_2 cis, the enhancement of the signal at δ 2.00 must be accounted for. The latter could be due to nuclear Overhauser effect (NOE) that occurred accidentally or spontaneously, as a result of coupling between two nuclei through space instead of through bonding electrons. Experimentally the NOE effects have been used to gain information about the spatial arrangement of nuclei in a molecule. The NOE is a change in the integrated NMR absorption intensity of a nuclear spin when the NMR absorption of another spin is saturated.¹¹³

In case of PdL_2 Species I it is believed that due to intermolecular interaction involving the Pd nucleus

with spin $5/2$, the relaxation time of the methine proton was shortened, leading to an enhancement of its signal.

Experiments can be suggested to confirm or modify the two proposed effects that could account for the NMR spectrum of Species I. Inasmuch as the pseudo-contact shift observed for the methine proton is upfield, one should choose a shift reagent, i.e. a complex of europium, that is known to produce a downfield shift. If adding such a shift reagent to Species I would shift some of the signal at $\delta = 2.0$ downfield from TMS, the experiment would serve to verify the proposed pseudo-contact observed. In an alternative experiment one might actually investigate Species I as shift reagent for other substrates.

The design of experimental conditions to confirm the intermolecular interactions leading to the enhancement of the signal, is more complicated. This effect — a type of nuclear Overhauser effect — is due to intermolecular interactions leading to enhancement of the signal. In ordinary NOE experiments one is largely interested in intramolecular NOE and in the elimination of intermolecular NOE effects.

In 1965 Kaiser¹²² had observed intermolecular NOE between protons of cyclohexane and chloroform. He had

suggested that such experiments should be of interest in studying the structure of liquid and intermolecular forces. In a review of chemical applications of NOE studies Noggle and Schirmer¹²³ suggest that such investigations of intermolecular NOE effects should be useful in studying association and solvation phenomena. They point out, however, that the lack of such studies may be due to the theoretical difficulties in treating both intermolecular relaxation and the theory of liquid mixtures.

The relaxation rate is proportional to several factors. It is important to note here that it is proportional to the spins causing the relaxation, is smaller at higher temperatures, and is larger in a more viscous solvent.¹²³ In ordinary NOE experiments the sample concentration must be kept low, so that intermolecular contributions are small compared to intramolecular effects. Since the postulated enhancement of the signal is believed to be caused by intermolecular effects, the proposed experiments should be designed to maximize intermolecular interactions. Suitable solvents would have to be selected and investigated, and the NMR spectrum of Species I investigated in a series of different dilutions. If the signal enhancement proves greater at higher concentrations, it would indicate that the proposed effect is intermolecular.

In view of the limited solubility of PdL₂ Species I, the selection of suitable solvents and studies at varying concentrations involve problems that were considered beyond the scope of this investigation. In addition, as pointed out by Noggle and Schirmer,¹²³ the theoretical treatment of the effects observed would prove quite difficult.

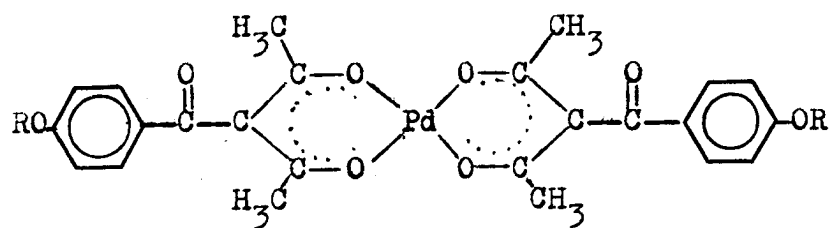
Two alternative structures might be considered for PdL₂ Species I, that could account for its anomalous NMR spectrum. In each of those two structures the ligand coordinated to the palladium in Species I is different from the ligand coordinated in Species II. Such a ligand is presumed to have formed during the reaction of the original ligand with PdCl₂, by a retrograde Claisen condensation. In both of the alternative structures the molecular formula of the palladium complex would correspond to PdC₄₀H₅₄O₈, and not to the PdC₃₆H₅₀O₆ found in PdL₂ Species II. Certain aspects common to both structures can be discussed together, then each structure will be considered separately.

The elemental analysis obtained on the purest sample of Species I, as judged by DTA criteria, showed 62.81% carbon, 7.15% hydrogen and 13.3% palladium by ash residue, or 13.56% by atomic absorption. Calculations based on

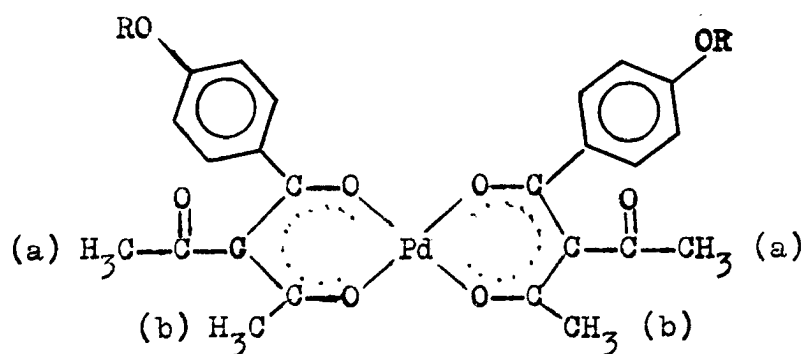
$\text{PdC}_{36}\text{H}_{50}\text{O}_6$ would require 63.10% C, 7.36% H and 15.52% Pd, while calculations based on $\text{PdC}_{40}\text{H}_{54}\text{O}_8$ would require 62.45% C, 7.08% H and 13.83% Pd. The experimental findings of the percentages of carbon and hydrogen could fit either formula, but the percent of palladium seems to be closer to that calculated for the heavier molecule.

On the other hand, the $\text{PdC}_{40}\text{H}_{54}\text{O}_8$ molecule would have a molecular weight of 769.3, while the molecular weight of $\text{PdC}_{36}\text{H}_{50}\text{O}_6$ corresponds to 684.8. Osmometrically determined molecular weights of Species I yielded values of 705 in benzene and 673 in chloroform, with an average value of 689, and a relative deviation of each experimental value of 1.7% and 2.9% from the calculated value of 684.8. A molecular weight of 769.3 would require a relative error of 12.6% or 9.2% on the respective experimental values, which is not considered likely. Thus, while the experimental low percentage of Pd supports formula $\text{PdC}_{40}\text{H}_{54}\text{O}_8$, the two molecular weight determinations support $\text{PdC}_{36}\text{H}_{50}\text{O}_6$.

As shown in Figure 56-B, structure X would be a highly symmetrical structure. All the methyl groups would be chemically and magnetically equivalent, and all would show the same signal in the NMR spectrum. This structure could account for the absence of the signal around $\delta = 6.0$,



Structure X



Structure Y

Figure 56-B

Alternative Structures for PdL₂ Species I

as well as the single strong signal at $\delta = 2.0$. However, like $\text{Pd}(\text{acac})_2$, this structure would be of overall D_{2h} symmetry, with some local D_{4h} symmetry around the $-\text{PdO}_4^-$ subunit of the molecule. As discussed in a previous section, the comparisons of far IR and low frequency Raman Pd-O fundamental bands suggest that Species I has C_{2v} symmetry.

Structure Y would correspond to a cis configuration and be of C_{2v} symmetry. However, it seems unlikely that the NMR signal of the acetyl groups (protons labeled a) would coincide with the signals of the methyl groups substituted on the chelate ring (protons labeled b). Only one signal is seen at $\delta = 2.0$ in the NMR spectrum, which makes structure Y also an unlikely alternative.

A further experimental way of distinguishing between the three alternative structures for Species I, would involve synthesis of the ligand proposed for complexes with structure X and Y. Such a ligand -- i.e. the (p-octyloxy)-1-phenyl-2-aceto-1,3-butanedione -- could then be directly coordinated to the Pd^{+2} , and the properties of the complex formed could be compared with those of PdL_2 Species I.

Each of the structures considered as alternatives fits better with some data, but is not supported by all the data. It should probably be pointed out that PdL_2

Species I was the more difficult to purify, and showed less potential for mesomorphic behavior than Species II. It was felt, therefore, that an extensive investigation to distinguish between the three alternative structures suggested for Species I was not justified. Although the evidence is not completely conclusive for either of the structures proposed for Species I, the weight of the combined evidence seems to favor the idea that Species I is the cis isomer of Species II.

Finally, it should be pointed out that the NMR spectra of the organo-palladium compounds that are the subject of this investigation, show no signal in the region of 3.5 to 4.50, where Baba et al⁷⁹ had reported the methine proton of the Pd-carbon bonded ligands. Since the far infrared spectra of these compounds show no evidence of Pd-carbon bonds either, we feel quite confident that these compounds do not contain any palladium-carbon bonded ligands.

Discussion of DTA Data and Potential Mesomorphism

Very interesting data, obtained by differential thermal analysis (DTA), can be used to compare the behavior of the PdL_2 compounds with other organo-palladium compounds. The DTA thermograms of most ordinary compounds show endotherms during phase changes that correspond to the melting point or boiling point (Fig. 57). Mesomorphic compounds (Figs. 34, 58) which are also called "liquid crystalline" substances, produce DTA thermograms with additional endotherms due to any solid-smectic and/or smectic-nematic and/or nematic isotropic phase transitions. For example, the p-n-octyloxy benzoic acid (Fig. 58) has been reported⁹ to undergo a solid-solid transition at 75°C, a solid-smectic transition at 101°C, a smectic-nematic transition at 108°C, and finally a nematic-isotropic transition at 146°C. The changes in molecular arrangements in each of these mesophases have been discussed in the Introduction. Upon cooling, mesomorphic substances show the corresponding exotherms, with some supercooling. Figure 58 shows the exotherms of p-octyloxy benzoic acid. The p-octyloxy-benzoylacetone prepared in this laboratory and identified as "Ligand" or L is not a mesomorphic compound. The DTA of the ligand (Fig. 57) shows ligand

Figure 57

DTA thermogram of ligand. A_1 and A_2 represent two parts of a heating curve, at different temperature scale shifts. B_1 and B_2 represent two parts of a cooling curve, with scale shifts.

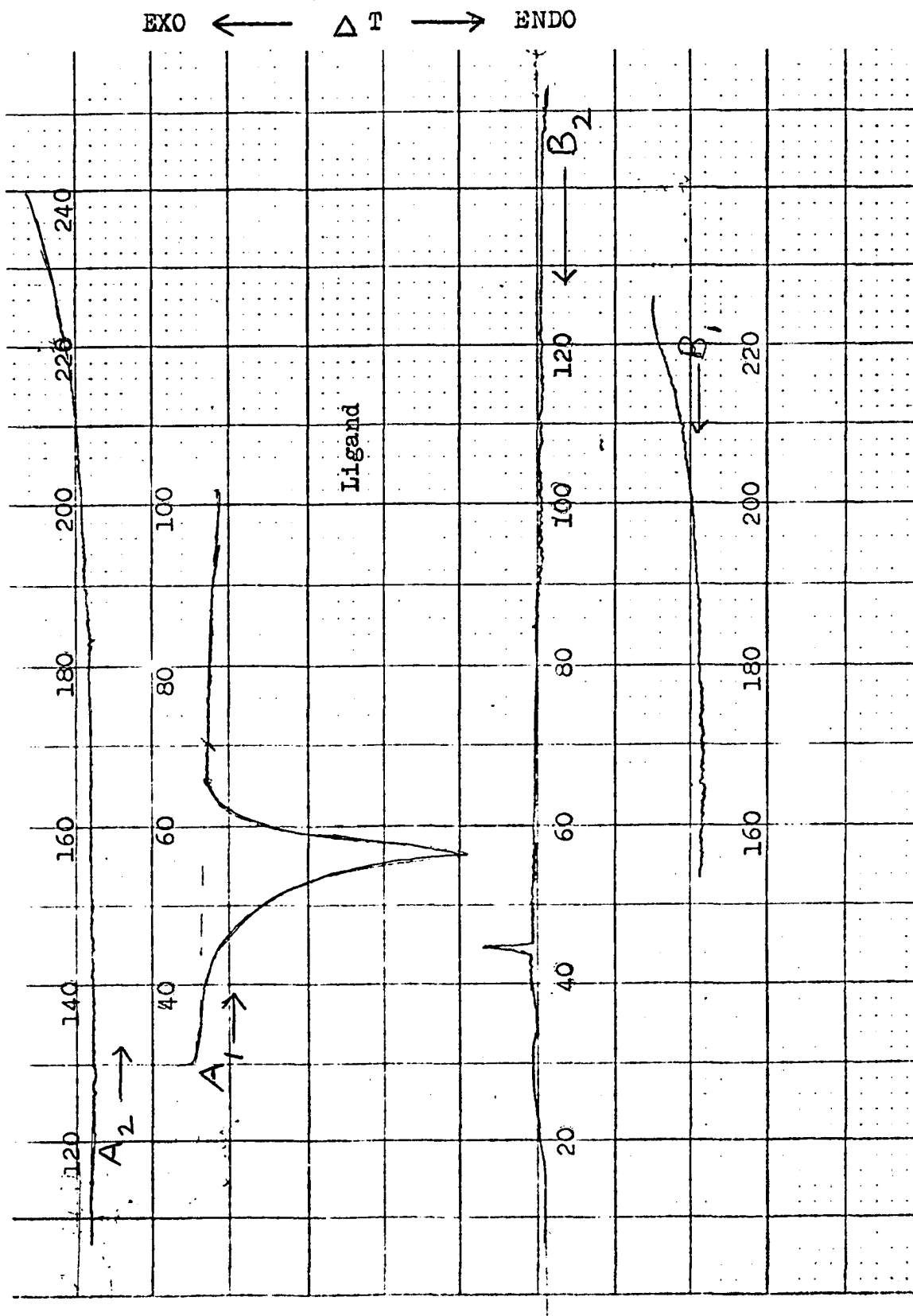


Figure 57

Figure 58

DTA thermogram of p-octyloxy-benzoic acid.
The lower curve A is the heating curve,
while the upper curve B is the cooling curve.

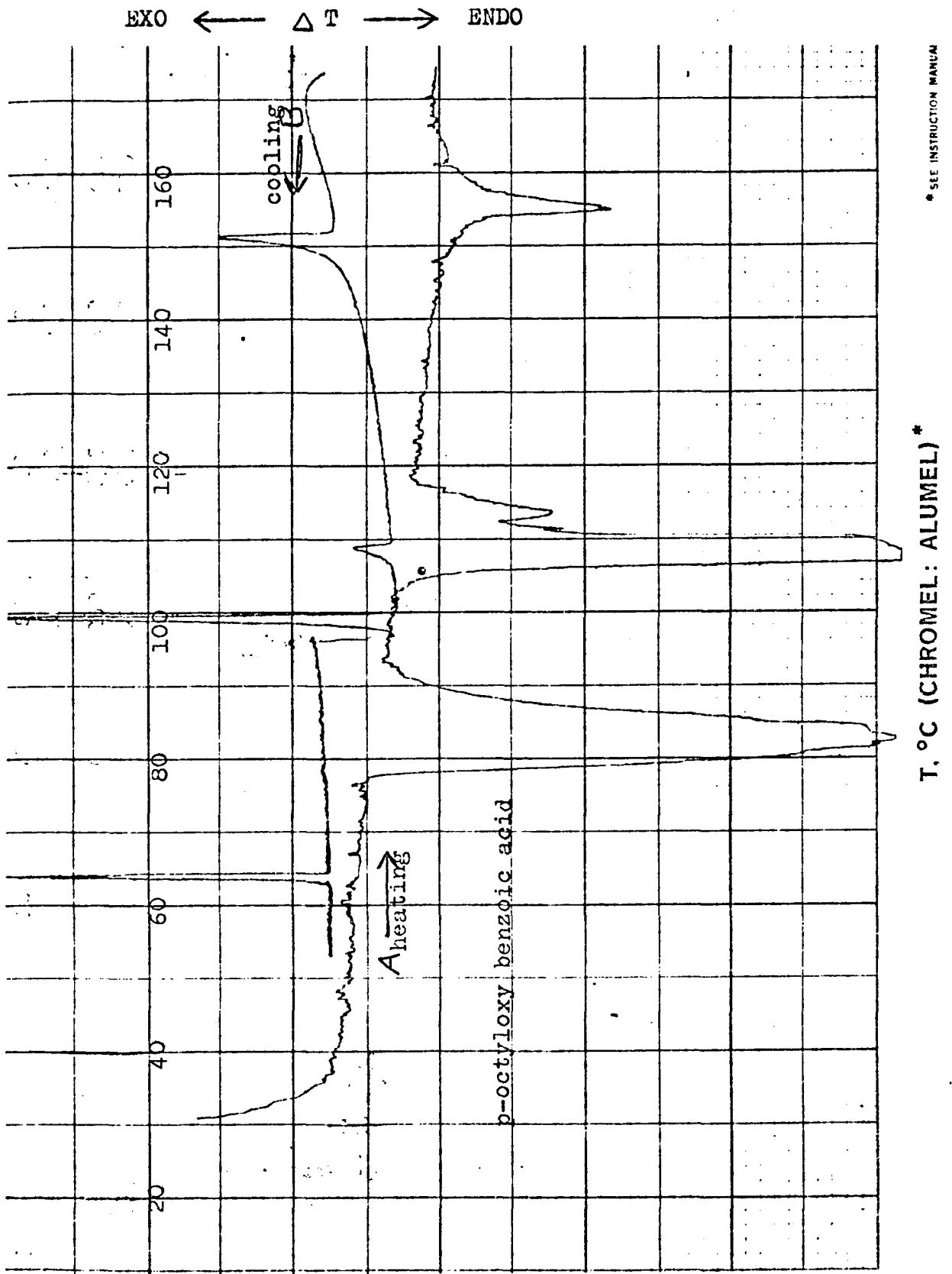


Figure 58

endotherm at 54-56°C due to the solid-liquid transition; and upon cooling the exotherm is seen at 40 or 45°C, due to supercooling.

DTA thermograms can also be used to detect the decomposition of compounds: a line with a positive slope indicates decomposition. Most organo-palladium compounds containing a Pd-O bond or bonds, melt with decomposition. The DTA thermograms of those compounds do not show an endotherm; instead, a gradually rising curve is seen at and above the decomposition temperature. Fig. 59-C is the DTA of palladium acetate with a decomposition temperature of 200°C (reported¹⁹ m.p. 205° with decomposition). Fig. 59-B shows the DTA of Pd(acac)₂, with decomposition at 200°C. Its melting point cannot be determined, but it has been reported by Grinberg and Simonova²⁸ to decompose with charring when heated above 180°C. Fig. 59-A is the DTA of Pd(bzac)₂ prepared in this laboratory, with decomposition around 220°C. The melting point of Pd(bzac)₂ has not been reported by Hon et al²⁰, nor by any of the other investigators who studied Pd(bzac)₂.^{84,74} Nesmeyanov et al⁹⁸ have reported that Pd(3-phenyl-acac)₂ melts with decomposition at 213-216°C. As can be seen from the DTA thermograms of some of the compounds mentioned above, none

Figure 59

DTA thermograms of three organo-palladium compounds.

Curve A is the heating curve of $\text{Pd}(\text{bzac})_2$

Curve B is the heating curve of $\text{Pd}(\text{acac})_2$

Curve C is the heating curve of $\text{Pd}(\text{acetate})_2$

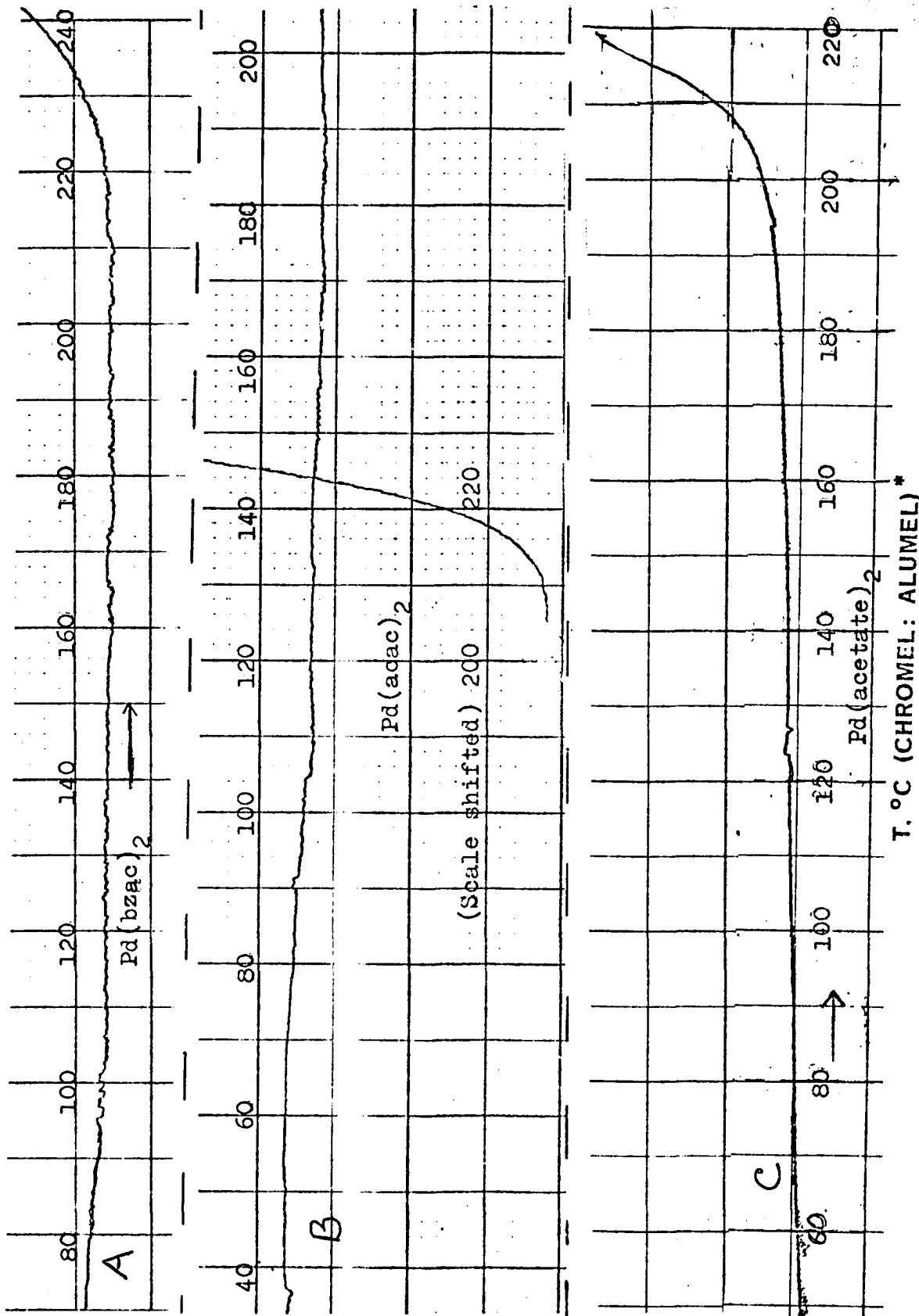


Figure 59

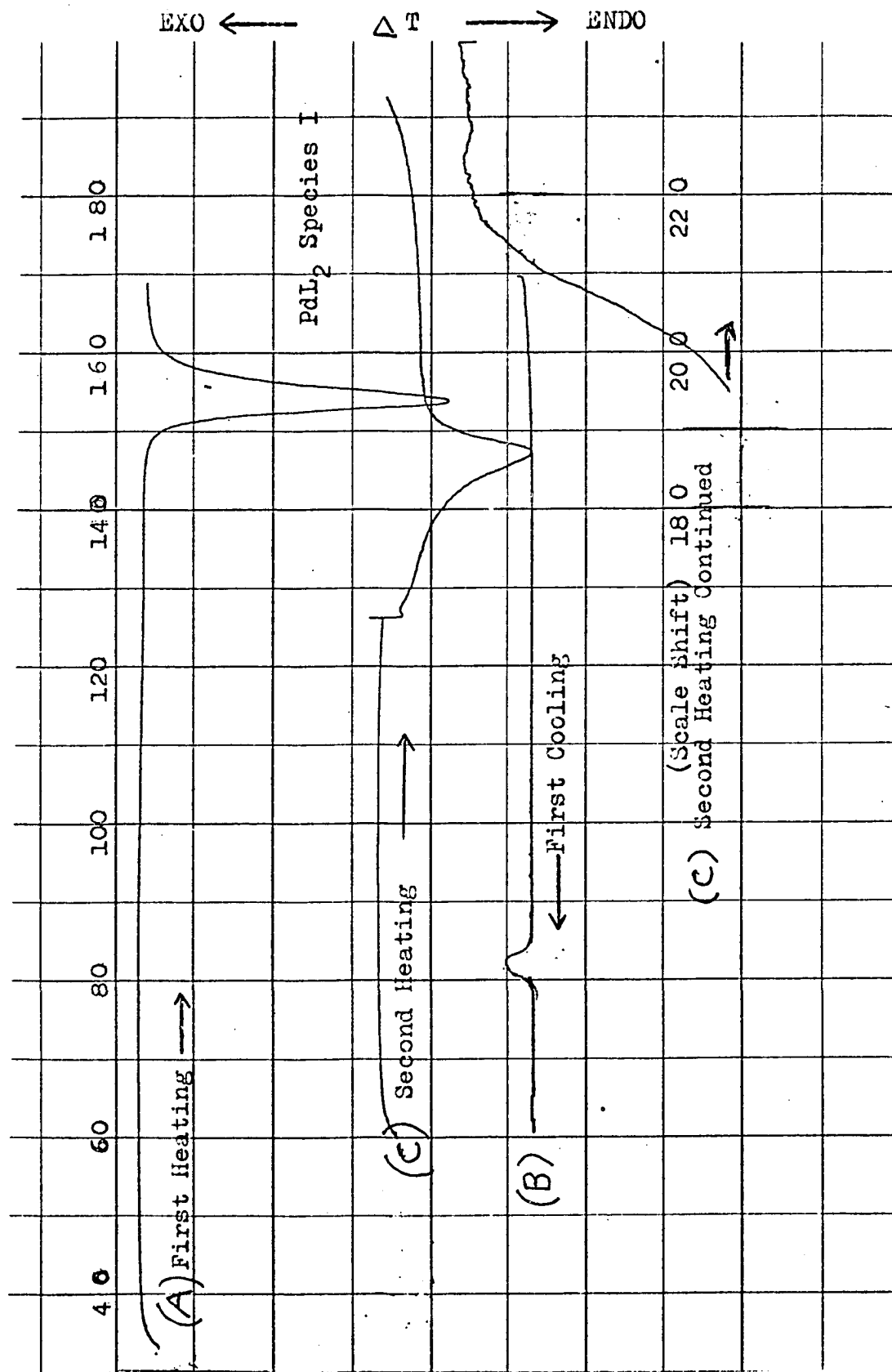
of them show an endotherm prior to decomposition.

It is very interesting to observe that the introduction of the long p-octyloxy chain into benzoylacetone which is coordinated to palladium, has apparently altered the balance of intermolecular forces operating in the solid organo-palladium compounds. It should be pointed out that the DTA of compounds PdL_2 , Species I cis as well as Species II trans, show a definite endotherm prior to their respective decomposition temperatures. Fig. 60 shows the DTA of Species I, with an endotherm at ca. 135°C , and with decomposition starting above 170°C . When the melting point of Species I is determined in a capillary tube, or using the heated stage of a Mettler FP-21 apparatus with observations through a microscope, it can be clearly seen that the yellow compound can be melted, then allowed to cool and crystallize, and it can be reheated to its normal melting point. This reversible process can be repeated several times with the temperature maintained below 145° . Species I cis begins to darken ca. 150°C , then decomposes ca. 165°C .

The thermal properties of Species II trans, as judged by its DTA pattern, differ even more markedly from those of the "unsubstituted" palladium-oxygen coordination

Figure 60

DTA thermogram of PdL₂ Species I, cis.
Curve A is the first heating curve,
Curve B is the first cooling curve,
Curve C, shown in two sections with a
temperature scale shift, is the final
heating curve.



T, °C (CHROMEL: ALUMEL) *

* SEE INSTRUCTION MANUAL FOR SCALE CORRECTION

Figure 60

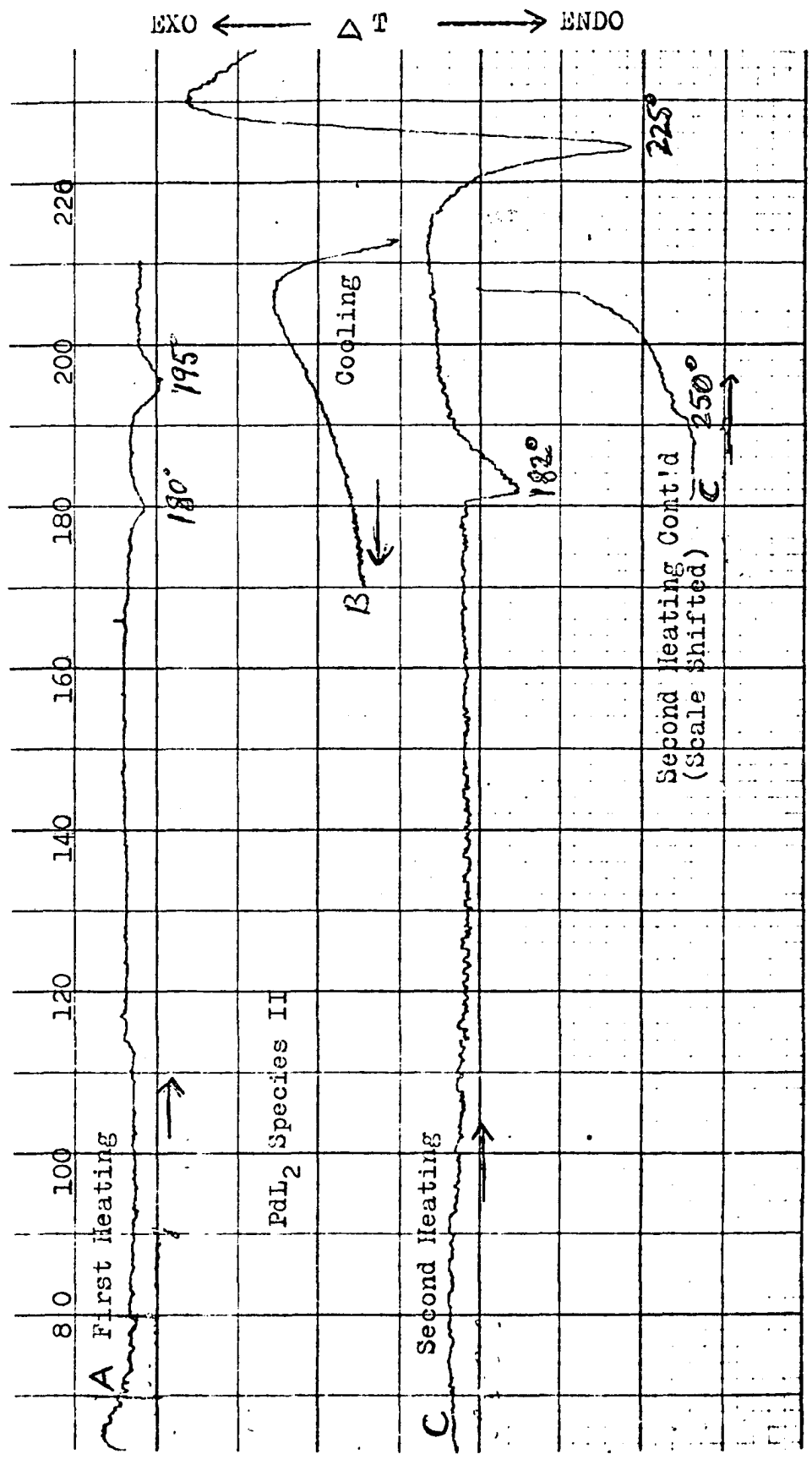
compounds, especially those discussed before. The DTA of Species II is similar in appearance to that of mesomorphic compounds. Fig. 61 shows two small endotherms at 180°C and 195°C , which precede the main endotherm at 225°C , with decomposition following above 250 or 260°C . However, if the compound has been heated above 220°C , the changes are no longer reversible.

Figures 61 and 62 show what happens when Species II is heated only to 200°C , then allowed to cool, and then reheated again. The region above 150° will be considered first. In Figure 61 curve A represents the first heating, curve B is the cooling curve, and curve C shows the second heating. The two endotherms about 180 and 195°C in curve A have merged into one endotherm about 182° in curve C, then the main endotherm is seen at 225° , with decomposition following.

In Figure 62, with a smaller sample of Species II, the heating and cooling processes were repeated. Curves A_1 and A_2 are two sections of the first heating curve; curve B is the first cooling curve; curves C_1 and C_2 represent the second heating; curves D -- the second cooling, and curves E_1 and E_2 the final heating. In each case there was a shift of the temperature scale between A_1 and A_2

Figure 61

DTA thermogram of PdL₂ Species II, trans.
Curve A is the first heating curve.
Curve B is the cooling curve.
Curve C, shown in two sections with a
temperature scale shift, is the second
heating curve.



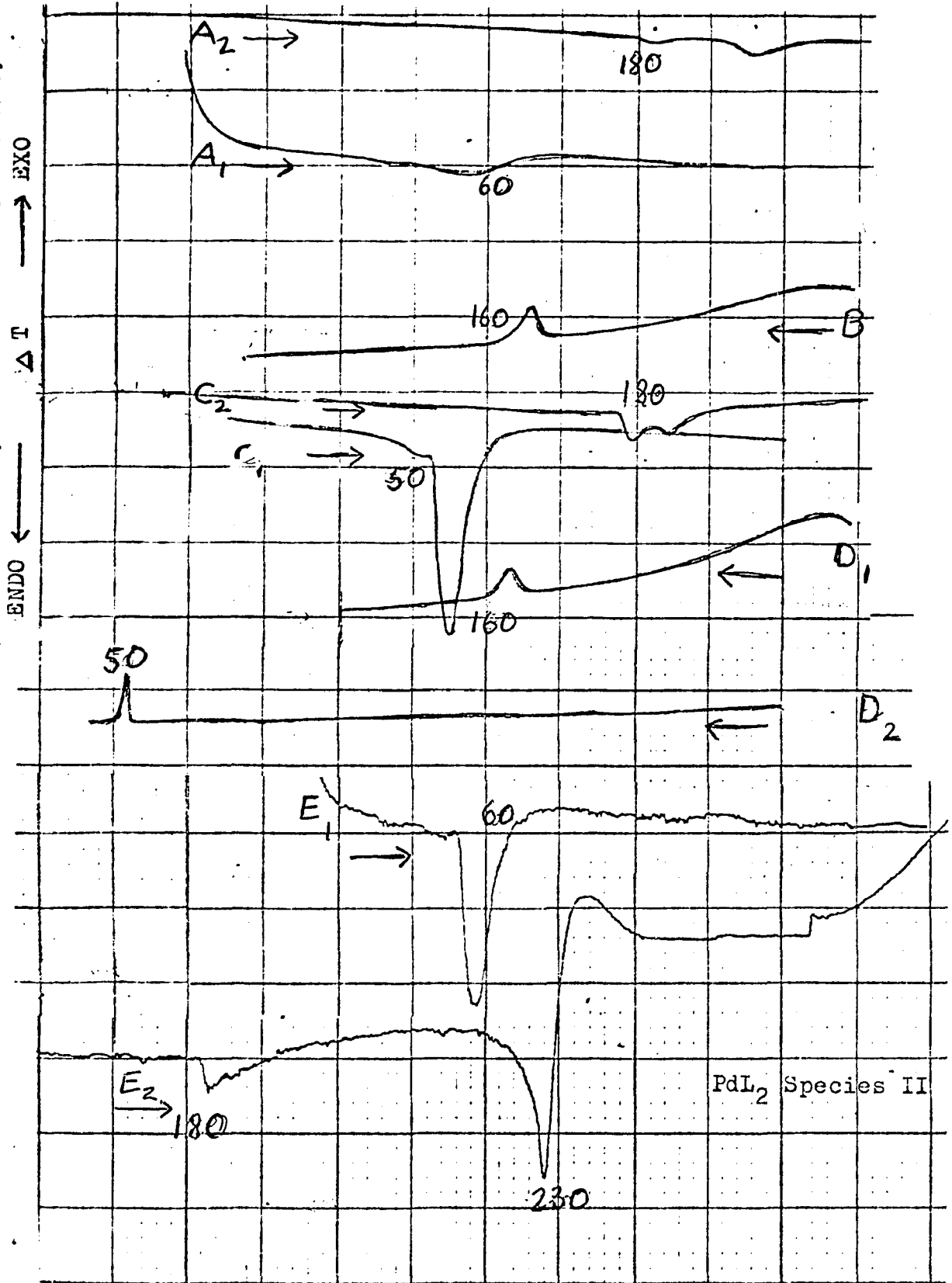
* SEE INSTRUCTION MANUAL FOR SCALE CORRECTIO

T. °C (CHROMEL: ALUMEL) *

Figure 61

Figure 62

DTA thermogram of PdL₂ Species II, trans, showing several heating and cooling curves. Curves A₁ and A₂ represent the first heating. Curve B is the first cooling curve. Curves C₁ and C₂ represent the second heating. Curves D₁ and D₂ represent the second cooling. Curves E₁ and E₂ represent the third and final heating.



T. °C (CHROMEL: ALUMEL)*

* SEE INSTRUCTION MANUAL FOR

Figure 62

between C_1 and C_2 and between E_1 and E_2 from lower to higher temperatures, respectively. Cooling curve D_1 is on the higher scale, followed by D_2 on the lower temperature scale.

As can be seen in Figure 62, the first heating curve A_2 shows the two endotherms around 180 and 195°C, and the first cooling curve B shows an exotherm about 166°C. The second heating curve C_2 shows two closely spaced endotherms at 178° and 185°, with a corresponding exotherm at 160° seen in cooling curve D_1 . In the final heating curve E_2 one larger "merged" endotherm is seen at 185°C, followed by the final "melting" endotherm at 226°, and decomposition above 240°.

An interesting change in the DTA pattern is also observed in the region around 60°C. In Figure 62 only a small endotherm is noted in curve A_1 around 58°, but it becomes much more pronounced during the second heating. Curve C_1 shows a large endotherm at 53°, with a corresponding exotherm at 50° seen in cooling curve D_2 . The final heating curve E_1 shows that same endotherm, essentially identical to that seen in C_1 , in both area and temperature.

One might speculate that the low temperature endo-

therm is a solid-solid transition, similar to that observed in the p-octyloxy-benzoic acid at 75°C. Herbert⁹ has suggested that in the p-alkoxy-benzoic acid series some apparently anomalous effects in magnitude of transition energies, could be explained by assuming several changes that could take place in compounds with longer alkoxy chains. He suggested that these changes could involve the onset of chain rotation, or a change in the angle of tilt within the planes of the molecule. It is conceivable that such changes can also occur in PdL₂ Species II trans, and that these are responsible for the endotherms around 60°C. Since the thermal energy is still fairly low during the first heating, the changes are not complete until the second heating, and this initial "disorganization" in the alkoxy chain persist through subsequent cooling and heating.

The DTA thermograms of PdL₂ Species II suggested that the compound may be mesomorphic. Based on the crystal structure reported by Hon et al²⁰ for Pd(bzac)₂ trans, it was expected that only the trans isomer of PdL₂ would have the proper geometry associated with the dimer of the model system of alkoxy-benzoic acids; i.e. it would have the dipolar alkoxy groups located at opposite ends of the

longest molecular axis. The potentially mesomorphic nature of Species II had to be investigated by other methods that would either complement and reinforce, or disprove the data from differential thermal analysis.

Investigations of Species II, by measuring changes in light scattering as a function of temperature, were inconclusive. In this attempt the Mettler FP-11 apparatus, described by Santoro and Esposito in 1974,¹¹⁴ was used. Since the sample darkened considerably upon heating, the light it might have scattered was not easily detectable. Efforts to detect mesomorphic behavior of thin films by reflected light were also unsuccessful. Measurements of changes in viscosity had been considered as a possible technique. The anomalous sudden changes in viscosity at the mesophase had been reported by Ostwald in 1933 in his study of mesomorphic melts.^{115,116} However, attempts to determine viscosity changes in Species II over the entire range of temperatures from 180° to 240° presented experimental difficulties that were considered outside the scope of this investigation.

The two techniques that finally proved most helpful were observations of the sample being heated in a capillary tube, and the examination of very thin films heated on the

stage of a polarizing microscope. The changes observed in Species II in a capillary tube suggested that the compound may be changing from a solid into a mesophase. But these changes were not as clear cut as changes observed with known "liquid crystals". The changes in Species II could also be interpreted as changes in crystal structure from an opaque solid to one that is more translucent, rather than from an opaque solid to a mesophase.

Thin films of PdL₂ Species II trans were carefully examined over the temperature range from ambient to 280°C. A polarizing microscope with an illuminated stage (Richards Model LB-46), attached to the FP-21 heated stage of Mettler FP-21 apparatus, was used. By this technique changes in Species II were compared with those observed on heating films of known mesomorphic substances that also undergo solid-solid transitions, in order to be able to distinguish the solid-solid changes from mesomorphic changes. In particular Species II was compared with p-octyloxy-benzoic acid (which goes through a solid-solid, solid-smectic, smectic-nematic and nematic isotropic transition), with p-heptyloxy-benzoic acid (smectic, nematic and isotropic transitions),⁹ and with p-propoxy-benzoic acid (solid-solid, solid-nematic, nematic-isotropic transitions).⁹

Our PdL₂ Species II did not show the optical anisotropy expected of a mesomorphic compound. It must be concluded either that PdL₂ Species II does not exist in the "isotropic form"; or that its isotropic form could not be detected, because the compound became darker on heating and eventually decomposed. The endotherms observed in the DTA thermograms of Species II just prior to the final endotherm at 225° could be attributed to some type of solid-solid transitions or "pseudo" mesophases. From the combined studies and evidence compiled in our laboratory it seems clear, however, that in synthesizing the Pd(p-octyloxy-1,3-butanedionato) complex we did succeed in modifying the thermal behavior associated with Pd-beta-diketones and other Pd-oxygen coordination compounds which decompose at their melting point.

In evaluating our attempts to synthesize a new class of organometallic mesomorphic compounds, and in attempting to assess the merits of this approach to the problem, several factors must be discussed and evaluated. One of the important factors to be considered is the strength of intermolecular attractions that operate in the system.

In general, intermolecular attractive forces can be classified as one of the following three:

(a) dipole-dipole attractions, which are the direct interactions between permanent dipoles in the molecules;

(b) induced dipole attractions arising from the mutual polarization of the molecules by their permanent dipole moments;

(c) dispersion forces, which are the attractions between instantaneous dipoles produced by spontaneous oscillations of the electron clouds of the molecules.

It is not the purpose of this discussion to examine each of the above classes of intermolecular forces, but rather to show how the interplay and balance of these forces is affected by the factors of molecular structure. This can best be done by comparing the effects on mesomorphic behavior due to small changes in the molecular structure, as within an homologous series of compounds. It will be shown that one of the important considerations is the so-called length-to-breadth ratio of the molecule. Another important factor is the melting point of the compound, which is affected by several factors, including some unpredictable aspects of the packing of the molecules in the crystal lattice and the crystal lattice adopted by the particular solid material investigated.

The review by Gray³ provides some guidelines on the importance of the factors to be considered, and their relationship to each other. In trying to assess the effect of molecular length on mesomorphic thermal stabilities, the p-n-alkoxy-benzoic acids are compared with those of their "aromatic homologues", the 4'-n-alkoxy-biphenyl-4-carboxylic acids. The mesomorphic thermal stabilities of the biphenyl acids are much greater than those of the benzoic acids. It should be noted that in the biphenyl compounds there are four aromatic rings per dimeric molecule, while in the benzoic acid analogues there are only two aromatic rings per molecule. Gray emphasizes, however, that the enhanced smectic and nematic thermal stabilities in the biphenyls are not simply a function of the greater lengths of the biphenyl acid molecules, but are also due to the greater polarizability of the two additional aromatic rings.

The introduction of a large atom, or groups of atoms into a molecule, will increase the polarizability of the system. Generally, the mesomorphic potential, or the mesomorphic thermal stability of the compound will be reduced. This effect can be understood if one remembers that any bulky atom or group, introduced into the "interior"

section of the molecule (i.e. in some position other than the end of the molecule), will broaden the rod-like molecule appreciably. As a result of this broadening, the molecules which are oriented parallel to one another, are forced apart further.

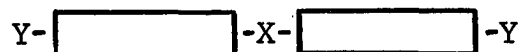
The interaction energy associated with all three types of intermolecular attractions mentioned before, is inversely proportional to the y power of r , where r is the distance between the attracting centers, and $y=6$ for the gas phase.

$$\text{Interaction energy} \propto \frac{1}{r^y} \quad (14)$$

As is apparent from the above equation, the interaction energy will fall off rapidly with an increase in r , and this effect is likely to counterbalance the increase in the energy of attraction arising from the increased polarizability due to the introduction of the large atom or group into the "interior" portion of the molecule.

It should be reemphasized in this discussion, that the basic requirement of an essentially linear molecule, coupled with the presence of groups that will produce suitably high intermolecular attractions, are most important factors in determining potentially mesomorphic

behavior. However, any increase in the molecular breadth will reduce the length-to-breadth ratio, and the rod-like molecule will become transformed into one that is more spherical than rod-like. Such a "broadened" molecule would no longer be a potentially mesomorphic structure. In a general sense, the thermal stabilities of the mesophase in a liquid crystalline material are likely to be high if the dipolar or polarizable groups occur terminally (Y in the figure shown below), or centrally (X in the figure) in the rod-like molecule. The thermal, stability and the likelihood of mesomorphic behavior would be low, if the dipolar groups occur along the side of the molecule and significantly increase the molecular breadth.



To be able to compare the various factors affecting mesomorphic or potentially mesomorphic behavior in terms of the organo-palladium compounds, it is necessary to estimate the length-to-breadth ratio of the model system we considered (the p-alkoxy-benzoic acids), as well as the ratio of the length/breadth in the trans isomer of the PdL₂ (Species II), and the cis isomer of PdL₂ (Species I). Based on qualitative considerations of the structures of the cis and trans isomers

of PdL_2 , one would expect the trans isomer, to have the higher length-to-breadth ratio, and to be the one that is more likely to be potentially mesomorphic.

Regarding the length-to-breadth ratio in p-octyloxybenzoic acid which is mesomorphic, some approximations are available in Herbert's discussion⁹ of the relationship between liquid crystalline behavior of the several p-alkoxybenzoic acid dimers and their molecular structure. Different parts of the molecule affect different regions of mesomorphic behavior. Herbert points out that when the length of the molecule is similar to its width, as for example in p-ethoxybenzoic acid, there are no mesomorphic properties. With the addition of $-\text{CH}_2-$ units to the alkoxy chain, up to the point where the physical length of the bent alkoxy chain is comparable to the length of the -oxybenzoic acid segment, largely nematic properties are observed. When the length of the alkyl chain becomes the dominant portion of the length of the molecule, pure smectic properties are observed. Herbert also points out that smectic properties in the acids of the even-numbered series are first noticed in the p-n-octyloxy benzoic acid, in which the "alkyl chain is almost exactly half the length of the whole molecule".⁹

In Gray's discussion of the significance of the length of the geometrically anisotropic molecule upon mesomorphic behavior, the author emphasizes that the effect of structural changes must be carefully evaluated. The effect on the mesomorphic thermal stability will depend on the nature of the mesophase, as well as on the effect of the structural modification on the average intermolecular attractive forces. For example, one could compare the effect of adding an aromatic ring with the addition of four methylene groups. In terms of molecular length, both of these structural modifications are approximately equal. However, in case of the aromatic ring, the length of the molecule is increased by a unit which contributes strongly to intermolecular attractions. The four methylene groups, on the other hand, will contribute much less to intermolecular cohesions. Gray cautions that "unless it is quite clear in what way a given substituent ... will affect the overall intermolecular attractions, it is unwise to make predictions about (its) effect on the mesomorphic thermal stability of a compound".³

Since in all mesomorphic systems one is dealing with a delicate balance between the intermolecular attractions that exist between the planes, the sides, and ends

of the molecules, specific changes in the length, in the breadth, etc. of the molecule will exert specific effects on either the smectic or the nematic thermal stabilities, or on the thermal stabilities of both mesophases. While one is tempted to make generalizations concerning the relationship between mesomorphism and chemical constitution, we found that it is not always possible to make predictions about mesomorphic or potentially mesomorphic behavior. We suggest that the modifications in the thermal behavior of the organo-palladium compounds as a result of the introduction of the p-alkoxy group into the molecule, justify the merit of such attempted generalizations. This difference in thermal behavior can best be appreciated by comparison of DTA data of PdL_2 trans with other unsubstituted palladium-beta-diketonates, like $\text{Pd}(\text{acac})_2$ and $\text{Pd}(\text{bzac})_2$; as well as other organo-palladium compounds in which the Pd is coordinated to oxygen, like $\text{Pd}(\text{acetate})_2$.

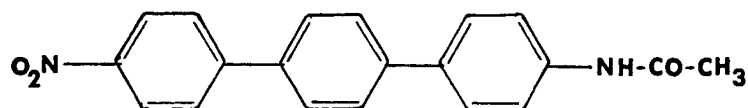
We might speculate that our PdL_2 system is potentially mesomorphic, but we are unable to detect its mesomorphic behavior because of the high melting point. It has been recognized³ that the melting point of the solid material is one more difficult factor to be considered in making predictions about mesomorphic behavior. A potentially mesomorphic system, made up of molecules that are

long, narrow and linear, with the appropriate dipolar groups, might be one in which strong intermolecular attractions would be expected. "If, however, these intermolecular attractions are too strong, selective weakening of the cohesive forces may not occur until high temperatures are reached; and when the melting process does begin, the thermal vibrations may be too great to allow an ordered arrangement of the molecules to persist".³ One of the real difficulties in making predictions about mesomorphic behavior seems to be the unpredictable nature of the melting point of the compound. In our case, the high melting point of trans PdL₂, (Species II), which is followed by decomposition, certainly presented real difficulties in attempts to detect or prove mesomorphic behavior.

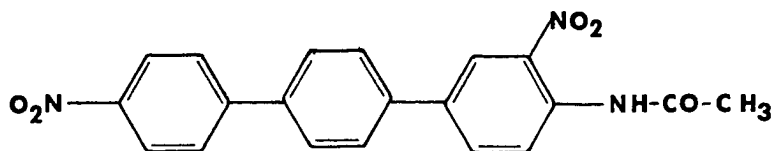
Several examples are cited by Gray in connection with the discussion of the effect of the high melting point: (1) p-ethoxybenzoic acid (not mesomorphic), which should be compared with the other members of this homologous series, especially the p-n-propyloxy-benzoic acid. The melting point of the ethoxy b.a. is higher than the nematic-isotropic transition temperature predicted from the smooth curve relationship for mesomorphic transition temperatures for this homologous series. In this case the isotropic

liquid does not supercool sufficiently for a monotropic nematic mesophase to be obtained or observed.

(2) The 4-acetamido-4''-nitro-p-terphenyl compound is compared with the 3,4''-dinitro-p-terphenyl compound (structures shown below). The dinitro compound is mesomorphic, with a nematic-isotropic transition at 228°. At first consideration, we would expect the mono-nitro analogue to be even more suitable for mesomorphic behavior, since there



4-acetamido-4''-nitro-p-terphenyl



4-acetamido-3,4''-dinitro-p-terphenyl

is no 3-nitro group to broaden the molecule. In fact, the 4''-nitro-compound melts much higher than the dinitro compound, at 333°, and it is not mesomorphic. In Gray's discussion this last example is probably the clearest illustration of the principle that the high melting point of the compound is responsible for the absence of mesomorphic properties.

In summarizing the conclusions about the intermolecular forces and their relationship to mesomorphic properties, it should be stressed that these forces must be suitably balanced. They cannot be too weak, or the ordered arrangement of the molecules will not persist after melting (as is the case in ordinary molecules which have no geometric anisotropy). Nor should those forces be too strong, or the crystal lattice will persist up to the temperatures that are too high for retention of the mesomorphic molecular orientation.

In our PdL_2 trans compound it is probably true that the intermolecular forces are too strong, and that the crystal lattice persists up to the "decomposition" temperatures. It is possible that some of the intermolecular forces also involve some weak intermetallic interactions between Pd atoms of different molecules. At present one can only speculate about such intermetallic interactions; their existence could be established by findings of a shortened Pd-Pd distance in the crystal structure of the compound.^{117,118,119,120} Intermetallic interactions could also be established by evidence of metal-metal vibrations in the 100 to 250 cm^{-1} region.¹²¹ However, we did not observe any bands in those regions of the Raman or IR spectra that

were intense enough to be assigned to metal-metal fundamental vibrations.

The X-ray crystallographic results of Hon et al²⁰ on Pd(bzac)₂ trans show that the metal atom of one molecule in the unit cell is in contact with a methyl groups of the other molecule (a distance of 3.75 Å). Hon et al also point out that there are van der Waals contacts between the phenyl rings that project on the sides. If one assumes that PdL₂ Species II trans crystallizes in a pattern similar to the Pd(bzac)₂ trans analogue, such van der Waals interactions between phenyl groups and the interactions between metal and methyl groups of adjacent molecules might be among the forces that help maintain the crystal lattice, and interfere with attempts to establish potentially polymorphic behavior. In more general terms, these types of interactions are only some of the examples of interactions that affect the delicate balance of intermolecular forces, and might account for the high melting point of PdL₂ Species II.

APPENDIX I. Correction of b.p. to Standard Pressure

This correction can be calculated by using the equation of H. B. Hass and R. F. Newton:

$$\Delta t = \frac{(273.1 + t) (2.8808 - \log p)}{\emptyset + 0.15 (2.8808 - \log p)}$$

where Δt = degrees C to be added to the observed boiling point
 t = observed boiling point
 p = observed pressure in torrs
 \emptyset = the entropy of vaporization at 760 torr

The value of \emptyset may be estimated from graphs and tables,¹⁰⁸ according to the group of compounds with close physical or structural resemblance. The \emptyset values used for the calculations on p-octyloxy-benzoyl chloride were 6.3 (first approximation), and 6.5

From the data reported by Pierce et al²⁴ for the p-2-octyloxy-benzoyl chloride (b.p. 224-229° at 40 torr), it was estimated that the p-n-octyloxy-benzoyl chloride should boil at 240° at 40 torr. Using the Hass-Newton equation, the Δt correction was calculated to be 98°, or the b.p. at standard pressure estimated around 338°C.

Similarly, the Hass-Newton equation was used on the data observed in the laboratory. The aroyl chloride prepared boiled at 147°C at 0.60 torr. The calculated Δt was 186°, or the estimated b.p. at standard pressure

was $147 + 186 = 333^{\circ}\text{C}$.

Using the other set of conditions, the b.p. of 170° at 2.0 torr, and the Hass-Newton equation, Δt was calculated to be 165.6° , and the b.p. $170 + 165.6 = 335.6^{\circ}\text{C}$.

mode	* $C_2' \rightarrow C_2''$ $C_2'' \rightarrow C_2'$											
	D_{4h}	D_4	D_{2d}	D_{2d}	C_{4v}	C_{4h}	D_{2h}	D_{2h}	C_4	S_4	D_2	D_2
\checkmark_1	A_{1g}	A_1	A_1	A_1	A_1	A_g	A_g	A_g	A	A	A	A
\checkmark_2	A_{2g}	A_2	A_2	A_2	A_2	A_g	B_{1g}	B_{1g}	A	A	B_1	B_1
\checkmark_3	B_{1g}	B_1	B_1	B_2	B_1	B_g	A_g	B_{1g}	B	B	A	B_1
\checkmark_4	B_{2g}	B_2	B_2	B_1	B_2	B_g	B_{1g}	A_g	B	B	B_1	A
\checkmark_5	E_g	E	E	E	E	E_g	$B_{2g} + B_{3g}$	$B_{2g} + B_{3g}$	E	E	$B_2 + B_3$	$B_2 + B_3$
\checkmark_6	A_{1u}	A_1	B_1	B_1	A_2	A_u	A_u	A_u	A	B	A	A
\checkmark_7	A_{2u}	A_2	B_2	B_2	A_1	A_u	B_{1u}	B_{1u}	A	B	B_1	B_1
\checkmark_8	B_{1u}	B_1	A_1	A_2	B_2	B_u	A_u	B_{1u}	B	A	A	B_1
\checkmark_9	B_{2u}	B_2	A_2	A_1	B_1	B_u	B_{1u}	A_u	B	A	B_1	A
\checkmark_{10}	E_u	E	E	E	E	E_u	$B_{2u} + B_{3u}$	$B_{2u} + B_{3u}$	E	E	$B_2 + B_3$	$B_2 + B_3$

(cont.)	**											
	C_{2v}	C_2	σ_v	C_2	σ_d	C_2'	C_2''	C_2	C_2'	C_2''	C_2	
\checkmark_1	A_{1g}	A_1	A_1	A_1	A_1	A_1	A_1	A_g	A_g	A_g	A	A
\checkmark_2	A_{2g}	A_2	A_2	B_1	B_1	B_1	B_1	A_g	B_g	B_g	A	B
\checkmark_3	B_{1g}	A_1	A_2	A_1	B_1	B_1	A_g	A_g	B_g	B_g	A	B
\checkmark_4	B_{2g}	A_2	A_1	B_1	B_1	A_1	A_g	B_g	A_g	B_g	A	B
\checkmark_5	E_g	$B_1 + B_2$	$B_1 + B_2$	$A_2 + B_2$	$A_2 + B_2$	$2B_g$	$A_g + B_g$	$A_g + B_g$	$A_g + B_g$	$2B$	$A + B$	$A + B$
\checkmark_6	A_{1u}	A_2	A_2	A_2	A_2	A_u	A_u	A_u	A_u	A	A	A
\checkmark_7	A_{2u}	A_1	A_1	B_2	B_2	A_u	B_u	B_u	A	B	A	B
\checkmark_8	B_{1u}	A_2	A_1	A_2	B_2	A_u	A_u	B_u	A	A	A	B
\checkmark_9	B_{2u}	A_1	A_2	B_2	A_2	A_u	B_u	A_u	A	B	A	B
\checkmark_{10}	E_u	$B_1 + B_2$	$B_1 + B_2$	$A_1 + B_1$	$A_1 + B_1$	$2B_u$	$A_u + B_u$	$A_u + B_u$	$2B$	$A + B$	$A + B$	$A + B$

*, ** D_{4h} , D_{2h} and C_{2v} subgroups used here

Character Tables for D_{4h} , D_{2h} and C_{2v} Symmetry Groups

D_{4h}	I	$2C_4(z)$	$C_4^2=C_2''$	$2C_2$	$2C_2'$	σ_h	$2\sigma_v$	$2\sigma_d$	$2S_4$	$S_2=i$		
A_{1g}	+1	+1	+1	+1	+1	+1	+1	+1	+1	+1	R_z Z	$\alpha_{xx} + \alpha_{yy}, \alpha_{zz}$
A_{1u}	+1	+1	+1	+1	+1	-1	-1	-1	-1	-1		$\alpha_{xx} - \alpha_{yy}$
A_{2g}	+1	+1	+1	-1	-1	+1	-1	-1	+1	+1		α_{zz}
A_{2u}	+1	+1	+1	-1	-1	-1	+1	+1	-1	-1		(R_x, R_y)
B_{1g}	+1	-1	+1	+1	-1	+1	+1	-1	-1	+1		(x, y)
B_{1u}	+1	-1	+1	+1	-1	-1	-1	+1	+1	-1		
B_{2g}	+1	-1	+1	-1	+1	+1	-1	+1	-1	+1		
B_{2u}	+1	-1	+1	-1	+1	-1	+1	-1	+1	-1		
E_g	+2	0	-2	0	0	-2	0	0	0	0		
E_u	+2	0	-2	0	0	+2	0	0	0	0		

$D_{2h} \equiv V_h$	I	$\sigma(xy)$	$\sigma(xz)$	$\sigma(yz)$	i	$C_2(z)$	$C_2(y)$	$C_2(x)$		
A_g	+1	+1	+1	+1	+1	+1	+1	+1	R_x Z R_y Y R_z X	$\alpha_{xx}, \alpha_{yy}, \alpha_{zz}$
A_u	+1	-1	-1	-1	-1	+1	+1	+1		α_{zz}
B_{1g}	+1	+1	-1	-1	+1	+1	-1	-1		α_{xx}
B_{1u}	+1	-1	+1	+1	-1	+1	-1	-1		α_{yy}
B_{2g}	+1	-1	+1	-1	+1	-1	+1	-1		α_{zz}
B_{2u}	+1	+1	-1	+1	-1	-1	+1	-1		α_{xx}
B_{3g}	+1	-1	-1	+1	+1	-1	-1	+1		α_{yy}
B_{3u}	+1	+1	+1	-1	-1	-1	-1	+1		α_{zz}

C_{2v}	E	C_2	$\sigma_v(xz)$	$\sigma_v'(yz)$		
A_1	1	1	1	1	z	x^2, y^2, z^2
A_2	1	1	-1	-1	R_z	xy
B_1	1	-1	1	-1	x, R_y	xz
B_2	1	-1	-1	1	y, R_x	yz

BIBLIOGRAPHY

1. D. Vorlaender, "Kristallinisch-fluessige Substanzen", Ferdinand Enke, Stuttgart, 1908
2. O. Lehman, Ann. Physik. 21, 181 (1906)
3. G. W. Gray, "Molecular Structure and the Properties of Liquid Crystals", Academic Press, London, 1962
4. G. W. Gray, "The Influence of Molecular Structure on Liquid Crystalline Properties", in "Liquid Crystals", Gordon and Breach Science Publishers, New York, 1966, p. 129 ff
5. G. H. Brown and W. G. Shaw, Chem. Reviews, 57, 1049 (1957)
6. W. Kast, "Landolt-Boernstein Zahlenwerte und Funktionen", 6th ed., Springer Verlag, Berlin, 1960, Vol. II, Part 2a, p. 266
7. H. W. Foote, "International Critical Tables", p. 314
8. G. W. Gray and B. Jones, J. Chem. Soc., 1953 4179
9. A. J. Herbert, Trans. Farad. Soc., 63, 555 (1967)
10. G. W. Gray and G. Jones, J. Chem. Soc., 1954 1467
11. D. Vorlaender, Chem. Ber., 43, 3120 (1910)
12. R. Walter, Chem. Ber., 59, 962 (1926)
13. R. Urban, Dissertation, Universitaet Halle (1922)
14. D. Vorlaender, "Chemische Kristallographie der Fluessigkeiten!" Akademische Verlagsgesellschaft, Leipzig, 1924
15. C. Eaborn and N. H. Hartshorne, J. Chem. Soc., 1955, 549

16. W. R. Young, I. Haller and D. C. Green, *Molecular Crystals and Liquid Crystals*, 13, 305 (1971)
17. F. A. Cotton and G. Wilkinson, "Advanced Inorganic Chemistry", 2nd ed. Interscience Publishers, New York, 1966, p. 1023
18. S. M. Morehouse, A. R. Powell, J. P. Heffer, T. A. Stephenson and G. Wilkinson, *Chemistry and Industry*, 1964, 544
19. T. A. Stephenson, S. M. Morehouse, A. R. Powell, J. P. Heffer and G. Wilkinson, *J. Chem. Soc.*, 1965, 3632
20. P. K. Hon, C. E. Pfluger and R. L. Belford, *Inorg. Chem.*, 6, 730 (1967)
21. L. R. Blaine, E. K. Plyler and W. S. Benedict, *J. Res. Nat. Bureau of Standards*, 66A, 223 (1962)
- 22a. R. S. Baxter, "Thermal Analysis, Vol. I", edited by R. F. Schwenker and P. D. Garn, Academic Press, Inc., New York, 1969
- 22b. R. W. Brandon and D. V. Claridge, *Chem. Comm.*, 1968, 677
23. S. M. McElvain and T. P. Carney, *J. Am. Chem. Soc.*, 68, 2592 (1946)
24. J. S. Pierce, *J. Am. Chem. Soc.*, 64, 1961 (1942)
25. S. S. Sabnis, K. D. Kulkarni and C. V. Deliwala, *J. Sci. Industr. Res.*, 17A, 421 (1958)
26. V. N. Andrievskii, *Izv. Akad. Nauk SSSR, Seria Khim.* (in Russian), 1966, 882
27. J. W. Carmichael, Jr., private communication, July 1972
28. A. A. Grinberg and L. K. Simonova, *Zh. Priklad, Khim.* (in Russian), 26, No. 8, 880 (1953)
29. P. R. Singh and R. Sahai, *Journ. Indian Chem. Soc.*, 46, 945 (1969)

30. M. S. Kharash, R. C. Seylor and F. R. Mayo, J. Am. Chem. Soc., 60, 882 (1938)
31. T. A. Stephenson, E. Bannister and G. Wilkinson, J. Chem. Soc., 1964, 2538
32. T. A. Stephenson and G. Wilkinson, J. inorg. nucl. chem., 29, 2122 (1967)
33. J. H. Talbot, Acta Cryst. 6, 720 (1953)
34. K. Nakamoto, "Infrared Spectra of Inorganic and Coordination Compounds", John Wiley and Sons, Inc., New York, 1963, p. 198
35. J. N. van Niekerk and F. R. L. Schoening, Acta Cryst., 6, 501 (1953)
36. J. N. van Niekerk and F. R. L. Schoening, Acta Cryst., 6, 227 (1953)
37. W. H. Bragg and G. T. Morgan, Proc. Roy. Soc., A104, 437 (1923)
38. H. Koyama and Y. Saito, Bull. Chem. Soc. Jap. 27, 113 (1954)
39. A. C. Skapski and M. L. Smart, Chem. Comm., 1970, 659
40. F. A. Cotton "The Infrared Spectra of Transitional Metal Complexes" in "Modern Coordination Chemistry", J. Lewis and R. G. Wilkins, eds., Interscience Publishers, New York, 1960, 379 ff
41. K. Nakamoto, "Infrared Spectra of Inorganic and Coordination Compounds, 2nd. ed., Interscience Publishers, New York, 1970, p. 247 ff
42. J. F. Ferraro, "Low-Frequency Vibrations of Inorganic and Coordination Compounds," Plenum Press, New York, 1971, p. 89 ff
43. B. Bock, K. Flatau, H. Junge, M. Kuhr and H. Musso, Angew. Chem. internat. Edit., 10 225 (1971)

44. R. S. Rasmussen, D. D. Tunnicliff, and R. R. Brattain, J. Amer. Chem. Soc., 71, 1068 (1949)
45. H. S. Jarrett, M. S. Sadler and J. N. Shoolery, J. Chem. Phys. 21, 2092 (1953)
46. K. Nakamoto, C. Udovich and J. Takemoto, J. Am. Chem. Soc., 92, 3973 (1970)
47. K. Nakamoto, P. J. McCarthy, and A. E. Martell, Nature, 183, 459 (1959)
48. J. U. Lowe, Jr. and L. N. Ferguson, J. Org. Chem., 30, 3001 (1965)
49. C. Y. Liang, E. J. Schimitschek and J. A. Trias, J. inorg. nucl. Chem., 32, 811 (1970)
50. L. J. Bellamy and L. Beecher, J. Chem. Soc., 1954, 4487
51. H. F. Holtzclaw, Jr. and J. P. Collman, J. Am. Chem. Soc., 79, 3318 (1957)
52. H. F. Holtzclaw, Jr. and J. P. Collman, Document No. 5129, ADI Auxiliary Publication Project, Library of Congress.
53. E. R. Blout, M. Fields and R. Karplus, J. Am. Chem. Soc., 70, 194 (1948)
54. I. M. Hunsberger, R. Ketcham and H. S. Gutowsky, J. Am. Chem. Soc., 74, 4839 (1952)
55. L. Kahovec and K. W. F. Kohlrausch, Chem. Ber. 73, 1304 (1940)
56. D. N. Shigorin, Akad. Nauk SSSR, Ser. Fiz., 17, 595 (1953); (Chem. Abstr. 48, 5651h)
57. D. N. Shigorin, Zh. fiz. Khim, 27, 554 (1953); (Chem. Abstr. 48, 748i)
58. R. E. Hester and R. A. Plane, Inorg. Chem., 3, 513 (1964)
59. F. A. Cotton and R. H. Holm, J. Am. Chem. Soc., 80, 5658 (1958)

60. M. Calvin and K. W. Wilson, J. Am. Chem. Soc., 67, 2003 (1945)
61. K. Nakamoto and A. E. Martell, J. Chem. Phys. 32, 588 (1960)
62. K. Nakamoto, P. J. McCarthy and A. E. Martell, J. Am. Chem. Soc., 83, 1272 (1961)
- 63a. S. Pinchas, B. L. Silver and I. Laulicht, J. Chem. Phys., 46, 1506 (1967)
- 63b. H. Ogoshi and K. Nakamoto, J. Chem. Phys., 45, 3113 (1966)
64. H. Musso and H. Junge, Tetrahedron Lett., 33, 4003, 4009 (1966)
65. M. Mikami, I. Nakagawa and T. Shimanouchi, Spectrochim. Acta, 23A, 1037 (1967)
66. L. J. Bellamy and R. F. Branch, J. Chem. Soc., 1954, 4491
67. R. West and R. Riley, J. inorg. nucl. Chem., 5, 295 (1958)
68. G. T. Behnke and K. Nakamoto, Inorg. Chem., 6, 433 (1967)
69. G. T. Behnke and K. Nakamoto, *ibid.*, p. 440
70. K. Nakamoto, Angew. Chem. internat. Edit., 11, 666 (1972)
71. L. B. Van Uitert, W. C. Fernelius and B. E. Douglas, J. Am. Chem. Soc., 75, 2736 (1953)
72. H. F. Holtzclaw, Jr., A. H. Carlson and J. P. Collman, J. Am. Chem. Soc., 78, 1838 (1950)
73. K. Nakamoto, Y. Morimoto and A. E. Martell, J. Phys. Chem., 66, 346 (1962)
74. P. R. Singh and R. Sahai, Aust. J. Chem., 22, 263 (1969)

75. P. R. Singh and R. Sahai, *Aust. J. Chem.*, 20, 649 (1967)
76. K. Nakamoto, H. J. McCarthy, A. Ruby and A. E. Martell, *J. Am. Chem. Soc.*, 83, 1066 (1961)
77. J. P. Collman, R. A. Moss, H. Maltz and C. C. Heindel, *J. Am. Chem. Soc.*, 83, 531 (1961)
78. R. P. Dryden and A. Winston, *J. Phys. Chem.*, 62, 635 (1958)
79. S. Baba, T. Ogura, S. Kawaguchi, *Bull. Chem. Soc. Japan*, 47, 665 (1974)
80. F. A. Cotton, "Chemical Applications of Group Theory", Interscience Publishers, New York, 1963, p. 263 ff
81. D. M. Adams, "Metal-Ligand and Related Vibrations", Edward Arnold Publishers, Ltd., London, 1967
82. P. K. Hon, C. E. Pfluger and R. L. Belford, *Inorg. Chem.* 5, 516 (1966)
83. P. K. Hon, R. L. Belford and C. E. Pfluger, *J. Chem. Phys.*, 43, 1323 (1965)
84. E. A. Shugam, L. M. Shkol'nikova and V. V. Zelentsov, *Zh. Strukt. Khimii (in Russian)*, 7, 128 (1966)
- 85a. L. L. Ingraham, "Steric Effects on Certain Physical Properties", in "Steric Effects in Organic Chemistry", M. S. Newman, ed., John Wiley and Sons, Inc., New York, 1956, p. 481 ff
- 85b. M. J. S. Dewar, *J. Am. Chem. Soc.*, 74, 3341 (1952)
- 85c. R. B. Turner and D. M. Voitle, *J. Am. Chem. Soc.*, 73, 1403 (1951)
86. P. R. Singh and R. Sahai, *Inorg. Nucl. Chem. Letters*, 4, 513 (1968)
87. S. I. Mizushima and T. Shimanouchi, *J. Am. Chem. Soc.*, 71, 1320 (1949)

88. R. F. Schaufele and T. Shimanouchi, *J. Chem. Phys.*, 47, 3605 (1967)
89. J. M. Schnur, *Molecular Crystals and Liquid Crystals*, 23, 155 (1973)
90. S. P. Gubin, L. I. Denisovich and A. Z. Rubezhov, *Dokl. Akad. Nauk SSSR (in Russian)*, 169, No. 1, 103 (1966)
91. R. Eistert and E. Merkel, *Chem. Ber.*, 86, 904 (1953)
92. T. Sasaki, K. Kanematsu and G. Kinoshita, *J. Org. Chem.*, 33, 680 (1968)
93. C. A. Coulson, "Conference on Quantum Mechanical Methods in Valence Theory", U. S. Government Printing Office, 1951, p. 42
94. D. W. Barnum, *J. Inorg. Nucl. Chem.*, 22, 183 (1961)
95. J. P. Fackler, Jr., F. A. Cotton and D. W. Barnum, *Inorg. Chem.*, 2, 97 (1963)
96. J. P. Fackler, Jr. and F. A. Cotton, *ibid*, p. 103
97. M. Blackstone, J. Van Thuiji and C. Romero, *Rec. Trav. Chim.*, 35, 557 (1966)
98. A. N. Nesmeyanov, A. Z. Rubezhov, S. P. Gubin and Z. B. Mitroshina, *Izv. Akad. Nauk SSSR, Ser, Khim. (in Russian)*, 1966, No. 4, 739; (*Chem. Abstr.* 65, 8318g)
99. J. W. Carmichael, Jr., L. K. Steinrauf and R. L. Belford, *J. Chem. Phys.*, 43, 3595 (1965)
100. L. W. Reeves, *Can. J. Chem.*, 35, 1351 (1957)
101. M. Calvin, *J. Am. Chem. Soc.*, 67, 2003 (1945)
102. D. E. Williams, *Acta Crystallogr.*, 21, 340 (1966)
103. E. A. Shugam, *Doklady Akad. Nauk SSSR, (in Russian)*, 81, 853 (1951); (*Chem. Abstr.* 46, 3894)

104. E. A. Lingafelter and R. L. Brawn, J. Am. Chem. Soc., 88, 2951 (1966)
- 105a. J. C. Hammet, J. A. S. Smith and E. J. Wilkins, J. Chem. Soc. A, 1969, 146
- 105b. J. C. Hammet and J. A. S. Smith, *ibid*, 1970, 1852
106. M. Kuhr and H. Musso, Angew. Chem. internat. Edit., 8, 147 (1969)
107. J. Lewis and C. Oldham, J. Chem. Soc. A, 1966, 1453
108. Handbook of Chemistry and Physics, 45th ed., The Chemical Rubber Company, Cleveland, 1965, Table E-42
109. "Nuclear Magnetic Shift Reagents", R. E. Sievers, ed. Academic Press, Inc., New York, 1973
110. C. C. Hinckley, J. Am. Chem. Soc., 91, 5160 (1969)
111. J. R. Campbell, Aldrichimica Acta (Aldrich Chemical Co.), 4, 55 (1971)
112. T. J. Marks, R. Porter, J. S. Kristoff and D. F. Shriver, "Organometallic Aspects of Shift Reagent Chemistry", p. 247 ff in Reference 109
113. R. M. Silverstein, G. C. Bassler and T. C. Morrill, "Spectrometric Identification of Organic Compounds", 3rd ed., John Wiley and Sons, Inc., New York, 1974, p. 194
114. A. Santoro and M. Esposito, J. Thermal Analysis, 6, 101 (1974)
115. W. Ostwald, Trans. Faraday Soc., 29, 1002 (1933)
116. *ibid*, p. 1080
117. S. D. Robinson and B. L. Shaw, J. Organometal. Chem., 3, 367 (1965)
118. M. R. Churchill and R. Mason, Nature, 204, 777 (1964)

119. M. Zocchi, J. Organometal. Chem., 33, C-47 (1971)
120. J. Hiraishi, I. Nakagava and T. Shimanouchi, Spectrochim. Acta, 24A, 819 (1968)
121. M. J. Ware, "Vibrational Studies of Metal-Metal Bonding", in "Essays in Structural Chemistry", A. J. Downs, ed., Plenum Press, New York, 1971, p. 404 ff
122. R. Kaiser, J. Chem. Phys., 42, 1838 (1965)
123. J. H. Noggle and R. E. Schirmer, "The Nuclear Overhauser Effect, Chemical Applications", Academic Press, New York, 1971, p. 31 ff